ELECTRONIC

TRANSFORMERS AND CIRCUITS

ELECTRONIC

TRANSFORMERS AND CIRCUITS

Reuben Lee

Advisory Engineer
Westinghouse Electric Corporation

SECOND EDITION

NEW YORK · JOHN WILEY & SONS, INC.
LONDON · CHAPMAN & HALL, LIMITED

Library of Congress Catalog Card Number: 55–10001

PRINTED IN THE UNITED STATES OF AMERICA

PREFACE TO SECOND EDITION

In the years since the first edition of this book was published, several new developments have taken place. This second edition encompasses such new material as will afford acquaintance with advances in the art. Some old topics which were inadequately presented have received fuller treatment. Several sections, especially those on electronic amplifiers and wave filters, have been deleted because more thorough treatments of these subjects are available in current literature. Thus the original objectives of a useful book on electronic transformers and related devices, with a minimum of unnecessary material, have been pursued in the second edition. Wherever the old material appeared adequate, it has been left unchanged, and the general arrangement is still the same, except for the addition of new Chapters 9 and 11. More information in chart form, but few mathematical proofs, are included.

In a book of general coverage, there is room only for a brief treatment of any phase of the subject. Thus the new chapter on magnetic amplifiers is a condensed outline of the more common components and circuits of this rapidly growing field. It is hoped that this chapter will be helpful as a general introduction to circuit and transformer designers alike. Recent circuit developments are reported in the *AIEE Transactions*.

In response to inquiry it should be stated that, where a mathematical basis is given, graphical performance is always calculated. There has been good general correspondence between the graphs and experimental tests. This correspondence is quite close in all cases except pulse transformers; for these, the graphs presented in this book predict wave shape with fair accuracy, but to predict exactly all the superposed ripples would be impracticable. This is pointed out in Chapter 10.

Although technical words usually have the same meaning as in the first edition, there are several new magnetic terms in the second edition. These terms conform with ASTM Standard A127-48.

Pascal said that an author should always use the word "our" rather than "my" in referring to his work, because there is in it usually more of other people's than his own. Never was this more true than of the present volume. Acknowledgment is due many Westinghouse engineers, especially R. M. Baker, L. F. Deise, H. L. Jessup, J. W. Ogden, G. F. Pittman, R. A. Ramey, T. F. Saffold, and D. S. Stephens, all of whom

assisted immeasurably by their constructive comments on the manuscript. D. G. Little's continued interest was most encouraging.

Helpful comment has been received from men outside Westinghouse. Mr. P. Fenoglio of the General Electric Co. kindly pointed out an omission in the first edition. Output wave shapes given for the front or leading edge of a pulse transformer were accurate for a hard-tube modulator, but not for a line-type modulator. The missing information is included in the second edition.

Finally, to my wife Margaret, my heartfelt thanks not only for her understanding of the long disruption of normal social life but also for her patience in checking proofs.

REUBEN LEE

Baltimore, Maryland
August, 1955

ACKNOWLEDGMENTS

Figures 23 and 24 were furnished through the courtesy of the Armco Steel Corp. Figures 50, 51, 52, 53, and 86 first appeared in a paper by O. H. Schade, *Proc. I.R.E.*, July, 1943, p. 341. Figure 150 is reprinted from *Proc. I.R.E.*, April, 1945. Figure 63 first appeared in the I.R.E. *Transactions on Component Parts*, April, 1955.

Figure 71 is reprinted from *Electronics*, March, 1955. Figures 89, 90, and 91 are reprinted from, and Section 52 (p. 123) is based on, "Solving a Rectifier Problem," *Electronics*, April, 1938. Figures 100 and 101 are reprinted from *Electronics* for September, 1949. Figure 180 and Section 97 (p. 232) are based on "A Study of R-F Chokes," which appeared in *Electronics* in April, 1934. Sections 123, 124, 125, and 127 (p. 294 et seq) are based on "Iron-Core Components in Pulse Amplifiers," *Electronics*, August, 1943. Figures 73, 258, and 259 are reprinted from this article.

Figure 88 is reprinted from *Tele-Tech and Electronic Industries*, October, 1953 (copyright Caldwell-Clements, 480 Lexington Avenue, New York).

Figures 107 and 110, and part of Section 67 (p. 153), first appeared in *Radio Engineering*, June, 1937.

Figure 142 is reprinted from the *General Radio Experimenter*, November, 1936.

Figures 163, 164, and 165 are reprinted from "Magnetic Ferrites—Core Materials for High Frequencies," by C. L. Snyder, E. Albers-Schoenberg, and H. A. Goldsmith, *Electrical Manufacturing*, December, 1949. Figure 191 is reprinted from *Electrical Manufacturing* for September, 1954.

The magnetic amplifier analysis on p. 276 is based on an unpublished paper by D. Lebell and B. Bussell, presented at the I.R.E. Convention, New York, March, 1952.

Figures 235, 252, 254, and 255, and Table XVII, are reprinted from *Proc. I.R.E.*, August, 1954.

PREFACE TO FIRST EDITION

The purpose of this book is twofold: first, to provide a reference book on the design of transformers for electronic apparatus and, second, to furnish electronic equipment engineers with an understanding of the effects of transformer characteristics on electronic circuits. Familiarity with basic circuit theory and transformer principles is assumed. Conventional transformer design is treated adequately in existing books, so only such phases of it as are pertinent to electronic transformers are included here. The same can be said of circuit theory; only that which is necessary to an understanding of transformer operation is given. It is intended that in this way the book will be encumbered with a minimum of unnecessary material. Mathematical proofs as such are kept to a minimum, but the bases for quantitative results are indicated. The A.I.E.E. "American Standard Definitions of Electrical Terms" gives the meaning of technical words used. Circuit symbols conform to A.S.A. Standards Z32.5—1944 and Z32.10—1944.

Chapter headings, except for the first two, are related to general types of apparatus. This arrangement should make the book more useful. Design data are included which would make tedious reading if grouped together. For instance, the design of an inductor depends on whether it is for power or wave filter work, and the factors peculiar to each are best studied in connection with their respective apparatus.

Parts of the book are based on material already published in the *Proceedings of the Institute of Radio Engineers, Electronics,* and *Communications.* Much of it leans heavily upon work done by fellow engineers of the Westinghouse Electric Corporation, the warmth of whose friendship I am privileged to enjoy. To list all their names would be a difficult and inadequate expression of gratitude, but I should be guilty of a gross omission if I did not mention the encouragement given me by Mr. D. G. Little, at whose suggestion this book was written.

R. L.

July 1947

CONTENTS

LIST OF SYMBOLS

Page numbers are those on which the corresponding symbol first appears. A symbol formed from one of the tabulated letters, with a subscript or prime added, is not listed unless it is frequently and prominently used in the book. Sometimes the same symbol denotes more than one property; the meaning is then determined by the context. Units are given wherever symbols are used. Small letters indicate instantaneous or varying electrical quantities, and capital letters indicate steady, effective, or scalar values.

a	Coil radius, 228
a	Coil winding height, 75
a	N_2/N_1, 147
A	Area, 172
A_c	Core area, 10
A_n	Ripple amplitude, 114
b	Winding traverse, 76
B	X_C/R_1 at frequency f_r, 150
B	Core flux density, 10
B_m, $B_{\max}$	Maximum operating flux density, 23, 97
B_r	Residual flux density, 23
c	Insulation thickness, 75
c	Specific heat, 57
C	Capacitance, 64
C_1, C_p	Primary capacitance, 147
C_2, C_s	Secondary capacitance, 147
C_e	Effective capacitance, 172
C_g	Capacitance of winding to ground, 245
C_w	Capacitance across winding, 245
d	Core tongue width, 38
d	Toroid diameter, 288
D	Winding height, 38
D	X_C/R_2 at frequency f_r, 159
e	Voltage (instantaneous value), 5
e_g	Alternating grid voltage, 141
e_p	Alternating plate voltage, 141

E	Emissivity, 57
E	Voltage (effective value), 6
E_B	Plate voltage, 141
E_o	Output voltage, 178
E_1	Primary voltage, 7
E_2	Secondary voltage, 7
E_S	Secondary no-load voltage, 7
E_L	Secondary full-load voltage, 7
E_{pk}	Peak value of alternating voltage, 111
E_{dc}	D-c voltage, 111
E_a	Voltage at top of pulse, 295
f	Frequency, 6
f_m	Midband frequency, 190
f_r	Resonance frequency, 150
f_c	Cut-off frequency, 185
$f(\ )$	Function of, 114
F	Factor, 230
g_m	Mutual conductance, 144
G	Gap loss constant, 191
H	Magnetizing force, 10
H_c	Coercive force, 23
i	Current (instantaneous value), 10
I, $\lvert I \rvert$, I_{rms}	Current (effective value), 6, 15
I_{dc}	Direct component of current, 16
$\hat{I}$, I_{pk}	Peak value of current, 16, 66
$\bar{I}$, I_{av}	Average value of current, 15, 66
I_P, I_B	Plate current (d-c), 142
I_L	Load current, 7
I_E	Loss component of exciting current, 10
I_M	Magnetizing current, 9
I_N	Exciting current, 9
I_G	Grid current (d-c), 142
j	$\sqrt{-1}$ (vector operator), 146
J	Low-frequency permeability/pulse permeability, 335
k	Thermal conductivity, 57
k	Coefficient of coupling, 225
k	½ ratio of impedance/circuit resistance $= \sqrt{L/C}/2R$, 104
K	Constant, 82
l_c	Mean length of core (or magnetic path), 10
l_g	Air gap, 88
L	Inductance, 90
L_e	Open-circuit inductance (*OCL*), 26

L_s	Short-circuit inductance, 76
L_m	Mutual inductance, 224
m	Decrement, 104
m	Order of harmonic, 114
M	Modulation factor, 16
MT	Mean turn length, 38
n	Number (e.g., of anodes), 76
N	Turns, 5
N_1	Primary turns, 5
N_2	Secondary turns, 5
N_L	Number of layers (of wire in coil), 173
OCL	Open-circuit inductance, 106
p	Density, 26
p	Ratio of voltages (in autotransformer), 250
p	Rectifier ripple frequency/line frequency (number of phases), 113
P_a	Volt-amperes per pound, 26
P_c	Core loss, 26
P_A	Ripple amplitude/E_{dc} (in rectifier), 114
P_R	Ripple amplitude/E_{dc} (across load), 114
PFN	Pulse forming network, 332
PRF	Pulse repetition frequency, 338
Q	$\omega L/R$ = coil reactance/coil a-c resistance, 106
r	Radius, 38
r_e	Equivalent radius, 57
r_p	Plate resistance, 144
R	Resistance, 6
R_1	Source resistance, 146
R_2	Load resistance, 146
R_L	Load resistance, 8
R_e	Equivalent core-loss (shunt) resistance, 8
S	Secondary winding, 71
S	Core window width, 102
t	Time (independent variable), 5
t	Thickness of insulation, 172
T	Period of a wave, 15
T	$2\pi\sqrt{L_sC_2}$ (undamped period of oscillatory wave), 295
V	Commutation voltage, 120
V	Volume (of core), 91
w	Core-stacking dimension, 38
W_g	Gap loss, 191
W_e	Core loss, 82

W_s	Copper loss, 82
X	Reactance, 6
X_N	Open-circuit reactance = $2\pi f L_e$, 9
X_C	Capacitive reactance = $1/(2\pi f C)$, 112
X_L	Inductive reactance = $2\pi f L$, 112
Z	Impedance, 8
Z_G	Source impedance, 141
Z_L	Load impedance, 141
Z_0	Characteristic impedance, 145
α	Amplifier gain, 174
α	$\sqrt{C_g/C_w}$, 245
α	Damping factor, 319
β	Feedback constant, 178
β	Natural angular frequency, 304
δ	Small interval of time, 15
Δ	Increment (e.g., of flux), 25
Δ	Exciting current/load current, 299
ϵ	Base of natural logarithms (= 2.718), 57
ϵ	Dielectric constant of insulation, 172
η	Efficiency, 14
θ	Temperature, 57
θ	Phase angle, 120
μ	Amplification factor, 141
μ	Permeability, 24
μ_Δ	Incremental permeability, 25
π	3.1416, 6
ϕ	Phase angle, 195
ϕ	Flux (varying), 6
$\Phi_{\max}$	Peak value of flux, 6
Σ	Summation (of a series of elements), 38
τ	Pulse duration, 298
ω	$2\pi f$ (angular frequency), 6

1. INTRODUCTION

1. What Is a Transformer? In its most elementary form, a transformer consists of two coils wound of wire and inductively coupled to each other. When alternating current at a given frequency flows in either coil, an alternating voltage of the same frequency is induced in the other coil. The value of this voltage depends on the degree of coupling and the flux linkages in the two coils. The coil connected to a source of alternating voltage is usually called the primary coil, and the voltage across this coil is the primary voltage. Voltage induced in the secondary coil may be greater than or less than the primary voltage, depending on the ratio of primary to secondary turns. A transformer is termed a step-up or a step-down transformer accordingly.

Most transformers have stationary iron cores, around which the primary and secondary coils are placed. Because of the high permeability of iron, most of the flux is confined to the core, and a greater degree of coupling between the coils is thereby obtained. So tight is the coupling between the coils in some transformers that the primary and secondary voltages bear almost exactly the same ratio to each other as the turns in the respective coils or windings. Thus the *turns ratio* of a transformer is a common index of its function in raising or lowering voltage. This function makes the transformer an important adjunct of modern electrical power systems. Raising the voltage makes possible the economical transmission of power over long distances; lowering the voltage again makes this power available in useful form. It is safe to say that, without transformers, modern industry could not have reached its present state of development.

2. Electronic Transformers. Although no exact line of demarcation can be drawn between power transformers and electronic transformers, in general electronic transformers are smaller. The source of power on a 60-cycle network is extremely large and may be the combined generating capacity of half a continent. Power in electronic equipment is limited to the capabilities of electron tubes, of which even the largest is small compared to a power station generator.

Transformers are needed in electronic apparatus to provide the different values of plate, filament, and bias voltage required for proper tube operation, to insulate circuits from each other, to furnish high impedance to alternating but low impedance to direct current, and to maintain or modify wave shape and frequency response at different potentials. The very concept of impedance, so characteristic of electronics, almost necessarily presupposes a means of changing from one impedance level to another, and that means is commonly a transformer.

Impedance levels are usually higher in electronic, as compared with power, equipment. Consider the connected kva on an 11,000-volt power line; it may easily total 1,000,000. Compare this with a large broadcast transmitter operating at the same voltage and drawing 70 kva. The currents in the two cases are 90,000 amp and 6 amp, respectively. For the power line, the load impedance is 11,000/90,000, or slightly more than 0.1 ohm; for the transmitter it is 11,000/6, or nearly 2,000 ohms. Source impedances are approximately proportional to these load impedances. In low-power electronic circuits the source impedance often exceeds the load impedance and influences the transformer performance even further.

Weight and space are usually at a premium in electronic equipment, and reliability is of paramount importance. Transformers account for a considerable portion of the weight and space, and form a prime component of the reliability.

These and other differences of application render many power transformers unsuitable for electronic circuit use. The design, construction, and testing of electronic transformers have become separate arts, directed toward the most effective use of materials for electronic applications.

3. New Materials. Like all electronic apparatus, transformers are subject to continual change. This is especially so since the introduction of new materials such as

(*a*) Grain-oriented core steel.
(*b*) Solventless impregnating varnish.
(*c*) Inorganic insulating tape.
(*d*) Improved wire enamel.
(*e*) Low-loss, powdered iron cores.
(*f*) Ferrite cores.

Through the application of these materials, it has been possible to

(*a*) Reduce the size of audio and power transformers and reactors.

(*b*) Increase the usefulness of saturable reactors as magnetic amplifiers.

(*c*) Reduce the size of high-voltage units.

(*d*) Design filters and reactors having sharper cut-off and higher Q than previously was thought possible.

(*e*) Make efficient transformers for the non-sinusoidal wave shapes such as are encountered in pulse, video, and sweep amplifiers.

(*f*) Extend the upper operating frequency of transformers into the high-frequency r-f range.

Occasionally someone asks why electronic transformers cannot be designed according to curves or charts showing the relation between volts, turns, wire size, and power rating. Such curves are very useful in designing the simpler transformers. However, this idea has not been found universally practicable for the following reasons:

(*a*) *Regulation.* This property is rarely negligible in electronic circuits. It often requires care and thought to use the most advantageous winding arrangement in order to obtain the proper IX and IR voltage drops. Sometimes the size is dictated by such considerations.

(*b*) *Frequency Range.* The low-frequency end of a wideband transformer operating range in a given circuit is determined by the transformer open-circuit inductance. The high-frequency end is governed by the leakage inductance and distributed capacitance. Juggling the various factors, such as core size, number of turns, interleaving, and insulation, in order to obtain the optimum design constitutes a technical problem too complex to solve on charts.

(*c*) *Voltage.* It would be exceedingly difficult, if not impossible, to reduce to chart form the use of high voltages in the restricted space of a transformer. Circuit considerations are very important here, and the transformer designer must be thoroughly familiar with the functioning of the transformer to insure reliable operation, low cost, and small dimensions.

(*d*) *Size.* Much electronic equipment is cramped for space, and, since transformers often constitute the largest items in the equipment, it is imperative that they, too, be of small size. An open-minded attitude toward this condition and good judgment may make it possible to meet the requirements which otherwise might not be fulfilled. New materials, too, can be instrumental in reducing size, sometimes down to a small fraction of former size.

In succeeding chapters the foregoing considerations will be applied

to the performance and design of several general types of electronic transformers. The remainder of this chapter is a brief review of fundamental transformer principles. Only iron-core transformers with closed magnetic paths are considered in this introduction. Air-core transformers, with or without slugs of powdered iron, are discussed in a later chapter on high-frequency transformers. Most transformers operate at power frequencies; it is therefore logical to begin with low-frequency principles. These principles are modified for other conditions in later chapters.

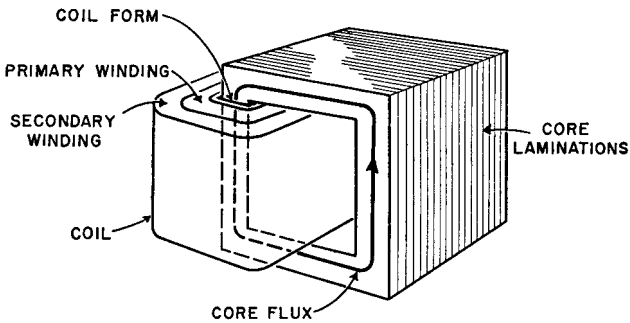

FIG. 1. Transformer coil and core.

A simple transformer coil and core arrangement is shown in Fig. 1. The primary and secondary coils are wound one over the other on an insulating coil tube or form. The core is laminated to reduce losses. Flux flows in the core along the path indicated, so that all the core flux threads through or links both windings. In a circuit diagram the transformer is represented by the circuit symbol of Fig. 2.

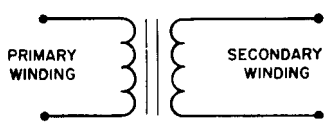

FIG. 2. Simple transformer.

4. Transformer Fundamentals. The simple transformer of Fig. 2 has two windings. The left-hand winding is assumed to be connected to a voltage source and is called the primary winding. The right-hand winding is connected to a load and is called the secondary. The transformer merely delivers to the load a voltage similar to that impressed across its primary, except that it may be smaller or greater in amplitude.

In order for a transformer to perform this function, the voltage across it must vary with respect to time. A d-c voltage such as that of a storage battery produces no voltage in the secondary winding or power

in the load. If both varying and d-c voltages are impressed across the primary, only the varying part is delivered to the load. This comes about because the voltage e in the secondary is induced in that winding by the core flux ϕ according to the law

$$e = -\frac{N\,d\phi}{dt} \times 10^{-8} \tag{1}$$

This law may be stated in words as follows: The voltage induced in a coil is proportional to the number of turns and to the time rate of change of magnetic flux in the coil. This rate of change of flux may be large or small. For a given voltage, if the rate of change of flux is small, many turns must be used. Conversely, if a small number of turns is used, a large rate of change of flux is necessary to produce a given voltage. The rate of change of flux can be made large in two ways, by increasing the maximum value of flux and by decreasing the period of time over which the flux change takes place. At low frequencies, the flux changes over a relatively large interval of time, and therefore a large number of turns is required for a given voltage, even though moderately large fluxes are used. As the frequency increases, the time interval between voltage changes is decreased, and for a given flux fewer turns are needed to produce a given voltage. And so it is that low-frequency transformers are characterized by the use of a large number of turns, whereas high-frequency transformers have but few turns.

If the flux ϕ did not vary with time, the induced voltage would be zero. Equation 1 is thus the fundamental transformer equation. The voltage variation with time may be of any kind: sinusoidal, exponential, sawtooth, or impulse. The essential condition for inducing a voltage in the secondary is that there be a flux *variation*. Only that part of the flux which links both coils induces a secondary voltage.

In equation 1, if ϕ denotes *maxwells* of flux and t time in seconds, e denotes *volts* induced.

If all the flux links both windings, equation 1 shows that equal volts per turn are induced in the primary and secondary, or

$$\frac{e_1}{e_2} = \frac{N_1}{N_2} \tag{2}$$

where e_1 = primary voltage
e_2 = secondary voltage
N_1 = primary turns
N_2 = secondary turns.

5. Sinusoidal Voltage. If the flux variation is sinusoidal,

$$\phi = \Phi_{max} \sin \omega t$$

where Φ_{max} is the peak value of flux, ω is angular frequency, and t is time. Equation 1 becomes

$$e = -N\Phi_{max}\omega \cos \omega t \times 10^{-8} \tag{3}$$

or the induced voltage also is sinusoidal. This voltage has an effective value

$$E = 0.707 \times 2\pi f N \Phi_{max} \times 10^{-8}$$
$$= 4.44 f N \Phi_{max} \times 10^{-8} \tag{4}$$

where f is the frequency of the sine wave. Equation 4 is the relation between voltage and flux for sinusoidal voltage.

Sufficient current is drawn by the primary winding to produce the flux required to maintain the winding voltage. The primary *induced* voltage in an unloaded transformer is just enough lower than the *impressed* voltage to allow this current to flow into the primary winding. If a load is connected across the secondary terminals, the primary induced voltage decreases further, to allow more current to flow into the winding in order that there may be a load current. Thus the primary of a loaded transformer carries both an exciting current and a load current, but only the load part is transformed into secondary load current.

Primary induced voltage would exactly equal primary impressed voltage if there were no resistance and reactance in the winding. Primary current flowing through the winding causes a voltage drop IR, the product of primary current I and winding resistance R. The winding also presents a reactance X which causes an IX drop. Reactance X is caused by the *leakage* flux or flux which does not link both primary and secondary windings. There is at least a small percentage of the flux which is not common to both windings. Leakage flux flows in the air spaces adjacent to the windings. Because the primary turns link leakage flux an inductance is thereby introduced into the winding, producing leakage reactance X at the line frequency. The larger the primary current, the greater the leakage flux, and the greater the reactance drop IX. Thus the leakage reactance drop is a series effect, proportional to primary current.

6. Equivalent Circuit and Vector Diagram. For purposes of analysis the transformer may be represented by a 1:1 turns-ratio *equivalent circuit*. This circuit is based on the following assumptions:

(*a*) Primary and secondary turns are equal in number. One winding is chosen as the *reference* winding; the other is the *referred* winding. The voltage in the referred winding is multiplied by the actual turns ratio after it is computed from the equivalent circuit. The choice between primary and secondary for the reference winding is a matter of convenience.

(*b*) Core loss may be represented by a resistance across the terminals of the reference winding.

(*c*) Core flux reactance may be represented by a reactance across the terminals of the reference winding.

(*d*) Primary and secondary IR and IX voltage drops may be lumped together; the voltage drops in the referred winding are multiplied by a factor derived at the end of this section, to give them the correct equivalent value.

(*e*) Equivalent reactances and resistances are linear.

As will be shown later, some of these assumptions are approximate, and the analysis based on them is only accurate so far as the assumptions are justified. With proper attention to this fact, practical use can be made of the equivalent circuit.

With many sine-wave electronic transformers, the transformer load is resistive. A tube filament heating load, for example, has 100 per cent power factor. Under this condition the relations between voltages and currents become appreciably simplified in comparison with the same relations for reactive loads. In what follows, the secondary winding will be chosen as the reference winding. At low frequencies such a transformer may be represented by Fig. 3(*a*). The transformer equivalent circuit is approximated by Fig. 3(*b*), and its vector diagram for 100 per cent p-f load by Fig. 3(*c*). Secondary load voltage E_L and load current I_L are in phase. Secondary induced voltage E_S is greater than E_L because it must compensate for the winding resistances and leakage reactances. The winding resistance and leakage reactance voltage drops are shown in Fig. 3(*c*) as IR and IX, which are respectively in phase and in quadrature with I_L and E_L. These voltage drops are the sum of secondary and primary winding voltage drops, but the primary values are multiplied by a factor to be derived later. If voltage drops and losses are temporarily forgotten, the same power is delivered to the load as is taken from the line. Let subscripts 1 and 2 denote the respective primary and secondary quantities.

$$E_1 I_1 = E_2 I_2 \tag{5}$$

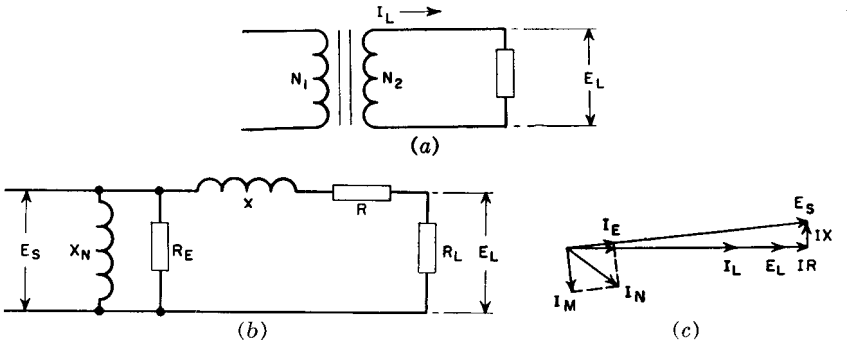

FIG. 3. (*a*) Transformer with resistive load; (*b*) equivalent circuit; (*c*) vector diagram.

or
$$\frac{E_1}{E_2} = \frac{I_2}{I_1} \tag{6}$$

so that the voltages are inversely proportional to the currents. Also, from equation 2, they are directly proportional to their respective turns.

$$\frac{E_1}{E_2} = \frac{N_1}{N_2} \tag{2a}$$

Now the transformer may be replaced by an impedance Z_1 drawing the same current from the line, so that

$$I_1 = E_1/Z_1$$

Likewise

$$I_2 = E_2/Z_2$$

where Z_2 is the secondary load impedance, in this case R_L. If these expressions for current are substituted in equation 6,

$$\frac{Z_1}{Z_2} = \left(\frac{E_1}{E_2}\right)^2 = \left(\frac{N_1}{N_2}\right)^2 \tag{7}$$

Equation 7 is strictly true only for negligible voltage drops and losses. It is approximately true for voltage drops up to about 10 per cent of the winding voltage or for losses less than 20 per cent of the power delivered, but it is not true when the voltage drops approach in value the winding voltage or when the losses constitute most of the primary load.

Not only does the load impedance bear the relation of equation 7

to the equivalent primary load impedance; the winding reactance and resistance may also be referred from one winding to the other by the same ratio. This can be seen if the secondary winding resistance and reactance are considered part of the load, across which the secondary induced voltage E_S appears. Thus the factor by which the primary reactance and resistance are multiplied, to refer them to the secondary for addition to the secondary drops, is $(N_2/N_1)^2$. If the primary had been the reference winding, the secondary reactance and resistance would have been multiplied by $(N_1/N_2)^2$.

In Fig. 3(*c*) the IR voltage drop subtracts directly from the terminal voltage across the resistive load, but the IX drop makes virtually no difference. How much the IX drop may be before it becomes appreciable is shown in Fig. 4. If the IX drop is 30 per cent of the induced voltage, 4 per cent reduction in load voltage results; 15 per cent IX drop causes but 1 per cent reduction.

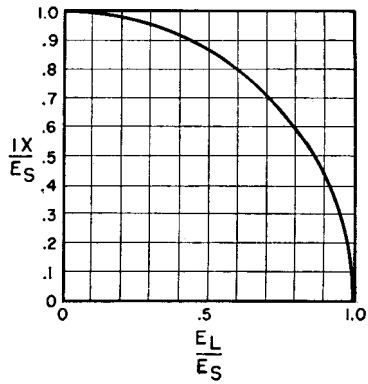

FIG. 4. Relation between reactive voltage drop and load voltage.

7. Magnetizing Current. In addition to the current entering the primary because of the secondary load, there is the core exciting current I_N which flows in the primary whether the secondary load is connected or not. This current is drawn by the primary core reactance X_N and equivalent core-loss resistance R_E and is multiplied by N_1/N_2 when it is referred to the secondary side. It has two components: I_M, the magnetizing component which flows 90° lagging behind induced voltage E_S; and I_E, the core-loss current which is in phase with E_S. Ordinarily this current is small and produces negligible voltage drop in the winding.

Core-loss current is often divided into two components: eddy current and hysteresis. Eddy-current loss is caused by current circulating in the core laminations. Hysteresis loss is the *power* required to magnetize the core first in one direction and then in the other on alternating half-cycles. Hysteresis loss and magnetization are intimately connected, as can be seen from Fig. 5. Here induced voltage e is plotted against time, and core flux ϕ lags e by 90°, in accordance with equation 3. This flux is also plotted against magnetizing current in the loop at the right. This loop has the same shape as the B-H loop

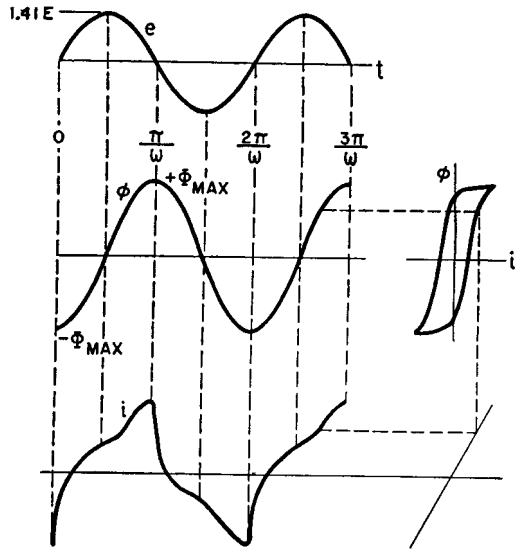

FIG. 5. Transformer voltage, flux, and exciting current.

for the grade of iron used in the core, but the scales are changed so that

$$\left.\begin{aligned} \phi &= BA_c \\ i &= Hl_c/0.4\pi N \end{aligned}\right\} \tag{8}$$

where B = core flux density in gauss
A_c = core cross-sectional area in cm^2
H = core magnetizing force in oersteds
l_c = core flux path length in cm.

Current is projected from the ϕ-i loop to obtain the alternating current i at the bottom of Fig. 5. This current contains both the magnetizing and the hysteresis loss components of current. In core-material research it is important to separate these components, for it is mainly through reduction of the B-H loop area (and hence hysteresis loss) that core materials have been improved. Techniques have been developed to separate the exciting current components, but it is evident that these components cannot be separated by current measurement only. It is nevertheless convenient for analysis of measurements to add the loss components and call their sum I_E, and to regard the magnetizing component I_M as a separate lagging current, as in Fig. 3. As long as the core reactance is large, the vector sum I_N of I_M and I_E is

small, and the non-sinusoidal shape of I_N does not seriously affect the accuracy of Fig. 3.

Core flux reactance may be found by measuring the magnetizing current, i.e., the current component which lags the applied voltage 90° with the secondary circuit open. Because of the method of measurement, this is often called the *open-circuit* reactance, and this reactance divided by the angular frequency is called the open-circuit inductance. The secondary and primary winding leakage reactances are found by short-circuiting the secondary winding and measuring the primary voltage with rated current flowing. The component of primary voltage which leads the current by 90° is divided by the current; this is the sum of the leakage reactances, the secondary reactance being multiplied by the (turns ratio)^2, and is called the *short-circuit* reactance.

Practical cases sometimes arise where the magnetizing component becomes of the same order of magnitude as I_L. Because current I_M flows only in the primary, a different equivalent circuit and vector diagram are necessary, as shown in Fig. 6. Note that the leakage react-

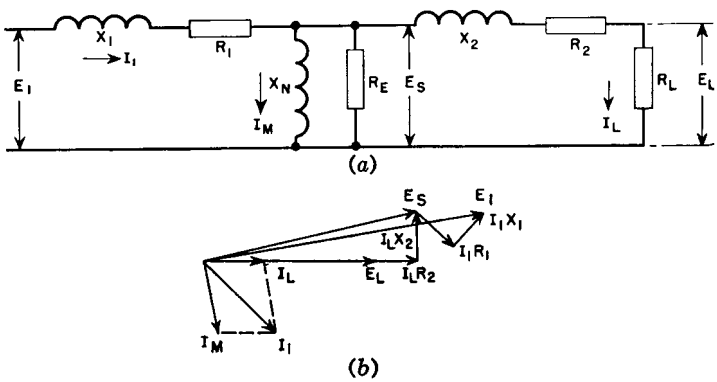

FIG. 6. (*a*) Equivalent circuit and (*b*) vector diagram for transformer with high magnetizing current.

ance voltage drop has a marked effect upon the load voltage, and this effect is larger as I_M increases relative to I_L. Therefore, the statement that IX voltage drop causes negligible difference between secondary induced and terminal voltages in transformers with resistive loads is true only for small values of exciting current. Moreover, the total primary current I_1 has a largely distorted shape, so that treating the IR and IX voltage drops as vectors is a rough approximation. For

accurate calculation of load voltage with large core exciting current, a point-by-point analysis would be necessary.

8. Flux and Average Voltage. If the variables are separated in equation 1, thus

$$e\,dt = -N \times 10^{-8}\,d\phi$$

an expression for flux may be found:

$$\int e\,dt = -N \times 10^{-8} \int d\phi$$

Now if we consider the time interval 0 to π/ω, we have

$$\int_0^{\pi/\omega} e\,dt = -N \times 10^{-8} \int_{-\Phi_{max}}^{+\Phi_{max}} d\phi$$

$$= -2N\Phi_{max} \times 10^{-8} \tag{9}$$

Equation 9 gives the relation between maximum flux and the time integral of voltage. The left side of the equation is the area under the voltage-time wave. For a given frequency, it is proportional to the *average* voltage value. This is perfectly general and holds true regardless of wave form. If the voltage wave form is alternating, the average value of the time integral over a long period of time is zero. If the voltage wave form is sinusoidal, the flux wave form is also sinusoidal but is displaced 90° as in Fig. 5, and the integral over a half-cycle is

$$-1.41E \left[\frac{\cos \omega t}{\omega}\right]_0^{\pi/\omega} = \frac{2.82E}{\omega}$$

whence

$$\Phi_{max} = \frac{1.41 \times 10^8 E}{\omega N} \tag{10}$$

Equation 10 is the relation between maximum flux, effective voltage, frequency, and turns. It is a transposed form of equation 4.

9. Ideal Transformer. The use of equivalent circuits enables an engineer to calculate many transformer problems with comparative ease. It is always necessary to multiply properties in the referred winding by the proper ratio. This has led to the interposition of a transformer of the right turns ratio somewhere in the equivalent circuit, usually across the load. The transformer thus used must introduce no additional losses or voltage drops in the circuit. It is called an

ideal transformer,[1] and it has negligibly small winding resistances, leakage flux, core loss, magnetizing current, and winding capacitances. Some power and audio transformers very nearly approach the ideal transformer at some frequencies. For example, in a typical 50-kva plate transformer, the winding resistance IR drops total 1 per cent and the leakage reactance IX drops 3 per cent of rated voltage, the core loss 0.6 per cent of output power and magnetizing current 2 per cent of rated primary current. When the term *ideal transformer* is used, it should be borne in mind that *negligibly small* is not *zero*. Particularly in electronic work, where frequency may vary, a limiting frequency may be reached at which the transformer is no longer ideal. Moreover, even if the limiting frequency is very low, it is never zero. There must be voltage variation if transformation is to take place. The assumptions of equations 5 to 7 were the same as for an ideal transformer.

10. Polarity. Let turns from equation 2*a* be substituted in equation 5. Then we have

$$N_1 I_1 = N_2 I_2 \tag{11}$$

or the primary and secondary ampere-turns are equal and opposite. This equality holds for only the load component of I_1; that is, exciting current has been regarded as negligibly small. If there is a direct current in the load, but not in the primary, or vice versa, equation 11 is true for only the a-c components.

A 1:1 turns-ratio transformer is shown diagramatically in Fig. 7. Impressed voltage is E_1, and primary current is I_1. Induced voltage E_i is slightly less than E_1, and is the same in magnitude and direction for both windings. Secondary current I_2 flows in the opposite direction to I_1. Instantaneous polarities are indicated by + and − signs. That is, when E_1 reaches positive maximum so do E_i and E_2. Dots are conventionally used to indicate terminals of the same polarity; dots in the circuit symbol at the right of Fig. 7 are used to indicate the same winding directions as in the left-hand figure.

11. Regulation, Efficiency, and Power Factor. Transformer regulation is the difference in the secondary terminal voltage at full load and at no load, expressed as a percentage of the full-load voltage. For the resistive load of Fig. 3(*a*), (*b*), and (*c*),

$$\text{Per cent regulation} = 100\ \frac{(E_S - E_L)}{E_L} \tag{12}$$

[1] See *Magnetic Circuits and Transformers*, M.I.T. Electrical Engineering Staff, John Wiley & Sons, New York, 1943, p. 269.

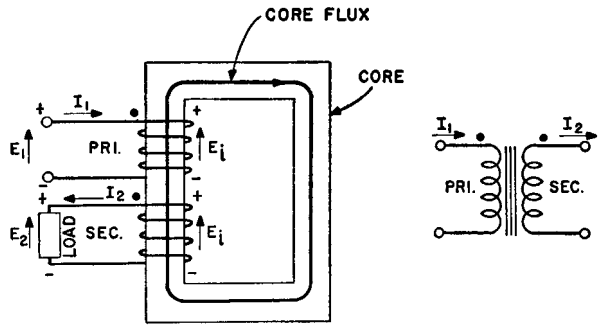

FIG. 7. Transformer polarity.

Since with low values of leakage reactance $E_S - E_L = IR$,

$$\text{Per cent regulation} = 100IR/E_L \tag{13}$$

provided that R includes the primary winding resistance multiplied by the factor $(N_2/N_1)^2$ as well as the secondary winding resistance. If leakage reactance is not negligibly small, approximately

$$\text{Per cent regulation} = 100\left[\frac{IR}{E_L} + \frac{1}{2}\left(\frac{IX}{E_L}\right)^2\right] \tag{14}$$

Efficiency is the ratio

$$\eta = \frac{\text{Output power}}{\text{Output power plus losses}} \tag{15}$$

where losses include both core and winding losses.

A convenient way of expressing power factor is

$$\text{Power factor} = \frac{\text{Output power plus losses}}{\text{Input volt-amperes}} \tag{16}$$

Equation 16 gives the power factor of a transformer plus its load.

One of the problems of transformer design is the proper choice of induction to obtain low values of exciting current and high power factor. Low power factor may cause excessive primary winding copper loss, low efficiency, and overheating.

12. Wave Shapes. Transformers in electronic circuits may be subjected to alternating and direct currents simultaneously, to modified sine waves, or to other non-sinusoidal waves. Although there is a relation between current and voltage wave shapes in a transformer, the two are frequently not the same, as has already been seen in Fig.

5. D-c components of primary voltage are not transformed; only the varying a-c component is transformed. Secondary current may be determined by the connection of the load. For example: if the load is a rectifier, the current will be some form of rectified wave; if the load is a modulator, the secondary current may be the superposition of two waves. If the primary voltage is non-sinusoidal, then the secondary current almost certainly will be non-sinusoidal.

If the primary voltage comes from an alternating source only, and the load is a half-wave rectifier, the secondary current has a d-c component, but the primary current has no d-c component except under changing conditions. That is to say, in the steady state there is no primary d-c component resulting from secondary d-c component alone. This is true, because any direct current in the primary requires a d-c source. But by the initial assumption there is no direct current present in the primary. Under these conditions, the core flux may be very much distorted because the flux excursions go into saturation in one direction only.

In succeeding chapters, two values of current will be of interest in circuits with non-sinusoidal waves, the average and the rms. Average current causes core saturation unless there is an air gap. Rms current determines the heating of the windings and is limited by the permissible temperature rise. Voltage wave form will be dealt with in subsequent chapters. Common current wave forms are tabulated here for convenience. (See Table I.)

Root-mean-square or rms current values are based upon the equation

$$I_{\text{rms}} = \sqrt{f\int_0^T i^2\,dt} \tag{17}$$

where i = current at any instant
f = frequency of repetition of current waves per second
T = duration of current waves in seconds
t = time in seconds.

Average current values are

$$I_{\text{av}} = f\int_0^T i\,dt \tag{18}$$

In the first wave shape, $T = 1/f$. In the fifth wave shape, $T + 2\delta$ is the current wave duration.

TABLE I. NON-SINUSOIDAL CURRENT WAVE FORMS

Current Wave Shape	Description	I_{rms}	I_{av}
	Direct current with superposed sine wave	$I_{dc}\sqrt{1+\frac{M^2}{2}}$	I_{dc}
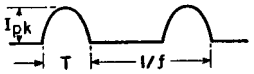	Half-sine loops of T duration and f repetition rate	$I_{pk}\sqrt{\frac{fT}{2}}$	$\frac{2I_{pk}fT}{\pi}$
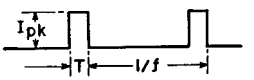	Square waves of T duration and f repetition frequency	$I_{pk}\sqrt{fT}$	$I_{pk}fT$
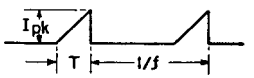	Sawtooth wave of T duration and f repetition frequency	$I_{pk}\sqrt{\frac{fT}{3}}$	$\frac{I_{pk}fT}{2}$
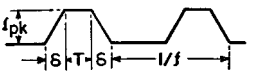	Trapezoidal wave of f repetition frequency	$I_{pk}\sqrt{\frac{f(2\delta+3T)}{3}}$	$I_{pk}f(\delta+T)$

In both equations 17 and 18, T refers to a full period. This is in contrast to steady-state sinusoidal alternating currents, the rms and average values of which are developed over a half-period because of the symmetry of such currents about the zero axis.

2. TRANSFORMER CONSTRUCTION, MATERIALS, AND RATINGS

13. Construction. Most electronic transformers are small, and for small transformers the shell-type core is usually most suitable because only one coil is required. Figure 8 shows shell-type transformer assemblies.

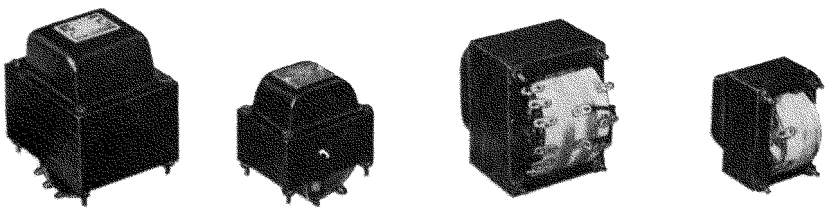

FIG. 8. Transformers with shell-type core.

The magnetic path is divided, half the flux enclosing one side of the coil and half the other. The coil opening is called the window. Between the windows is the core tongue, which is twice as wide as the

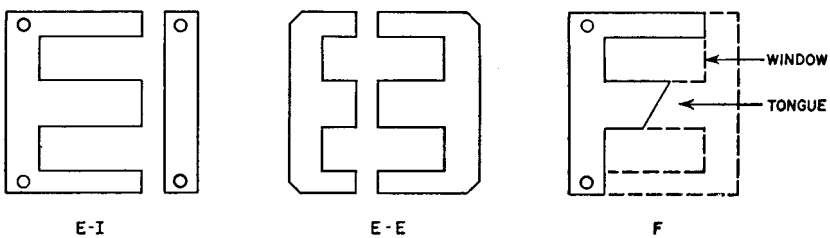

FIG. 9. Shell-type laminations.

iron around the rest of the window. The core is built up of thin laminations to reduce eddy-current losses; typical shapes are shown in Fig. 9. Alternate stacking of the lamination pairs may be used to reduce magnetic reluctance and keep magnetizing current small. To reduce assembly cost, this alternate stacking is sometimes done in groups of

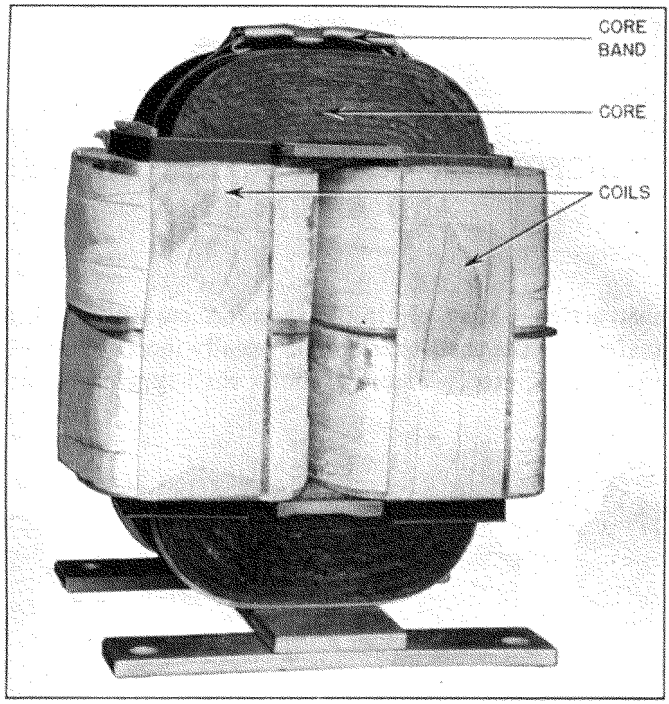

FIG. 10. Core-type transformer.

two or more laminations, with some increase in magnetizing current. A wide range of sizes of shell-type laminations is available. At 60 cycles, common thicknesses are 0.014 in., 0.019 in., and 0.025 in.

Shell-type laminations are made with proportions to suit the transformer. In the E-I shape a scrapless lamination is widely used. Two E's facing each other are first punched, and the punched-out strips are of the right dimensions to form two I's. Then the E's are cut apart. This economy of material is not justified in transformers in which turns per layer, and hence window width, must be reduced relative to window height.

For some applications, the core-type transformer is preferable. In these there is only one magnetic path, but there are two coils, one on each leg of the core. A core-type transformer is shown in Fig. 10, and some core-type laminations in Fig. 11.

Cores wound from continuous steel strip are widely used. One common shape is illustrated in Fig. 12; it is known as the type C core. Steel strip is first wound to the proper build-up on a mandrel. The

wound core is then annealed, impregnated with a bond, and cut in two to permit assembly with the coil. After assembly with the coil, the core is held together with a steel band as in Fig. 10. Several advantages accrue from this construction, which will be discussed in Section 15.

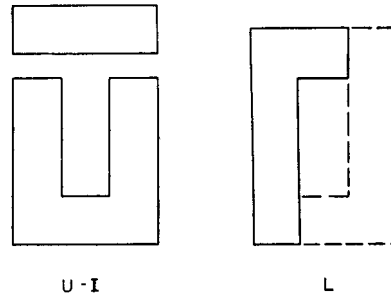

FIG. 11. Core-type laminations.

Typical assemblies using two type C cores are shown in Figs. 13 and 14; they correspond to shell-type laminations. Because it is simpler to assemble a single-core loop, a single core is often used, especially in small sizes. See Fig. 15. In 60-cycle service the laminations are usually stacked alternately to produce an overlapping joint. This is approximated in the type C cores with ground gap surfaces which fit closely together. Either type of core can be used with core gaps; laminations are stacked butting, with no overlap. The desired amount of gap material, such as fish-paper, is inserted between the gap surfaces.

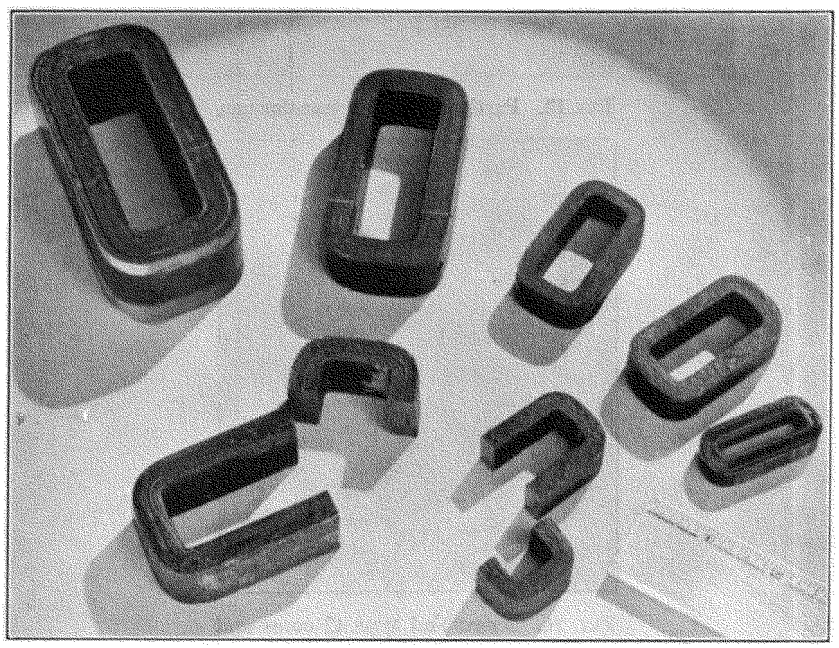

FIG. 12. Type C cores.

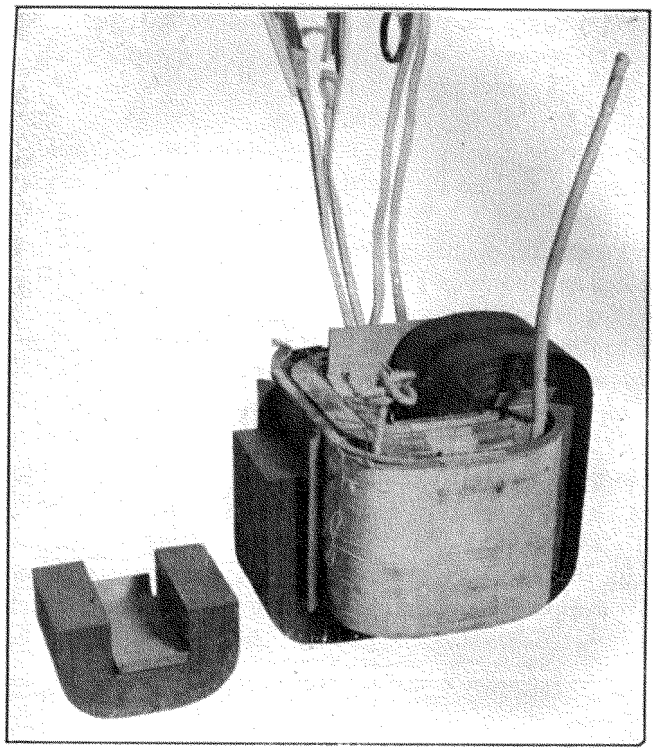

FIG. 13. Partly assembled transformer.

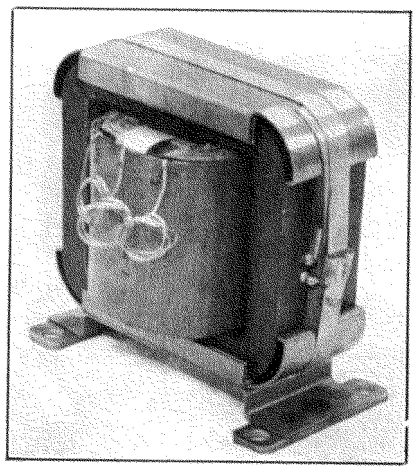

FIG. 14. Assembled type C cores and coil.

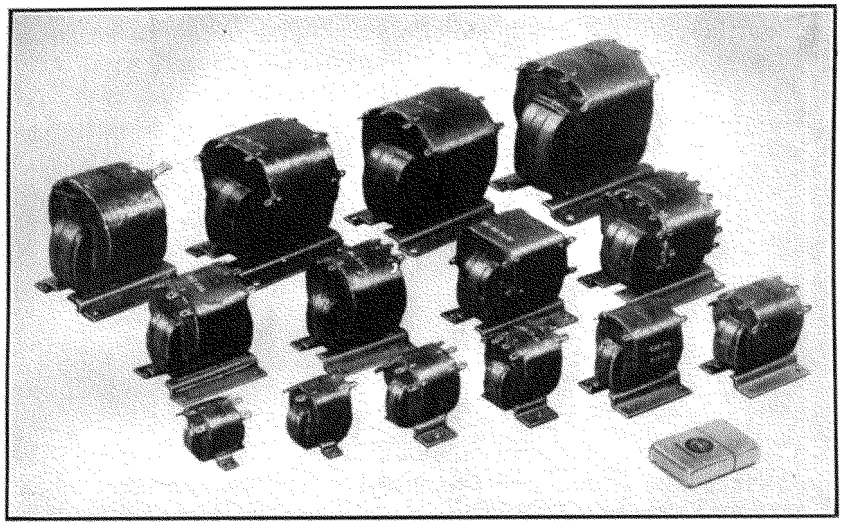

FIG. 15. Single-coil, single-core assemblies.

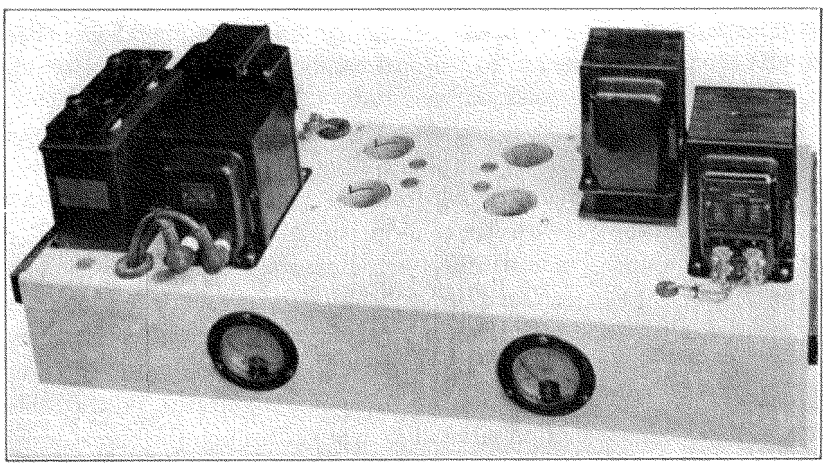

FIG. 16. Transformers mounted on amplifier chassis.

14. Mountings. Both types of cores may be built into neat assemblies with the laminations exposed, and the coils covered by end cases, such as those in the amplifier of Fig. 16. When complete enclosure is desired, assemblies like those in Fig. 17 are used.

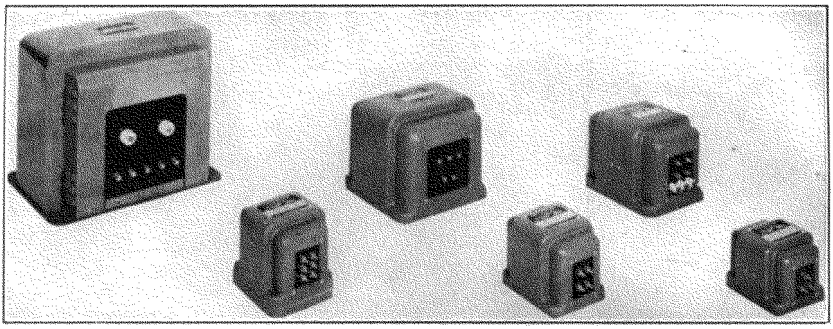

FIG. 17. Fully enclosed transformers.

The degree of enclosure depends on many conditions, among them the following:

(*a*) *Climate.* In a humid climate, especially in the tropics, copper corrodes readily. Transformers containing fine wire may have open circuits soon after exposure to tropical conditions, and it is preferable to seal them against the entry of moisture.

(*b*) *Temperature Rise.* Transformers handling large amounts of power may become hot because of the electrical losses. To seal them in containers imposes additional obstacles to the dissipation of this heat. Fortunately the wire size is large enough to withstand corrosion without developing open circuits. Such units may be of the open type.

(*c*) *Space.* Sealing a transformer usually requires more space than mounting the core and coil directly on the chassis or panel. End cases like those in Fig. 16 do not require much space but do reduce cooling by convection. When air is used to cool other apparatus, power tubes for instance, it is very often circulated near or through the transformer to prevent the coils from overheating.

(*d*) *Voltage.* In high-voltage dry-type transformers, enclosure in a metal case may add to the difficulties of insulating the windings. In oil-filled transformers, a tank is required for the oil and enclosure is thereby provided.

(*e*) *Appearance.* Generally speaking, enclosed transformers are neater than the open type. This fact is given consideration where space is available, especially in broadcast apparatus.

15. Core Materials. Electronic transformers make use of a large variety of core materials. In this chapter, the more useful magnetic properties of several grades of core materials are presented for reference and comparison. To guard against possible ambiguity, definitions of magnetic terms are first reviewed.

Referring to the typical hysteresis loop of Fig. 18, curve OB_m is the manner in which completely unmagnetized steel becomes magnetized by a magnetizing force H gradually increasing up to value H_m. Flux density or induction is not proportional to H but rises more gradually as it approaches H_m, B_m. Once the material reaches this state, it does not retrace curve OB_m if H is reduced. Instead, it follows the left side of the solid-line loop in the direction of the arrow until, with negative H_m, it reaches the maximum negative induction $-B_m$. If H is now reversed, the induction increases as indicated by the right side of the loop, which is symmetrical in that the upper and lower halves are equal in area and have the same shape.

In laboratory tests of magnetic material, the changes in H are made slowly by means of a permeameter. The solid curve of Fig. 18 is then called the *d-c hysteresis loop.* If the changes are made more rapidly, for example at a 60-cycle rate, the loop is wider, as shown by the dotted lines. If a higher frequency is used, the loop becomes still wider, as shown by the dot-dash lines. At any frequency, energy is expended in changing induction from B_m to $-B_m$ and back to B_m; this energy is called the *hysteresis loss* and is proportional to the area of the B-H loop. Increase in loop width with frequency is usually attributed to eddy currents which flow, even in laminated cores, to some degree.

If a closed magnetic core is magnetized to induction B_m and then the magnetizing force completely removed, induction decreases to *residual* induction B_r and remains at this value in the absence of magnetizing force, or for $H = 0$. The value of H required to reduce B to zero is called the *coercive force* (H_c). From Fig. 18 it is evident that B_r and H_c may change with frequency for the same B_m and grade of core material, and the design of transformers and reactors may be affected by the influence of frequency on core steel properties.

According to equation 10, p. 12, the core flux is proportional to effective alternating voltage for a given frequency and number of turns, and so is flux density in a given core. Therefore the largest loop of

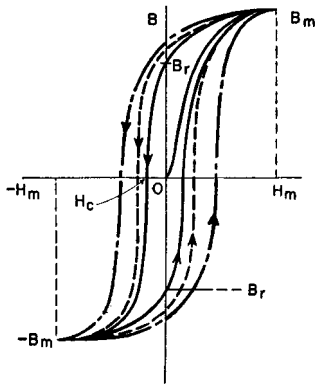

FIG. 18. A-c and d-c hysteresis loops.

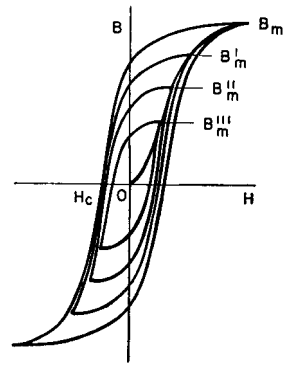

FIG. 19. Normal induction.

Fig. 19 corresponds to a definite effective voltage and frequency, applied across a coil linking a definite core, and magnetizing it to maximum flux density B_m. If effective voltage is reduced 20 per cent a smaller B-H loop results, with lower maximum flux density B'_m. If effective voltage is reduced further, still lower maximum flux density B''_m is reached. The locus of points B_m, B'_m, B''_m, etc., is drawn in Fig. 19, and is called the *normal induction* curve. It is similar in shape to, but not identical with, the *virgin curve* OB_m of Fig. 18. Each time the maximum flux density is lowered, a short time elapses before the new loop is traced each cycle. Thus the loops of Fig. 19 represent symmetrical steady-state or cyclic magnetization at different levels of maximum induction.

A normal induction curve is drawn in Fig. 20. The ratio of B to H at any point on the curve is the *normal permeability* for that value of B. For the maximum flux density B_m, the normal permeability is

$$\mu = B_m/H_m \tag{19}$$

It is the slope of a straight line drawn through the origin and B_m. A similar line drawn tangent to the curve at its "knee" is called the *maximum* permeability and is the ratio $\mu_m = B'/H'$. The slope B_0/H_0 of normal induction at the origin (enlarged in Fig. 20) is the permeability for very low induction B_0; it is called *initial* permeability and is usually much less than μ_m.

Maximum permeability as here defined is really the average slope of the normal induction curve up to induction B'. Actual slope from

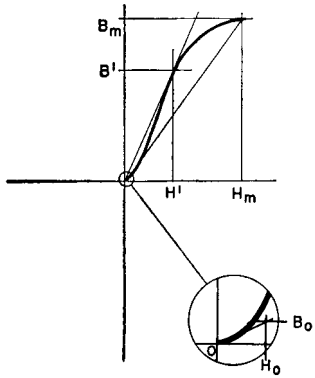

FIG. 20. Normal permeabilities.

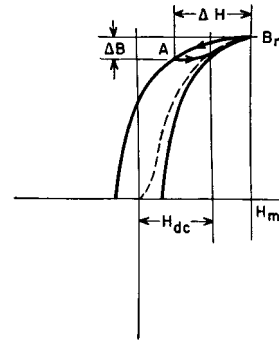

FIG. 21. Incremental permeability.

O to B' is greater at some points than maximum permeability, because the curve is steepest below B'. The slope at any induction is called *differential* permeability.

From inspection of Fig. 19 it will be noticed that, for $H = 0$, the sides of the B-H loop are steeper than any part of the normal induction curve and hence the slopes exceed μ_m. This fact has practical significance in the design of magnetic amplifiers.

In the foregoing, symmetrical magnetization has been assumed. If a core is magnetized with d-c magnetizing force H_{dc} as in Fig. 21, and a-c magnetization ΔH is superimposed, the cyclic magnetization follows a minor loop AB_m. Decreasing induction follows the left side of a major loop whose maximum induction is B_m, down to induction $A = B_m - \Delta B$. Increasing induction follows a line which joins the right side of the major loop. The area of this loop is small, but so is the average slope, or *incremental* permeability. This permeability is important in reactor design. It is defined by

$$\mu_\Delta = \Delta B/\Delta H \tag{20}$$

and is generally smaller than μ_m. The dotted line in Fig. 21 is the normal induction curve, the locus of the tops of minor loops as H_{dc} is decreased.

Returning now to Fig. 19, if H_m is increased, an induction is finally reached at which unit increase of H produces only unit increase in B_m. This is known as *saturation induction* B_s. The value of H at which B_s is first reached is very large compared to H_c for most core materials.

A striking development has been the production of core materials with *rectangular* hysteresis loops. In such materials B_s is reached at small values of H, as shown in Fig. 22. Core material having a rectangular hysteresis loop is especially useful in magnetic amplifiers, and is discussed in Chapter 9.

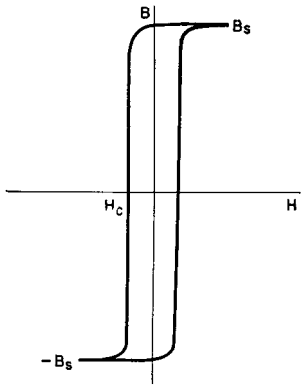

FIG. 22. Rectangular hysteresis loop.

The *volt-amperes per pound* or apparent core loss (P_a) of a magnetic material is the product of rms induced voltage and rms exciting current drawn from the source when a pound of the material is subjected to sinusoidally varying induction of a specified maximum value B_m and of a specified frequency f. Exciting current is non-sinusoidal, as can be seen from Fig. 5, Chapter 1. The power component of P_a is the core loss P_c. The reactive component is usually the larger and is called VARS per pound. It is related to permeability in the following way:

Let it be assumed that for conditions B_m, H_m in a core the magnetizing current is approximately sinusoidal, of effective value I_M, drawn from a supply of frequency f and effective voltage E. If we combine

1. Open-circuit inductance $L_e = E/2\pi f I_M$ (21)

$$= \frac{B_m A_c N}{\sqrt{2}\, I_M \times 10^8} \tag{22}$$

2. Magnetizing force $H_m = \dfrac{0.4\pi N I_M \sqrt{2}}{l_c}$ (23)

3. VARS/lb $= \dfrac{E I_M p}{A_c l_c}$ (24

convert to inches, and put density $p = 0.27$ lb/in.^{3}, then

$$\mu = \frac{152 f B_m^2}{\text{VARS/lb} \times 10^8} \tag{25}$$

At 60 cycles, $\mu = \dfrac{B_m^2}{11{,}000\ \text{VARS/lb}}$. Because of the non-linearity of I_M, this equation is approximate. Moreover, there is no allowance for core gap.

In usual electronic transformer practice, it is necessary to avoid reaching saturation flux densities, because high exciting currents pro-

duce high winding *IR* drops, high losses, low efficiency, and large size. Curves of induction and core loss are available from manufacturers of laminations. Grades and thickness are designated by numbers such as Armco Trancor M15 and Allegheny Transformer A. A wide choice of silicon-steel laminations is available in 0.014-in., 0.019-in., and 0.025-in. thicknesses, with silicon content of approximately 3 to 4%,

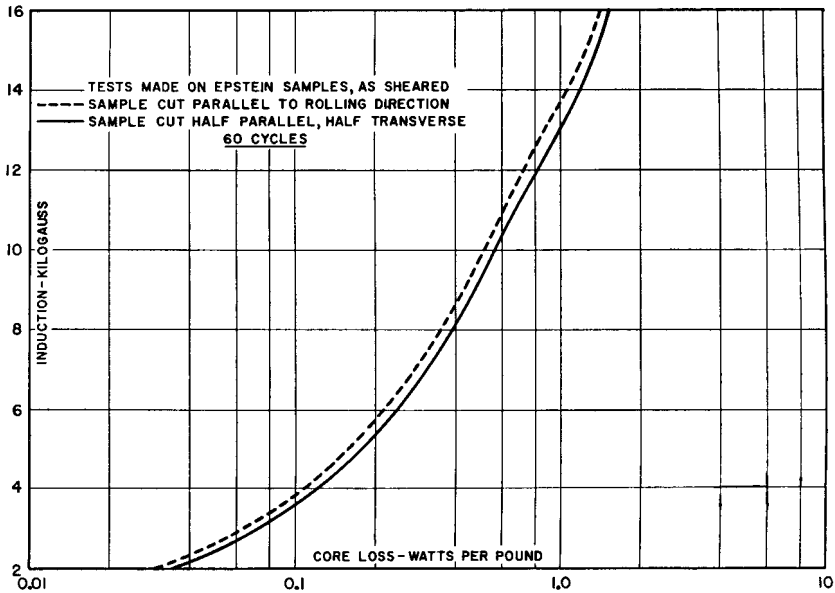

FIG. 23. Core loss at high induction. Armco Trancor M15 grade, 29 gage.

and with core losses ranging from 0.6 to 1.2 watts per pound at 10,000 gauss, 60 cycles (64,500 lines per square inch). Figures 23 and 24 are core-loss and exciting va/lb for a widely used grade of electronic transformer core steel at 60 cycles.

Much work has been done in developing grain-oriented core materials. These materials have a composition similar to that of older, non-oriented core material, but grains in the material are oriented by cold-rolling in the direction illustrated by Fig. 25. Magnified sections of laminations are shown in this figure; (*a*) shows the random directions of "easy" magnetization in grains of non-oriented silicon steel. When magnetic flux is established in the lamination, the grains must be aligned in the same direction, as in Fig. 25(*b*). If the grains are already oriented in this direction during the rolling process, much

smaller magnetizing force is required to produce the desired flux. Coercive force and hysteresis loss are smaller than in non-oriented steel; permeability is greater, and so is B_r, so that the rectangular loop of Fig. 22 is approached in grain-oriented steel.

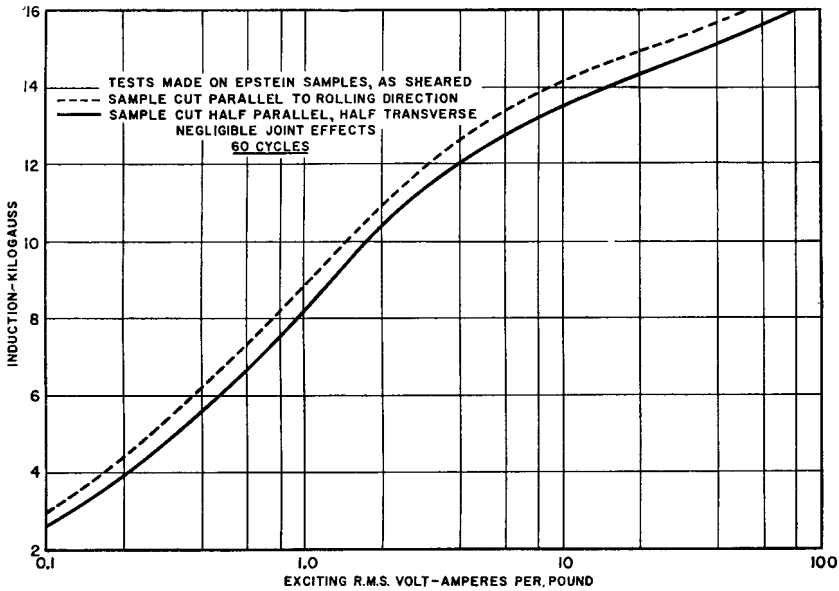

FIG. 24. Exciting rms volt-amperes per pound, Armco Trancor M15 grade, 29 gage.

Grain-oriented core materials are of two major types: silicon-steel and nickel-iron alloy. Electronic power transformers (i.e., plate and filament supply transformers) formerly comprised only hot-rolled silicon-steel cores. The development of grain-oriented silicon steel has had a marked effect on size and performance of such transformers. To

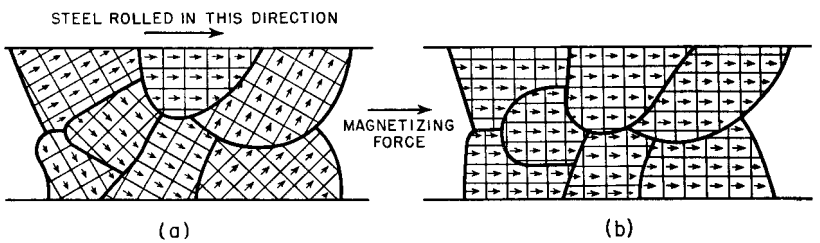

FIG. 25

illustrate this effect, a comparison is made below between the older non-oriented steel (termed, for simplicity, silicon steel) and Hipersil, a cold-rolled steel in which grain orientation is carried out to a high degree. If core flux flows in the grain-oriented direction, high core inductions may be realized. Type C cores fulfill this requirement, because the strip is wound in the same direction as the flux path.

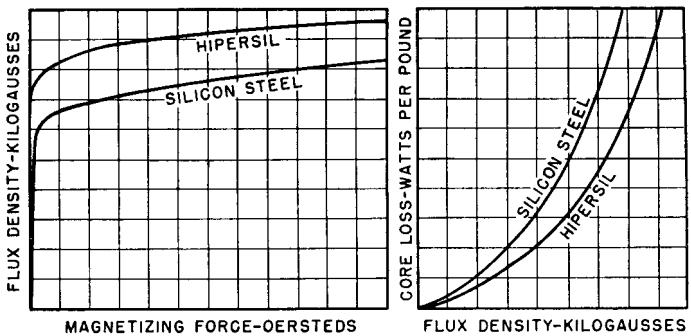

FIG. 26. Induction and core-loss curves of silicon steel and Hipersil at 60 cycles.

The material is rolled in three major thicknesses:

No. 29 gage (about 12 to 14 mils thick) for frequencies up to 400 cycles.

5 mils thick for frequencies 400 cycles and higher.

2 mils thick for frequencies in the low and medium r-f bands.

Probably the most remarkable property of this material is its high saturation point. In Fig. 26 the comparison is given in terms of a hypothetical 60-cycle working induction using high-grade, conventional silicon steel. If this value is assumed to be 100 per cent, the induction obtained with grain-oriented steel is 130 to 150 per cent, with no increase in magnetizing force. Another way of expressing this improvement is shown in Fig. 27 as a comparison of the permeability of the two steels. The permeability of grain-oriented steel is much higher at the maximum point, and has the same percentage increase as in Fig. 26 for normal working inductions. Iron loss in Hipersil is less than in silicon steel, as Fig. 26 shows. The decrease in iron loss is chiefly due to a reduction in hysteresis loss; the eddy-current loss is less affected by grain orientation. Future comparisons may widen these differences.

The increase in induction is beneficial in several ways. First, it permits a reduction of core area for the same magnetizing current. Second, it results in a smaller mean length of turn and thus in a reduction in the amount of copper needed. In distribution and power transformers, for maximum benefit the iron and copper losses are reproportioned. In small electronic transformers, the iron loss is usually a small part of the total loss, and the reduction in copper loss is of greater significance. Within certain limits, the sum of the two losses determines the size of a transformer, and here the usefulness of grain-oriented steel becomes most apparent.

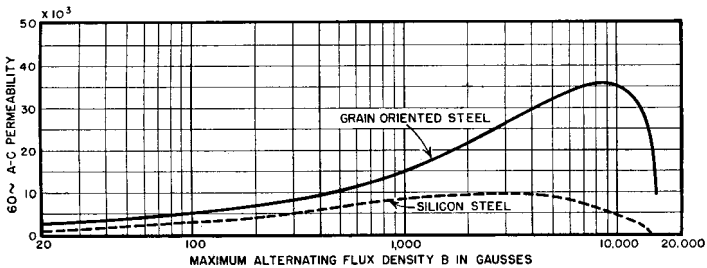

FIG. 27. Permeability of silicon and grain-oriented silicon steel.

The foregoing was written with 60-cycle applications particularly in mind. At higher power supply frequencies, such as the 400- and 800-cycle supplies encountered in aircraft and portable equipment, the results are somewhat different. The decrease in iron loss is not so marked, because the eddy current loss forms a larger proportion of the total iron loss. However, it is usual practice to use thin-gage laminations at these frequencies, and much better space factor can be obtained in wound cores than in stacked cores. The increase in permeability is just as effective in these higher frequency applications as at 60 cycles. The net result is a smaller transformer than was formerly possible, though for different reasons and in different proportions.

Reactors which carry direct current are usually smaller when made with grain-oriented than with ordinary silicon steel. At low voltages, where low inductions are involved, grain-oriented steel has greater incremental permeability, and maintains it at high flux densities also. Consequently, a reduction of 50 per cent in weight is often feasible.

Grain-oriented silicon steel does not replace high nickel-iron alloys for audio transformers, when they work at low inductions, and with little or no direct current. Some nickel-iron alloys have higher permea-

bility at low flux densities, and their use for this purpose continues. But at high inductions, or where considerable amounts of direct current are involved, grain-oriented silicon steel is used. Lower distortion, extended frequency range, or small size is the result, and sometimes a combination of all three occurs.

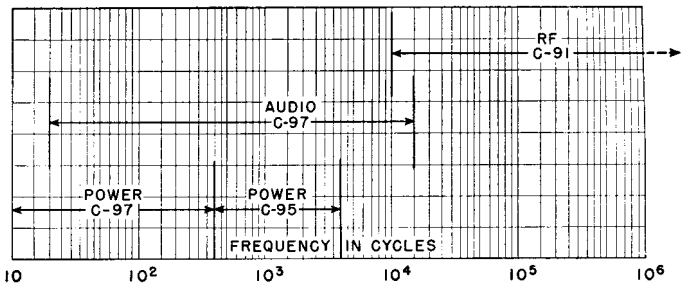

FIG. 28. Use of Hipersil in various frequency zones.

Hipersil can be used for transformers in various applications in the low and medium r-f bands, at power levels ranging up to hundreds of kilowatts. The same is true of video and pulse transformers, which may be regarded as covering an extended frequency range down into the audio range and up into the medium r-f range. Such transformers are grouped rather loosely together as r-f transformers in the diagram shown in Fig. 28. In this figure the several classifications, r-f, audio, and power transformers, are shown with respect to their frequency ranges and the approximate gage of the material used for these ranges. The gage is indicated by the symbol number in Table II.

TABLE II. HIPERSIL CORE DATA

Hipersil	Thickness	Typical Hipersil Space Factor *	Typical Space Factor for Silicon Steel *
C-97	0.013 in.	95%	90%
C-95	0.005 in.	90%	80%
C-91	0.002 in.	85%	70%

* Refers to percentage of core volume occupied by metal. The Hipersil figure is for type C cores, and the silicon steel figure is for punched laminations.

Core-loss and exciting va/lb for 29-gage Hipersil are plotted in Figs. 29 and 30. Joint reluctance is neglected in Fig. 30.

An example of specialized core materials is the development of a new grain-oriented silicon steel especially for weight reduction in com-

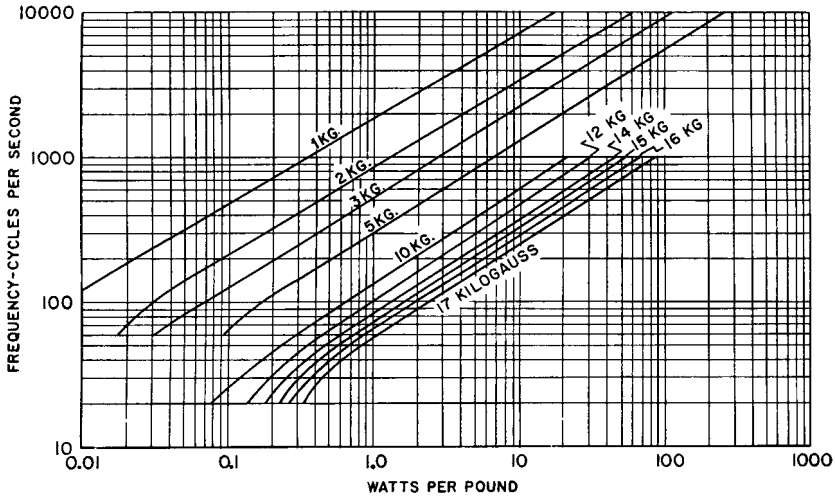

FIG. 29. Core loss in C-97 Hipersil cores (29 gage).

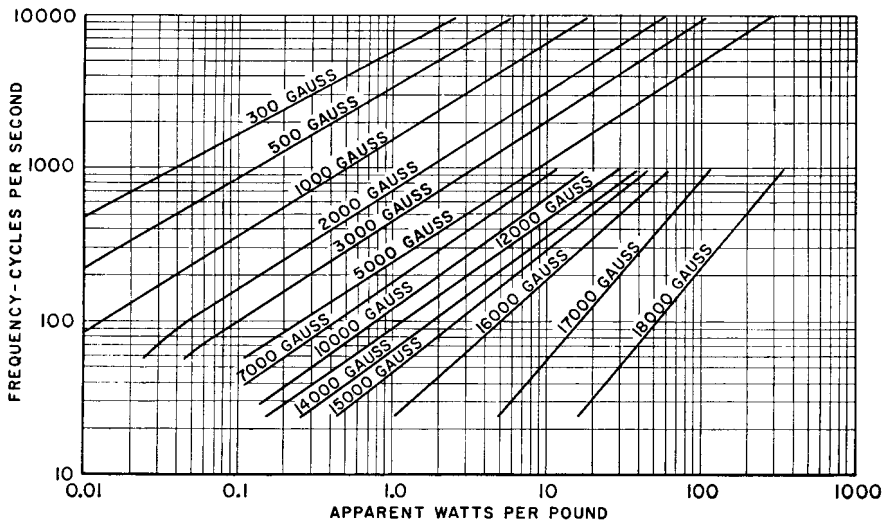

FIG. 30. A-c excitation curve, typical data. C-97 Hipersil cores (29 gage).

ponents for 400-cycle applications. By means of large reduction in core loss at 400 cycles and still larger increase in permeability at high induction, a 0.004-in.-thick core material was developed which operates satisfactorily in many instances at 17,000 gauss, 400 cycles. As a result, 40 per cent of the weight was eliminated in transformers designed to take advantage of the 0.004-in-thick core material. At lower inductions the core loss of this material tends to be larger than in the older 0.005-in.-thick material. Hence it is only where 17,000 gauss is a practicable working induction that the weight reduction is possible.

Grain-oriented steel alloys of approximately 50% nickel content are extensively used in saturable reactors. Electrical properties of cores wound from these materials are spoiled if the strip is bent or constrained mechanically. Usually the nickel-alloy strip is wound into cores in the form of a toroid, annealed, and enclosed in an insulating box to protect it from damage. Special machinery is then used to wind turns of wire around the core. With the proper precautions, it is possible to realize the advantages of a very rectangular, narrow hysteresis loop in the finished reactor. These properties have been found useful also in pulse transformers, and are discussed in Chapters 9 and 10 in detail.

In audio- or higher-frequency low-loss reactors or transformers, it may be desirable to use powdered iron or nickel-alloy cores. These cores are made of finely divided particles, coated with insulating compound, which separates them and introduces many fine air gaps in the magnetic path. The cores are molded into various shapes suitable for the application. Effective permeability of such cores is reduced to a figure much lower than that of laminations made from the same material.

Magnetic ferrites likewise are used at higher frequencies. These substances are characterized by high resistivity so that neither laminations nor powder particles are necessary to reduce eddy-current loss. Cores are molded and sintered at high temperature. After sintering they have ceramic hardness but relatively low Curie temperature.[1] Ferrites are useful at very high frequencies.

Some of the principal core materials are listed in Table III.

16. Windings. Current density in the winding copper is sometimes estimated for design purposes by rules such as 1,000 cir mils per amp. These rules are useful in picking out a first choice of wire size for a given current requirement but should not be regarded as final. In-

[1] The temperature at which a ferric substance loses its intrinsic permeability.

TABLE III. CORE MATERIALS

Approximate Description	Trade Names	Typical Maximum Permeability μ_m	Maximum Operating Flux Density B_m (gauss)	Coercive Force D-C Loop (oersteds)	Chief Uses
Silicon steel	Transformer Trancor M15 Power 58	8,500	12,000	0.5	Small power and voice frequency audio transformers
Grain-oriented silicon steel	Hipersil Trancor 3X	30,000	17,000	0.4	Larger sizes of power and wide-range audio transformers; low-frequency r-f transformers; saturable reactors
50% nickel steel	Hipernik Allegheny Electric Metal Nicaloi	50,000	10,000	0.06	Small, wide-range audio transformers and reactors (may have small d-c induction)
50% nickel steel, special heat treatment	Conpernik	1,400	*		Extremely linear and low-loss transformers
Grain-oriented 50% nickel steel	Hipernik V Orthonol Orthonik Deltamax Permenorm	50,000	14,500	0.15	Saturable reactors
80% nickel steel	Permalloy Mumetal Hymu	100,000	6,000	0.05	Small or wide-range audio transformers (no d-c induction)
80% nickel steel, special heat treatment	Supermalloy	200,000	6,000	0.01	Very small or wide-range transformers (no d-c induction)
Powdered iron	Crolite Polyiron	125	*		Wave filter reactors; low and medium r-f transformers
Ferrite	Ceramag Ferramic Ferroxcube	1,000	2,000	0.2	Sweep circuit transformers; r-f transformers and reactors

* These materials are used for low flux density, low-loss applications.

stead, the temperature rise, regulation, or other performance criterion should govern the final choice of wire size. Regulation is calculated as in Section 11, and temperature rise as in Sections 22 and 23. In Fig. 31 the circular mils per ampere are plotted for small enclosed dry-type transformers with Hipersil cores and a winding temperature rise of 55 centigrade degrees; it can be seen to vary appreciably over this range of sizes.

Space occupied by the wire depends on the wire insulation as well as on the copper section. This is especially noticeable in small wire sizes. Table IV gives the bare and insulation diameters for several common kinds of wire and Table V the turns per square inch of wind-

ing space. Space usually can be saved by avoiding cotton or silk wire covering, and instead using enameled wire with paper layer insulation as in Fig. 32. Thickness of layer paper may be governed by layer voltage; it is good practice to use 50 volts per mil of paper. In coils where layer voltage is low, the paper thickness is determined by the mechanical strength necessary to produce even layers and a tightly

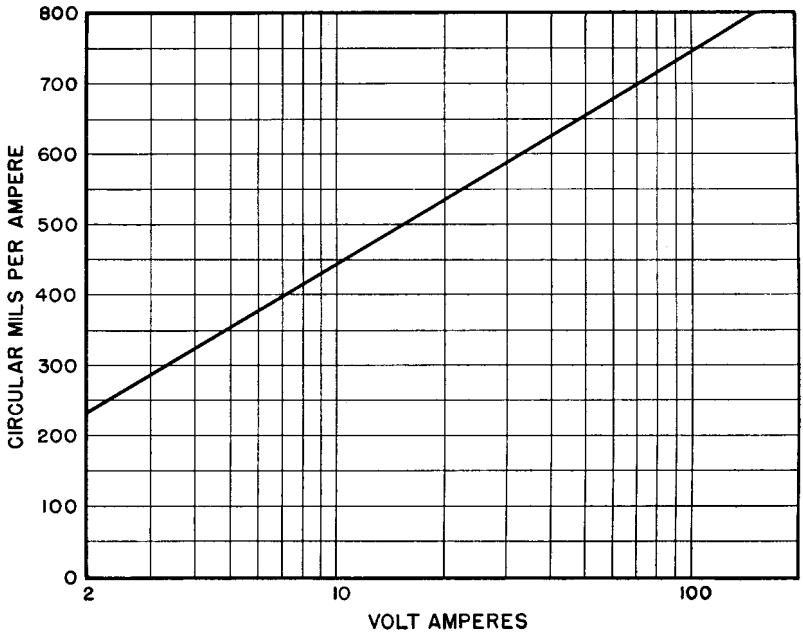

FIG. 31. Wire size in windings of small enclosed 60-cycle transformers.

wound coil. Table VI gives the minimum paper thickness based on this consideration.

Space factor may refer to linear spacing as across a layer, or to the total coil section area. It is more convenient to use linear space factor in designing layer-wound coils and area space factor in random-wound coils. The values in each case depend largely on the method of winding. For example, it is possible to wind No. 30 enameled wire with 97 per cent linear space factor by hand, but with only 89 per cent on an automatic multiple-coil winding machine. (See Fig. 33.) Moreover, values of space factor vary from plant to plant. An average for multiple-coil machines is given in Table VI.

TABLE IV. INSULATED WIRE SIZES

B & S Gage	Bare Diameter	Diameter of Insulated Wire								Area in Circular Mils	Ohms per 1000 Feet at 25°C	Feet per Ohm at 25°C	Pounds per 1000 Feet
		Single Enamel	Double Enamel	Single Cotton Enamel	Single Silk Enamel	Single Cotton	Double Cotton	Single Silk	Double Silk				
44	.0020	.0023								4.00	2,700	.3850	.012
43	.0022	.0025								4.84	2,150	.4670	.015
42	.0025	.0029								6.25	1,700	.6050	.019
41	.0028	.0032								7.84	1,350	.7630	.024
40	.0031	.0036	.0039							9.61	1,103	.9550	.030
39	.0035	.0040	.0044							12.25	864	1.204	.038
38	.0040	.0046	.0050							16.00	659	1.519	.048
37	.0045	.0051	.0055							20.30	522	1.915	.060
36	.0050	.0057	.0061	.0095	.0075	.0090	.0130	.0070	.0090	25.00	424	2.414	.076
35	.0056	.0064	.0067	.0102	.0082	.0096	.0136	.0076	.0096	31.40	338	3.045	.096
34	.0063	.0072	.0077	.0109	.0089	.0103	.0143	.0083	.0103	39.70	266	3.839	.120
33	.0071	.0080	.0085	.0117	.0097	.0111	.0151	.0091	.0111	50.40	210	4.841	.152
32	.0080	.0090	.0095	.0127	.0107	.0120	.0160	.0100	.0120	64.00	165	6.105	.19
31	.0089	.0100	.0104	.0137	.0117	.0129	.0169	.0109	.0129	79.20	134	7.698	.24
30	.0100	.0111	.0117	.0148	.0128	.0140	.0180	.0120	.0140	100	106	9.707	.31
29	.0113	.0125	.0130	.0162	.0142	.0153	.0193	.0133	.0153	128	83.1	12.24	.38
28	.0126	.0139	.0145	.0175	.0155	.0166	.0206	.0146	.0166	159	66.4	15.43	.48
27	.0142	.0155	.0161	.0192	.0172	.0182	.0222	.0162	.0182	202	52.5	19.46	.61
26	.0159	.0172	.0178	.0210	.0190	.0199	.0239	.0179	.0199	253	41.7	24.54	.77
25	.0179	.0193	.0200	.0234	.0211	.0222	.0262	.0199	.0219	320	33.0	30.95	.97
24	.0201	.0216	.0222	.0256	.0233	.0244	.0284	.0221	.0241	404	26.2	39.02	1.23
23	.0226	.0242	.0247	.0282	.0259	.0269	.0309	.0246	.0266	511	20.7	49.21	1.54
22	.0253	.0271	.0278	.0310	.0287	.0296	.0336	.0273	.0293	645	16.4	62.05	1.95
21	.0285	.0302	.0310	.0344	.0319	.0330	.0370	.0305	.0325	812	13.0	78.25	2.45
20	.0320	.034	.0345	.0385	.0355	.0370	.0410	.0340	.0360	1,020	10.3	98.66	3.09
19	.0359	.038	.0387	.0425	.0395	.0409	.0449	.0379	.0399	1,300	8.14	124.4	3.89
18	.0403	.042	.0431	.0469	.0439	.0453	.0493	.0423	.0443	1,600	6.59	156.9	4.9
17	.0453	.047	.0481	.0521	.0491	.0503	.0543	.0473	.0493	2,030	5.22	197.8	6.2
16	.0508	.053	.0536	.0576	.0546	.0558	.0608	.0528	.0548	2,600	4.07	249.4	7.8
15	.0571	.059	.0605	.0640	.0610	.0621	.0671	.0591	.0611	3,250	3.26	314.5	9.9
14	.0641	.066	.0675	.0711	.0681	.0691	.0741	.0661	.0681	4,100	2.58	396.6	12.4
13	.0719									5,180	2.00	499.3	15.7
12	.0808									6,530	1.59	629.6	19.8
11	.0907									8,235	1.26	794.0	24.9
10	.1019									10,380	1.00	1,001	31.4
9	.1144									13,090	.792	1,262	40.0
8	.1285									16,510	.628	1,592	50.0

TABLE V. TURNS PER SQUARE INCH OF INSULATED WIRE

B & S Gage	Single Enamel Wire	Double Enamel Wire	Single Cotton Enamel Wire	Single Silk Enamel Wire	Single Cotton-Covered Wire	Double Cotton-Covered Wire	Single Silk-Covered Wire	Double Silk-Covered Wire
42	119,000							
41	96,000							
40	77,000	66,200						
39	62,400	51,800						
38	47,300	40,000						
37	38,400	33,100						
36	30,900	26,900	11,100	17,900	12,350	5,920	20,400	12,350
35	24,500	22,300	9,600	14,900	10,900	5,430	17,200	10,900
34	19,300	16,900	8,430	12,700	9,430	4,900	14,500	9,430
33	15,600	13,900	7,280	10,650	8,130	4,380	12,100	8,130
32	12,350	11,100	6,210	8,740	6,940	3,900	10,000	6,940
31	10,000	9,260	5,330	7,300	5,900	3,510	7,780	5,900
30	8,180	7,300	4,580	6,100	5,100	3,090	6,940	5,100
29	6,430	5,920	3,810	4,950	4,270	2,760	5,670	4,270
28	5,200	4,770	3,280	4,170	3,640	2,360	4,690	3,640
27	4,170	3,880	2,720	3,390	3,030	2,080	3,810	3,030
26	3,380	3,160	2,270	2,780	2,520	1,940	3,120	2,520
25	2,690	2,500	1,820	2,240	2,080	1,460	2,530	2,080
24	2,150	2,030	1,530	1,850	1,690	1,230	2,050	1,720
23	1,710	1,650	1,260	1,490	1,380	1,050	1,650	1,420
22	1,370	1,300	1,045	1,220	1,140	883	1,345	1,160
21	1,100	1,045	846	925	915	729	1,075	943
20	860	850	675	793	730	595	862	836
19	693	668	555	640	597	495	700	628
18	568	540	455	518	490	412	563	510
17	455	432	368	417	395	340	450	412
16	357	350	303	338	320	270	360	335
15	288	273	244	270	260	222	287	268
14	230	220	198	216	210	182	229	222
13	179	176						
12	143	141						
11	114	113						
10	90	90						
9	72	72						
8	57	57						

Mean length of turn must be calculated for a coil in order to find its resistance in ohms. This may be found by referring to the side view of Fig. 32. Note that there is a small clearance space between core

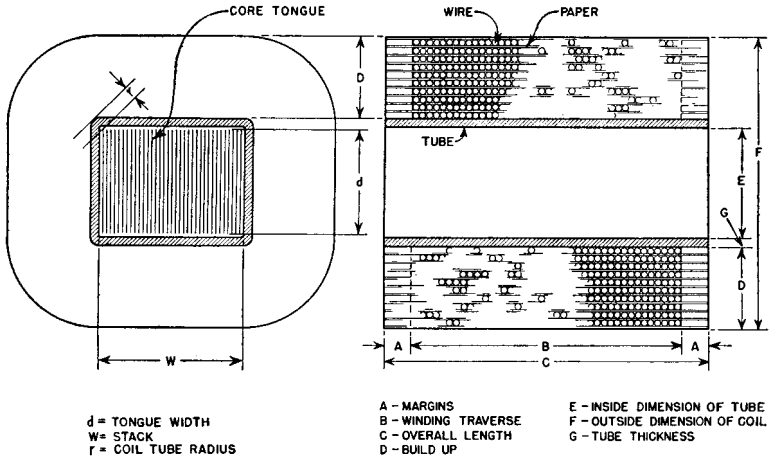

FIG. 32. Paper-insulated coil.

and coil form or tube. Let d be the core tongue and w the stack. Suppose there are several concentric windings. The length of mean turn of a winding V at distance r from the core and having height D, is

$$MT = 2w + 2d + 2\pi\left(r + \frac{D}{2}\right)$$

$$= 2(w + d) + \pi(2\Sigma D + D) \tag{26}$$

where ΣD is the sum of all winding heights and insulation thicknesses between winding V and the core.

The mean turn of the winding U just below V ordinarily is calculated before that of winding V. This fact simplifies the calculation of winding V, the mean turn of which is

$$MT_V = MT_U + \pi(D_U + D_V + 2c) \tag{27}$$

where c is the thickness of insulation between U and V.

Allowance must be made, with many coil leads, for bulging of the coil at the ends and consequent increase of mean turn length.

The placement, insulation, and soldering of leads constitute perhaps the most important steps in the manufacture of a coil. When coils

TABLE VI. PAPER-INSULATED COIL DATA

(Courtesy Phelps-Dodge Copper Products Corp.)

B & S Gage	Layer Insulation	Turns per Inch	Space Factor
44	.0005″	369	85%
43	.0005″	340	85%
42	.0005″	304	85%
41	.0007″	265	85%
40	.0007″	239	86%
39	.0007″	215	86%
38	.001″	193	87%
37	.001″	170	87%
36	.001″	155	87%
35	.001″	140	88%
34	.001″	124	88%
33	.0013″	110	88%
32	.0013″	98	88%
31	.0015″	88	88%
30	.0015″	80	89%
29	.0015″	71	89%
28	.0015″	64	89%
27	.0022″	57	89%
26	.0022″	52	89%
25	.0022″	47	90%
24	.0022″	42	90%
23	.005″	37	90%
22	.005″	33	90%
21	.005″	30	90%
20	.005″	26	90%
19	.007″	23	90%
18	.007″	21	90%
17	.007″	19	90%
16	.010″	17	90%
15	.010″	15	90%
14	.010″	13	90%
13	.010″	12	90%
12	.010″	10	90%
11	.010″	9	90%
10	.010″	8	90%

are wound one at a time, the leads can be placed in the coil while it is being wound. The start lead may be placed on the coil form, suitable insulation may be placed over it, and coil turns may be wound over the insulation. Tap leads can be arranged in the same way. Finish leads must be anchored by means of tape, string, or yarn, because

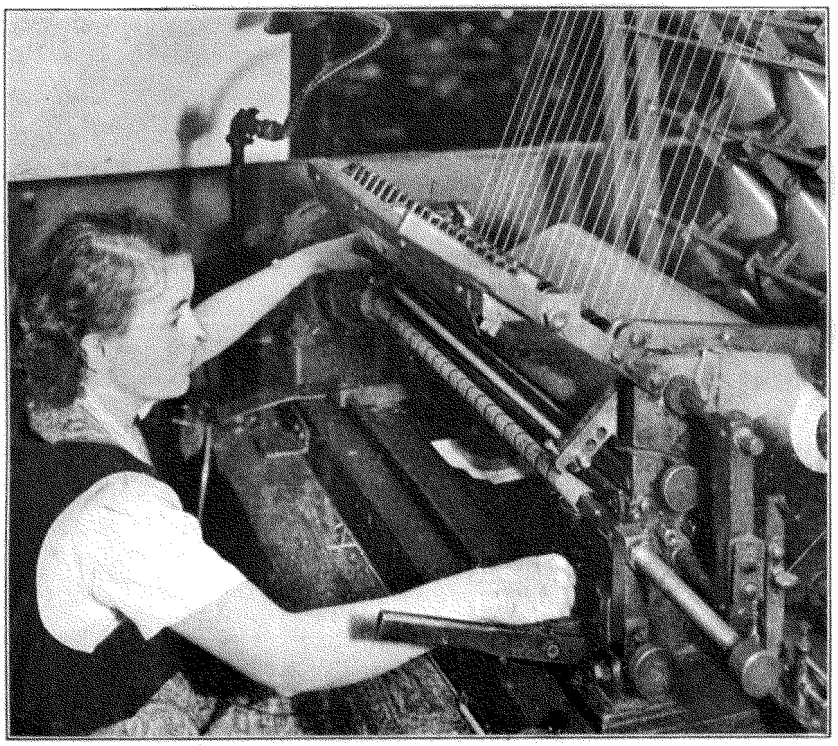

FIG. 33. Winding 20 coils in multiple machine: layer paper at right.

there are no turns of wire to wind over them. Typical lead anchoring is shown in Fig. 34.

In multiple-wound coils, the leads must be attached after the coils are wound. Extra wire on the start turn is pulled out of the coil and run up the side as shown in Fig. 35, with separator insulation between wire extension and coil. Outer insulation covers the wire extension up to the lead joint. A pad of insulation is placed under the joint, and one or more layers of insulation, which insulate and anchor the joint, are wound over the entire coil and the lead insulation. Electrical-grade

scotch tape is widely used for anchoring leads. It is important to avoid corrosive adhesives.

Leads should be large enough to introduce only a small amount of voltage drop and should have insulation clearances adequate for the test voltage. These clearances can be found as explained in Section 19.

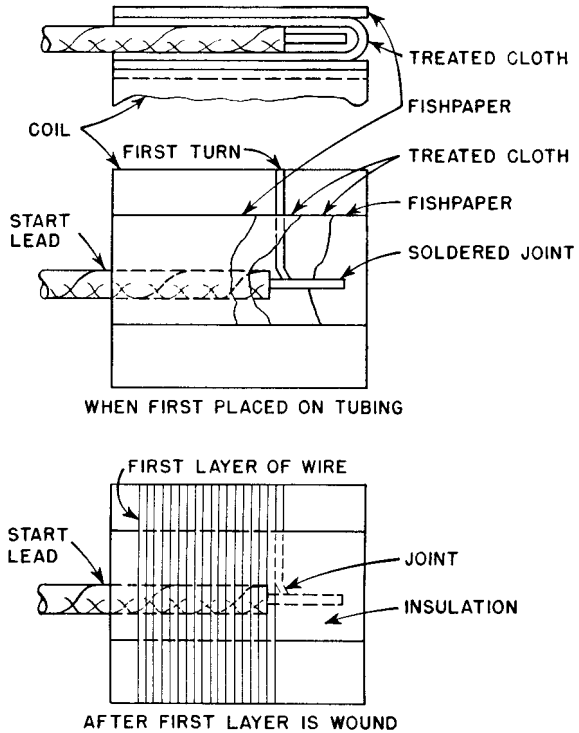

FIG. 34. Start-lead insulation in hand-wound coils.

In high-voltage transformers it would often be possible to seal the windings if there were no leads; hence lead placement calls for much care and skill. Leads and joints should also be mechanically strong enough to withstand winding, impregnating, and handling stresses without breakage.

17. Insulation. Three classes of insulation are used in dry-type transformers. Class A insulation is organic material such as paper, cotton, silk, varnish, or wire enamel. Class B insulation is mica, asbestos, glass, porcelain, or other inorganic material with organic binders such as varnish for embedding the insulation. A small amount of

other class A material is permissible in a class B coil "for structural reasons," but it should be kept to a minimum.

In general, the vital difference between these classes of insulation is one of operating temperature. Glass-covered wire is preferable to asbestos for space reasons; it is available in approximately the same dimensions as cotton-covered wire. Built-up mica is the usual insulation wrapper material. With special bonds it is flexible enough to

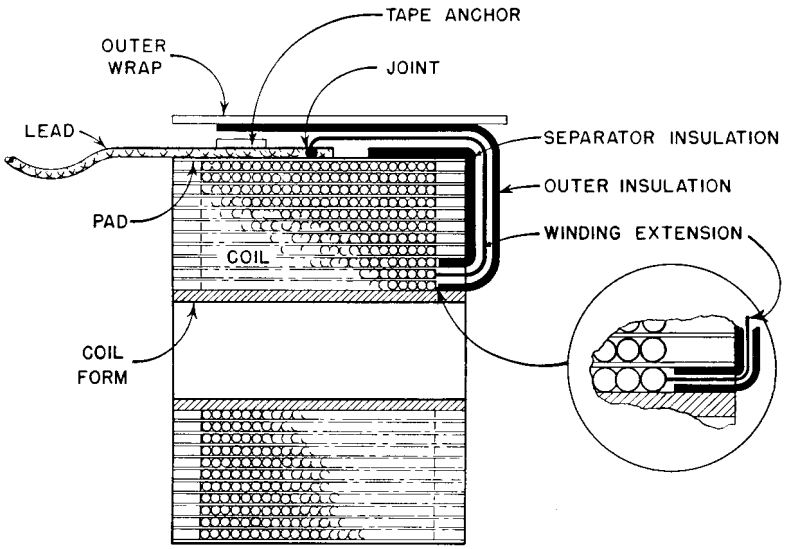

FIG. 35. Start-lead insulation in multiple-wound coils.

wind over coils or layers of wire. Stiff mica plate for lead insulation and mica tubing for coil forms are usually bonded with heat-resistant varnish. Class B insulating material is more expensive than class A and is used only when other advantages outweigh the cost.

The necessity for small size in aircraft or mobile apparatus is continually increasing the tendency to use materials at their fullest capabilities. As size decreases, the ability of a transformer to radiate a given number of watts loss also decreases. Hence, it operates at higher temperature. Transformers for 400- and 800-cycle power supplies can be made in smaller overall dimensions by using class B insulation (see Section 20). As a result, from 30 to 50 per cent decrease in size (as compared with class A insulation), in addition to increased ability to withstand extremes of ambient temperature, humidity, and altitude, is obtained. Class B insulation is thus of special importance in

aircraft apparatus. Usually at 60 cycles enough room is available to use class A insulation, but mica may be used to reduce the size of high-voltage units.

A third class of insulation is the *silicones,* organic silicates with remarkable thermal and mechanical properties. These materials are coming into use at operating temperatures approaching 200°C. Silicone-treated cloth, silicone rubber, and silicone varnish are already in use. Under development are silicone wire enamel and silicone-bonded mica. They are generally designated as class H insulation.

For apparatus having long service life, AIEE Standard 1 limits the "hottest spot" temperature of impregnated [1] coils as follows:

Class A insulation	105°C
Class B insulation	130°C
Class H insulation	200°C

Life test data are plotted in Fig. 36 for class A and class B insulation. The temperature scale is special, based on T. W. Dakin's data,[2] showing that insulation life is proportional to the reciprocal of absolute temperature. The two lines indicate how operating temperature may be increased for a given life when class B insulation is used. Equal life is obtained when class A insulation is operated at 105°C maximum (40°C ambient, 55°C rise, 10°C hottest spot gradient), and when class B insulation is operated at 130°C maximum (40°C ambient, 80°C rise, 10°C hottest spot gradient). Intermittent load temperatures may be high for short periods. These periods are additive. For example, class A insulation has approximately the same life whether it is operated at 115°C continuously or half the time at 123°C and half the time at 25°C. Figure 36 shows only the influence of temperature on insulation life. Life is further reduced by moisture, vibration, and corona. It is therefore important that insulation be protected against damage caused by all these factors. Such protection is discussed in Section 20.

18. Dielectric Strength. The usual figure given for dielectric strength is the breakdown value in rms volts at 60 cycles in a 1-minute test. It is not possible to operate class A insulation anywhere near this value because of the cellular structure of all organic materials. Even after these materials are treated with varnish, many small holes exist throughout a coil structure which ionize and form corona at voltage

[1] For the definition of impregnation, see Section 20.

[2] See "Electrical Insulation Deterioration Treated as a Chemical Rate Phenomenon," by T. W. Dakin, *Trans. AIEE, 67,* 113 (1948).

far below breakdown. With class A insulation (organic materials), the designer must be governed more by resistance of the insulation to corona over a long period than by breakdown strength of the insulation in a 1-minute test. For example, a 20-mil thickness of treated cloth will withstand 10,000 volts for 1 minute. However,

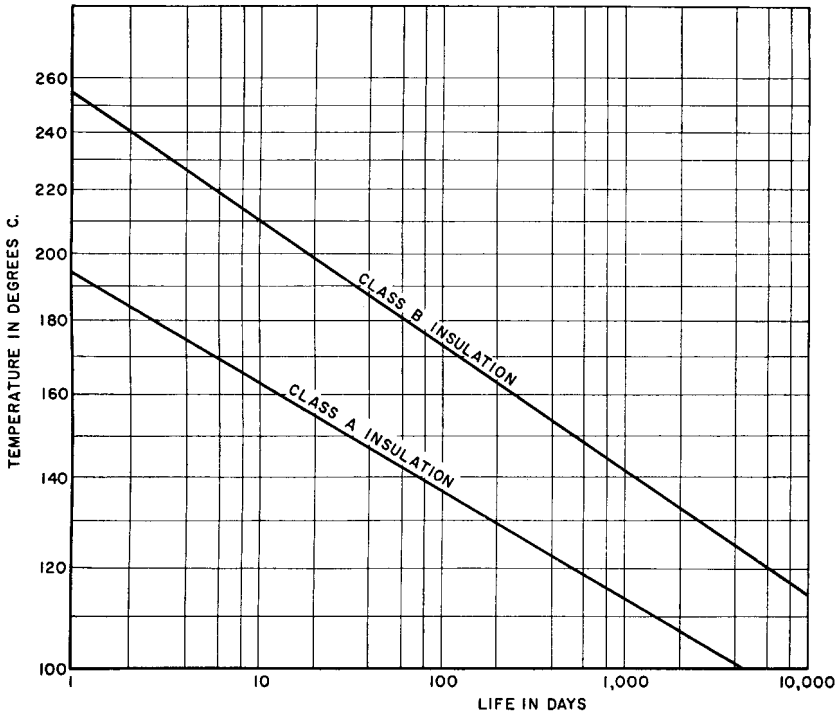

FIG. 36. Approximate life expectancy of electrical insulation.

corona starts at 1,250 volts, and operation at any higher voltage would puncture the insulation in a few weeks. It is much wiser to keep a reasonable margin, say 20 to 30 per cent, below the corona limit than to use a fraction of the 1-minute breakdown test. Approximate voltages at which corona is audible are plotted in Fig. 37 as a function of insulation thickness.

Differences in hearing ability between persons make a corona measurement desirable. This is done by means of the standard NEMA circuit of Fig. 38.[1] With the transformer connected as shown, receiver

[1] See "Radio Influence Characteristics of Electrical Apparatus," by P. L. Bellaschi and C. V. Aggers, *Trans. AIEE, 57,* 626 (November, 1938).

output meter is adjusted to half-scale by a volume control potentiometer in the receiver. Next, the transformer is replaced by a modulated 1-mc signal generator, the output of which is varied until the noise meter output is again half-scale. The signal generator output in microvolts is read on an attenuator; this is then a measurement of the corona present.

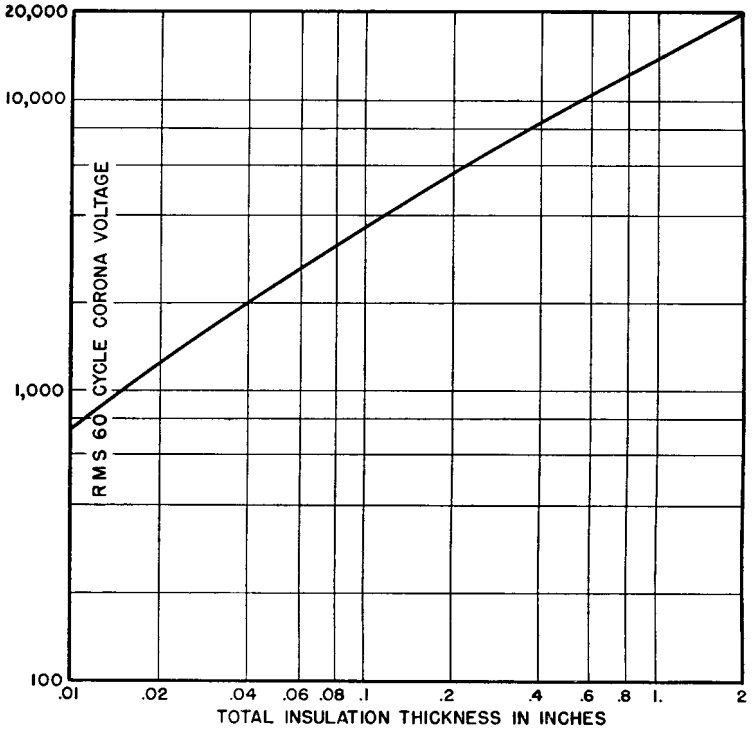

FIG. 37. Corona limit for treated cloth and paper.

Class B insulation can be worked much closer to the ultimate dielectric strength, but the latter is less a factor in determining size than creepage distance to the core. For mica an approximate working voltage rule is 100 volts rms per mil thickness.

Insulated coils in air are subject to a two-dielectric effect that is peculiarly troublesome. If the path of electric stress is partly through solid material and partly through air, the air may be overstressed because it has the lower dielectric constant (unity, compared with 3 to 5 for most coil materials). If this condition exists, it is usually imprac-

ticable to increase the air distance and so reduce the volts per inch to a value below the corona limit. The addition of more solid insulation over the whole coil may make it too large. Often the only feasible remedy is to fill the air space with more solid material, either in the form of filling compound or strips of insulation like micarta or pressboard.

It is important, when dealing with insulation voltage, to make a

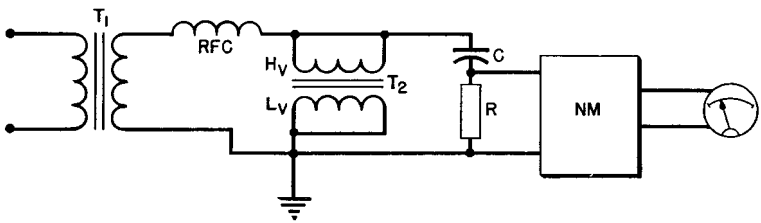

T_1	TESTING TRANSFORMER	R	INPUT RESISTOR (600 OHMS)
T_2	TRANSFORMER UNDER TEST	NM	NOISE METER (RECEIVER WITH METER OUTPUT)
C	COUPLING CAPACITOR	RFC	RADIO FREQUENCY CHOKE

FIG. 38. Standard NEMA radio-influence measuring circuit.

distinction between test voltage and operating voltage. Of the two, operating voltage is the better value to specify.

19. Creepage Distance. Although solid insulation dielectric strength is important, the usual bottleneck for high voltage is creepage distance, such as margins between wire and core along the layers of insulation, or margins between lead joints and frame along the leads and coil sides. A common way of increasing the direct creepage distance across the margins is to use an insulating channel as in Fig. 39(*a*). This is especially helpful when the part of the coil adjacent to the core tongue is at low potential and the upper part is at high potential, as in some plate transformers. When the whole coil is at high potential it may be insulated by taping the coil, but taping is expensive and is avoided wherever creepage safely provides the necessary insulation strength.

Creepage distances over treated cloth or other organic material in air are shown in Fig. 40 for breakdown voltages up to 100 kv. The primary purpose of these curves is to find the proper margins for coils adjacent to the core.

Insulation between the start (or finish) turn of the first layer and the core consists of creepage along the margin plus the thickness of the coil form. This is not a relevant distance, however, if the coil lead

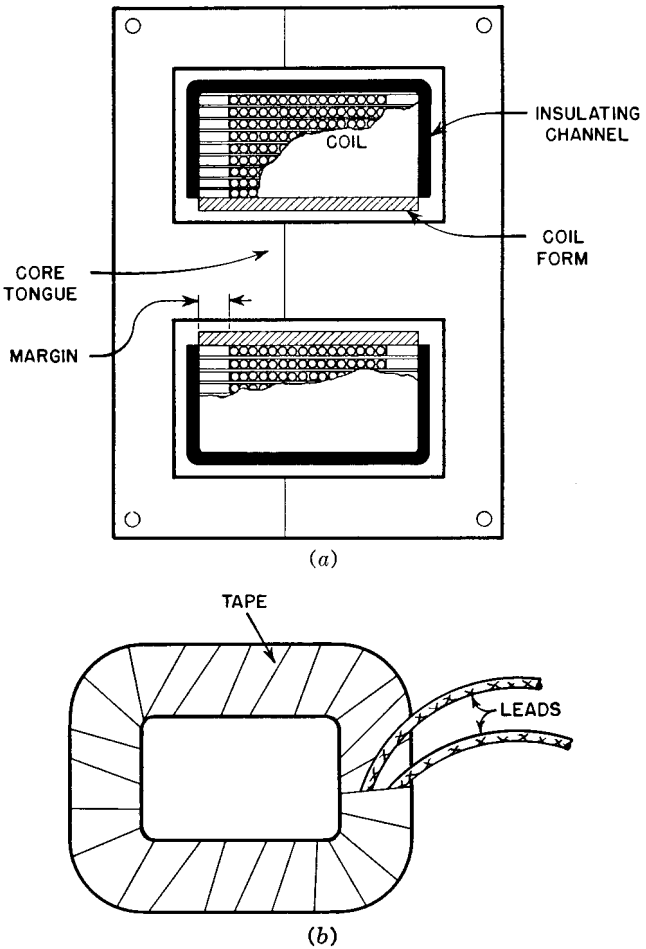

FIG. 39. (*a*) Use of insulating channel; (*b*) taped coil.

is brought across the margin and up the side of the coil. In such a case, the only creepage distance is the thickness of the coil form. In low-voltage coils this may be enough; in higher-voltage coils, a barrier of insulating material is needed between the coil form and the core, under the spot where the lead is brought out of the coil. Such a

barrier is provided by outer insulation in Fig. 35. Dimensions of the insulating barrier should be such that a distance at least equal to the coil margin should intervene between the start lead and the core in all directions and the thickness may be the same as the coil form.

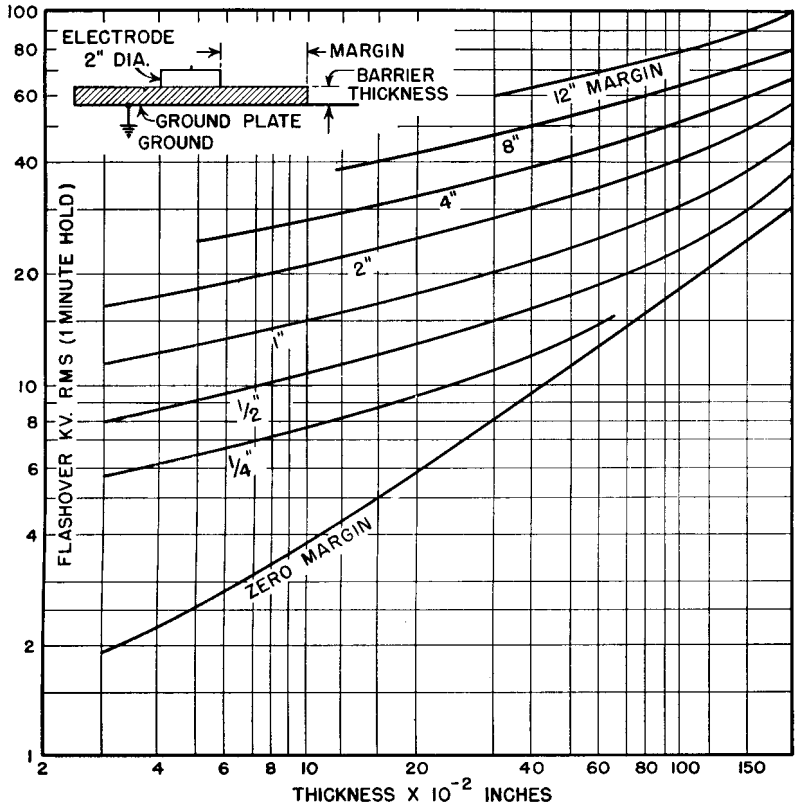

FIG. 40. Creepage curves in air over smooth organic insulation.

In any coil where the finish lead is at the top of the coil, there is less difficulty in insulating the finish lead. The finish lead has a longer creepage distance to the core if the height of the coil is a greater distance than the margin. It is necessary to avoid using materials on the sides of the coil which would result in any decrease of dielectric strength. In this respect, the creepage strength of some materials with high puncture strength is not good. The last layer of wire may be insulated from the core with a channel as in Fig. 39(*a*).

When practical coil margins, even with barriers, are insufficient to

support the induced or applied voltage, coils are taped as in Fig. 39(*b*). Taping is the most time-consuming but the safest method of insulation. Separate secondaries may be taped and then assembled over the primary. If the whole transformer winding is taped, the coil form must be large enough to allow room for the taping between the core and coil form. It is also important that the leads be taped, to prevent breakdown from joints to ground.

Ordinarily, a winding is separated from the winding under it by wraps of Kraft paper or other insulation. In the coil of Fig. 41 the insulation thickness between winding 1 and winding 2 is shown divided

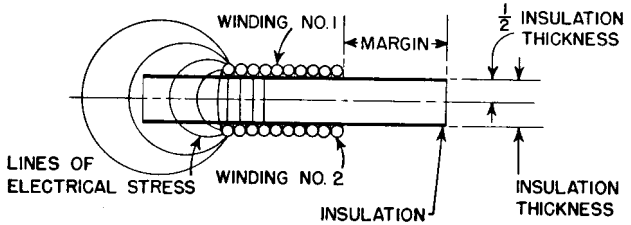

FIG. 41. Adaptation of Fig. 40 for insulation between coils.

by an imaginary center line. With equal margins in the two windings, the voltage stress is symmetrical about this center line. Margins should be such that there is sufficient creepage distance, in conjunction with one-half the insulation thickness, to withstand one-half the test voltage between these adjacent windings. That is, when full test voltage is applied between the windings, only half of it appears between the first layer of winding 1 and the center line of the insulation between the windings. If the margins are unequal, the sum of the two margins, in conjunction with the total insulation thickness, should be large enough to withstand the full test voltage, in accordance with Fig. 40.

Coils may be divided into "part coils" or sections, to reduce insulation stresses, but such coils should be closely integrated with the circuit. For this reason, part coils are discussed in later chapters.

20. Impregnation. After a coil is wound the best practice is to impregnate it in some sort of insulating liquid which hardens after filling. This is done for several reasons. First, it protects the wire from movement and possible mechanical damage. Second, it prevents the entrance of moisture and foreign matter which might corrode the wire or cause insulation deterioration. Third, it increases the dielectric

strength of fibrous insulating materials. Fourth, it assists in heat dissipation from the coil. Single-layer coils may be dipped in the liquid, drained, and dried, but deeper, thicker coils require the use of vacuum to remove air from the coil and admit the liquid to all parts of the interior. The best mechanical result is obtained when coils are assembled with cores before treatment.

Insulation is considered to be impregnated when a suitable substance replaces the air between its fibers, even if this substance does not completely fill the spaces between the insulated conductors.

Coils having little or no temperature rise in normal use are impregnated with chemically neutral mineral wax. The wax is melted in a sealed tank and is drawn into another tank in which preheated coils have been placed, and a vacuum is maintained. Coils are removed from the tank, drained, and allowed to cool. Wax treatment provides good dielectric qualities and moisture protection. It is a quick, simple process.

Transformers having operating temperatures of 65°C or higher are impregnated with varnish. Varnish of good grade and close control is essential to achieve thorough filling and dry coils after impregnation. Oleoresinous varnishes, which polymerize to a hard state by baking, are notably useful for the purpose. A high degree of vacuum, fresh varnish, and accurate baking temperature control are necessary for good results. Plasticizers are sometimes added to the varnish to prevent brittleness in finished coils. Varnish may attack wire enamel (which itself is a kind of varnish), and so the soaking and baking time periods must be regulated carefully.

Varnishes for impregnation of electrical coils have until lately been diluted by solvents to lower the viscosity so as to permit full penetration of the windings. When the coils are baked, the varnish dries and the solvent is driven off. The drying leaves very small holes through which moisture can penetrate and in which corona may form. Eventually, the insulation deteriorates. It is, therefore, necessary to allow large clearances for high voltages or to immerse the coils in oil. Either of these alternatives increases the size of a high-voltage transformer in relation to that of a low-voltage transformer. For this reason, *solventless resins* have come into use as filling compounds for dry-type coils. They are known by trade names such as Fosterite, Paraplex, and Stypol. These resins have the advantage of changing from a liquid to a solid state by heat polymerization, so that small holes formed by drying of the solvent are eliminated. Filling of the coil

may be accomplished by casting the transformer in a mold, or by encapsulation. Encapsulation is readily adapted to irregular coil surfaces and is accomplished by a leak-proof coat before filling. In either process, a good vacuum is necessary to insure complete filling.

Silicone materials are moisture-resistant. Basic insulation should be inorganic, or silicone-treated cloth, tape, laminated sheets, and tubes. Through the use of silicones, some transformers may be designed to have very small dimensions for their ratings. This may be achieved most successfully if the coil insulation comprises only silicone or inorganic materials, including impregnation with silicone varnish. Dielectric strength of silicones is about the same as class A materials. Hence the thickness of silicone coil insulation is similar to that for organic materials.

Continual development improves all classes of insulation; present A, B, and H insulation classes may be superseded eventually by new classes based entirely on functional evaluation. Life tests have been proposed [1] which classify a transformer according to its ability to withstand the effects of voltage, moisture, and vibration, as well as temperature.

In encased high-voltage units, air around the coils, bushings, and leads is especially subject to the formation of corona. To reduce this tendency, the containers are filled with asphaltic compound which replaces the air with solid, non-ionizing material. A similar compound is often used to fill containers of low-voltage transformers to avoid the need for mechanically fastening the core to the case. This is a permissible practice if the melting point of the compound is higher than the highest operating temperature and if its cracking point is below the lowest operating temperature.

21. Oil Insulation. Although, in electronic apparatus, there is a tendency toward the use of dry-type transformers, frequently voltages are so high that air clearances are impracticable and oil-filled containers must be used. In Fig. 42 the curves show rms breakdown voltage versus creepage distance under oil. An example will show the advantage of oil filling. From Figs. 40 and 42 it will be seen that 10-in. creepage distance is required in air to withstand a 1-minute breakdown test of 60 kv on insulation 0.5 in. thick, whereas in oil only 2-in. creepage distance is required.

[1] See "Functional Evaluation of Insulation for Small Dry-Type Transformers Used in Electronic Equipment," by R. L. Hamilton and H. B. Harms, *AIEE Tech. Paper* 54–121.

Curves of Fig. 42 are for pressboard or Micarta under oil. Some kinds of porcelain have less creepage strength than these materials. On the other hand, some grades of glass and polystyrene are much better and withstand 150 kv for 1 minute with 2 in. of creepage path.

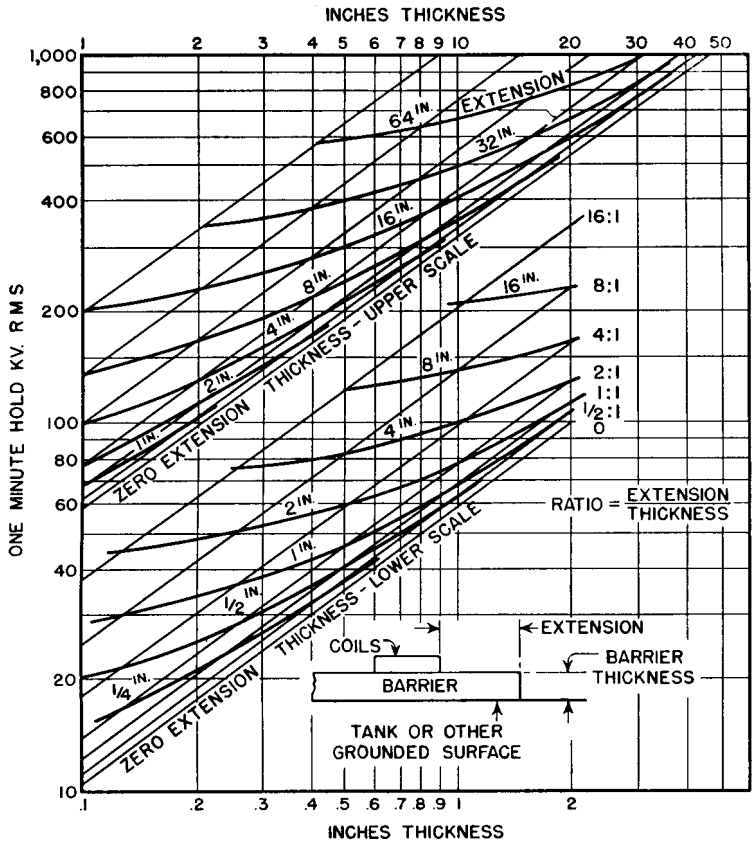

FIG. 42. Creepage curves of solid insulation under oil.

In high-voltage low-current power supplies, these special materials are used to save weight and space. At 50 kv or more, sharp edges and points should be avoided by the use of round terminals, leads, and coils.

Only high grades of insulating oil are used for this purpose. Tests are run continually to check condition of the oil. Oil is stored in such a manner as to keep out moisture and dirt and avoid extremes of

temperature. Where very high voltages are used, as in X-ray apparatus, oil filling is done under vacuum to remove air bubbles, and containers are sealed afterwards to prevent moisture from entering. Mica insulation is not used in oil because oil dissolves flexible bonds.

Often a high-voltage transformer can be integrated with some other component, such as a tube socket, capacitor, or another transformer. This is desirable from the standpoint of space conservation, provided that adequate clearances to the case are maintained. "Packaged" power supplies are sometimes made in this fashion to facilitate assembly and repair.

22. Size versus Rating. Core area depends upon voltage, induction, frequency, and turns. For a given frequency and grade of core material, core area depends upon the applied voltage. Window area depends upon coil size, or for a given voltage upon the current drawn. Since window area and core area determine size, there is a relation between size and v-a rating.

With other factors, such as frequency and grade of iron, constant, the larger transformers dissipate less heat per unit volume than the smaller ones. This is true because dissipation area increases as the square of the equivalent spherical radius, whereas volume increases as its cube. Therefore larger units are more commonly of the open type, whereas smaller units are totally enclosed. Where enclosure is feasible, it tends to cause size increase by limiting the heat dissipation. Figure 43 shows the relation between size and rating for small, enclosed, low-voltage, two-winding, 60-cycle transformers having Hipersil cores and class A insulation and operating continuously in a 40°C ambient. The size increases for the same volt-amperes over that in Fig. 43 for any of the following reasons:

High voltage	Silicon-steel cores
High ambient temperature	Low regulation
Lower frequency	More windings

The size decreases for

Higher frequencies	Open-type units
Class B insulation	Intermittent operation

If low-voltage insulation is assumed, two secondary windings reduce the rating of a typical size by 10 per cent; six secondaries by 50 per cent. The decreased rating is due partly to space occupied by insulation and partly to poorer space factor. The effects of voltage, temperature, and core steel on size have been discussed in preceding sec-

tions. Frequency and regulation will be considered separately in succeeding chapters.

Open-type transformers like those in Fig. 8 have better heat dissipation than enclosed units. The lamination-stacking dimension can

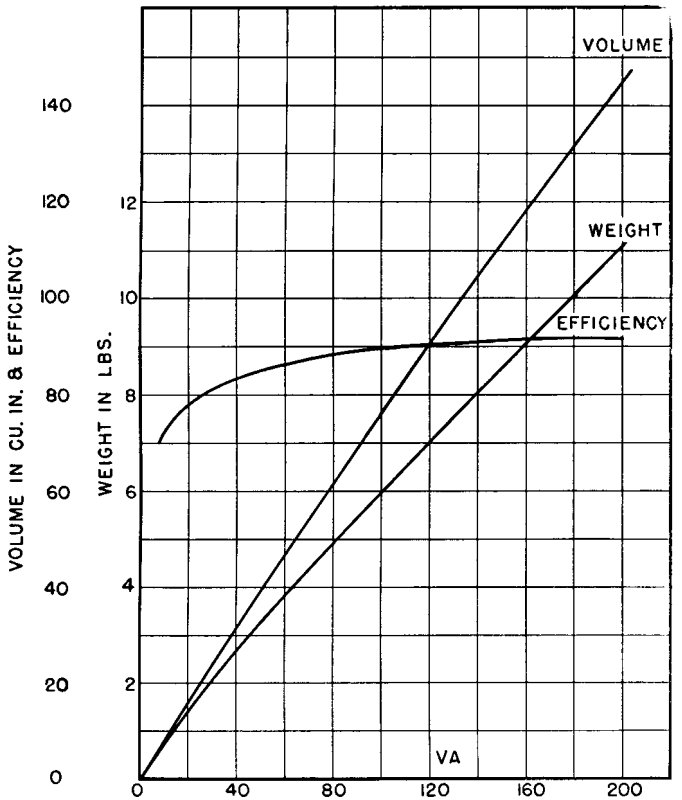

FIG. 43. Size of enclosed 60-cycle transformers.

be made to suit the rating, so that one size of lamination may cover a range of v-a ratings. Heat dissipation from the end cases is independent of the stacking dimension, but that from the laminations is directly proportional to it. This is shown in Fig. 44 for several lamination sizes. For each size the horizontal line represents heat dissipation from the end cases; the sloping line represents dissipation from end cases, plus that from the lamination edges which is proportional to the stacking dimension. At ordinary working temperature, heat is dis-

sipated at the rate of 0.008 watt per square inch per centigrade degree rise. In Fig. 44 the watts per centigrade degree of temperature rise are given as a function of lamination stack. This refers to temperature rise at the core surface only. In addition, there is a temperature

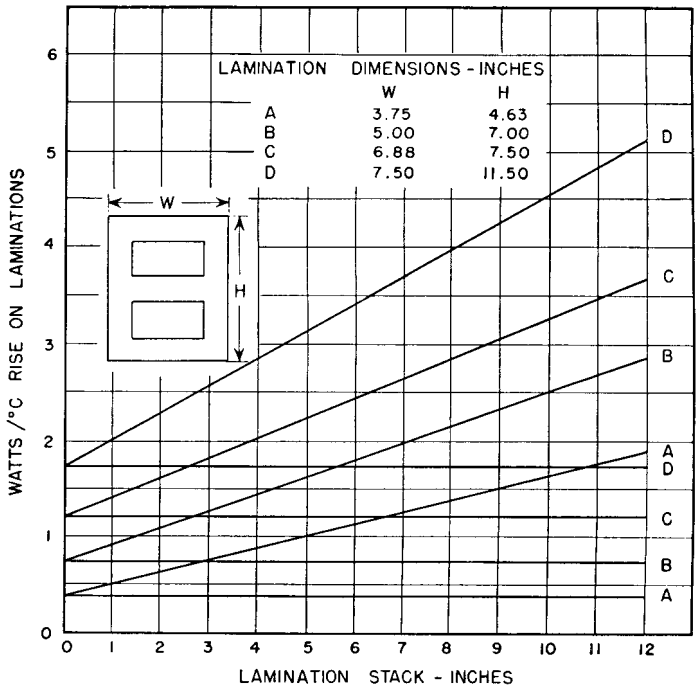

FIG. 44. Heat dissipation from open-type transformers with end cases.

gradient between coil and core which is given in similar manner in Fig. 45.

To find the average coil temperature rise, divide the *copper* loss by the watts per centigrade degree from the sloping line of Fig. 45. To this add the *total* of copper and iron losses divided by the appropriate ordinate from Fig. 44. That is, the total coil temperature rise is equal to the sum of the temperature drop across the insulation (marked Cu-Fe gradient in Fig. 45) and the temperature drop from the core to the ambient air. Data like those in Figs. 44 and 45 can be established for any lamination by making a heat run on two transformers, one having a core stack near the minimum and one near the maximum that is likely to be used. Usually stacking dimensions lie between the ex-

tremes of ½ to 3 times the lamination tongue width, and poor use of space results from stacking outside these limits. If end cases are omitted, coil dissipation is improved as much as 50 per cent.

The same method can be used for figuring type C Hipersil core designs; here the strip width takes the place of the stacking dimension of punched laminations, and the build-up corresponds to the tongue

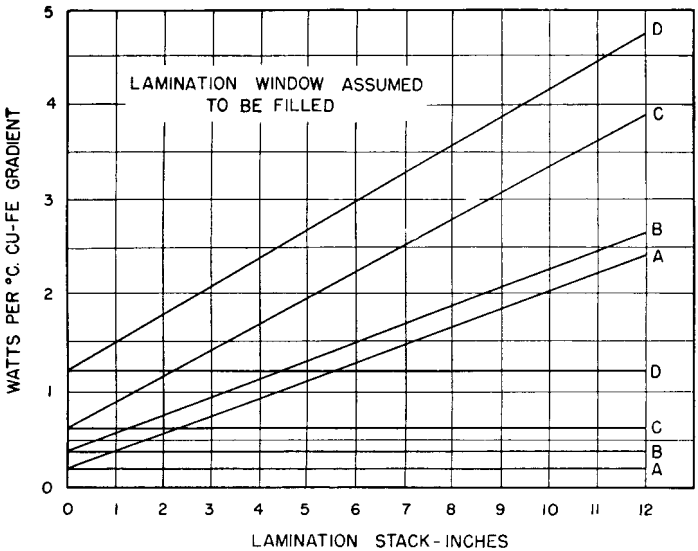

FIG. 45. Winding-to-core gradient for open-type transformers with end cases. For lamination sizes, see Fig. 44.

width. When two cores are used, as in Fig. 14, the heating can be approximated by using data for the nearest punching.

For irregular or unknown heat dissipation surfaces, an approximation to the temperature rise can be found from the transformer weight, as derived in the next section.

23. Intermittent Ratings. It often happens that electronic equipment is operated for repeated short lengths of time, between which the power is off. In such cases the average power determines the heating and size. Transformers operating intermittently can be built smaller than if they were operated continuously at full rating.

Intermittent operation affects size only if the "on" periods are short compared to the thermal time constant of the transformer; that is, small transformers have less heat storage capacity and hence rise to final

temperature more quickly than do large ones. It is important, therefore, to know the relation between size and thermal time constant, or the time that would be required to bring a transformer to 63 per cent of the temperature to which it would finally rise if the power were applied continuously.

The exact determination of temperature rise time in objects such as transformers, having irregular shapes and non-homogeneous materials, has not yet been attempted. Even in simple shapes of homogeneous material, and after further simplifying assumptions have been made, the solution is too complicated [1] for rapid calculation. However, under certain conditions, a spherical object can be shown to cool according to the simple law: [2]

$$\theta = \theta_0 \epsilon^{-\frac{3Et}{pcr}} \tag{28}$$

where θ = temperature above ambient at any instant t
θ_0 = initial temperature above ambient
E = emissivity in calories per second per centigrade degree per square centimeter
p = density of material
c = specific heat of material
r = radius of sphere
ϵ = 2.718.

The conditions involved in this formula are that the sphere is so small or the cooling so slow that the temperature at any time is sensibly uniform throughout the whole volume. Mathematically, this is fulfilled when the expression Er/k (where k is the thermal conductivity of the material) is small compared to unity. Knowing the various properties of the transformer material, we can tell (1) whether the required conditions are met, and (2) what the thermal time constant is. The latter is arrived at by the relation

$$t_c = pcr_e/3E \tag{29}$$

where r_e is the radius of the equivalent sphere.

In order to convert the non-homogeneous transformer into a homogeneous sphere the average product of density and specific heat pc is

[1] See *The Mathematical Theory of Heat Conduction*, by L. R. Ingersoll and O. J. Zobel, Ginn and Co., Boston, 1913, p. 142.

[2] Ingersoll and Zobel, *op. cit.*, p. 143.

found. Figures on widely different transformers show a variation from 0.862 to 0.879 in this product; hence an average value of 0.87 can be taken, with only 1 per cent deviation in any individual case.

Since the densities of iron and copper do not differ greatly, and insulation brings the coil density closer to that of iron, it may be further assumed that the transformer has material of uniform density 7.8 throughout. The equivalent spherical radius can then be found from

$$r_e = (\text{Weight}/1.073)^{1/3} \tag{30}$$

where r_e is in inches and weight is in pounds. The time constant is plotted from equations 29 and 30 in terms of weight in Fig. 46.

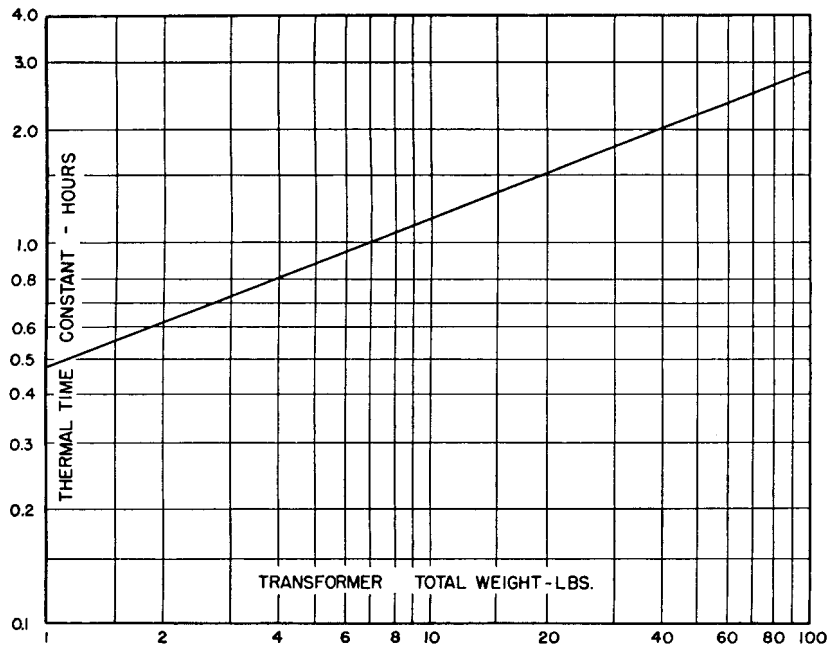

FIG. 46. Transformer time constant, or time required to reach 63 per cent of final temperature.

The condition that Er/k be small compared to unity is approximated by assuming that k is the conductivity of iron—a safe assumption, because the conductivity of copper is 7 to 10 times that of iron. A transformer weighing as much as 60 lb has $r_e = 5.45$ in., $E = 0.00028$ cal per sec per sq cm/°C, and $k = 0.11$. Changing r_e to metric units

gives $Er/k = (0.00028 \times 5.45 \times 2.54)/0.11 = 0.34$, which is small enough to meet the necessary condition of equation 28.

It will be noticed that equation 28 is a law for cooling, not temperature rise. But if the source of heat is steady (as it nearly is) the equation can be inverted to the form $\theta_0 - \theta$ for temperature rise, and θ_0 becomes the final temperature.

Temperature rise of a typical transformer is shown in Fig. 47, to-

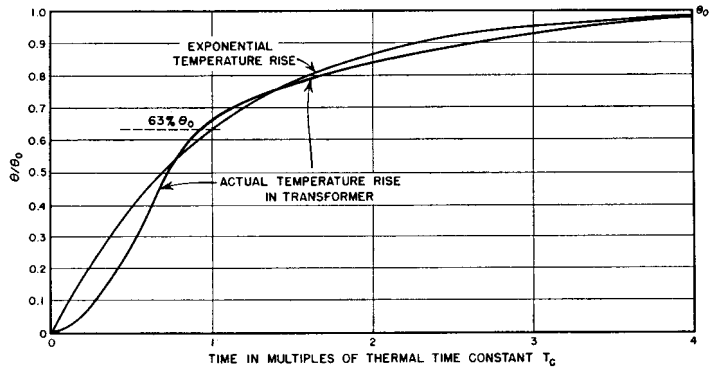

FIG. 47. Transformer temperature rise time.

gether with the exponential law which is $\theta_0 - \theta$, where θ is the temperature of equation 28. The actual rise is less at first than that of the foregoing simplified theory, then more rapid, and with a more pronounced "knee." The 63 per cent of final temperature is reached in about 70 per cent of the theoretical time constant t_c for transformers weighing between 5 and 200 lb. This average correction factor is included in Fig. 46 also.

If a transformer is operated for a short time and then allowed to cool to room temperature before operating again, the temperature rise can be found from Figs. 46 and 47. As an example, suppose that the continuously operated final coil temperature rise is 100 centigrade degrees, the total weight is 5 lb, and operating duty is infrequent periods of 2 hr. From Fig. 46, the transformer has a thermal time constant of 0.85 hr. This corresponds to $t_c = 1$ in Fig. 47. Two hours are therefore $2 \div 0.85 = 2.35$ times t_c, and the transformer rises to 90 per cent of final temperature, or a coil temperature rise of 90 centigrade degrees, in 2 hr.

If, on the other hand, the transformer has regular off and on intervals, the average watts dissipated over a long period of time govern the

temperature rise. A transformer is never so small that it heats up more in the first operating interval than at the end of many intervals.

From equation 30 can be found a relation between weight, losses, and final temperature rise. For, since heat is dissipated at 0.008 watt per sq in./°C rise, and the area A_S of the equivalent sphere is $4\pi r_e^2$,

$$\theta_0 = \frac{\text{Total watts loss}}{0.008A_S} = \frac{\text{Total watts loss}}{0.1\left(\dfrac{\text{Total weight in pounds}}{1.073}\right)^{\frac{2}{3}}} \tag{31}$$

where θ_0 is the final temperature rise in centigrade degrees. This equation is subject to the same approximations as equation 28; test results show that it is most reliable for transformers weighing 20 lb or more, with 55°C temperature rise at 40°C ambient.

3. RECTIFIER TRANSFORMERS AND REACTORS

Rectifiers are used to convert alternating into direct current. The tubes generally have two electrodes, the cathode and the anode. Both high vacuum and gas-filled tubes are used. Sometimes for control purposes the gas-filled tubes have grids, which are discussed in Chapter 8.

A high-vacuum rectifier tube characteristic voltage-current curve is shown in Fig. 48. Current flows only when the anode is positive with respect to the cathode. The voltage on this curve is the internal potential drop in the tube when current is drawn through it. This voltage divided by the current gives effective tube resistance at any point. Tube resistance decreases as current increases, up to the emission limit, where all the electrons available from the cathode are used. Filament voltage governs the emission limit and must be closely controlled. If the filament voltage is too high, the tube life is shortened; if too low, the tube will not deliver rated current at the proper voltage.

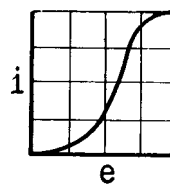

FIG. 48. High-vacuum rectifier voltage-current curve.

Gas-filled rectifier tubes have internal voltage drop which is virtually constant and independent of current. Usually this voltage drop is much lower than that of high vacuum tubes. Consequently, gas-filled tubes are used in high power rectifiers, where high efficiency and low regulation are important. In some rectifiers, silicon or germanium crystals or selenium disks are used as the rectifying elements.

In this chapter, the rectifier circuits are summarized and then rectifier transformers and reactors are discussed.

24. Rectifiers with Reactor-Input Filters. Table VII gives commonly used rectifier circuits, together with current and voltage relations in the associated transformers. This table is based on the use of a reactor-input filter to reduce ripple. The inductance of the choke is assumed to be great enough to keep the output direct current constant. With any finite inductance there is always some superposed

TABLE VII – TABLE OF RECTIFIER CIRCUITS

TYPE	SINGLE PHASE HALF WAVE	SINGLE PHASE FULL WAVE	SINGLE PHASE BRIDGE CIRCUIT	3 PHASE HALF WAVE	3 PHASE HALF WAVE ZIG ZAG	DOUBLE 3 PHASE WITH BALANCE COIL ‡	3 PHASE FULL WAVE (SEC. MAY BE Δ)	3 PHASE FULL WAVE ZIG ZAG *	SIX PHASE HALF WAVE
CIRCUITS	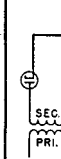		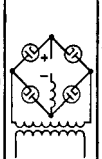	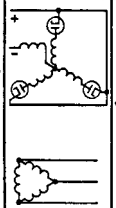	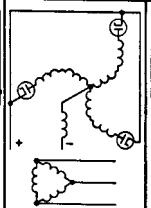	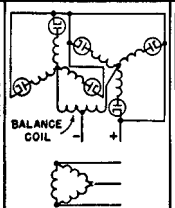	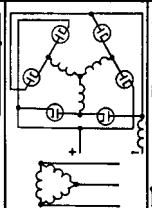	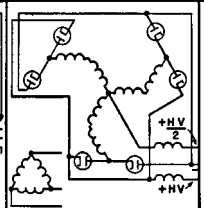	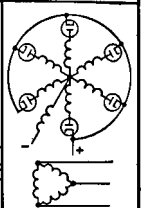
RECTIFIER PHASES AND NUMBER OF TUBES	1	2	2-4	3	3	6	6	6	6
PHASES OF A-C SUPPLY	1	1	1	3	3	3	3	3	3
SECONDARY VOLT PER LEG	2.22	1.11 (HALF SECT.)	1.11 (WHOLE)	0.855	0.985 (HALF LEG .493)	0.855	0.428	0.493 HALF LEG .247	0.74
PRIMARY VOLTAGE	2.22	1.11	1.11	0.855	0.855	0.855	0.428	0.428	0.74
SECONDARY CURRENT PER LEG	1.57	0.707	1.00	0.577	0.577	0.289	0.816	0.816	0.408
PRIMARY CURRENT PER LEG	1.21	1.000	1.00	0.471	0.408	0.408	0.816	0.816	0.577
SECONDARY K V A	3.48	1.57	1.11	1.48	1.71	1.48	1.05	1.21	1.81
PRIMARY K V A	2.68	1.11	1.11	1.21	1.05	1.05	1.05	1.05	1.28
AVERAGE OF PRIMARY AND SECONDARY K V A ∅	3.08	1.34	1.11	1.35	1.38	1.26	1.05	1.13	1.55
INVERSE PEAK VOLTAGE	3.14	3.14	1.57	2.09	2.09	2.09	1.05	1.05	2.09
RMS CURRENT PER TUBE	1.57	0.707	0.707	0.577	0.577	0.289	0.577	0.577	0.408
PEAK CURRENT PER TUBE	3.14	1.00	1.00	1.00	1.00	0.500	1.00	1.00	1.00
AVERAGE CURRENT PER TUBE	1.00	0.50	0.50	0.33	0.33	0.167	0.33	0.33	0.167
RIPPLE FREQUENCY	f	2f	2f	3f	3f	6f	6f	6f	6f
RMS RIPPLE VOLTAGE	1.11	0.472	0.472	0.177	0.177	0.04	0.04	0.04	0.042
RIPPLE PEAKS	+2.14 −1.00	+0.57 −1.00	+0.57 −1.00	+0.209 −0.291	+0.209 −0.291	+0.057 −0.077	+0.057 −0.077	+0.057 −0.077	+0.057 −0.077
LINE POWER FACTOR	0.373	0.90	0.90	0.826	0.955	0.955	0.955	0.955	0.955

NOTE: THE VALUES OF VOLTAGE AND CURRENT ARE EFFECTIVE OR R.M.S., UNLESS OTHERWISE STATED; THEY ARE GIVEN IN TERMS OF THE AVERAGE D.C. VALUES, AND THE KILOVOLT-AMPERES IN TERMS OF D.C. KILOWATT OUTPUT. PERFECT TRANSFORMERS, RECTIFIERS AND D.C. CHOKE ARE ASSUMED, AND $N_1/N_2 = 1$, EXCEPT IN ZIG-ZAG CIRCUITS. SECONDARY AND PRIMARY REFER TO ANODE TRANSFORMER.
‡ FREQUENCY OF BALANCE COIL VOLTAGE 3f. BALANCE COIL VOLTAGE 0.356. PEAK BALANCE COIL VOLTAGE 0.605. BALANCE COIL K V A 0.173.
* USE COLUMN 5 VALUES FOR HALF VOLTAGE TAP. ∅ MAGNETIZING CURRENT ASSUMED NEGLIGIBLE IN ALL CASES.

This table is based mostly on "Polyphase Rectification Special Connections," by R. W. Armstrong, *Proc. I.R.E.*, Vol. 19, Jan. 1931.

ripple current which is neglected in the table, and which is considered further in Chapter 4.

The single-phase half-wave rectifier ordinarily has discontinuous output current, and its output voltage is therefore highly dependent upon the inductance of the input filter choke. For this reason, the currents and voltages are given for this rectifier without a filter.

The difference between primary and secondary v-a ratings in several of these rectifiers does not mean that instantaneous v-a values are different; it means that because of differences in current wave form the rms values of current may be different for primary and secondary.

Unbalanced direct current in the half-wave rectifiers requires larger transformers than in the full-wave rectifiers. This is partly overcome in three-phase transformers by the use of zigzag connections. The three-phase full-wave rectifier can be delta-connected on both primary and secondary if desired; the secondary current is multiplied by 0.577 and the secondary voltage by 1.732. Anode windings have more turns of smaller wire in the delta connection. Single-phase bridge and three-phase full-wave rectifiers require notably low a-c voltage for a given d-c output, low inverse peak voltage on the tubes, and small transformers.

25. Rectifiers with Capacitor-Input Filters. When the filter has no reactor intervening between rectifier and first capacitor, rectifier current is not continuous throughout each cycle and the rectified wave form changes. During the voltage peaks of each cycle, the capacitor charges and draws current from the rectifier. During the rest of the time, no current is drawn from the rectifier, and the capacitor discharges into the load.

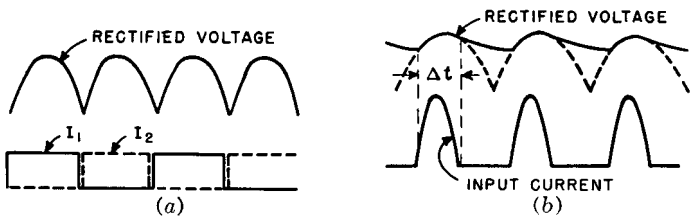

FIG. 49. Voltage and current comparisons in reactor-input and capacitor-input circuits.

Comparison between the rectified voltage of reactor-input and capacitor-input filters in a single-phase full-wave rectifier may be seen in Figs. 49(*a*) and (*b*), respectively. The two tube currents I_1 and I_2 in (*a*) add to a constant d-c output, whereas in (*b*) the high-peaked tube currents flow only while the rectified voltage is higher than the

average d-c voltage. *Average* current per tube in both cases is half the rectifier output. With large values of capacitance, the rectified voltage

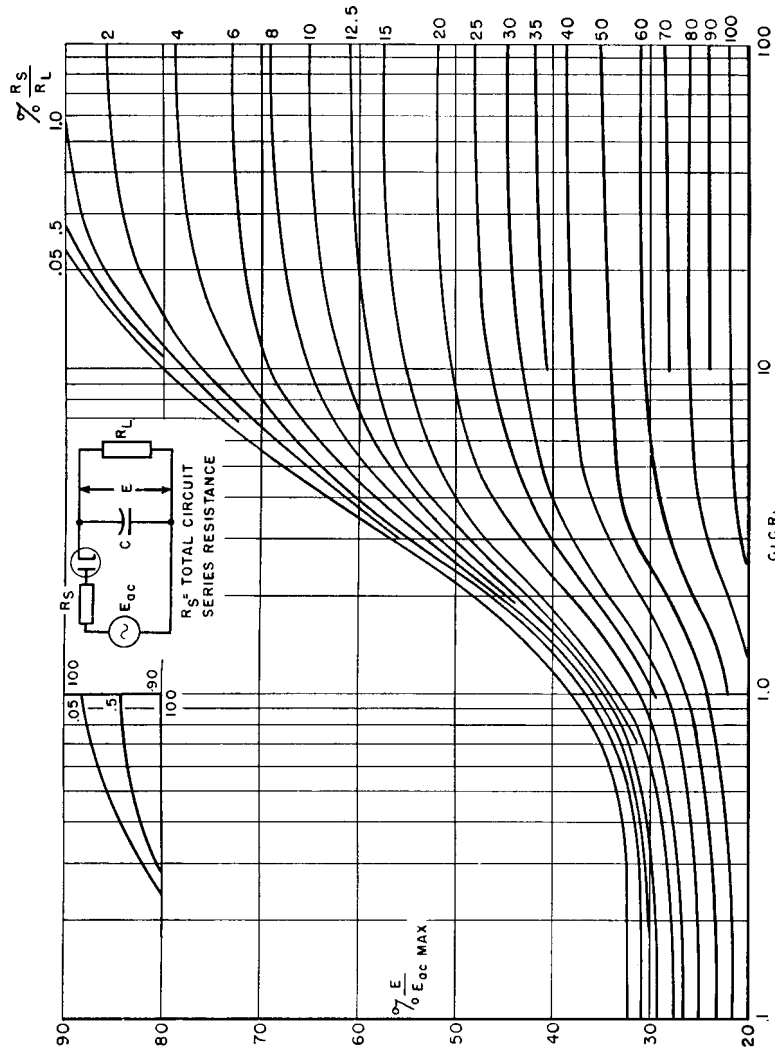

FIG. 50. Relation of peak sine voltage to d-c voltage in half-wave capacitor-input circuits.

in Fig. 49(*b*) increases to within a few per cent of the peak voltage. Ripple, average rectified voltage output, and rectifier current are dependent on the capacitance, the supply line frequency, and the load resistance. They are dependent also on rectifier internal resistance because it affects the peak value of current which the filter capacitor can draw during the charging interval Δt.

Analysis of this charge-discharge action involves complicated Fourier series which require a long time to calculate.[1] Satisfactory

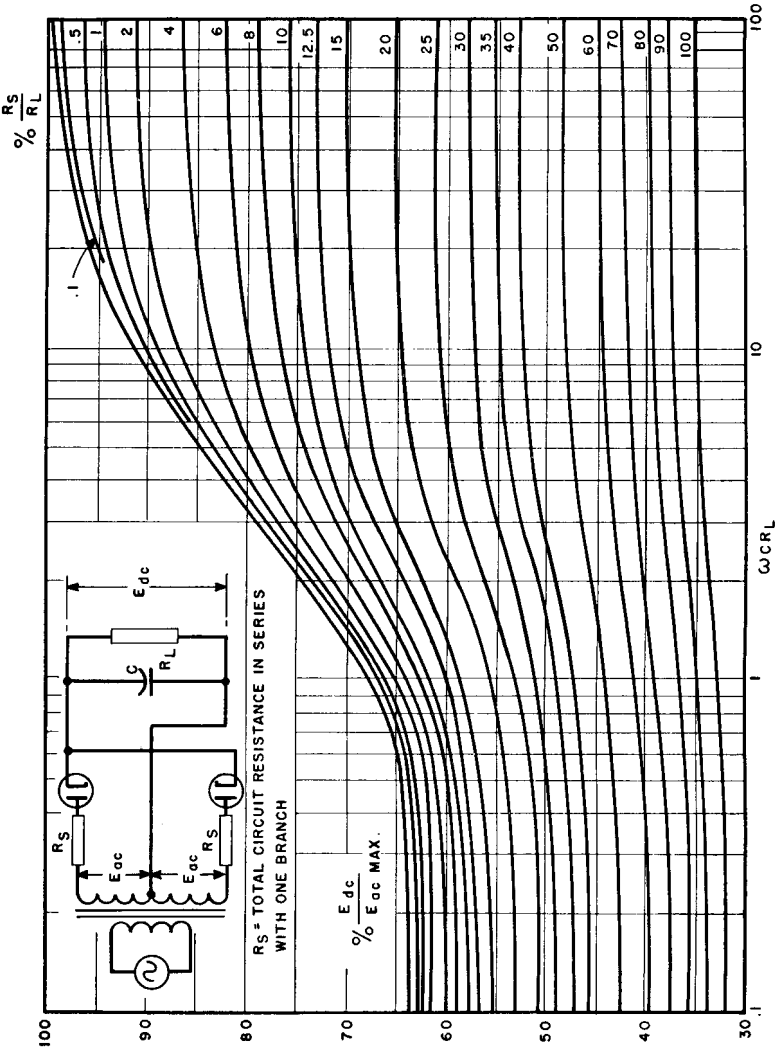

FIG. 51. Relation of peak sine voltage to d-c voltage in full-wave capacitor-input circuits.

voltage and current values have been obtained from experimental measurements by Schade [2] and are shown in Figs. 50, 51, and 52 for

[1] See "Diode Rectifying Circuits with Capacitance Filters," by D. L. Waidelich, *Trans. AIEE, 61,* 1161 (December, 1941).

[2] "Analysis of Rectifier Operation," by O. H. Schade, *Proc. I.R.E., 31,* 341 (July, 1943).

single-phase half-wave and full-wave rectifiers. In these figures R_S is the rectifier series resistance, including the transformer resistance.

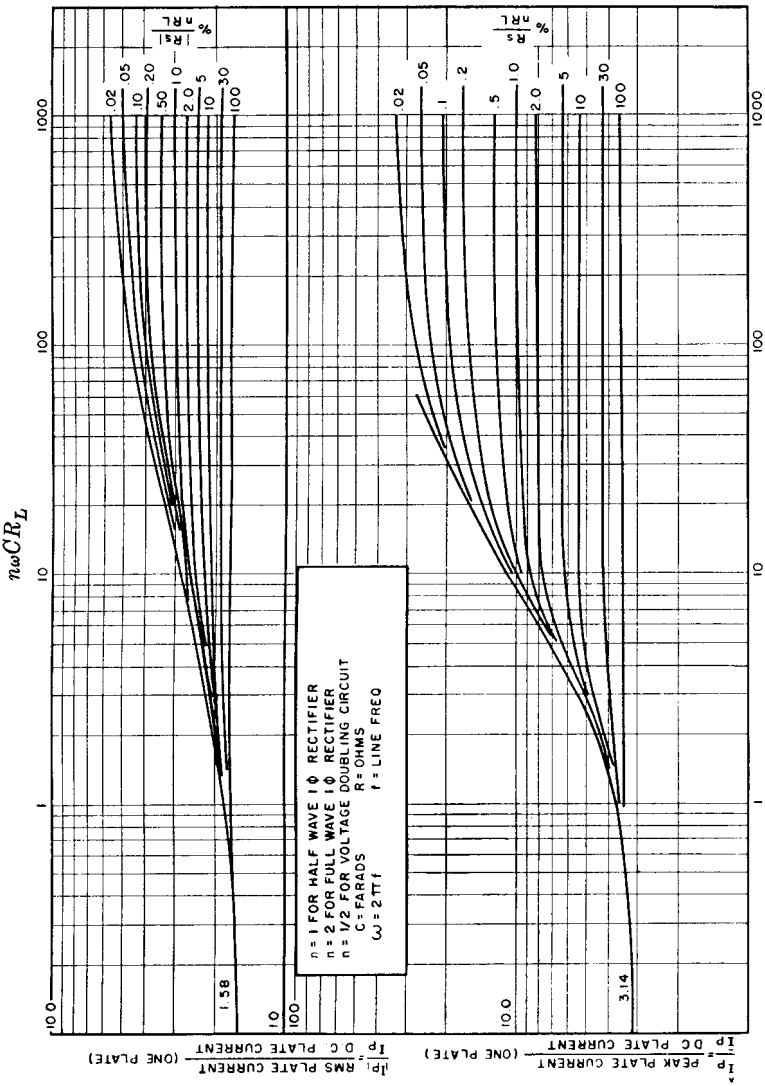

FIG. 52. Relation of peak, average, and rms diode current in capacitor-input circuits.

Results accurate to within 5 per cent are obtained if the rectifier resistance corresponding to peak current $\hat{I}_P$ is used in finding R_S. The process is cut-and-try, because $\hat{I}_P$ depends on R_S, and vice versa, but two trials usually suffice. Resistance is in ohms, capacitance is in

farads, and ω is 2π times the supply frequency. Three-phase rectifiers are rarely capacitor-input because of their larger power.

In Fig. 52 the peak current indicates whether the peak current of a given tube is exceeded, and the rms current determines the transformer secondary heating. The v-a ratings are greater, but *ratios* of primary to secondary v-a ratings given in Table VII hold for capacitor-input transformers also.

26. Voltage Doublers. To obtain more d-c output voltage from a rectifier tube, the circuit of Fig. 53 is often used. With proper values of circuit elements the output is nearly double the a-c peak voltage. Tube inverse peak voltage is little more than the d-c output voltage, and no d-c unbalance exists in the anode transformer. Current output available from this circuit is less than from the single-phase full-wave circuit for a given rectifier tube. Current relations are given in Fig. 52.

Voltage tripling and quadrupling circuits also are used, either to increase the d-c voltage or to avoid the use of a transformer.[1]

27. Filament Transformers. Low-voltage filament transformers are used for heating tube filaments at or near ground potential. Often the filament windings of several tubes are combined into one transformer. Sometimes this requires several secondary windings. In terms of a single secondary transformer a 5 or 6 secondary unit requires about 50 per cent greater size and weight. But these multiwinding transformers are smaller than five or six separate units; this warrants designing them specially in many instances.

Rectifier tube filaments often operate at high d-c voltages and require windings with high voltage insulation. It is usually not feasible to combine high-voltage windings with low-voltage windings when the high voltage is more than 3,000 volts direct current because of insulation difficulties, particularly in the leads. Large rectifier filaments are usually heated by separate transformers; in polyphase rectifiers, all tube filaments are at high voltage, and some secondary windings may be combined. See the three-phase full-wave rectifier in Table VII, where the $+HV$ lead connects to a winding which heats the filaments of three tubes.

Low capacitance filament windings are sometimes required for high-frequency circuits. The problem is not particularly difficult in small v-a ratings and at moderate voltages. Here air occupies most of the space between windings. In larger ratings the problem is more difficult, because the capacitance increases directly as the coil mean turn

[1] See "Analyses of Voltage Tripling and Quadrupling Circuits," by D. L. Waidelich and H. A. Taskin, *Proc. I.R.E., 33,* 449 (July, 1945).

length for a given spacing between windings. As voltage to ground increases, there comes a point beyond which creepage effects necessitate

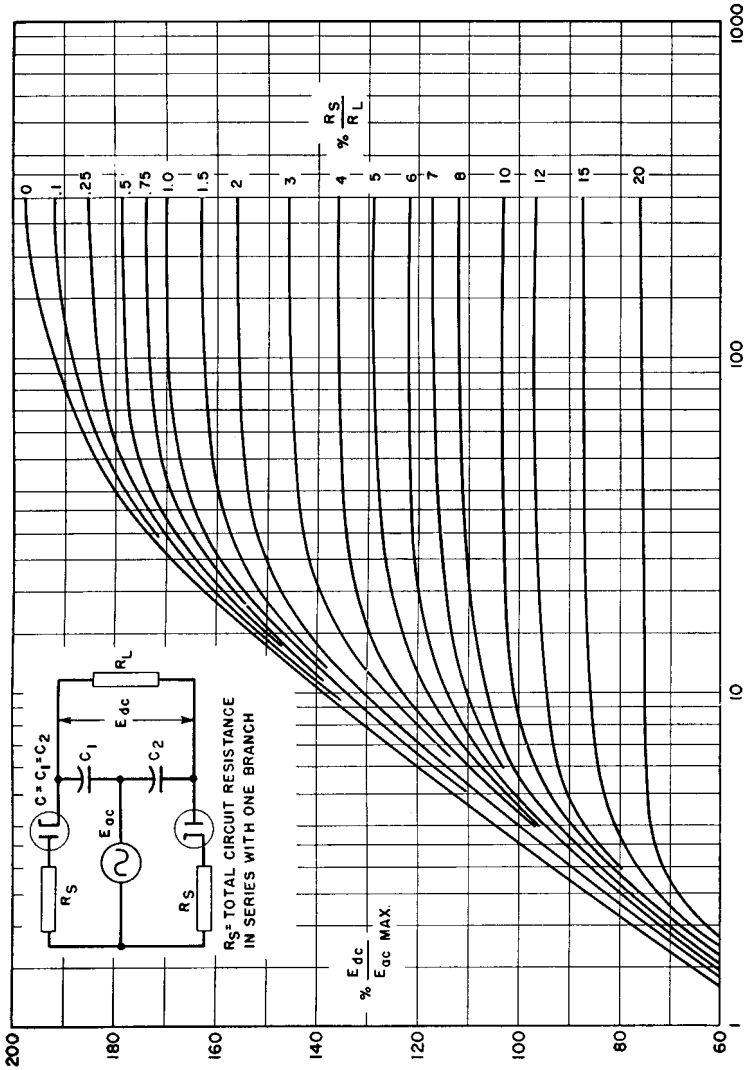

FIG. 53. Relation of peak sine voltage to d-c voltage in voltage-doubling circuit.

oil-insulated windings, whereupon the capacitance jumps 2 to 1 for a given size and spacing. There is a value of capacitance below which it is impossible to go because of space limitations in the transformer. What this value is in any given case may be estimated from the fact

that the capacitance in $\mu\mu$f of a body in free space is roughly equal to one-half its largest dimension in centimeters.

Except for the differences just mentioned, the design of filament transformers does not differ much from that of small 60-cycle power

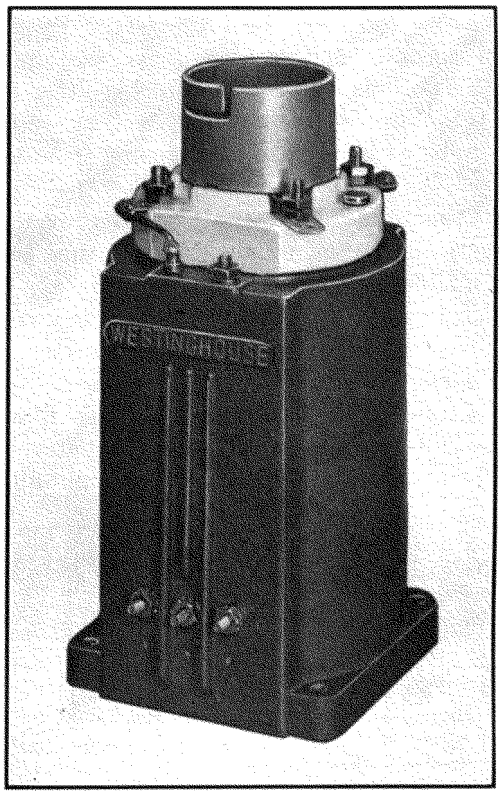

FIG. 54. 15 kv filament transformer enclosed in insulating case.

transformers. The load is constant and of unity power factor. Leakage reactance plays practically no part, because of its quadrature relationship to the load. Output voltage may therefore be figured as in Fig. 3(*c*) (p. 8). It should be *accurately* calculated, however, to maintain the proper filament emission and life.

When a tube filament is cold, the filament resistance is a small fraction of its operating value. In large tubes it is often necessary to protect the tube filaments against the high initial current they would draw at rated filament voltage. This is done by automatically reducing the starting voltage through the use of a current-limiting trans-

former having magnetic shunts between primary and secondary windings. The design of these transformers is somewhat special, and is included in Chapter 8.

High-voltage filament transformers are sometimes mounted in an insulating case, as in Fig. 54, with the tube socket on top. This arrangement eliminates the need for high-voltage wiring between the transformer and the tube, and provides the insulation for the socket. The problem of air pockets at the base of high-voltage bushings is also eliminated. It is still necessary to insulate well between windings and to fill the case fully with insulating compound in order to eliminate corona.

28. Filament Transformer Design. It is important that design work be done systematically to save the designer's time and to afford a ready means of finding calculations at a later date. To attain these ends a calculation form, such as that in Fig. 55, is used. The form is usually made to cover several kinds of transformers, and only the spaces applicable to a filament transformer are used.

Suppose that a transformer is required to supply filament power for four single-phase full-wave rectifiers having output voltages of 2,000, 500, 250, and 250 volts, respectively, with choke-input filters, as follows:

Primary voltage 100

Frequency 60 cycles

Four secondaries for the following tube filaments:

2—872 tubes:	5 volts	13.5 amp	Insulated for +2000 v d-c
2—866 tubes:	2.5 volts	10 amp	Insulated for + 500 v d-c
1—5U4G tube:	5 volts	3 amp	Insulated for + 250 v d-c
1—5Y3GT tube:	5 volts	2 amp	Insulated for + 250 v d-c

Ambient temperature: 40°C

First comes the choice of a core. Data such as those in Fig. 43 are helpful in this, and so is design experience in the modification of such data by the specified requirements. The core used here is a 2-in. stack of laminations A, Fig. 44, which is described more fully in Fig. 56, and has enough heat dissipation surface for this rating. For silicon steel, an induction of 70,000 lines per square inch is practical. The primary turns can be figured from equation 4 by making the substitution $\phi = BA_c$ and transposing to

$$N_1 = \frac{E \times 10^8}{4.44 f A_c B} \tag{32}$$

where A_c is the core cross-sectional area, or product of the core tongue width and stack dimension, and B is the core induction. In this transformer, with 90 per cent stacking factor, $A_c = 2 \times 0.9 \times 1.375 = 2.48$ sq in., and the primary turns are found to be 216.

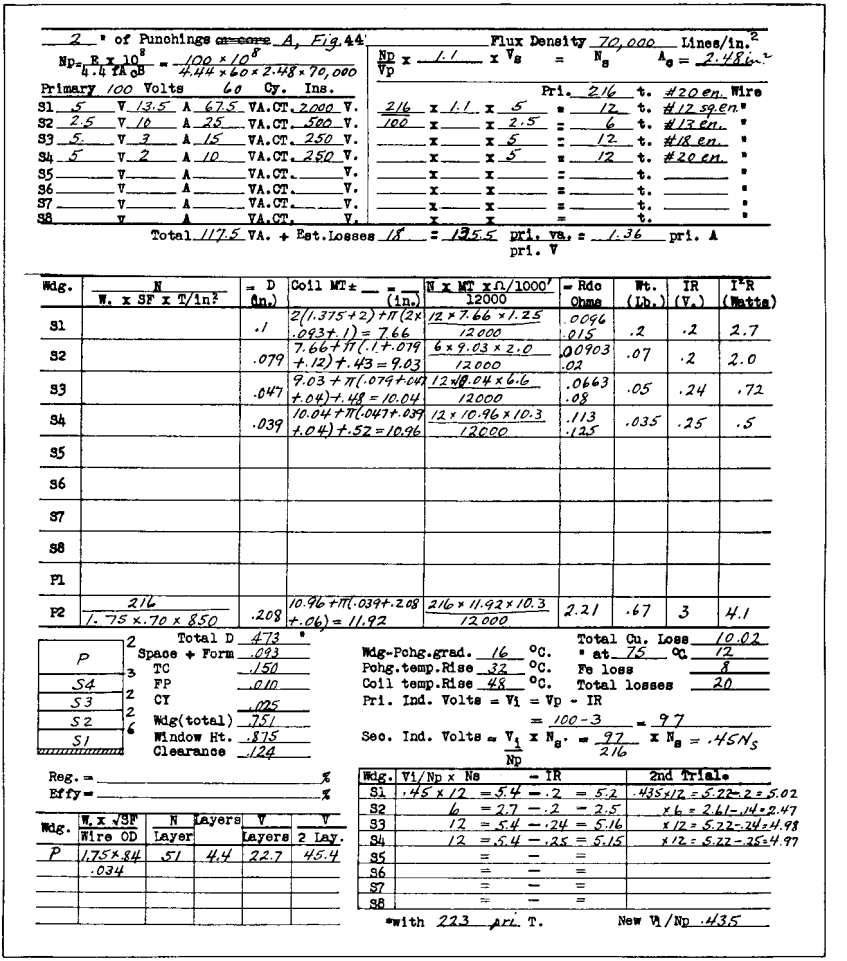

FIG. 55. Filament transformer design calculations.

Below this calculation are set down the primary voltage and frequency, and the voltage, current, volt-amperes, and insulation voltage for all secondary windings. These are designated S_1 to S_4 for identification. From the sum of the individual v-a figures, the transformer

rating is found. To it is added an estimate of losses to obtain the input volt-amperes, and the primary current.

Next an estimate of the regulation is made (10 per cent) and added to unity to obtain the multiplier 1.1 in the estimate of secondary turns near the top of the calculation form. From the currents listed, the wire size for each winding is chosen. Round enameled wire is used for

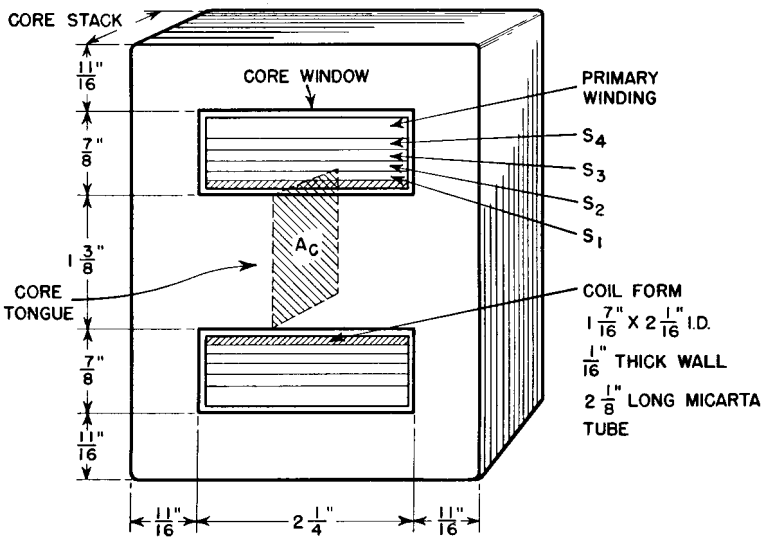

FIG. 56. Dimensions and coil section of filament transformer.

each winding except S_1, and for it No. 12 square wire is used to save space. The largest wire is placed next to the coil form to prevent damage in winding to the smaller wires.

The next task is to find out whether the wire chosen will fit in the core window space. Winding height D is entered for each winding. For each secondary this is the wire diameter, because the wire is wound in a single layer. D for S_1 is slightly larger than the wire dimension to allow for the bulge that occurs when square wire is wound. The twelve turns of S_1 occupy about $1\frac{1}{4}$ in. of horizontal winding space. The core window is $2\frac{1}{4}$ in. wide. From this is subtracted $\frac{1}{8}$ in. for clearance, leaving $2\frac{1}{8}$ in. total coil width. Margins on each side of S_1 are therefore $\frac{1}{2}(2\frac{1}{8} - 1\frac{1}{4}) = \frac{7}{16}$ in. According to Fig. 40 (p. 48) this provides over 8 kv breakdown strength, which is well above the 5-kv test voltage for S_1. Other secondary windings have lower test voltages and wider margins, and hence have more than adequate creepage distances.

The $\frac{1}{16}$-in.-thick Micarta rectangular tube used for the coil form has a corona voltage of 2,700 rms, which affords about 23 per cent safety factor over the normal operating voltage at the tube filaments. Over S_1 are wound six wraps of 0.010-in.-thick treated cloth, which has 2,600-volt corona limit. Winding S_2 supplies a filament at 500 volts of the same polarity as S_1. Hence only 1,500 volts direct current or 1,660 volts alternating current occur across this insulation. At the right of the small sketch in Fig. 55 are listed the number of wraps of 0.010-in.-thick treated cloth over each section of winding. These are added together to give the columnar figure of 0.150 for TC.

The primary winding is wound without layer insulation and with an area space factor of 70 per cent. Cotton is wound in with the wire to form walls $\frac{3}{16}$ in. thick on either side of the primary; this accounts for the low space factor and for the $1\frac{3}{4}$-in. winding traverse. The coil is finished with two layers of treated cloth, a layer of 0.010-in. fishpaper for mechanical protection, and a 0.025-in. serving of untreated cotton yarn or tape to hold it together. The total winding adds up to 0.751 in., leaving 0.124 in. clearance, about the right allowance for winding slack for four secondaries.

Mean turns are figured from equations 26 and 27, with 5 per cent incremental increase in S_2, S_3, and S_4 for leads. With the mean turn values the winding resistances, weights of copper, and IR and I^2R for each winding can be found. To S_1, S_2, and S_3 winding resistance is added lead resistance, and the lower figure is the sum of the two in each case. Total copper loss is multiplied by 1.3 to correct for 75°C operating temperature. The core weight is 6.8 lb, and the grade of steel used has 1.17 watts per pound at 70,000 lines per square inch. This gives a core loss of 8 watts, and a total of copper and core loss of 20 watts. After these losses are divided by the appropriate ordinates from Figs. 44 and 45 (pp. 55 and 56) the coil temperature rise is figured at 48 centigrade degrees, which is safe for class A insulation.

We know by now that the design is safe, but secondary voltages still must be checked. The method of equation 13 is used. Output voltages on first trial range from 0 to 4 per cent high. S_2 voltage is correct but out of line with the rest. Changing S_2 leads to a larger size makes the per cent voltage drops more nearly alike, and increasing the primary turns to 223 brings all output voltages to correct value within 1.2 per cent. Filament voltage should be kept within 2 per cent for these tubes, to allow for meter error. Primary voltage per layer is checked at the lower left; this is equivalent to 22.7 volts per mil of wire enamel, which is safe practice.

If the design were deficient in any respect, even down to the last things figured, some change would have to be made which would require recalculation of all or part of the transformer; hence the importance of good estimating all the way along.

The filament transformer outlined above had a center tap (C.T.) in each filament winding. Such taps are used with directly heated cathodes, especially when plate current is large, to prevent uneven distribution of filament emission. In windings for supplying filaments of small tubes, center taps are sometimes omitted. Ripple in the rectified output then increases, and transformer core flux density becomes asymmetrical. Whether these effects are permissible depends on operating conditions. Usually plate current is much smaller than filament current, so that center-tap leads may be smaller in copper section than start and finish leads. A certain amount of space is required for these leads; rectifier wiring is also more time-consuming when there are center taps. Nevertheless, the extra work and size may be justified by improved performance.

An even number of turns, such as were used in the transformer windings described in this section, results in center-tap placement on the same coil end as the start and finish leads; if there were an odd number of turns, the tap lead would be at the opposite end. In a single-core, single-coil design, an odd number of turns cannot be center-tapped exactly. Usually the unbalance caused by the tap being a half-turn off center is not serious, but it should not be disregarded without calculation.

29. Anode Transformers. Anode transformers differ from filament transformers in several respects.

(*a*) *Currents* are non-sinusoidal. In a single-phase full-wave rectifier, for instance, current flows through one half of the secondary during each positive voltage excursion and through the other half during each negative excursion. For half of the time each half-secondary winding is idle.

(*b*) *Leakage inductance* not only determines output voltage but also affects rectifier regulation in an entirely different manner than with a straight a-c load. This is discussed in Chapter 4.

(*c*) *Half-wave rectifiers* carry unbalanced direct current; this may necessitate less a-c flux density, hence larger transformers, than full-wave rectifiers. Unbalance in the three-phase half-wave type can be avoided by the use of zigzag connections, but an increase in size over full-wave results because of the out-of-phase voltages. These connec-

tions are desirable in full-wave rectifiers when half voltage is obtained from a center tap. See Table VII.

(*d*) *Single-phase full-wave rectifiers with two anodes* have higher secondary volt-amperes for a given primary v-a rating than a filament transformer. Bridge-type (four-anode) rectifiers have equal primary and secondary volt-amperes, as well as balanced direct current, and plate transformers for these rectifiers are smaller than for other types. Three-phase rectifier transformers are smaller in total size but require more coils. The three-phase full-wave type has equal primary and secondary v-a ratings.

(*e*) *Induced secondary voltage* is much higher. Filament transformers are insulated for this voltage but have a few secondary turns

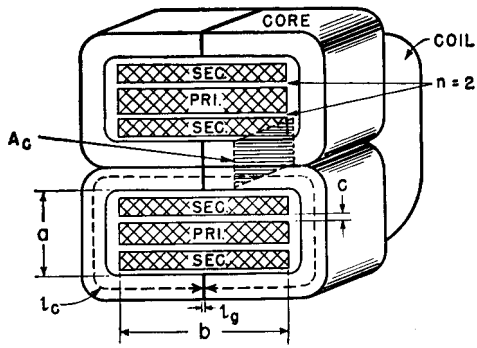

FIG. 57. Dimensions and coil section of anode transformer. Construction shown is for shell-type transformer with 2 Hipersil cores.

of large wire, whereas anode transformers have many turns of small wire. For this reason the volts per layer are higher in anode transformers, and core windows having proportionately greater height and less width than those in Fig. 56 are often preferable. This trend runs counter to the conditions for low leakage inductance and makes it necessary to interleave the windings. Figure 57 shows the windings of a single-phase full-wave rectifier transformer with the primary interleaved between halves of the secondary. This arrangement is especially adaptable to transformers with grounded center tap. The primary-secondary insulation can be reduced to the amount suitable for primary to ground. This is called *graded* insulation.

In large power rectifiers of the gas-filled or pool types, anode current under short-circuit conditions may be very great, and anode transformer windings must be braced to prevent damage. If the conductors

are small, solventless varnish is useful for solidly embedding the conductors.

30. Leakage Inductance. Flux set up by the primary winding which does not link the secondary, or vice versa, gives rise to leakage or self-inductance in each winding without contributing to the mutual flux. The greater this leakage flux, the greater the leakage inductance, because the inductance of a winding equals the flux linkages with unit current in the winding. In Fig. 57, all flux which follows the core path l_c is mutual flux. Leakage flux is the relatively small flux which threads the secondary winding sections, enters the core, and returns to the other side of the secondaries, without linking the primary. The same is true of flux linking only the primary winding. But it is almost impossible for flux to leave the primary winding, enter the core, and re-enter the primary without linking part of the secondary also. The more the primary and secondary windings are interleaved, the less leakage flux there is, up to the limit imposed by flux in the spaces c between sections. These spaces contain leakage flux also; indeed, if there is much interleaving or if the spaces c are large, most of the leakage flux flows in them. Large coil mean turn length, short winding traverse b, and tall window height a all increase leakage flux.

Several formulas have been derived for the calculation of leakage inductance. That originated by Fortescue [1] is generally accurate, and errs, if at all, on the conservative side:

$$L_S = \frac{10.6N^2MT(2nc + a)}{10^9n^2b} \tag{33}$$

where L_S = leakage inductance of both windings in henrys, referred to the winding having N turns
MT = mean length of turn for whole coil in inches
n = number of dielectrics between windings ($n = 2$ in Fig. 57)
c = thickness of dielectric between windings in inches
a = winding height in inches
b = winding traverse in inches.

The greatest gain from interleaving comes when the dielectric thickness c is small compared to the window height; when nc is comparable to the window height, the leakage inductance does not decrease much as n is increased. It is often difficult to reduce the leakage inductance which occurs in high-voltage transformers because of leakage flux in

[1] See *Standard Handbook for Electrical Engineers,* McGraw-Hill Book Co., New York, 1922, 5th ed., p. 413.

spaces c. A small number of turns, short mean turn, and low, wide core windows all contribute to a low value of leakage inductance.

31. Anode Transformer Design. Let the requirements of a rectifier be

1,200 volts 115 ma rectifier d-c output
Single-phase full-wave circuit with 866 tubes
Primary 115 volts 60 cycles
Rectifier regulation 5 per cent maximum
Ambient 55°C

To fulfill these requirements, a reactor-input filter must be used. If 1 per cent is allowed for reactor IR drop, a maximum of 4 per cent regulation is left in the anode transformer. The approximate secondary output voltage is $1{,}200 \times 2.22 = 2{,}660$, say 2,700 volts. The center tap may be grounded. Suppose that a transformer like the one in Fig. 57 is used. The calculations are given in Fig. 58. The various steps are performed in the same order as in filament transformers. The grain-oriented type C core is worked at 38 per cent higher induction, with but 60 per cent of the core loss of Fig. 55; its strip width is 2¼ in., build-up ⅝ in., and window 1 in. by 3 in. for each core loop. Note the difference in primary and secondary volt-amperes and winding heights. Since the primary and secondary are symmetrical about the primary horizontal center line, they have the same mean turn length. Losses and temperature rise are low. Regulation governs size. Secondary layer voltage is high enough to require unusually thick layer paper. This coil is wound on a multiple-coil machine. Winding height is figured on the basis of layer paper adequate for the voltage instead of from Table VI (p. 39), but turns per layer are taken from this table. Since adjacent layers are wound with opposite directions of traverse, the highest voltage across the layer insulation is twice the volts per layer. Layer insulation is used at 46 volts per mil in the secondary; this counts the 1.7 mils of double enamel, which must withstand impregnation without damage. Anode leads and margins withstand 5 kv rms test voltage. Since the secondary center tap is grounded, two thicknesses of 0.010-in. insulation between windings are sufficient. Clearance of 0.253 in. allows room for in-and-out coil taping.

Secondary leakage inductance, from equation 33, is

$$\frac{10.6 \times 4{,}200^2 \times 10.2(4 \times 0.020 + 0.747)}{4 \times 2.375 \times 10^9} = 0.166 \quad \text{henry}$$

At 60 cycles this is $6.28 \times 60 \times 0.166 = 63$ ohms, which would be 240 ohms if the secondary were a single section, and which would increase regulation as set forth in Chapter 4. The regulation calcu-

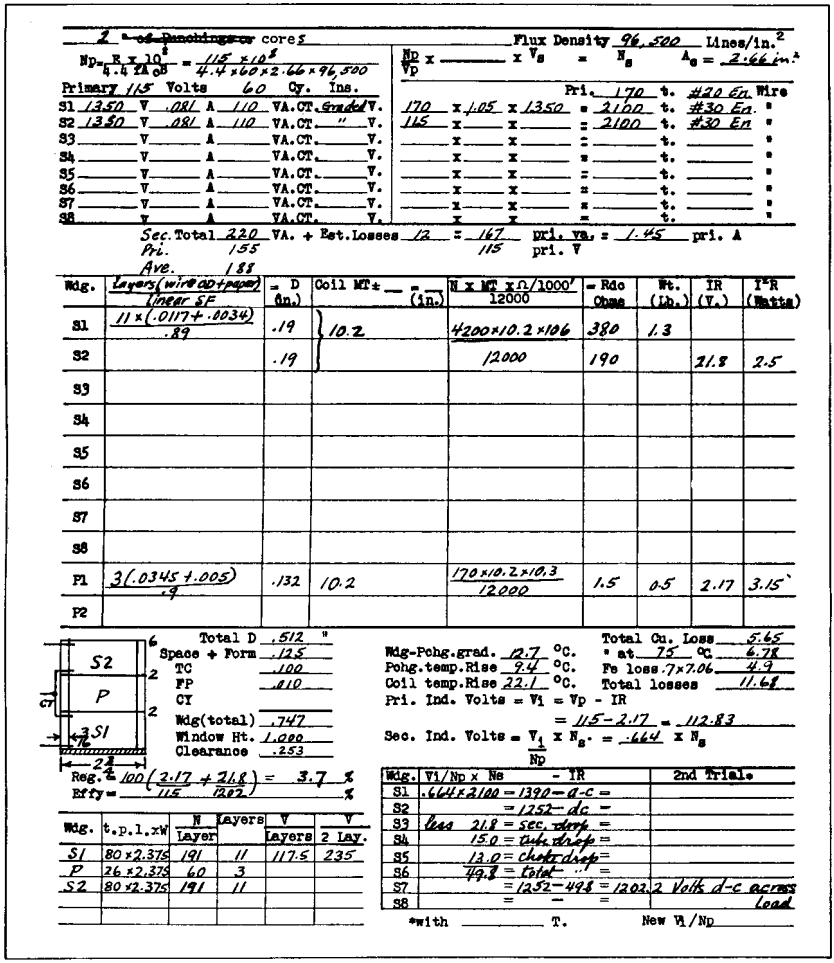

FIG. 58. Anode transformer design calculations.

lated in Fig. 58 is that due to primary IR calculated in the normal manner, plus I_{dc} times one-half the secondary winding resistance.

When high voltage is induced in a winding, the layer insulation and coil size may often be reduced by using the scheme shown in Fig. 59. This is applicable to a plate transformer of the single-phase full-wave

type with center tap grounded. It then becomes practical to make the secondary in two separately wound vertical halves or part coils. One of the part coils is assembled with the turns in the same direction as those of the primary, and the other part coil is reversed so that the turns are in the opposite direction. The two start leads are connected together and to ground as in Fig. 59. It is necessary then to provide only sufficient insulation between windings to withstand the primary test voltage. Channels may be used to insulate the secondaries from the core. With higher voltages, it may be necessary to provide pressboard spacers between the secondary part coils, or to tape the secondary coils separately, but margins must be provided sufficient to prevent creepage across the edges of the spacers.

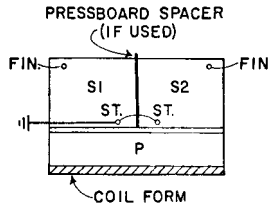

FIG. 59. Anode transformer with C.T. grounded.

32. Combined Anode and Filament Transformers. Anode and filament windings are combined into a single transformer mainly in low-power ratings such as those in receivers and grid bias power supplies.

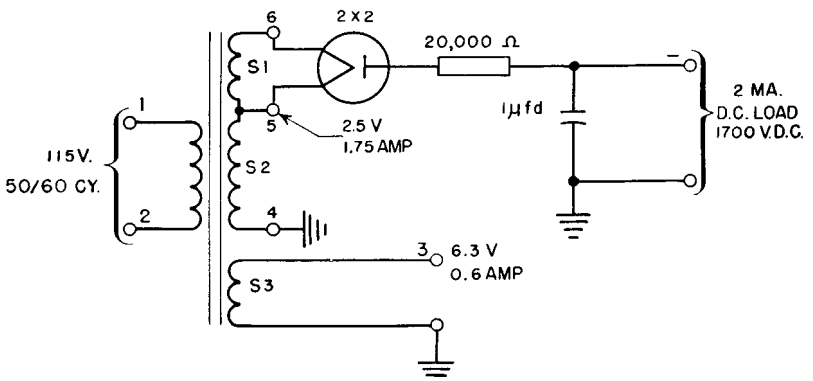

FIG. 60. Power supply transformer.

One widely used combination includes the anode and filament windings for a rectifier and a filament winding for the amplifier tubes. Figures 60 and 61 show how winding insulation sometimes may be graded to require a minimum of insulation and space. The high-voltage filament winding S_1 is placed over the coil form to take advantage of its thick insulation. Layer insulation is sufficient between S_1 and S_2, and between S_2 and S_3. Over and under the primary winding is 115-volt

insulation. Thus Fig. 61 is a high-voltage transformer with no high-voltage insulation in it except what is incidental to the coil form.

Combined anode and filament transformers are difficult to test for regulation or output voltage aside from operation in the rectifier circuit itself, because a-c loads do not duplicate rectifier action. Most transformers of this kind are used in rectifiers with capacitor-input filters or with fixed loads in which regulation is not important.

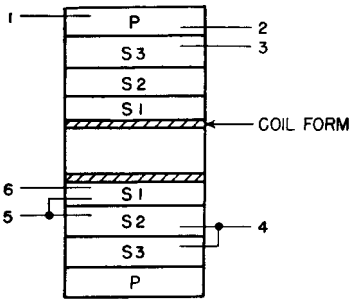

FIG. 61. Winding arrangement to save insulation.

Ratings are easier to predict. Anode secondary v-a rating is the product of rms voltage and current, but the corresponding portion of primary v-a rating depends on the rectifier and is found as mentioned in Sections 24 and 25. To this is added the sum of filament winding v-a ratings, and the primary current can then be calculated from the total volt-amperes.

33. Power Supply Frequency. Foregoing examples were based on a 60-cycle supply. Twenty-five-cycle transformer losses are lower for a given induction. It follows that induction can be increased somewhat over the 60-cycle value, but saturation currents prevent a decided increase. Larger size results, nearly 2:1 in volume. Otherwise 25-cycle transformers are not appreciably different from 60-cycle transformers.

Power supply frequencies of 400 and 800 cycles are used mainly in aircraft and portable equipment to save weight and space. Silicon-steel core materials 0.005 in. thick are principally used at these frequencies to reduce eddy currents. Losses at 400 and 800 cycles for three core materials are shown in Fig. 62. These losses can be the controlling factors in determining transformer size, because a given material saturates at nearly the same induction whether the frequency is 60 cycles or 800 cycles, but the core loss is so high at 800 cycles that the core material cannot be used near the saturation density. The higher the induction the higher the core heating. For this reason, class B insulation can be used in many 400- and 800-cycle designs to reduce size still further. If advantage is taken of both the core material and insulation, 800-cycle transformers can be reduced to 10 per cent of the size of 60-cycle transformers of the same rating. Typical

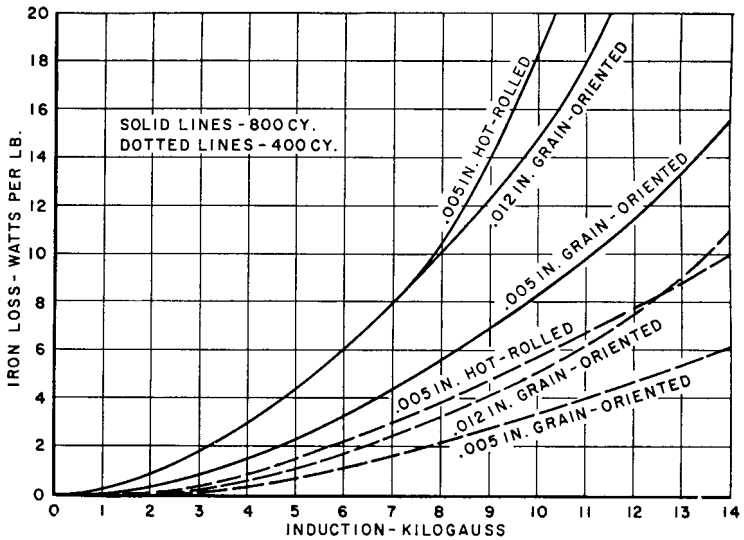

FIG. 62. Silicon-steel core loss at 400 and 800 cycles.

combinations of grain-oriented core material and insulation are as follows:

Frequency	Strip Thickness	*B*-Gauss	Class of Insulation	Operating Temperature
60	0.014	15,000	A	95°C
400	0.005	12,500	B	140°C
800	0.005	8,500	B	140°C

In very small units, these flux densities may be used at lower temperatures and with class A insulation because of regulation. The special 4-mil steel developed for 400 cycles makes possible size reduction comparable to that for 800 cycles. The necessity for small dimensions, especially in aircraft apparatus, continually increases the tendency to use materials at their fullest capabilities.

Many small 60-cycle transformers have core loss which is small compared to winding or copper loss. This condition occurs because inductance is limited by exciting current rather than by core loss. As size or frequency increases, this limitation disappears, and core loss is limited only by design considerations. Under such circumstances, the ratio of core to copper loss for maximum rating in a given size may be found as follows. Let

W_e = core loss
W_s = copper loss
K_1, K_2, etc. = constants
E = secondary voltage
I = secondary current

For a transformer with a given core, winding, volt-ampere rating, and frequency, $W_e \approx K_1E^2$. For a given winding, $W_s = K_2I^2$. Also, for a given size, $W_e + W_s = K_3$, a quantity determined by the permissible temperature rise. Hence the transformer volt-ampere rating is approximately

$$EI = \sqrt{\frac{W_eW_s}{K_1K_2}}$$
$$= K_4\sqrt{W_e(K_3 - W_e)}$$

For a maximum, the rating may be differentiated with respect to W_e, and the derivative equated to zero:

$$0 = K_3 - 2W_e$$

whence

$$W_e = K_3/2$$

so that $W_s = K_3/2$, or copper and core losses are equal for maximum rating.

Although this equality is not critical, and is subject to many limitations such as core shape, voltage rating, and method of cooling, it does serve as a guidepost to the designer. If a transformer design is such that a large disparity exists between core and copper losses, size or temperature rise often may be reduced by a redesign in the direction of equal losses.

34. An 800-Cycle Transformer Design.

Primary 120 volts 800 cycles
Rectifier to deliver 0.2 amp at +450 volts using 5U4G in single-phase full-wave circuit with 0.5-μfd capacitor input filter.

Figures 51 and 52 tell whether the product ωCR_L will produce the necessary d-c output without exceeding the rectifier tube peak inverse voltage rating and peak current rating.

$$\omega CR_L = 6.28 \times 800 \times 0.5 \times 10^{-6} \times (450/0.2) = 5.65$$

For R_S assume a peak current of 0.5 amp. Average anode character-

istics show 97 volts tube drop, or $97 \div 0.5 = 194$ ohms at peak current. $R_S/R_L = 194/2{,}250 = 0.086$. Add 5 per cent for transformer windings; estimated $R_S/R_L = 13.6$ per cent.

Check on Peak Current from Fig. 52.

$$n\omega CR_L = 11.3$$

$$\hat{I}_p = 5I_p = 5 \times 0.1 = 0.5 \text{ amp}$$

the peak value assumed. Rms current in tube plates and secondary windings is $2 \times 0.1 = 0.2$ amp. Output voltage, from Fig. 51, is 0.69 peak a-c voltage per side. Hence secondary rms voltage per side is $450 \times 0.707 \div 0.69 = 460$ volts, and secondary volt-amperes $= 2 \times 460 \times 0.2 = 184$. The anode transformer must deliver $2 \times 460 = 920$ volts at 0.2 amp rms. Primary volt-amperes $= 0.707 \times 184 = 130$.

Inverse peak voltage is the peak value of this voltage plus the d-c output, because the tube filament is at d-c value, plus a small amount of ripple, while one anode has a maximum of peak negative voltage, during the non-conducting interval. Thus peak inverse voltage is $460 \times 1.41 + 450 = 1{,}100$ volts, which is within the tube rating.

Choice of core for this transformer is governed by size and cost considerations. Assume that the core works at 8,500 gauss. The loss per pound for 0.005-in. silicon steel and grain-oriented steel is 12.2 and 6.6, respectively. (See Fig. 62.) But punchings have 80 per cent stacking factor, whereas the type C core has 90 per cent. In this thickness 0.005-in. grain-oriented steel compares still better with ordinary silicon steel than Fig. 62 would indicate and so will be used for the core.

Let two type C cores be used with the following dimensions:

Strip width	¾ in.	Window height	⅝ in.
Build	⅜ in.	Window width	1½ in.
Total net core area	0.506 sq in.	Core weight	0.75 lb

Turns could be figured from equation 32, except that the induction is in gauss. Since many core data are given in gauss, equation 32 is changed for convenience to

$$N_1 = \frac{3.49E \times 10^6}{fA_cB} \tag{34}$$

where dimensions are in inches and B is in gauss. Primary turns are then

$$\frac{3.49 \times 120 \times 10^6}{800 \times 0.506 \times 8{,}500} = 122$$

Final design figures are:

Primary 122 turns	No. 26 glass-covered wire	d-c resistance 1.8 ohms
Secondary 900 turns	No. 29 glass-covered wire	d-c resistance 38 ohms

Primary copper loss at 100°C	=	3.35 watts
Secondary copper loss at 100°C	=	2.04 watts
Core loss 6.6 × 0.75	=	4.95 watts
Total losses		10.34 watts

With an open-type mounting and mica insulation this transformer has a temperature rise of 75 centigrade degrees.

35. Polyphase Transformers. In large power rectifiers three-phase supplies are generally used. Accurate phase voltages must be maintained to avoid supply frequency ripple in the output. Delta-connected primaries are shown in Table VII for the various rectifiers; these are preferable to open-delta because phase balance is better, and to Y-connections because of possibly high third harmonics. Open-delta connections require only two single-phase transformers instead of three, but a similar saving may be had by using a single core-type three-phase unit which retains the phase-balance advantage. The main drawback to a three-phase core is its special dimensions. Often, to use standard parts, three single-phase units are employed in the smaller power ratings. But if the power is hundreds or thousands of kilowatts, the cores are built to order, and the weight saving in a three-phase core is significant.

Two- and three-phase filament transformers are used with output tubes for large broadcast stations to heat filaments uniformly and reduce hum in the r-f output.

36. Design Chart. In preceding sections, it has been stated that special conditions require tailored designs. Windings for simple low-voltage 60-cycle transformers may be chosen from the chart of Fig. 63. This chart is based upon the following conditions:

(*a*) Two untapped concentric windings; primary wound first.
(*b*) Operating voltage in both windings less than 1,000 volts.
(*c*) Power supply frequency 60 cycles.
(*d*) Maximum temperature rise 40°C in 65°C ambient.
(*e*) Resistive loads.

(*f*) Equal I^2R losses in primary and secondary.
(*g*) Solventless resin impregnated coils.
(*h*) Open-type assemblies like those of Fig. 15.
(*i*) Grain-oriented silicon-steel cores.

It was found that 40°C rise in the four smallest sizes resulted in excessive voltage regulation. For example, a small filament transformer would deliver correct filament voltage at room ambient temperature of 25°C, but at 105°C this voltage dropped to less than the published tube limit. Hence the winding regulation in the two smallest transformers was limited to 15 per cent, and in the next two larger sizes to 10 per cent. In still larger sizes, the 40°C temperature limit held the regulation to less than 10 per cent.

In using the chart, ratings rarely fall exactly on the v-a values assigned to each core. Hence a core is generally chosen with somewhat greater than required rating. Lower regulation and temperature rise than maximum then result. Wire size in quadrant I also increases in discrete sizes, and if the chart indication falls between two sizes the smaller size should be used.

Instructions for Using Fig. 63.

1. Choose a core from Table VIII which has a v-a rating equal to or greater than that required.
2. From rated primary and secondary voltages, find number of turns for both windings in quadrant IV.
3. From rated primary and secondary currents, find wire size for both windings in quadrant I.
4. Project turns across to quadrant III to obtain winding resistances.

TABLE VIII. TRANSFORMER SIZE, RATING, AND REGULATION

Core	Maximum V-A Rating	% Regulation	Total Weight (lb)	Overall Dimensions (inches)
1	5	15	0.38	1¾ × 1¾ × 1¾
2	10	15	0.68	1⅞ × 2⅜ × 1¾
3	25	10	1.2	2¼ × 2⅞ × 2¼
4	50	10	2.2	2½ × 3⅛ × 2½
5	100	8	3.8	3⅛ × 3¾ × 3
6	200	6	6.4	3⅞ × 4¾ × 3⅝
7	350	4	11.0	4⅜ × 5⅜ × 4
8	500	3	15	5⅛ × 6⅛ × 5
9	1,000	2.2	24	5⅞ × 6¾ × 6⅛
10	1,600	1.8	36	7¼ × 8¼ × 7½
11	3,200	1.2	75	9¾ × 12¾ × 8

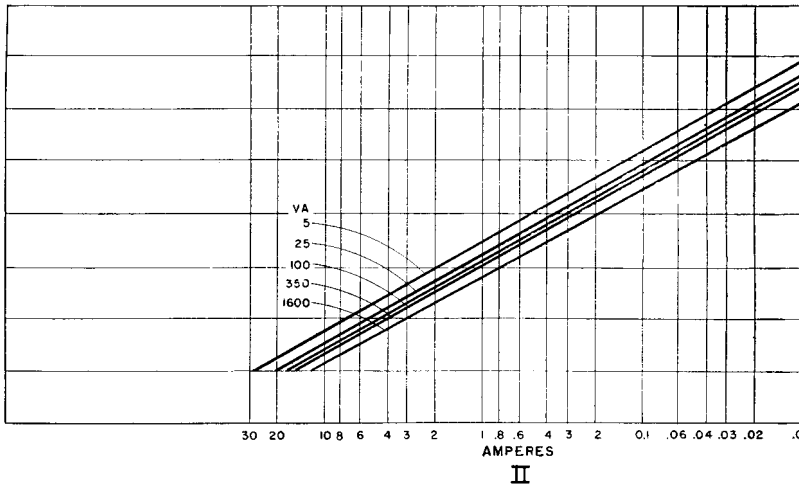

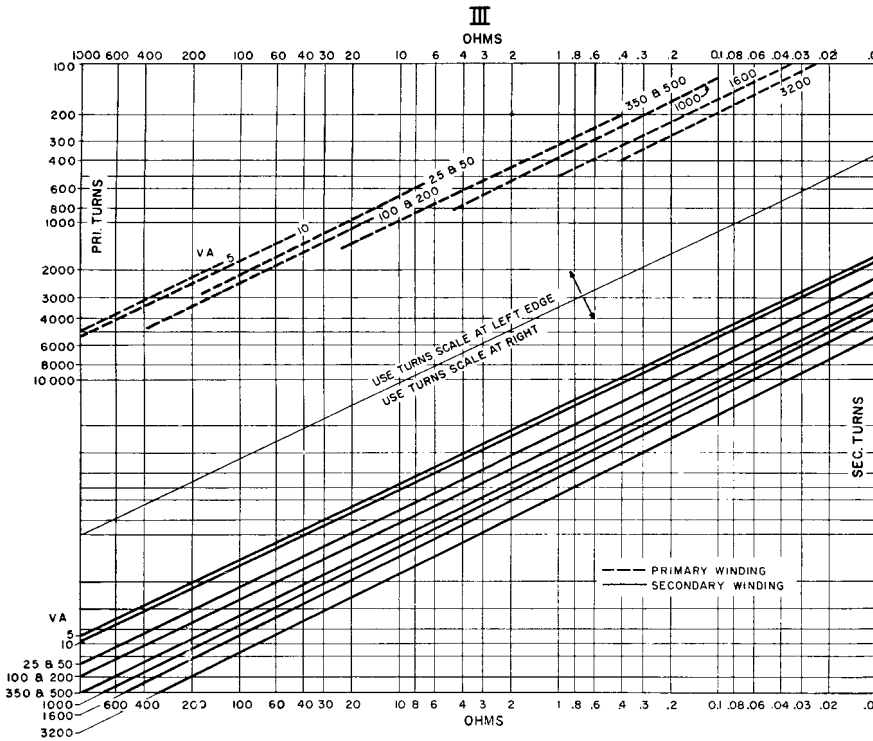

FIG. 63. Low-voltage 60-cycle transformer design chart.

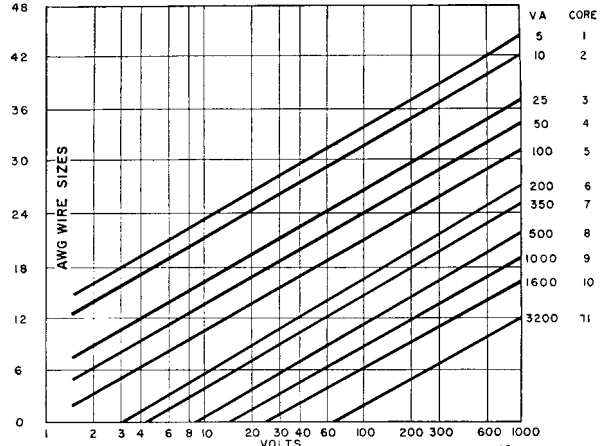

I

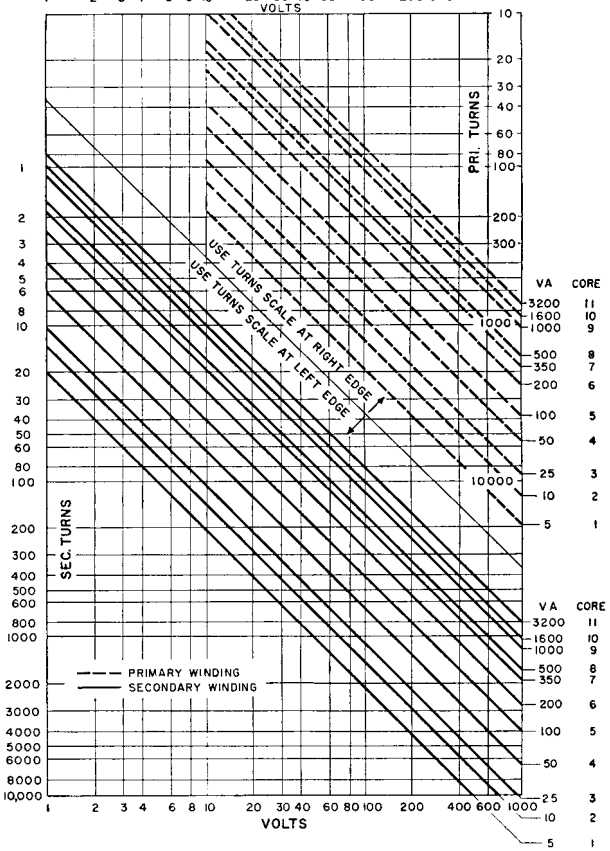

IV

FIG. 63. *(Continued)*

Departures from the assumed conditions preclude direct application of Fig. 63, but the chart is still useful as a starting point in design. For some common modifications, the following notes apply:

1. For each additional secondary winding reduce core maximum rated volt-amperes by 10 per cent. Choose wire size from quadrant II.
2. For 50-cycle transformers, reduce core maximum rated v-a 10 per cent.
3. When permissible temperature rise is higher than 40°C, core maximum volt-amperes equal (v-a in table) $\times \sqrt{\text{temperature rise}/40°\text{C}}$.

Example. A transformer is required for 115/390 volts, 60 cycles, to deliver 77 volt-amperes. This rating falls between the maxima for cores 4 and 5. Using core 5 at 115 volts, we read, from Fig. 63, for the primary, 440 turns of No. 22 wire and 3 ohms d-c resistance; for the secondary, 1,700 turns of No. 27 wire and 40 ohms d-c resistance.

37. Reactors. Reactors are used in electronic power equipment to smooth out ripple voltage in d-c supplies, so they carry direct current in the coils. It is common practice to build such reactors with air gaps in the core to prevent d-c saturation. The air gap, size of the core, and number of turns depend upon three interrelated factors: inductance desired; direct current in the winding; and a-c volts across the winding.

The number of turns, the direct current, and the air gap determine the d-c flux density, whereas the number of turns, the volts, and the core size determine the a-c flux density. If the sum of these two flux densities exceeds saturation value, noise, low inductance, and nonlinearity result. Therefore a reactor must be designed with knowledge of all three of the conditions above.

Magnetic flux through the coil has two component lengths of path: the air gap l_g, and the length of the core l_c. The core length l_c is much greater geometrically than the air gap l_g, as indicated in Fig. 57, but the two components do not add directly because their permeabilities are different. In the air gap, the permeability is unity, whereas in the core its value depends on the degree of saturation of the iron. The effective length of the magnetic path is $l_g + (l_c/\mu)$, where μ is the permeability for the steady or d-c component of flux.

Reactor design is, to a large extent, the proportioning of values of air gap and magnetic path length divided by permeability. If the air gap is relatively large, the reactor inductance is not much affected by

changes in μ; it is then called a *linear* reactor. If the air gap is small, changes in μ due to current or voltage variations cause inductance to vary; then the reactor is non-linear.

When direct current flows in an iron-core reactor, a fixed magnetizing force H_{dc} is maintained in the core. This is shown in Fig. 64 as the vertical line H_{dc} to the right of zero H in a typical a-c hysteresis loop, the upper half DB_mD' of which corresponds to that in Fig. 21. Increment ΔH of a-c magnetization, superposed on H_{dc}, causes flux density increment ΔB, with permeability μ_Δ equal to the slope of dotted line AB_m. ΔB is twice the peak a-c induction B_{ac}. It will be recalled from Fig. 19 that the normal induction curve OB_m is the locus of the end points of a series of successively smaller major hysteresis loops. Since the top of the minor loop always follows the left side of a major loop, as H_{dc} is reduced in successive steps the upper ends of corresponding minor loops terminate on the normal induction curve.

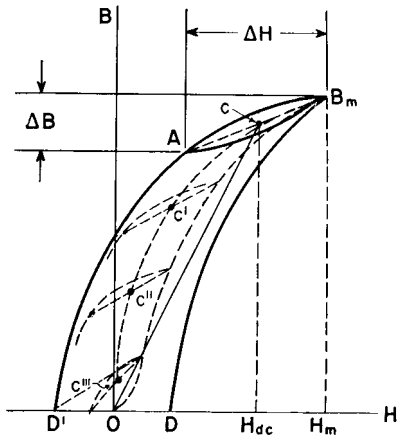

FIG. 64. Incremental permeability with different amounts of d-c magnetization.

Dotted-line slopes of a series of minor loops are shown in Fig. 64, the midpoints of which are C, C', C'', and C'''. Increment of induction ΔB is the same for each minor loop. It will be seen that the width of the loop ΔH is smaller, and hence μ_Δ is greater, as H_{dc} is made smaller.

Midpoints C, C', etc., form the locus of d-c induction. The slope of straight line OC is the d-c permeability for core magnetization H_{dc}. It is much greater than the slope of AB_m. Hence incremental permeability is much smaller than d-c permeability. This is true in varying degree for all the minor loops. The smaller ΔB is, the less the slope of a minor loop becomes, and consequently the smaller the value of incremental permeability μ_Δ. The curve in Fig. 65 marked μ is the normal permeability of 4% silicon steel for steady values of flux, in other words, for the d-c flux in the core. It is 4 to 20 times as great as the incremental permeability μ_Δ for a small alternating flux superposed upon the d-c flux. The ratio of μ to μ_Δ gradually increases as d-c flux density increases.

Because of the low value of μ_Δ for minute alternating voltages, the effective length of magnetic path $l_g + (l_c/\mu_\Delta)$ is considerably greater for alternating than for steady flux. But the inductance varies inversely as the length of a-c flux path. If, therefore, the incremental permeability is small enough to make l_c/μ_Δ large compared to l_g, it follows that small

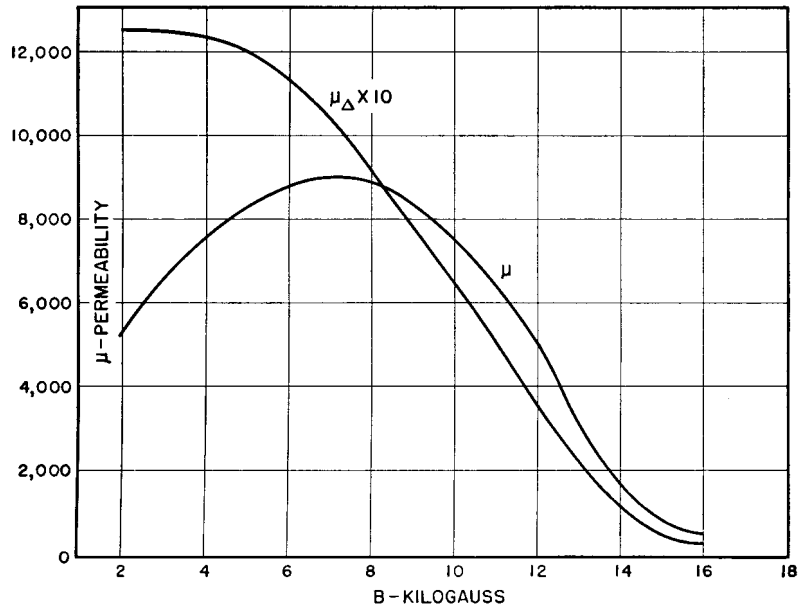

FIG. 65. Normal and incremental permeability of 4% silicon steel.

variations in l_g do not affect the inductance much. For this reason the exact value of the air gap is not important with small alternating voltages.

Reactor size, with a given voltage and ratio of inductance to resistance, is proportional to the stored energy LI^2. For the design of reactors carrying direct current, that is, the selection of the right number of turns, air gap, and so on, a simple method was originated by C. R. Hanna.[1] By this method, magnetic data are reduced to curves such as Fig. 66, plotted between LI^2/V and NI/l_c from which reactors can be designed directly. The various symbols in the coordinates are:

[1] "Design of Reactances and Transformers Which Carry Direct Current," by C. R. Hanna, *J. AIEE, 46,* 128 (February, 1927).

L = a-c inductance in henrys
I = direct current in amperes
V = volume of iron core in cubic inches
= $A_c l_c$ (see Fig. 57 for core dimensions)
A_c = cross section of core in square inches
l_c = length of core in inches
N = number of turns in winding
l_g = air gap in inches

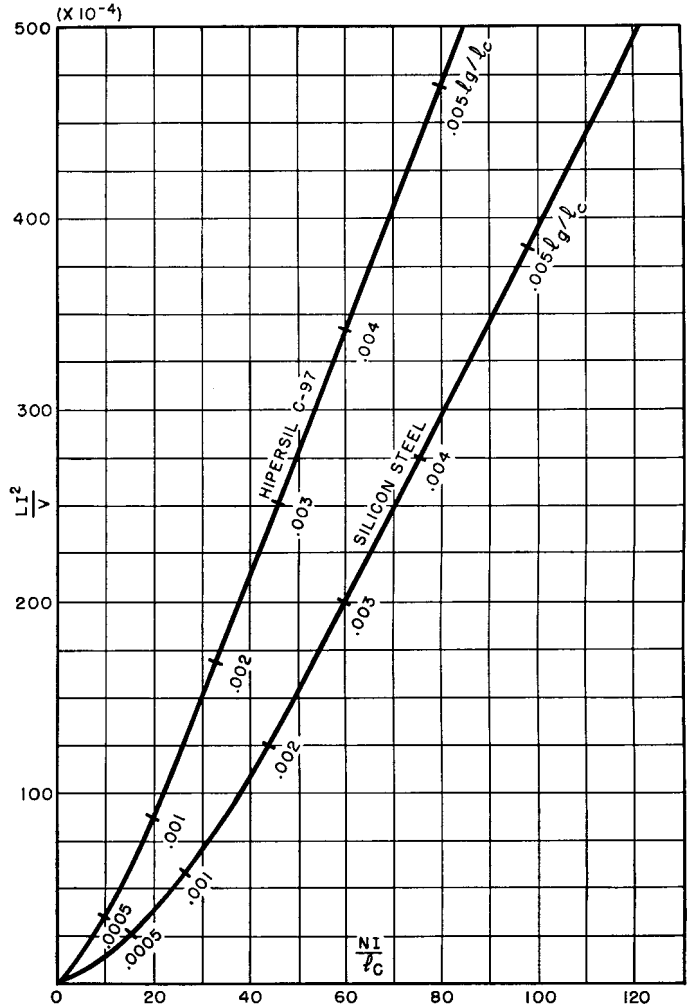

FIG. 66. Reactor energy per unit volume versus ampere-turns per inch of core.

Each curve of Fig. 66 is the envelope of a family of fixed air-gap curves such as those shown in Fig. 67. These curves are plots of data based upon a constant small a-c flux (10 gauss) in the core but a large

and variable d-c flux. Each curve has a region of optimum usefulness, beyond which saturation sets in and its place is taken by a succeeding curve having a larger air gap. A curve tangent to the series of fixed air-gap curves is plotted as in Fig. 66, and the regions of optimum use-

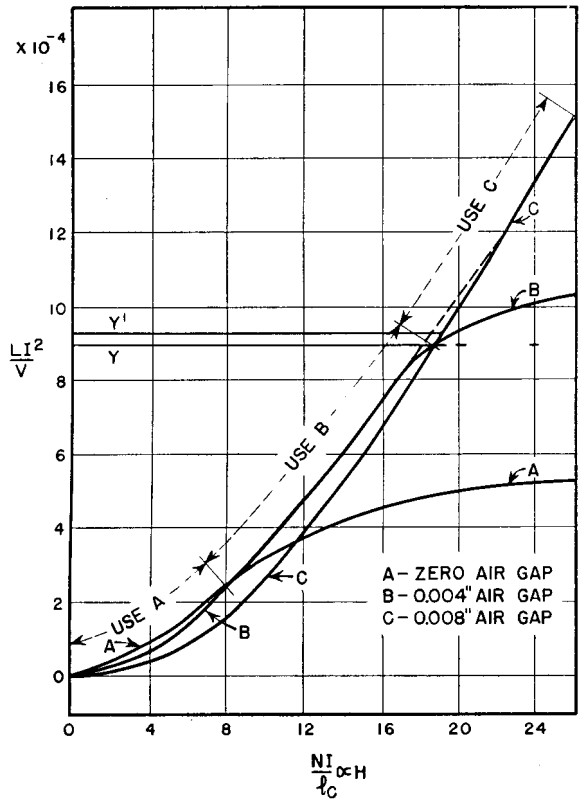

FIG. 67. Fixed air-gap curves. For $B_{dc} \gg B_{ac}$, air gap is not critical.

fulness are indicated by the scale l_g/l_c. Hence Fig. 66 is determined mainly by the d-c flux conditions in the core and represents the most LI^2 for a given amount of material.

Figure 67 illustrates how the exact value of air gap is of little consequence in the final result. The dotted curve connecting B and C is for a 6-mil gap. Point Y' represents the maximum inductance that could be obtained from a given core for $NI/l_c = 19$. Point Y is the inductance obtained if a gap of either 4 or 8 mils is used. The differ-

ence in inductance between Y and Y' is 4 per cent, for a difference in air gap of 33 per cent.

An example will show how easy it is to make a reactor according to this method.

Example. Assume a stack of silicon-steel laminations having a cross section ⅞ in. by ⅞ in., and with iron filling 92 per cent of the space. The length of the flux path l_c in this core is 7½ in. It is desired to know how many turns of wire and what air gap are necessary to produce 70 henrys when 20 ma direct current are flowing in the winding.

This problem is solved as follows:

$$A_c = (0.875)^2 \times 0.92 = 0.71 \text{ sq in.}$$

$$V = 0.71 \times 7.5 = 5.3$$

$$\frac{LI^2}{V} = \frac{70 \times 4 \times 10^{-4}}{5.3} = 53 \times 10^{-4}$$

In Fig. 66 the abscissa corresponding to $LI^2/V = 53 \times 10^{-4}$ is $NI/l_c = 25$ for silicon steel. The ratio of air gap to core length l_g/l_c is between 0.0005 and 0.001.

$$NI/l_c = 25$$

$$N = (25 \times 7.5)/0.020 = 9{,}350 \text{ turns}$$

The total air gap is nearly $0.001 \times 7\frac{1}{2}$ or 7.5 mils; the gap at each joint is half of this value, or 3.75 mils.

The conditions underlying Hanna's method of design are met in most applications. In receivers and amplifiers working at low audio levels, the alternating voltage is small and hence the alternating flux is small compared to the steady flux. Even if the alternating voltage is of the same order as the direct voltage, the alternating flux may be small, especially if a large number of turns is necessary to produce the required inductance; for a given core the alternating flux is inversely proportional to the number of turns. D-c resistance of the coil is usually fixed by the regulation or size requirements. Heating seldom affects size.

38. Reactors with Large A-C Flux. With the increasing use of higher voltages, it often happens that the a-c flux is no longer small compared to the d-c flux. This occurs in high-impedance circuits where the direct current has a low value and the alternating voltage has a high value. The inductance increases by an amount depending on the values of a-c and d-c fluxes. Typical increase of inductance is shown

in Fig. 68 for a reactor working near the saturation point. Increasing a-c flux soon adds to the saturation, which prevents further inductance

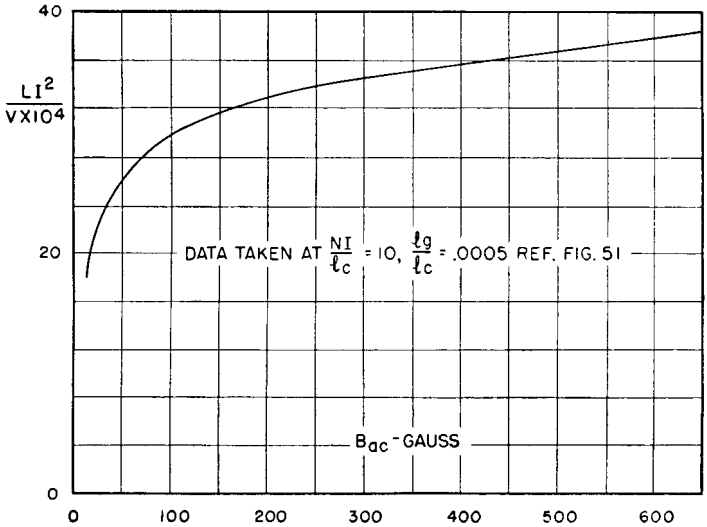

FIG. 68. Increase of inductance with a-c induction.

increase and accounts for the flattening off in Fig. 68. Saturation of this sort may be avoided by limiting the value of the d-c flux.

To illustrate the effect of these latter conditions, suppose that a reactor has already been designed for negligibly small alternating flux and operates as shown by the minor loop with center at G, Fig. 69. Without changing anything else, suppose that the alternating voltage across the reactor is greatly increased, so that the total a-c flux change is from zero to B_m. (Assume that the reactor still operates about point G.) The hysteresis loop, however, becomes the unsymmetrical figure $OB_mD'O$. The average permeability during the positive flux swing is represented by the line GB_m, and during the negative flux swing by OG. The slope of GB_m is greater than that of the minor loop; hence, the first effect exhibited by the reactor is an increase of inductance.

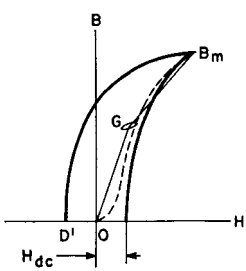

FIG. 69. Change of permeability with a-c induction.

The increase of inductance is non-linear, and this has a decided

effect upon the performance of the apparatus. An inductance bridge measuring such a reactor at the higher a-c voltage would show an inductance corresponding to the average slope of lines OG and GB_m. That is, the average permeability during a whole cycle is the average of the permeabilities which obtain during the positive and negative increments of induction, and it is represented by the average of the slopes of lines OG and GB_m. But if the reactor were put in the filter of a rectifier, the measured ripple would be higher than a calculated value based upon the bridge value of inductance. This occurs because the positive peaks of ripple have less impedance presented to them than do the negative peaks, and hence they create a greater ripple at the load. Suppose, for example, that the ripple output of the rectifier is 500 volts and that this would be attenuated to 10 volts across the load by a linear reactor having a value of inductance corresponding to the average slope of lines OG and GB_m. With the reactor working between zero and B_m, suppose that the slope of OG is 5 times that of GB_m. The expected average ripple attenuation of 50:1 becomes 16.7:1 for positive flux swings, and 83.3:1 for negative, and the load ripple is

$$\frac{1}{2}\left(\frac{500}{16.7}+\frac{500}{83.3}\right)=18 \text{ volts}$$

or an increase of nearly 2:1 over what would be anticipated from the measured value of inductance.

This non-linearity could be reduced by increasing the air gap somewhat, thereby reducing H_{dc}. Moreover, the average permeability increases, and so does the inductance. It will be apparent that decreasing H_{dc} further means approaching in value the normal permeability. This can be done only if the maximum flux density is kept low enough to avoid saturation. Conversely, it follows that, if saturation is present in a reactor, it is manifested by a decrease in inductance as the direct current through the winding is increased from zero to full-load value.

In a reactor having high a-c permeability the equivalent length of core l_c/μ is likely to be small compared to the air gap l_g. Hence, it is vitally important to keep the air gap close to its proper value. This is, of course, in marked contrast to reactors not subject to high a-c induction.

If a choke is to be checked to see that no saturation effects are present, access must be had to an inductance bridge. With the proper values of alternating voltage across the reactor, measurements of inductance can be made with various values of direct current through it.

If the inductance remains nearly constant up to normal direct current, no saturation is present, and the reactor is suitable for the purpose. If, on the other hand, the inductance drops considerably from zero direct current to normal direct current, the reactor very probably is non-linear. Increasing the air gap may improve it; otherwise, it should be discarded in favor of a reactor which has been correctly designed for the purpose.

Filter reactors subject to the most alternating voltage for a given direct voltage are those used in choke-input filters of single-phase rectifiers. The inductance of this type of reactor influences the following:

Value of ripple in rectified output.

No-load to full-load regulation.

Transient voltage dip when load is suddenly applied, as in keyed loads.

Peak current through tubes during each cycle.

Transient current through rectifier tubes when voltage is first applied to rectifier.

It is important that the inductance be the right value. Several of these effects can be improved by the use of swinging or tuned reactors. In a swinging reactor, saturation is present at full load; therefore the inductance is lower at full load than at no load. The higher inductance at no load is available for the purpose of decreasing voltage regulation. The same result is obtained by shunt-tuning the reactor, but here the inductance should be constant from no load to full load to preserve the tuned condition.

In swinging reactors, all or part of the core is purposely allowed to saturate at the higher values of direct current to obtain high inductance at low values of direct current. They are characterized by smaller gaps, more turns, and larger size than reactors with constant inductance ratings. Sometimes two parallel gaps are used, the smaller of which saturates at full direct current. When the function of the reactor is to control current by means of large inductance changes, no air gap is used. Design of such reactors is discussed in Chapter 9.

The insulation of a reactor depends on the type of rectifier and how it is used in the circuit. Three-phase rectifiers, with their low ripple voltage, do not require the turn and layer insulation that single-phase rectifiers do. If the reactor is placed in the ground side of the circuit one terminal requires little or no insulation to ground, but the other terminal may operate at a high voltage to ground. In single-phase

rectifiers the peak voltage across the reactor is E_{dc}, so the equivalent rms voltage on the insulation is $0.707E_{dc}$. But for figuring $B_{\max}$ the rms voltage is $0.707 \times 0.67E_{dc}$. Reactor voltages are discussed in Chapter 4.

39. Linear Reactor Design. A method of design for linear reactors is based on three assumptions which are justified in the foregoing:

(*a*) The air gap is large compared to l_c/μ, μ being the d-c permeability.

(*b*) A-c flux density depends on alternating voltage and frequency.

(*c*) A-c and d-c fluxes can be added or subtracted arithmetically.

From (*a*) the relation $B = \mu H$ becomes $B = H$. Because of fringing of flux around the gap, an average of $0.85B$ crosses over the gap. Hence $B_{dc} = 0.4\pi NI_{dc}/0.85l_g$. With l_g in inches this becomes

$$B_{dc} = 0.6NI_{dc}/l_g \quad \text{gauss} \tag{35}$$

Transposing equation 34

$$B_{ac} = (3.49E \times 10^6)/fA_cN \quad \text{gauss} \tag{36}$$

The sum of B_{ac} and B_{dc} is $B_{\max}$, which should not exceed 11,000 gauss for 4% silicon steel, 16,000 gauss for grain-oriented steel, or 10,000 gauss for a 50% nickel alloy. Curves are obtainable from steel manufacturers which give incremental permeability μ_Δ for various combinations of these two fluxes. Figure 70 shows values for 4% silicon steel.

By definition, inductance is the flux linkages per ampere or, in cgs units,

$$L = \frac{\phi N}{10^8 I_M} = \frac{B_{ac}A_cN}{10^8 I_M} \tag{37}$$

But

$$B_{ac} = \frac{0.4\pi NI_M}{l_g + (l_c/\mu_\Delta)}$$

If this is substituted in equation 37

$$L = \frac{3.19N^2A_c \times 10^{-8}}{l_g + (l_c/\mu_\Delta)} \quad \text{henrys} \tag{38}$$

provided that dimensions are in inches. The term A_c in equation 38 is greater than in equation 36 because of the space factor of the laminations; if the gap is large A_c is greater still because the flux across it

fringes. With large gaps, inductance is nearly independent of μ_Δ, at least with moderate values of B_{max}. With small gaps, permeability

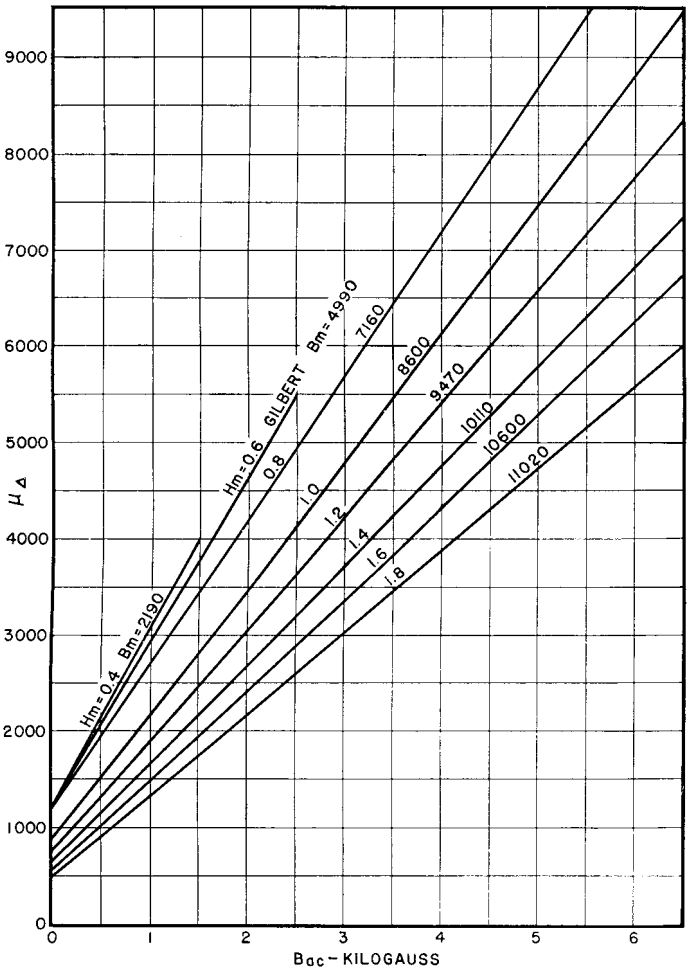

FIG. 70. Incremental permeability for 4% silicon steel with high a-c induction.

largely controls. There is always a certain amount of gap even with punchings stacked alternately in groups of 1. Table IX gives the approximate gap equivalent of various degrees of interleaving laminations for magnetic path l_c of 5.5 in.

TABLE IX. EQUIVALENT GAPS WITH INTERLEAVED LAMINATIONS

0.014-in. Laminations Alternately Stacked	Equivalent Air Gap in Inches (Total) with Careful Stacking
In groups of 1	0.0005
In groups of 4	0.001
In groups of 8	0.002
In groups of 12	0.003
In groups of 16	0.004
Butt stacking with zero gap	0.005

Example. An input reactor is required for the filter of a 1,300-volt, ¼-amp, single-phase, full-wave, 60-cycle rectifier. Let $N = 2{,}800$ turns, net $A_c = 2.48$ sq in., gross $A_c = 2.76$ sq in., $l_c = 9$ in., $l_g = 0.050$ in. The 120-cycle voltage for figuring B_{ac} is $0.707 \times 0.67 \times 1{,}300 = 605$ volts.

$$B_{dc} = \frac{0.6 \times 2{,}800 \times 0.25}{0.050} = 8{,}400$$

$$B_{ac} = \frac{3.49 \times 605 \times 10^6}{120 \times 2.48 \times 2{,}800} = 2{,}540$$

$$B_{\max} = 10{,}940 \text{ gauss}$$

Figure 70 shows

$$\mu_\Delta = 2{,}650$$

$$L = \frac{3.19 \times (2{,}800)^2 \times 2.76 \times 10^{-8}}{0.050 + \frac{9}{2650}} = 13.0 \text{ henrys}$$

40. Linear Reactor Chart. In the preceding section, it was assumed that the core air gap is large compared to l_c/μ, where μ is the d-c permeability. In grain-oriented steel cores the air gap may be large compared to l_c/μ_Δ, because of the high *incremental* permeability of these cores. When this is true, variations in μ do not affect the total effective magnetic path length or the inductance to substantial degree. Reactor properties may then be taken from Fig. 71. In order to keep the reactor linear, it is necessary to limit the flux density. For grain-oriented silicon-steel cores, inductance is usually linear within 10 per cent if the d-c component of flux B_{dc} is limited to 12,000 gauss and the a-c component B_{ac} to 3,000 gauss.

Dotted lines in quadrant I are plots of turns vs. core area for a given wire size and for low-voltage coils, where insulation and margins are governed largely by mechanical considerations. Core numbers in Fig. 71 have the same dimensions and weight as in Table VIII.

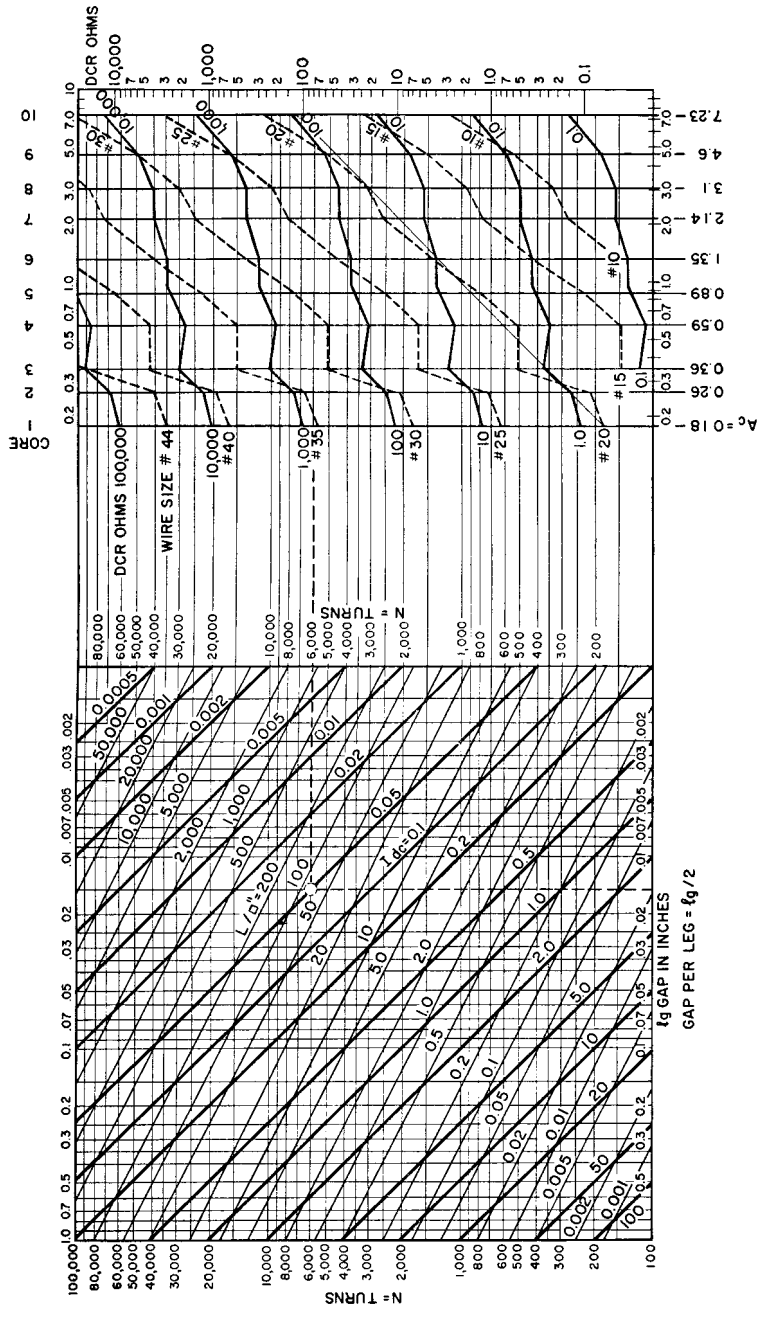

FIG. 71. Linear reactor design chart.

If the cores increased in each dimension by exactly the same amount, the lines in quadrant I would be straight. In an actual line of cores, several factors cause the lines to be wavy:

(*a*) Ratios of core window height to window width and core area deviate from constancy.
(*b*) Coil margins increase stepwise.
(*c*) Insulation thickness increases stepwise.

A-c flux density in the core may be calculated by equation 36, and B_{dc} by equation 35. If B_m materially exceeds 15,000 gauss, saturation is reached, and the reactor may become non-linear or noisy.

Instructions for Using Fig. 71.

1. Estimate core to be used.
2. Divide required inductance by area (A_c) of estimated core to obtain a value of L/sq in.
3. In second quadrant, locate intersection of L/sq in. and rated I_{dc}.
4. On this intersection, read total gap length (l_g) and number of turns (N). Gap per leg = $l_g/2$.
5. Project intersection horizontally into first quadrant to intersect vertical line which corresponds to estimated core. This second intersection gives d-c resistance and wire size.

Example. Required: 15 henrys at I_{dc} = 50 ma.
Estimate core No. 1.
L/sq in. = 84.3, l_g = 0.015 in., N = 6,000, DCR = 800 ohms.
Wire size = No. 36.
(Example shown starting with dotted circle.)

A similar chart may be drawn for silicon-steel laminations, but to maintain linearity lower values of flux density should be used.

41. Air-Gap Flux Fringing. In Section 39, equation 38 was developed for inductance of a linear reactor with an air gap. It is assumed that 85 per cent of the core flux is confined to the cross section of core face adjoining the gap. The remaining 15 per cent of the core flux "fringes" or leaves the sides of the core, thus shunting the gap. Fringing flux *decreases* the total reluctance of the magnetic path and *increases* the inductance to a value greater than that calculated from equation 38. Fringing flux is a larger percentage of the total for larger gaps. Very large gaps are sometimes broken up into several smaller ones to reduce fringing.

If it is again assumed that the air gap is large compared to l_c/μ, the

reluctance of the iron can be neglected in comparison with that of the air gap. For a square stack of punchings, the increase of inductance due to fringing is

$$\frac{L'}{L} = \left(1 + \frac{2l_g}{\sqrt{A_c}} \log_e \frac{2S}{l_g}\right) \tag{39}$$

Equation 39 is plotted in Fig. 72 with core shape $\sqrt{A_c}/S$ as abscissas and gap ratio l_g/S as parameter.[1]

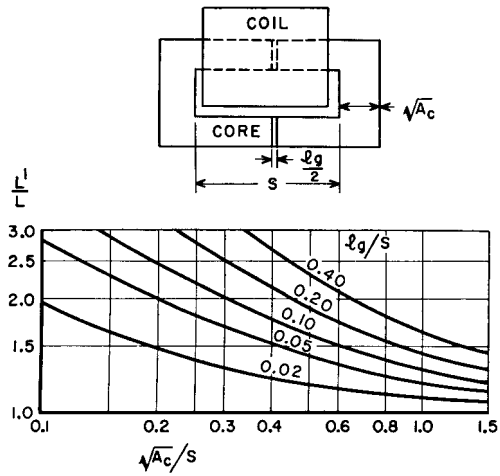

FIG. 72. Increase of reactor inductance with flux fringing at core gap.

If the air gap is enclosed by a coil, as at the top of Fig. 72, flux fringing is reduced because of the magnetizing force set up near the gap by the ampere-turns of the coil. A coil fitting tightly all around the core would produce no fringing at all. As the distance from inside of the coil to the core increases, so does the fringing. Fringing therefore depends upon the coil form thickness; if it materially exceeds the air gap per leg, fringing is nearly the same as it would be in a core gap which is not enclosed by a coil. Figure 72 is based on a thick coil form.

42. Similitude in Design. Charts such as Fig. 63 show that ratings are related to size in an orderly sequence, provided that certain proportions between core dimensions are maintained. Figure 63 is for 60

[1] See G. F. Partridge, *Phil. Mag., 22* (7th series), 675 (July–December, 1936).

cycles. If a transformer is desired for another frequency, its size may be estimated from Table VIII, provided that the same core proportions apply, and similar values of induction and temperature rise are used. If the new conditions are widely different, due allowance must be made for them or the estimate will not be accurate.

Table VIII and Figs. 63 and 71 are examples of *similitude*. If all variations between ratings are taken into account, similitude provides a very accurate basis for estimating new sizes; for the transformer designer there is no better basis for starting a new design.

43. Reactor Current Interruption. Sudden interruption of current through a reactor may cause high voltages to develop in the winding. This may be seen by considering the voltage across a reactor with linear inductance L and varying current i in the winding. Let current i be substituted for I_M in equation 37; it may be transposed to give

$$\phi = 10^8 Li/N \tag{37a}$$

where L is in henrys and i in amperes. If this expression for ϕ be substituted in equation 1, we obtain

$$e = -L\frac{di}{dt} \tag{40}$$

Equation 40 states that the magnitude of voltage across a reactor is equal to the inductance multiplied by the rate of current change with time. The sense or direction of this voltage is always such as to oppose the current change. Therefore, if current interruption takes place instantaneously, inductive voltage is infinitely large. In an actual reactor, losses and capacitance are always present; hence interruption of reactor current forces the reactor voltage to discharge into its own capacitance and loss resistance. The curves of Fig. 73 show how the reactor voltage e rises when steady current I flowing in the reactor is suddenly interrupted. The maximum value to which voltage e could rise under any condition is IR_2, where R_2 is the equivalent loss resistance. R_2 depends mostly on the reactor iron loss at the resonance frequency determined by reactor inductance L and capacitance C. This frequency is $1/T$, where T is $2\pi\sqrt{LC}$. Conditions for high voltage across the reactor occur with high values of k, the ratio of $\sqrt{L/C}$ to $2R_2$. If subject to sudden current interruptions, reactors must be insulated to withstand this voltage, or must be protected by spark gaps or other means. The curves of Fig. 73 are based on equation 41:

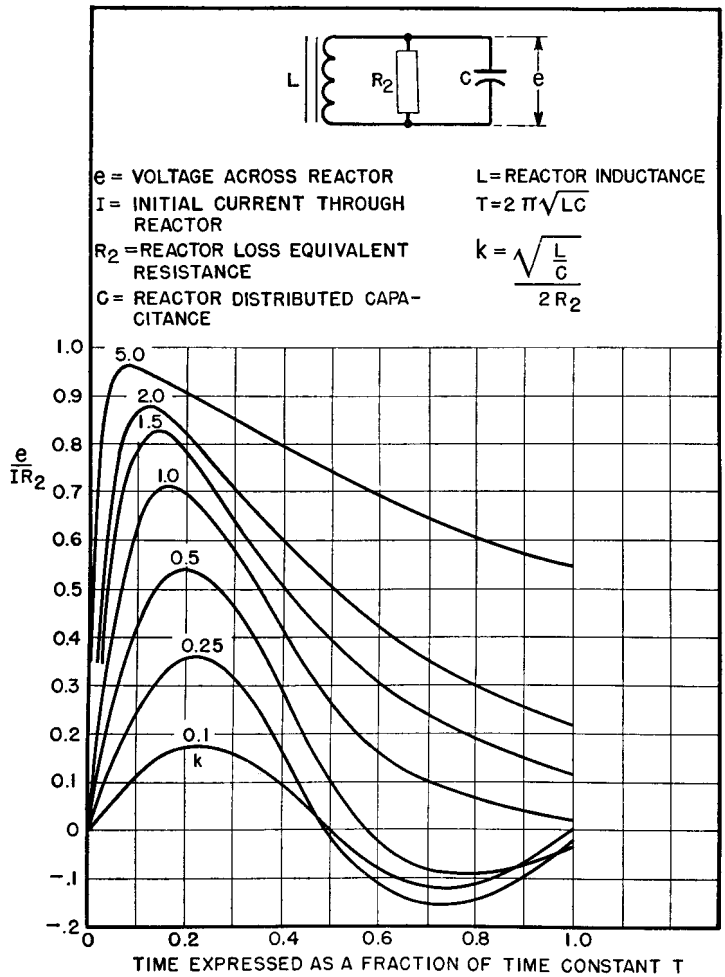

FIG. 73. Reactor voltage rise.

$$\frac{e}{IR_2} = \frac{k}{\sqrt{k^2 - 1}} (\epsilon^{m_2 t} - \epsilon^{m_1 t}) \tag{41}$$

where

$$m_1, m_2 = \frac{-2\pi}{T} (k \pm \sqrt{k^2 - 1})$$

If there is appreciable circuit or wiring capacitance shunting the reactor after it is disconnected, this contributes to the total reactor capacitance C.

44. Transformers with D-C Flux. When there is a net d-c flux in the core, as in single-phase half-wave anode transformers, the choice of core depends on the same principles as in reactors with large a-c flux. The windings carry non-sinusoidal load current, the form of which depends on the circuit. Winding currents may be calculated with the aid of Table I (p. 16). Generally the heating effects of these currents are large. Maximum flux density should be limited as described in Section 39. This precaution is essential in limited power supplies like aircraft or portable generators, lest the generator voltage wave form be badly distorted. On large power systems the rectifier is a minor part of the total load and has no influence on voltage wave form. The chief limitation then is primary winding current, and maximum induction may exceed the usual limits.

In single-phase half-wave transformers, air gaps are sometimes provided in the cores to reduce the core flux asymmetry described in Section 12. Transformers designed in this manner resemble reactors in that core induction is calculated as in Sections 37 to 41, depending on the operating conditions. Even in transformers with no air gap, there is a certain amount of incidental reluctance at the joints in both stacked laminations and type C cores. This small gap reduces the degree of core saturation that would exist in half-wave transformers with unbroken magnetic paths.

45. Power Transformer Tests. A power transformer is tested to discover whether the transformer will perform as required, or whether it will give reliable service life. Some tests perform both functions.

(*a*) *D-C Resistance.* This test is usually made on transformers at the factory as a check on the correctness of wire size in each winding. Variations are caused by wire tolerances, and by difference in winding tension between two lots of coils or between two coil machine operators. About 10 per cent variation can be expected in the d-c resistance of most coils, but this value increases to 20 per cent rather suddenly in sizes smaller than No. 40. The test is made by means of a resistance bridge or specially calibrated meter.

(*b*) *Turns Ratio.* Once the correct number of turns in each winding is established, correct output voltage can be assured for a coil of given design by measuring the turns. A simple way of doing this is by use of the turns-ratio bridge in Fig. 74. If the turns are correct, the null indicated by the meter occurs at a ratio of resistances

$$R_1/R_2 = N_1/N_2 \tag{42}$$

If there is an error in the number of turns of one winding, the null occurs at the wrong value R_1/R_2. A source of 1,000 cycles is preferable to one of 60 cycles for this test. The smaller current drawn by the transformer reduces IR and IX errors. Harmonics in the source obscure the null, and so the source should be filtered. The null is often made sharper by switching a small variable resistor in series with R_1 or R_2 to offset any lack of proportion in resistances of windings N_1 or N_2.

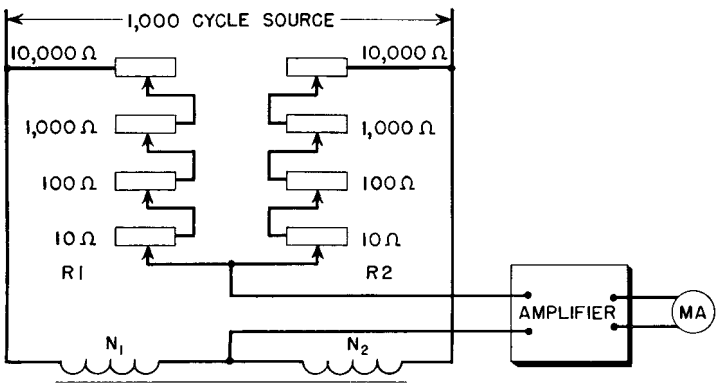

FIG. 74. Turns-ratio bridge.

An accuracy of 0.1 per cent can usually be attained with four-decade resistances. Polarity of winding is also checked by this test, because the bridge will not balance if one winding is reversed.

(*c*) *Open-Circuit Inductance* (*OCL*). There are several ways of measuring inductance. If the Q (or ratio of coil reactance to a-c resistance) is high, the check may be made by measuring the current drawn by an appropriate winding connected across a source of known voltage and frequency. This method is limited to those cases where the amount of current drawn can be measured. A more general method makes use of an inductance bridge, of which one form is shown in Fig. 75.

If direct current normally flows in the winding, it can be applied through a large choke as shown. Inductance is then measured under the conditions of use. Source voltage should be adjustable for the same reason and should be filtered to produce a sharp null. R_c is provided to compensate for coil a-c resistance. Without it an accurate measurement is rarely attained. Enough data are provided by the test to calculate a-c resistance as well as inductance.

When Q is low, as it is in coils with high resistance, better accuracy is obtained with the Maxwell bridge, which is like the Hay bridge except that X_c and R_c are paralleled. Then the equations for bridge balance become

$$L_x = R_1R_2C \qquad R_x = R_1R_2/R_c \tag{43}$$

The Maxwell bridge has the further advantage that the null is independent of the source frequency.

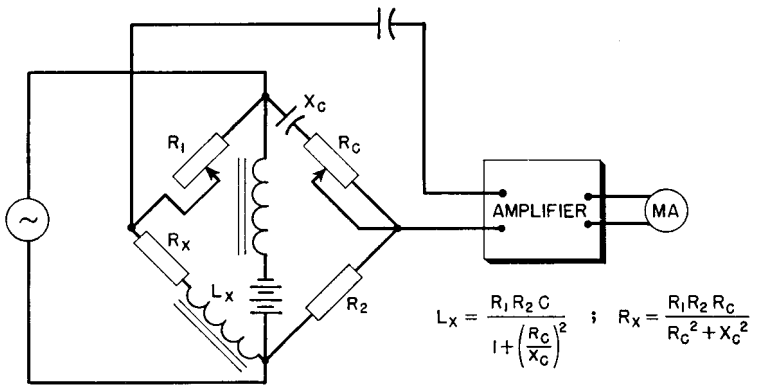

FIG. 75. Modified Hay bridge for measuring inductance.

(*d*) *Temperature Rise.* Tests to determine whether a transformer overheats are made by measuring the winding resistances before and after a heat run, during which the transformer is loaded up to its rating. Where several secondaries are involved, each should deliver rated voltage and current. Power is applied long enough to allow the transformer temperature to become stable; this is indicated by thermometer readings of core or case temperature taken every half hour until successive readings are the same. Ambient temperature at a nearby location should also be measured throughout the test. The average increase in winding resistance furnishes an indication of the average winding temperature. Figure 76 furnishes a convenient means for finding this temperature.

(*e*) *Regulation.* It is possible to measure voltage regulation by connecting a voltmeter across the output winding and reading the voltage with load off and on. This method is not accurate because the regulation is usually the difference between two relatively large quantities. Better accuracy can be obtained by multiplying the rated

winding currents by the measured winding resistances and using equation 13. If the winding reactance drop is small this equation works well for resistive loads. To measure winding reactance drop, a short-circuit test is used. With the secondary short-circuited, sufficient voltage is applied to the primary to cause rated primary current to

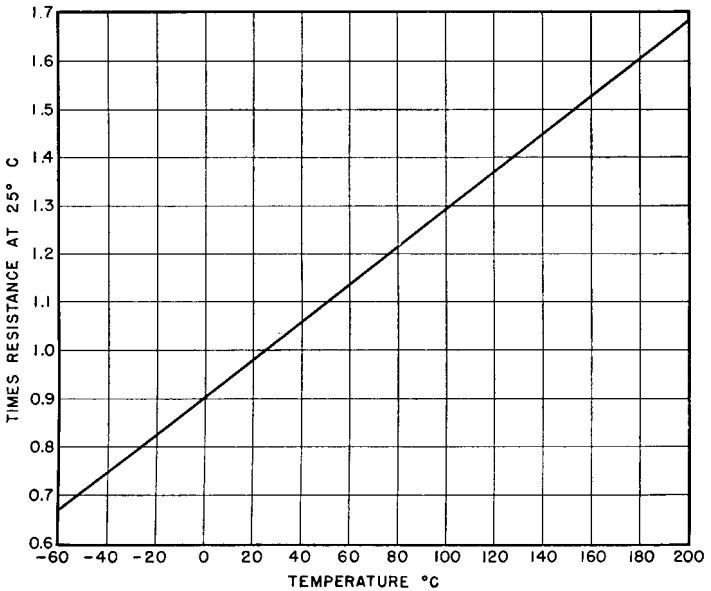

FIG. 76. Copper resistance versus temperature in terms of resistance at 25°C.

flow. The quotient E/I is the vector sum of winding resistances and reactances. Reactance is found from

$$X = \sqrt{Z^2 - R^2} \tag{44}$$

where R includes the resistance of both windings and the meter.

Sometimes it is more convenient to measure the leakage inductance with secondary short-circuited on a bridge and multiply by $2\pi f$.

(*f*) *Output Voltage.* Although the method described under (*e*) above is accurate for two-winding transformers, it is not applicable to multi-secondary transformers unless they are tested first with newly calibrated meters to see that all windings deliver proper voltage at full load. Once this is established, values of winding resistance and reactance thereafter can be checked to control the voltage. The interde-

pendence of secondary voltages when there is a common primary winding makes such an initial test desirable. This is particularly true in combined filament and plate transformers, for which the best test is the actual rectifier circuit.

(*g*) *Losses.* Often it is possible to reduce the number of time-consuming heat runs by measuring losses. The copper loss is readily calculated by multiplying the measured values of winding resistance (corrected for operating temperature) by the squares of the respective rated currents. Core loss is measured with open secondary by means of a low-reading wattmeter at rated voltage in the primary circuit. If these losses correspond to the allowable temperature rise, the transformer is safely rated.

(*h*) *Insulation.* There is no test to which a transformer is subjected which has such a shaky theoretical basis as the insulation test. Yet it is the one test it must pass to be any good. Large quantities of transformers can be built with little or no insulation trouble, but the empirical nature of standard test voltages does not assure insulation adequacy. It has been found over a period of years that, if insulation withstands the standard rule of twice normal voltage plus 1,000 volts rms at 60 cycles for 1 minute, reasonable insulation life is usually obtained. It is possible for a transformer to be extremely under-insulated and still pass this test (see p. 44); conversely, there are conditions under which the rule would be a handicap. Therefore it can only be considered as a rough guide.

The manner of making insulation tests depends upon the transformer. Low-voltage windings categorically can be tested by short-circuiting the terminals and applying the test voltage from each winding to core or case with other windings grounded. Filament transformers with secondaries insulated for high voltage may be tested in similar manner. But a high-voltage plate transformer with grounded center tap requires unnecessary insulation if it is tested by this method. Instead, a nominal voltage of, say, 1,500 volts is applied between the whole winding and ground; after that the center tap is grounded and a voltage is applied across the primary of such value as to test the end terminals at twice normal plus 1,000 volts. Similar test values can be calculated for windings operating at d-c voltages other than zero. Such a test is called an induced voltage test. It is performed at higher than normal frequency to avoid saturation. An advantage of induced voltage testing is that it tests the layer insulation.

If insulation tests are repeated one or more times they may destroy the insulation, because insulation breakdown values decrease with

time. Successive applications of test voltage are usually made at either decreased voltage or decreased time. In view of their dubious value, repeated insulation tests are best omitted.

Corona tests are not open to this objection. A voltage 5 per cent higher than normal is applied to the winding, and the leads are run through blocking capacitors to the input of a sensitive radio receiver as in Fig. 38.[1] RETMA standard noise values for this test are based primarily on radio reception, but they do indicate whether standard insulation practice is followed. See Table X.

TABLE X. CORONA VOLTAGE

RMS Working Voltage (kilovolts)	Corona Level (microvolts)
Up to 8.6	1,000
8.61 to 15	2,500

Transformers which are subjected to voltage surges may be given impulse tests to determine whether the insulation will withstand the surges. Power line surges are the most difficult to insulate for. The electric power industry has standardized on certain impulse voltage magnitudes and wave shapes for this testing.[2] The ratio of impulse voltage magnitude to 60-cycle, 1-minute insulation test voltage is called the *impulse ratio*. This ratio is much greater for oil-insulated transformers than for dry-type transformers, and is discussed further in Chapter 4.

[1] See RETMA Standard TR-102-B, "Power Transformers for Radio Transmitters."

[2] See ASA Standard C57.22-1948, paragraph 22.116.

4. RECTIFIER PERFORMANCE

46. Ripple. Filters used with rectifiers allow the rectified direct current to pass through to the load without appreciable loss, but ripple in the rectified output is attenuated to the point where it is not objectionable. Filtering sometimes must be carried out to a high degree. From the microphone to the antenna of a high-power broadcast station, there may be a power amplification of 2×10^{15}. The introduction of a ripple as great as 0.005 per cent of output voltage at the microphone would produce a noise in the received wave loud enough to spoil the transmitted program. A rectifier used at the low-power levels must be unusually well filtered to prevent noticeable hum from being transmitted.

Different types of rectifiers have differing output voltage waves, which affect the filter design to a large extent. Certain assumptions, generally permissible from the standpoint of the filter, will be made in order to simplify the discussion. These assumptions are:

1. The alternating voltage to be rectified is a sine wave.
2. The rectifying device passes current in one direction but prevents any current flow in the other direction.
3. Transformer and rectifier voltage drops are negligibly small.
4. Filter condenser and reactor losses are negligible.

47. Single-Phase Rectifiers. Single-phase half-wave rectified voltage across a resistive load R is shown in Fig. 77. It may be resolved by Fourier analysis into the direct component whose value is $0.318E_{pk}$ or $0.45E_{ac}$, and a series of alternating components. The fundamental alternating component has the same frequency as that of the supply.

Single-phase half-wave rectifiers are used only when the low average value of load voltage and the presence of large variations in this voltage are permissible. The chief advantage of this type of rectifier is its simplicity. A method of overcoming both its disadvantages is illustrated in Fig. 78 where a capacitor C shunts the load. By using the proper capacitor, it is often possible to increase the value of E_{dc} to

within a few per cent of the peak voltage E_{pk}. The principal disadvantage of this method of filtering is the large current drawn by the capacitor during the charging interval as shown in Fig. 49(*b*) (p. 63). This current is limited only by transformer and rectifier regulation; yet it must not be so large as to cause damage to the rectifier. The higher the value of E_{dc} with respect to E_{ac}, the larger is the charging current taken by C. (See Figs. 50 and 52, pp. 64 and 66.) Therefore, if a smooth current wave is desired, some other method of filtering must be used.

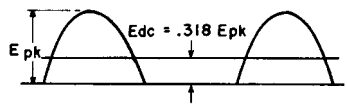

FIG. 77. Half-wave rectifier voltage.

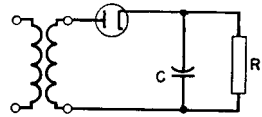

FIG. 78. Capacitor filter.

To obtain less voltage variation or ripple amplitude, after the limiting capacitor size has been reached, an inductive reactor may be employed. It may be placed on either the rectifier or the load side of the capacitor, depending on whether the load resistance R is high or low respectively. See Figs. 79(*a*) and (*b*). In the former, the voltage E_{dc} has less than the average value $0.45E_{ac}$, because the inductor delays the build-up of current during the positive half-cycle of voltage, and yet the inductor in this case should have a high value of reactance X_L, compared to the capacitive reactance X_C, in order to filter effectively. When R is low, reactance X_L should be high compared to R.

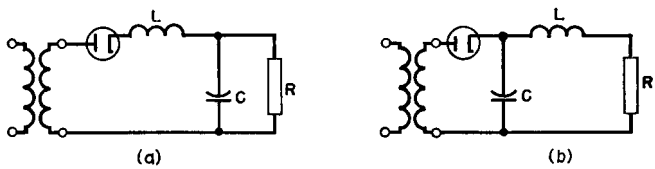

FIG. 79. (*a*) Inductor-input filter; (*b*) capacitor-input filter.

In Fig. 79(*a*) the ripple amplitude across R is $-X_C/(X_L - X_C)$ times the amplitude generated by the rectifier, if R is high compared to X_C. Also, in Fig. 79(*b*), the ripple amplitude across R is R/X_L times the ripple obtained with capacitor only. R here is small compared to X_L.

Large values of inductance are required to cause continuous current flow when the inductor is on the rectifier side of the capacitor in a half-

wave rectifier circuit. Since current tends to flow only half the time, the rectified output is reduced accordingly. This difficulty is eliminated by the use of the full-wave rectifier of Fig. 80. The alternating

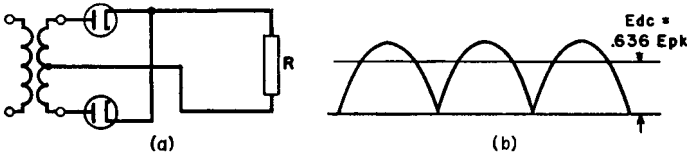

FIG. 80. (*a*) Single-phase full-wave rectifier; (*b*) rectified full-wave voltage.

components of the output voltage have a fundamental frequency double that of the supply, and the amplitudes of these components are much less than for the half-wave rectifier. The higher ripple frequency causes L and C to be doubly effective; the smaller amplitude results in smaller percentage of ripple input to the filter. Current flow is continuous and E_{dc} has double the value that it had in Fig. 77. For these reasons, this type of rectifier is widely used.

A full-wave rectifier uses only one-half of the transformer winding at a time; that is, E_{ac} is only half the transformer secondary voltage. A circuit which utilizes the whole of this voltage in producing E_{dc} is the single-phase bridge rectifier shown in Fig. 81. The output voltage relations are the same as those of Fig. 80(*b*). Although this circuit requires more rectifying tubes, it eliminates the need for a transformer midtap.

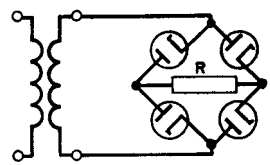

FIG. 81. Bridge rectifier.

48. Polyphase Rectifiers. The effect of rectifying more than one phase is to superpose more voltages of the same peak value but in different time relation to each other. Figures 82(*a*) and (*b*) give a comparative picture of the rectified output voltage for three-phase half-wave and full-wave rectifiers. Increasing the number of phases increases the value of E_{dc}, increases the frequency of the alternating components, and decreases the amplitude of these components. Ripple frequency is p times that of the unrectified alternating voltage, p being 1, 2, 3, and 6 for the respective waves. Roughly speaking, p may be taken to represent the number of phases, provided that due allowance is made for the type of circuit, as in Fig. 83. Rectifiers with $p = 3$ or 6 are derived from three-phase supply lines, and, by special connections, rectifiers with $p = 9$, 12, or more are obtained.

The frequency of any ripple harmonic is mp, where m is the order of the harmonic.

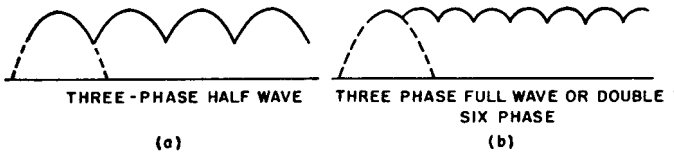

FIG. 82. Polyphase rectifier output waves.

Ripple voltage for any of these rectifiers can be found by the Fourier relation:

$$A_n = \frac{2}{T}\int_{-T/2}^{T/2} f(t)\cos n\omega t\, dt \tag{45}$$

where A_n = amplitude of nth ripple harmonic
T = ripple fundamental period
t = time (with peak of rectified wave as $t = 0$)
$\omega = 2\pi/Tp = 2\pi \times$ supply line frequency
$f(t)$ = ripple as a function of time
$= E_{pk}\cos\omega t$, $T/2 > \omega t > -T/2$.

The voltage peak is chosen as $t = 0$ to obtain a symmetrical function $f(t)$ and eliminate a second set of harmonic terms like those in equation 45, but with sin $n\omega t$ under the integral.

Ripple amplitude is given in Fig. 83 for the ripple fundamental, and second and third harmonics with reactor-input filters. In this curve, the ratio P_A of ripple amplitude to direct output voltage is plotted against the number of phases p. It should be noted that P_A diminishes by a considerable amount for the second and third harmonics. In general, if a filter effectively reduces the percentage of fundamental ripple across the load, the harmonics may be considered negligibly small.

49. Multistage Filters. In the inductor-input filter shown in Fig. 79(*a*), the rectifier is a source of non-sinusoidal alternating voltage connected across the filter. It is possible to replace the usual circuit representation by Fig. 84(*a*). For any harmonic, say the nth, the voltage across the whole circuit is the harmonic amplitude A_n, and the voltage across the load is $P_R E_{dc}$, P_R being ripple allowable across the load, expressed as a fraction of the average voltage. Since the load

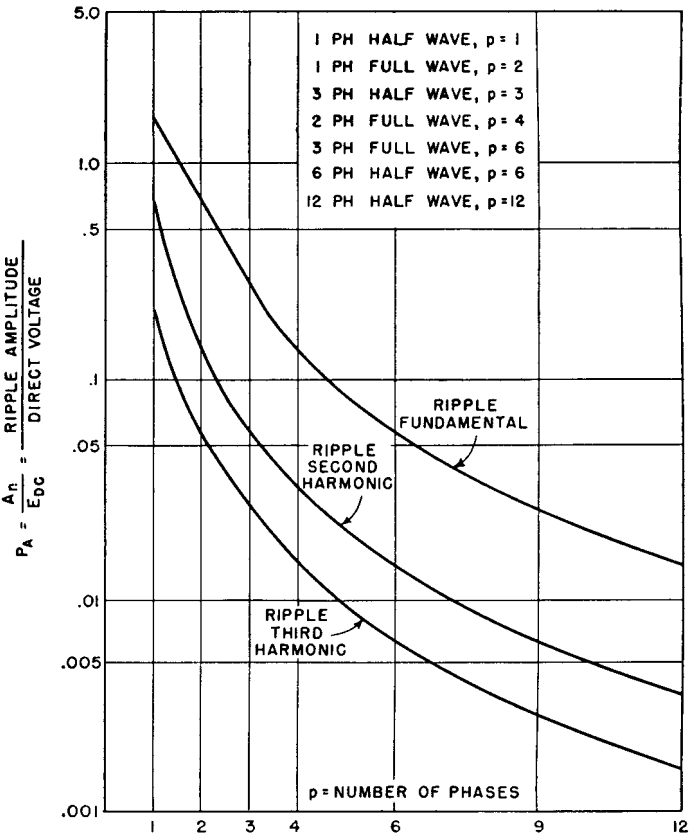

FIG. 83. Rectifier ripple voltage.

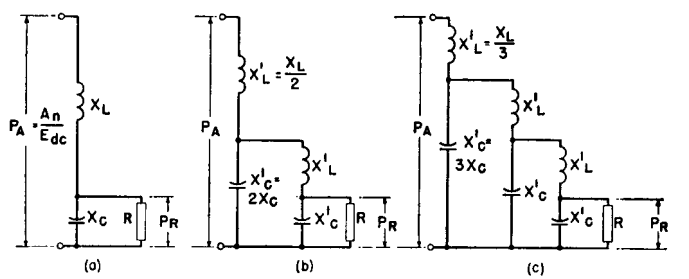

FIG. 84. Inductor-input filter circuits.

resistance R is high compared to X_C, the two voltages are nearly in phase, and they bear the same ratio to each other as their respective reactances, or

$$\frac{P_A}{P_R} = \frac{X_L - X_C}{X_C} = \frac{X_L}{X_C} - 1 \tag{46}$$

From the type of rectifier to be used, and the permissible amount of ripple in the load voltage, it is possible to determine the ratio of inductive to capacitive reactance.

When the magnitude P_R must be kept very small, the single-stage filter of Fig. 84(a) may require the inductor and the capacitor to be abnormally large. It is preferable under this condition to split both the inductor and the capacitor into two separate equal units, and connect them like the two-stage filter of Fig. 84(b). A much smaller total amount of inductance and of capacitance will then be necessary. For this filter

$$\frac{P_A}{P_R} = \left(\frac{X'_L - X'_C}{X'_C}\right)^2 \tag{47}$$

X'_L and X'_C being the reactances of each inductor and capacitor in the circuit. Likewise, the three-stage filter of Fig. 84(c) may be more practicable for still smaller values of P_R. In the latter filter,

$$\frac{P_A}{P_R} = \left(\frac{X'_L - X'_C}{X'_C}\right)^3 \tag{48}$$

and, in general, for an n-stage filter,

$$\frac{P_A}{P_R} = \left(\frac{X'_L - X'_C}{X'_C}\right)^n \tag{49}$$

It is advantageous to use more than one stage only if the ratio P_A/P_R is high. That the gain from multistage filters is realized only for certain values of P_A/P_R is shown by Fig. 85. The lower curve shows the relation between P_A/P_R and X_L/X_C for a single-stage filter. The second curve shows the increase in P_A/P_R gained by splitting up the same amount of L and C into a two-stage filter; as indicated in Fig. 84(b), the inductor and capacitor both have one-half their "lumped" value. The upper curve indicates the same increase for a three-stage filter, each inductor and capacitor of which have one-third

of their "lumped" or single-stage filter value. The attenuation in multistaging is enormous for high X_L/X_C. For lower ratios there

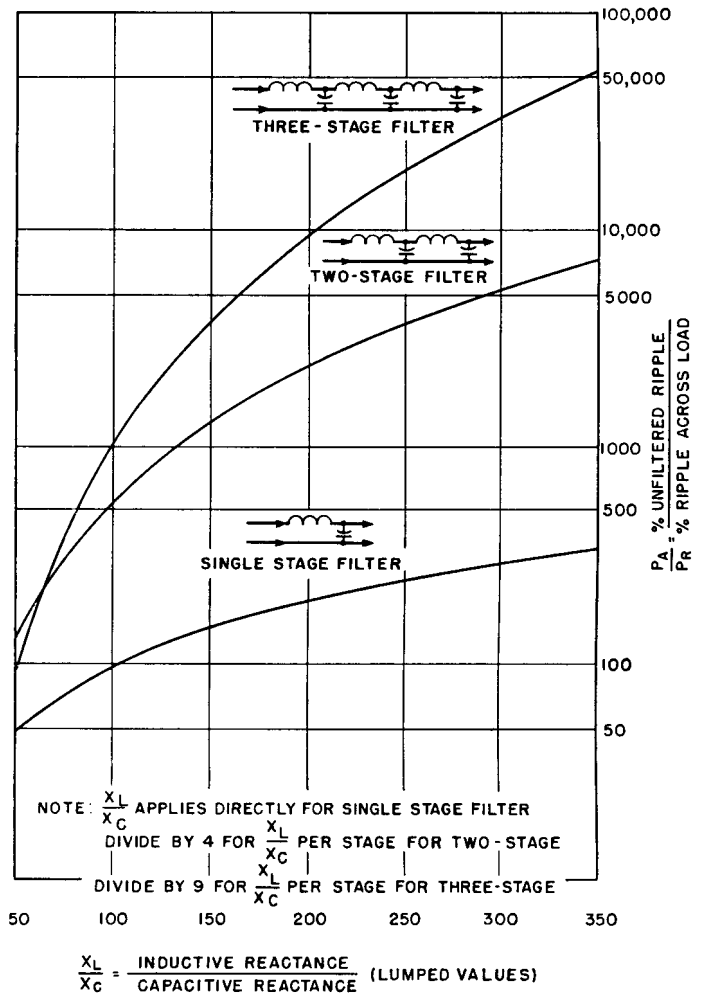

FIG. 85. Attenuation in one-, two-, and three-stage filters.

may be a loss instead of a gain, as shown by the intersection of the two upper curves. These curves intersect the lower curve if all are prolonged further to the left. This may be a puzzling condition; but consider that, for $X_L/X_C = 50$ in the single-stage filter, the ratio is

$\frac{1}{3}X_L/3X_C$ or 5% in the three-stage filter; the rather small advantage in the latter is not difficult to account for.

Other factors may influence the number of filter stages. In some applications, modulation or keying may require that a definite size of filter capacitor be used across the load. Usually these conditions result in a single-stage filter, where otherwise more stages might be most economical.

Table VII (p. 62) shows filter reactors in the negative lead, which may be either at ground or high potential. If low ripple is required in the filtered output, it is usually preferable to locate the filter reactors in the high-voltage lead. Otherwise, there is a ripple current path through the anode transformer winding capacitance to ground which bypasses the filter reactor. Ripple then has a residual value which cannot be reduced by additional filtering. In the three-phase, zigzag, full-wave circuit, with center tap used for half-voltage output, separate reactors should be used in the positive leads; placing a common reactor in the negative lead introduces high amplitude ripple in the high-voltage output.

In rectifiers with low ripple requirements, both filament and anode windings should be accurately center-tapped to avoid low-frequency ripple, which is difficult to filter. Three-phase leg voltages should be balanced for the same reason.

50. Capacitor-Input Filters. One of the assumptions implied at the beginning of this chapter, namely, that transformer and rectifier voltage drops are negligibly small, cannot usually be made when capacitor-input filters are used, because of the large peak currents drawn by the capacitor during the charging interval. Such charging currents drawn through finite resistances affect both the d-c output voltage and the ripple in a complicated manner, and simple analysis such as that given for inductor-input filters is no longer possible. Figure 86 is a plot of the ripple in the load of capacitor-input filters with various ratios of source to load resistance, and for three types of single-phase rectifiers. These curves are useful also when resistance is used in place of an inductor at the input of a filter. ω is 2π times the a-c supply frequency, C is the capacitance, R_L is the load resistance, and R_S the source resistance.

When L-C filter stages follow a capacitor-input filter, the ripple of the latter is reduced as in Fig. 85, except that the value of P_A must be taken from Fig. 86. When an R-C filter stage follows any type of filter,

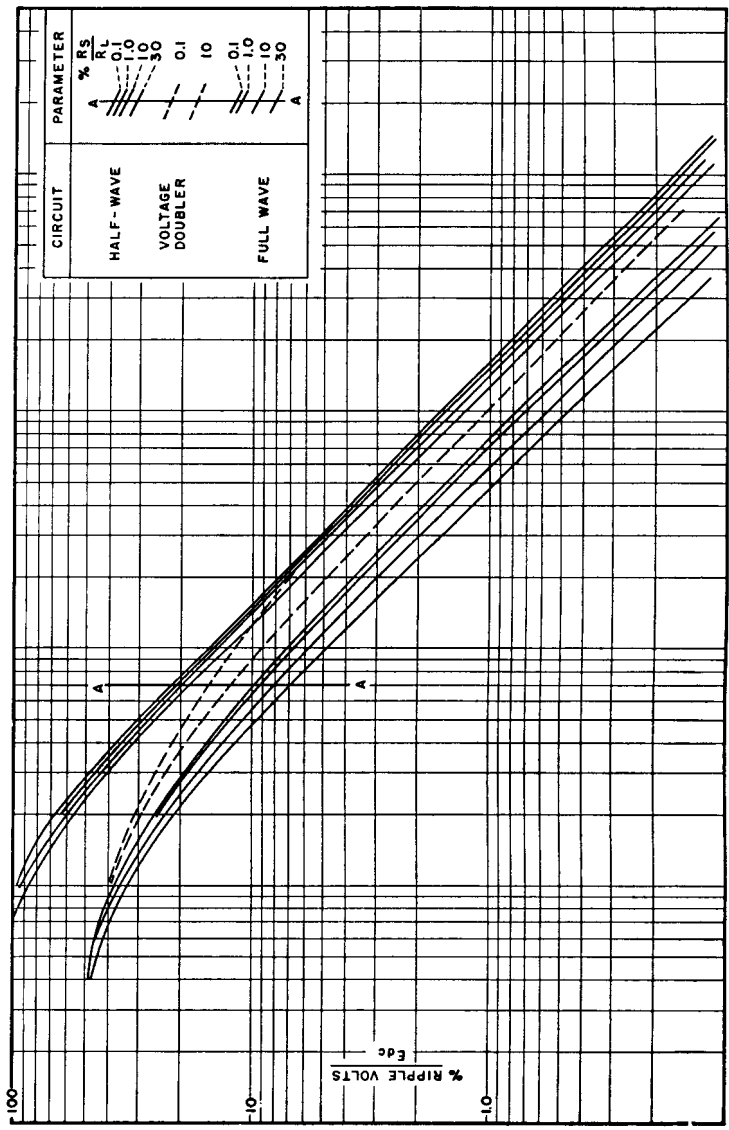

FIG. 86. Rms ripple voltage of capacitor-input filters.

the ripple is reduced in the ratio R/X_C represented by the R-C stage.

51. Rectifier Regulation. The regulation of a rectifier comprises three distinct components:

1. The d-c resistance or IR drop.
2. The commutation reactance or IX drop.
3. The capacitor charging effect.

The first component can be reduced to a small value by the use of tubes, transformers, and inductors having low resistance. Mercury-

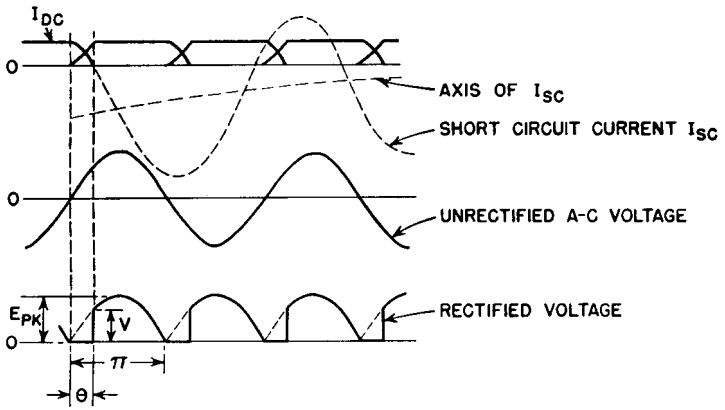

FIG. 87. Commutation current effect on rectifier voltage.

vapor tubes are of noteworthy usefulness in this respect, as the internal voltage drop is low and almost independent of load current variations.

Commutation reactance can be kept to a low value by proper transformer design, particularly where the ratio of short-circuit current to normal load is high.

During part of each cycle, both tubes of a single-phase full-wave rectifier are conducting. During this interval one tube loses its current and the other one builds up to normal current. Because of the inevitable reactance in the transformer, this change does not take place immediately but during an angle θ as in Fig. 87. Short-circuit current is initiated which would rise as shown by the dotted lines of Fig. 87, if it could pass through the rectifier tubes; it prevents the rectified voltage wave from retaining its normal shape, so that for a portion of each cycle the rectified output is zero.

Let the transformer winding resistance be temporarily neglected; if the current could rise to maximum, the short-circuit value would be

$2E_{pk}/X$, where X is the leakage reactance of the whole secondary, but it is limited by the rectifier to I_{dc}. The short-circuit current rises to $(1 - \cos \theta)$ times maximum in the commutation period, or

$$[2E_{pk}(1 - \cos \theta)]/X = I_{dc}$$

The average voltage from zero to the re-ignition point V is

$$(E_{pk}/\pi)(1 - \cos \theta)$$

Combining these relations gives, for the *average* voltage cut out of the rectified voltage wave by commutation,

$$V_{\text{av}} = I_{dc}X/2\pi \tag{50}$$

By similar reasoning, the commutation reactance drop for polyphase rectifiers is

$$pI_{dc}X'/2\pi \tag{51}$$

where X' = the transformer leakage reactance from line to neutral on the secondary side, and p = the number of phases in Fig. 83.

In this formula, the leakage reactance per winding is associated with the voltage across that winding. This is accurate when each phase is supplied by a separate transformer. But it fails for $p = 2$ in the single-phase full-wave rectifier, using one plate transformer, where half of the secondary voltage is rectified each half-cycle. In such a rectifier, during commutation the whole secondary voltage is effective, and so is the leakage reactance of the whole secondary. This reactance has 4 times the leakage reactance of each secondary half-winding, but only twice the half-winding voltage acts across it. Hence equation 50 must be used for the single-phase rectifier; here X = the reactance of the entire secondary.

When high winding resistance limits short-circuit current, commutation has less effect than equation 50 would indicate. This condition prevails in small rectifiers; the IX drop is negligibly small because of the small transformer dimensions. For example, in the plate transformer designed in Fig. 58 the leakage inductance is 0.166 henry. The commutation reactance drop is, from equation 50,

$$0.115 \times 0.166 \times 2\pi \times 60/2\pi = 1.15 \quad \text{volts}$$

or 0.1 per cent. This is negligible compared to the 3.7 per cent regulation calculated in Fig. 58. In this case the short-circuit current would be limited by winding resistance rather than by leakage inductance.

In large rectifiers, all rectifier components have low losses to prevent power wastage or overheating, and the IR drop is a very small percentage of the total. At the same time, a large transformer requires careful design in order to keep the IX drop reasonably small. Therefore, in large rectifiers the IX drop is the dominant cause of regulation. An example with 60 kva rating has 0.7 per cent IR drop and 6 per cent IX drop.

In medium-size rectifiers the IR and IX drops may be of equal, or at least comparable, value. In such rectifiers these two components of

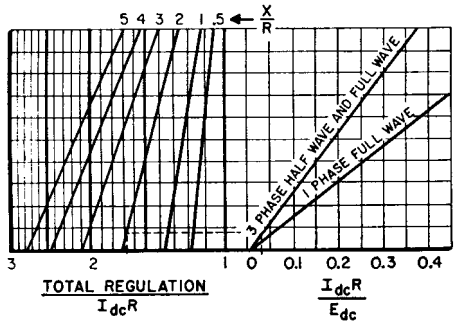

FIG. 88. Increase in rectifier regulation due to transformer reactance.

regulation do not add arithmetically. Commutation interval θ, Fig. 87, depends on the short-circuited reactance when resistance is negligible, but if resistance is appreciable θ is related to the ratio X/R exponentially.[1] The increase in regulation caused by commutation reactance may be found from Fig. 88, in terms of d-c output voltage E_{dc}. In this figure the regulation of three widely used rectifiers (single-phase full-wave, three-phase half-wave, and three-phase full-wave) is given in a manner which enables one to proceed directly from the IR component of regulation to total regulation.

X and R are ohms per phase except X/R ratio is for the whole secondary in single-phase full-wave rectifiers. R in X/R ratio includes primary R in all cases. R in $I_{dc}R/E_{dc}$ is for two windings in three-phase full-wave rectifiers. To obtain total regulation, project $I_{dc}R/E_{dc}$ vertically to one-phase or three-phase line. Project this point to the left to proper X/R line. Abscissa at left gives total regu-

[1] See *Mercury-Arc Rectifiers and Their Circuits*, by D. C. Prince and P. B. Vogdes, McGraw-Hill Book Co., New York, 1927, p. 216.

lation. An example is indicated by the dotted line. In this example, the rectifier is three-phase full-wave.

$E_{dc} = 2{,}000$ volts $\qquad \dfrac{X}{R} = 2$

$I_{dc} = 1$ amp

$R = 60$ ohms $\qquad \dfrac{I_{dc}R}{E_{dc}} = \dfrac{60}{2{,}000} = 3$ per cent

$X = 120$ ohms

Total regulation $= 1.68 \times 3 = 5.04$ per cent. If the IX regulation had been added directly to IR it would be 6 per cent + 3 per cent = 9 per cent, and the calculated regulation would be nearly 4 per cent higher than actual.

52. Capacitor Effect. If the rectifier had no filter capacitor, the rectifier would deliver the average value of the rectified voltage wave, less regulation components 1 and 2 of Section 51. But with a filter capacitor, there is a tendency at light loads for the capacitor to charge up to the peak value of the rectified wave. At zero load, this amounts to 1.57 times the average value, or a possible regulation of 57 per cent in addition to the IR and IX components, for single-phase full-wave rectifiers. This effect is smaller in magnitude for polyphase rectifiers, although it is present in all rectifiers to some extent.

Suppose that the rectifier circuit shown in Fig. 80(*a*) delivers single-phase full-wave rectifier output as shown in Fig. 80(*b*) to an inductor-input filter and thence to a variable load. In such a circuit, the filter inductor keeps the capacitor from charging to a value greater than the average E_{dc} of the rectified voltage wave at heavy loads. At light loads the d-c output voltage rises above the average of the rectified wave, as shown by the typical regulation curve of Fig. 89.

Starting at zero load, the d-c output voltage E_0 is 1.57 times the average of the rectified wave. As the load increases, the output voltage falls rapidly to E_1 as the current I_1 is reached. For any load greater than I_1, the regulation is composed only of the two components IR and IX. It is good practice to use a bleeder load I_1 so that the rectifier operates between I_1 and I_2.

Filter elements X_L and X_C determine the load I_1 below which voltage rises rapidly. The filter, if it is effective, attenuates the a-c ripple voltage so that across the load there exists a d-c voltage with a small ripple voltage superposed. A choke-input filter attenuates the harmonic voltages much more than the fundamental, and, since the harmonics are smaller to begin with, the main function of the filter is

to take out the fundamental ripple voltage. This has a peak value, according to Fig. 83, of 66.7 per cent of the average rectified d-c voltage for a single-phase full-wave rectifier. Since this ripple is purely a-c it encounters a-c impedances in its circuit. If we designate the choke impedance as X_L, and the capacitor impedance as X_C, both at the fundamental ripple frequency, the impedance to the fundamental component is $X_L - X_C$, the load resistance being negligibly high compared to X_C in an effective filter. The d-c voltage, on the other hand, produces a current limited mainly by the load resistance, provided that the choke IR drop is small.

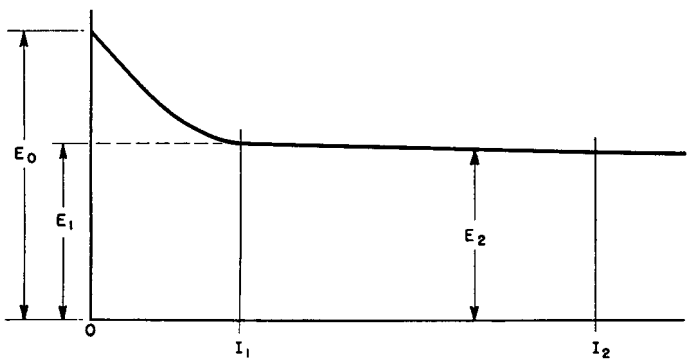

FIG. 89. Rectifier regulation curve.

A-c and d-c components are shown in Fig. 90, with the ripple current I_{ac} superposed on the load direct current I_{dc}. If the direct current is made smaller by increased load resistance, the a-c component is not affected because load resistance has practically no influence in determining its value. Hence a point will be reached, as the d-c load current is diminished, where the peak value of ripple current just equals the load direct current. Such a condition is given by d-c load I_1 which is equal to I_{ac}. If the d-c load is reduced further, say to the value I_x, no current flows from the rectifier in the interval A-B of each ripple cycle. The ripple current is not a sine wave, but is cut off on the lower halves, as in the heavy line of Fig. 91. Now the average value of this current is not I_x but a somewhat higher current I_y. That is, the load direct current is higher than the average value of the rectified sine wave voltage divided by the load resistance. This increased current is caused by the tendency of the capacitor to charge up to the peak of the voltage wave between such intervals as A-B; hence the

term capacitor effect which is applied to the voltage increase. The limiting value of voltage is the peak value of the rectified voltage, which is 1.57 times the sine-wave average, at zero load current.

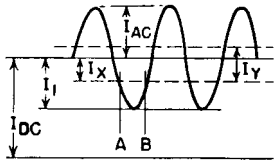

FIG. 90. A-c and d-c components of filter current.

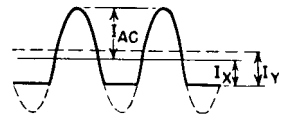

FIG. 91. Capacitor effect at light load.

To prevent capacitor effect the choke must be large enough so that I_{ac} is equal to or less than the bleeder current I_1. This consideration leads directly to the value of choke inductance. The bleeder current I_1 is E_1/R_1, where R_1 is the value of bleeder resistance. The ripple current is the fundamental ripple voltage divided by the ripple circuit impedance, or

$$I_{ac} = \frac{0.667E_1}{X_L - X_C}$$

Equating I_1 and I_{ac} we have, for a single-phase full-wave rectifier,

$$R_1 = \frac{X_L - X_C}{0.667} \tag{52}$$

Here we see that the value of capacitance also has an effect, but it is minor relative to that of the choke. In a well-designed filter, the choke reactance X_L is high compared to X_C. Therefore, the predominant element in fixing the value of R_1 (and of I_1) is the filter reactor.

Polyphase rectifiers have similar effects, but the rise in voltage is not so great because of the smaller difference between peak and average d-c output. The bleeder resistance for eliminating capacitor effect can be found in general from

$$R_1 = \frac{X_L - X_C}{P_1} \tag{53}$$

where P_1 is the fundamental ripple peak amplitude from Fig. 83, and X_L and X_C are the filter reactances at fundamental ripple frequency.

Between load I_1 and zero load, the rate of voltage rise depends upon the filter. Figure 92 shows the voltage rise as a function of the ratio

$(X_L - X_C)/R_L$ for a single-phase full-wave rectifier. A curve of ripple in terms of ripple at full load is given. Figure 92 is a plot of experimental data taken on a rectifier with $IR + IX$ regulation of 5 per cent. Reactances X_L and X_C are computed for the fundamental ripple frequency.

Capacitor-input filters have the voltage regulation curves shown in Figs. 50, 51, and 53) (pp. 64, 65, and 68) for their respective circuits. At light loads these filters may give reasonably good regulation, but it

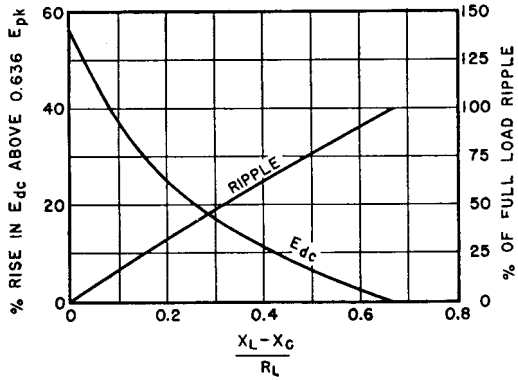

FIG. 92. Voltage rise in single-phase full-wave rectifier at light loads.

is possible to get very poor regulation at heavier loads, as can be seen from the curves. Rectifier series resistance plays an important part in the voltage regulation of this type of filter. The effect of anode transformer leakage inductance can be found from Fig. 92.

53. Tuned Rectifier Filters. Sometimes an inductor-input filter is tuned as in Fig. 93. The addition of capacitor C_1 increases the effective reactance of the inductor to the fundamental ripple frequency. Both regulation and ripple of this type of filter are improved. The filter is not tuned for the ripple harmonics, so the use of high-Q filter inductors is unnecessary. An increase in effectiveness of the filter inductor of about 3 to 1 can be realized in a single-phase full-wave rectifier circuit. Tuned filters are less effective with three-phase rectifiers because slight phase unbalance introduces low-frequency ripple which the filter does not attenuate.

Filters may be tuned as in Fig. 94, where the filter capacitor C_1 is connected to a tap near the right end of inductor L, and the other filter capacitor C_2 is chosen to give series resonance and hence zero

reactance across the load at the fundamental ripple frequency. Because of choke losses, the impedance across R_L is not zero, but the resulting ripple across load resistor R_L can be made lower than without

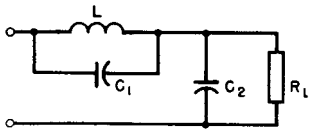

FIG. 93. Shunt-tuned filter.

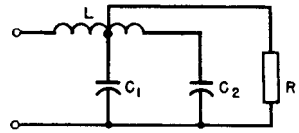

FIG. 94. Series-tuned filter.

the use of capacitor C_1. Ripple is attenuated more than in the usual inductor-input filter, but regulation is not substantially different.

54. Rectifier Currents. If the inductor in an inductor-input filter were infinitely large, the current through it would remain constant. If the commutation reactance effect is not considered, the current through each tube of a single-phase rectifier would be a square wave, as shown by I_1 and I_2 of Fig. 49(*a*) (p. 63). The peak value of this current wave is the same as the d-c output of the rectifier, and the rms value is $0.707I_{dc}$. With finite values of inductance, an appreciable amount of ripple current flows through the inductor and effectively modulates I_1 and I_2, thus producing a larger rms inductor current like the first wave of Table I (p. 16).

Capacitor-input filters draw current from the rectifier only during certain portions of the cycle, as shown in Fig. 49(*b*). For a given average direct current, the peak and rms values of these current waves are much higher than for inductor-input filters. Values for the single-phase rectifiers are given in Fig. 52 (p. 66). If an *L*-*C* filter stage follows the input capacitor, the inductor rms current is the output direct current plus the ripple current in quadrature.

Polyphase rectifiers are ordinarily of the choke-input type, because they are used mostly for larger power, and therefore any appreciable amount of series resistance cannot be tolerated. For this reason, the low *IR* drop tubes, such as mercury-vapor rectifiers, are commonly used. Such tubes do not possess sufficient internal drop to restrict the peak currents drawn by capacitor-input filters to the proper values.

In a shunt-tuned power supply filter such as shown in Fig. 93, the current drawn from the rectifier is likely to be peaked because two capacitors C_1 and C_2 are in series, without intervening resistance or inductance. This peak quickly subsides because of the influence of inductor L, but an oscillation may take place on top of the tube cur-

rent wave as shown in Fig. 95. The rectifier tube must be rated to withstand this peak current. At the end of commutation the voltage

FIG. 95. Anode current with shunt-tuned filter.

jumps suddenly from zero to V (Fig. 87). Peak rectifier current may be as much as

$$I_{pk} = V/\omega L_s \tag{54}$$

L_s is half the transformer leakage inductance, and $\omega = 2\pi \times$ frequency of oscillation determined by L_s in series with C_1 and C_2. This peak current is superposed on I_{dc}. It flows through the anode transformer and tube, but the current in choke L (Fig. 93) is determined by ripple voltage amplitude and choke reactance. Series resistance R_s reduces this peak current to the value

$$I_{pk} = \frac{V}{\omega L_s} \epsilon^{-\frac{\pi R_s}{4\omega L_s}} \tag{55}$$

It is obtained by applying a step function voltage to the series $R_s L_s C$ circuit. The criterion for oscillations is

$$R_s < 2\sqrt{\frac{L_s}{C}} \tag{56}$$

where C is the capacitance of C_1 and C_2 in series. Many rectifier tubes have peak current ratings which must not be exceeded by such currents.

Currents shown in Table VII (p. 62) and Figs. 49 and 95 are reflected back into the a-c power supply line, except that alternate current waves are of reverse polarity. Small rectifiers have little effect on the power system, but large rectifiers may produce excessive interference in nearby telephone lines because of the large harmonic currents inherent in rectifier loads. High values of commutation reactance reduce these line current harmonics, but, since good regulation requires low commutation reactance, there is a limit to the control possible by this means. A-c line filters are used to attenuate the

line current harmonics. A large rectifier, with three-phase series resonant circuits designed to eliminate the eleventh, thirteenth, seventeenth, and nineteenth harmonics of a 60-cycle system, is shown in Fig. 96. Smaller rectifiers sometimes have filter sections such as

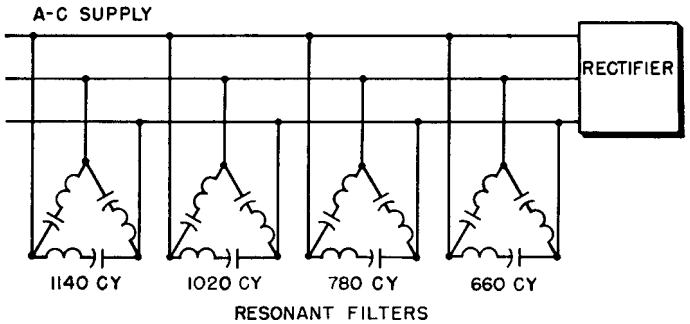

FIG. 96. A-c line filter for large power rectifier.

those in Fig. 97; these are rarely used in large installations because of the excessive voltage regulation introduced by the line inductors.

Filters designed to keep r-f currents out of the a-c lines are often

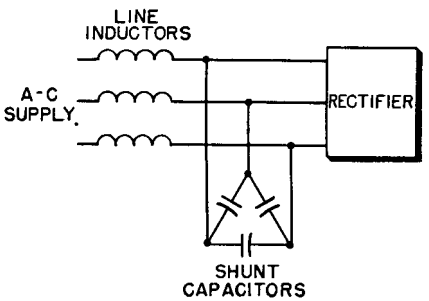

FIG. 97. A-c line filter for medium-sized power rectifier.

used with high-voltage rectifiers. Even if the anode transformer has low radio influence, commutation may cause r-f currents to flow in the supply lines unless there is a filter.

55. Rectifier Transients. The shunt-tuned filter currents mentioned in the preceding section are transient. Since the tube current is cut off during each cycle, a transient current may occur in each cycle. When power is first applied to the rectifier, another transient occurs, which may be smaller or larger than the cyclic transient, depending on the

filter elements. In reactor-input filters the transient current can be approximated by the formula given in Section 54 for a step function applied to the series circuit comprising filter L and C plus R_s. This circuit is valid because the shunting effect of the load is slight in a well-proportioned filter. In capacitor-input filters, the same method can be used, but here the inductance is the leakage inductance of the anode transformer. Therefore, equation 55 applies, except that the maximum step function voltage is E_{pk}.

Transients which occur when power is first applied differ from cyclic transients in that they are spasmodic. Power may be applied at any instant of the alternating voltage cycle, and the suddenly impressed rectifier voltage ranges from zero to E_{pk}. Starting transients are difficult to observe on an oscilloscope because of their random character. It is necessary to start the rectifier several times for one observation of maximum amplitude, and the trace is faint because it appears for a very brief time.

Excessive current inrush, which occurs when a power transformer is connected to a supply line, plagues rectifier design. The phenomenon is associated with core saturation. For example, suppose that the core induction is at the top of the hysteresis loop in Fig. 18 (p. 24) at the instant when power is removed from the rectifier, and that it decreases to residual value B_r for $H = 0$. Suppose that the next application of power is at such a point in the voltage cycle that the normal induction would be B_m. This added to B_r requires a total induction far above saturation value; therefore heavy initial magnetizing current is drawn from the line, limited only by primary winding resistance and leakage inductance. This heavy current has a peaked wave form which may induce momentary high voltages by internal resonance in the secondary coils and damage the rectifier tubes. Or it may trip a-c overload relays. The problem is especially acute in large transformers with low regulation. A common remedy is to start the rectifier with external resistors in the primary circuit and short-circuit them a few cycles later. Some rectifiers are equipped with voltage regulators which reduce the primary voltage to a low value before restarting.

A-c line transients may cause trouble in three-phase rectifiers, especially those having balance coils, by shifting the floating neutral voltage. Filters like that in Fig. 97 prevent such transients from appearing in the rectified output.

In some applications the load is varied or removed periodically. Examples of this are keyed or modulated amplifiers. Transients occur

when the load is applied (key down) or removed (key up), causing respectively a momentary drop or rise in plate voltage. If the load is a device which transmits intelligence, the variation in filter output voltage produced by these transients results in the following undesirable effects:

1. Modulation of the transmitted signal.
2. Frequency variation in oscillators, if they are connected to the same plate supply.
3. Greater tendency for key clicks, especially if the transient initial dip is sharp.
4. Loss of signal power.

A filter which attenuates ripple effectively is normally oscillatory; hence damping out the oscillations is not practicable. Nor would it remedy the transient dip in voltage, which may increase with non-oscillatory circuits. The filter capacitor next to the load should be large enough to keep the voltage dip reasonably small. An approximation for transient dip in load voltage which neglects the damping effect of load and series resistance is

$$\Delta E_D = \frac{1}{R}\sqrt{\frac{L}{C}} \tag{57}$$

where ΔE_D is the transient dip expressed as a fraction of the steady-state voltage across R, and L, C, and R are as shown in Fig. 79(a). The accuracy of this approximation is poor for dips in transient voltage greater than 20 per cent.

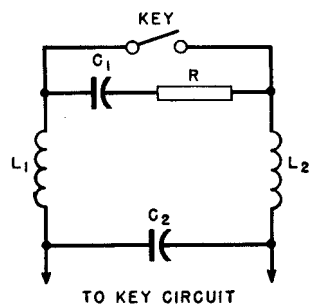

FIG. 98. Key-click filter.

Although the tendency for key clicks in the signal may be reduced by attention to the d-c supply filter elements, the clicks may not be entirely eliminated. Where key-click elimination is necessary, some sort of key-click filter is used, of which Fig. 98 is an example. This filter has inductance and capacitance enough to round off the top and back of a wave and eliminate sharp, click-producing corners. Figure 99 is an oscillogram showing a keyed wave shape with and without such a filter.

In a choke-input filter, voltage surges are developed across the choke under the following conditions:

1. *Ripple Voltage.* With large rectifier commutation angles, or with grid-controlled rectifiers, a surge occurs once each ripple cycle. In the limit, this surge equals the rectifier peak voltage.

2. *Initial Starting Surge.* This surge adds to output d-c voltage. Under the worst conditions it raises the voltage at this point to twice normal and occurs every time rectifier plate voltage is applied.

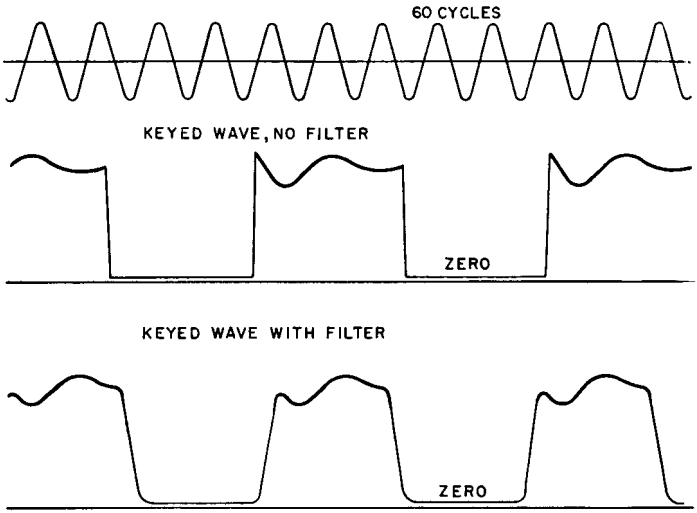

FIG. 99. Keyed wave shape with and without key-click filter.

3. *Keying or Modulation Transient.* Surge value depends upon constants L, C, and R_L, and is limited by considerations of wave shape. This occurs each time the key is opened or closed, or load is varied.

4. *Short-Circuit Surge.* If load R_L is suddenly short-circuited, it causes full d-c voltage to appear across the filter reactor until the circuit breaker opens. This occurs occasionally. Rectifiers are sometimes arranged so that, if the short circuit persists, the circuit breaker recloses 3 times and then remains open.

5. *Interruption of Reactor Current.* This surge voltage is limited only by losses and capacitance of the circuit, and it may be large, as shown by Fig. 73. Unless the reactor is designed to produce this voltage, it occurs only through accident.

Conceivably, surges 1, 2, and 3 may occur simultaneously and add arithmetically. A reactor insulated to withstand surges 1 plus 2 plus 3 also would withstand surge 4. A reasonable value of peak surge voltage comprising these factors is 2½ times the full d-c working voltage.

If surges 1 and 5 are too much for reasonable insulation, the reactor is protected by a gap or other means.

If a rectifier is disconnected from the supply line while the load is off, interruption of plate transformer peak magnetizing current may cause high voltages to appear at random in the windings in much the same way as reactor current interruption causes high voltages. This is especially true if the transformer operates at high core induction. The effect is partly mitigated by the arc energy incident to the opening of the disconnecting switch. But unless the plate transformer is insulated specifically to prevent dangerously high voltages, protective elements may have to be added in a rectifier subject to switching at light loads. The necessity for such protection may be estimated from exciting volt-ampere data plus the curves of Fig. 73.

Insufficient attention sometimes is given to the manner in which power supply lines are brought into buildings. This is particularly important where a rectifier is supplied by overhead high-voltage lines. Because of their relatively high surge impedance, lightning and switching surges occurring on such lines may cause abnormally high voltages to appear in a rectifier and break down the insulation of transformers or other component parts. The likelihood of such surges occurring should be taken into account before the transformers are designed.

Underground cable power lines impose much less severe hazards: first because they are protected from lightning strokes, and second because they have much lower impedance (about one-tenth that of overhead lines). Surges on these cables have much lower values compared to those on overhead lines carrying the same rated voltage. Protection against these surges varies with the type of installation.

The best protection of all is provided by an indoor power system with an underground cable connecting it to the rectifier. Good protection is afforded by oil-insulated outdoor surge-proof distribution transformers, stepping down to the rectifier a-c power supply voltage, with an underground cable between the distribution transformer and rectifier. No protection at all is provided when overhead lines come directly into the rectifier building.

With the trend to dry-type insulation, it is desirable to use lightning arresters on overhead lines where they enter the building. Because of their low impulse ratio, dry-type transformers require additional arresters inside the building. When a line surge is discharged by a lightning arrester, there is no power interruption.

56. Rectifier Filter Charts. From the preceding sections, it can be seen that various properties of rectifier filters, such as ripple, regula-

tion, and transients, may impose conflicting conditions on rectifier design. To save time in what otherwise would be a laborious cut-and-try process, charts are used. In Fig. 100 the more usual filter properties are presented on a single chart to assist in arriving at the best filter directly. This chart primarily satisfies ripple and regulation equations 46 and 53 for a choke-input filter.

Abscissa values of the right-hand scale are bleeder conductance in milliamperes per volt, and of the left-hand scale, filter capacitance in microfarads. Ordinates of the lower vertical scale are inductance in henrys. Lines representing various amounts of ripple in the load are plotted in quadrant I, labeled both in db and rms per cent ripple. In quadrant II, lines are drawn representing different types of rectifiers and supply line frequencies. A similar set of lines is shown in quadrant IV.

Two orthogonal sets of lines are drawn in quadrant III. Those sloping downward to the right represent resonant frequency of the filter L and C, and also load resistance R_L. The other set of lines is labeled $\sqrt{L/C}$, which may be regarded as the filter impedance. It can be shown that the transient properties of the filter are dependent upon the ratio of $\sqrt{L/C}$ to R_L.

The L scale requires a correction to compensate for the fact that ripple is not exactly a linear function of L but rather of $X_L - X_C$. The curves in the lower part of quadrant IV give the amount of correction to be added when the correction is greater than 1 per cent.

Instructions for Using Chart

1. Assume suitable value of bleeder resistance or bleeder current I_1 in millamperes per volt of E_{dc}. This is also steady-state peak ripple current in milliamperes.

2. Trace upward on assumed bleeder ordinate to intersect desired value of load ripple, and from here trace horizontally to the left to diagonal line for rectifier and supply frequency used. Directly under, read value of C.

3. Trace downward on same assumed bleeder ordinate to intersect diagonal line below for rectifier and supply frequency, and read value of L.

4. From desired ripple value, determine correction for L on graph at lower right, and add indicated correction to value of L.

5. Using corrected value of L and next standard value of C, find intersection in third quadrant, and read maximum resonant frequency f_r.

6. Using same values of L and C as in 5, read value of ratio $\sqrt{L/C}$.

7. Under intersection of $\sqrt{L/C}$ with load resistance R_L read values of the four transients illustrated in Fig. 101 (in per cent).

Example (shown dotted). Three-phase full-wave 60-cycle rectifier; E_{dc} = 3,000 v; I_2 = 1 amp; I_1 = 96 ma; load ripple = −50 db; balanced line.
Solution:

Bleeder ma/volt = 0.032.
C = 4.5 μf (use 5 μf).
Scale value of L = 0.78 h; corrected value = 0.82 h.
Resonant frequency = 75 cycles.
Load resistance R_L = 3,000 ohms.
$i_m = 7I_2 = 7$ amp; ΔE_D = 12 per cent; ΔE_R = 15 per cent; ΔE_s = 80 per cent.

In polyphase rectifiers the possibility exists of enough phase unbalance to impress a voltage on the filter having a frequency lower than the normal fundamental ripple frequency. If the filter L and C resonate near the unbalance frequency, then excessive ripple may be expected. Conversely, the L and C should have a resonant frequency lower than the unbalance frequency to avoid this trouble. Quadrant III of the chart has a series of lines labeled f_r, and the intersection of L and C thereon indicates this resonant frequency. It should be no higher than the value given in the small table on the chart if excessive ripple is to be avoided. This table is based on 2 per cent maximum unbalance in the phase voltages.

For most practical rectifier filters, transient conditions fall within the left-hand portion of the third quadrant. The other conditions sometimes help in the solution of problems in which L and C are incidental, e.g., the leakage inductance and distributed capacitance of a plate transformer.

Although the chart applies directly to single-stage, untuned filters with constant choke inductance, it can be used for other types with modifications:

(*a*) *Shunt-Tuned Choke per Fig. 93.* Figure 100 can be used directly for capacitance C, but, for a given amount of ripple, divide the chart values of inductance by 3 in order to obtain the actual henrys needed in the choke.

(*b*) *Swinging Choke.* If at light load the filter choke swings to S times the full-load value of henrys, multiply the capacitance obtained from the chart by the ratio S to find the capacitance needed (C_n). The

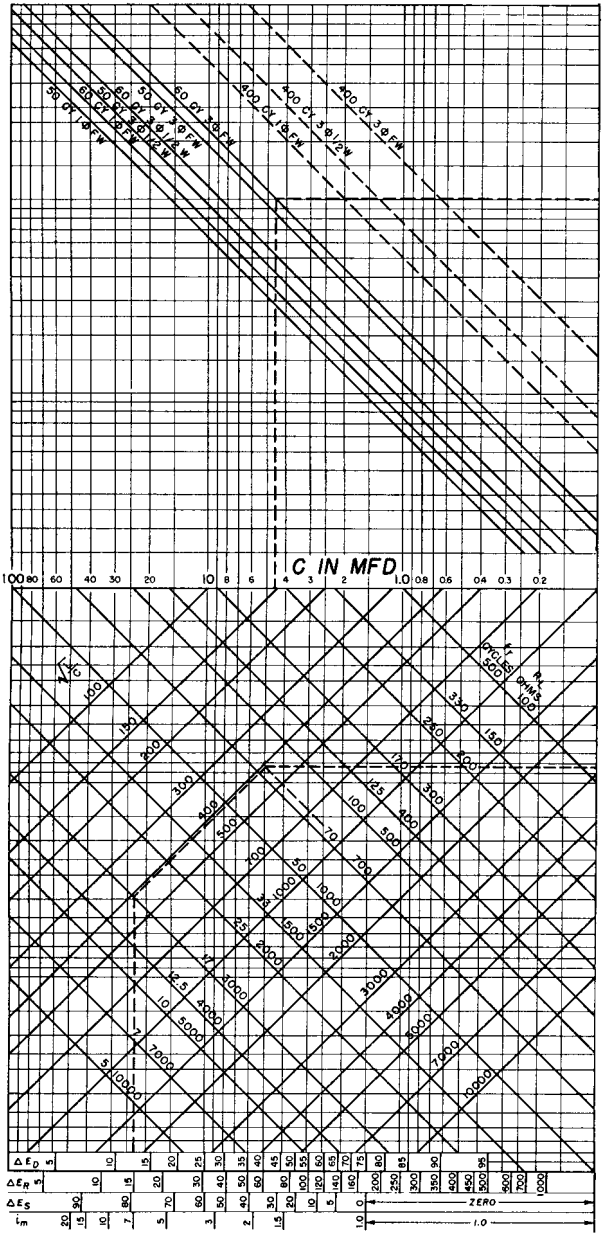

FIG. 100. Choke-input filter chart.

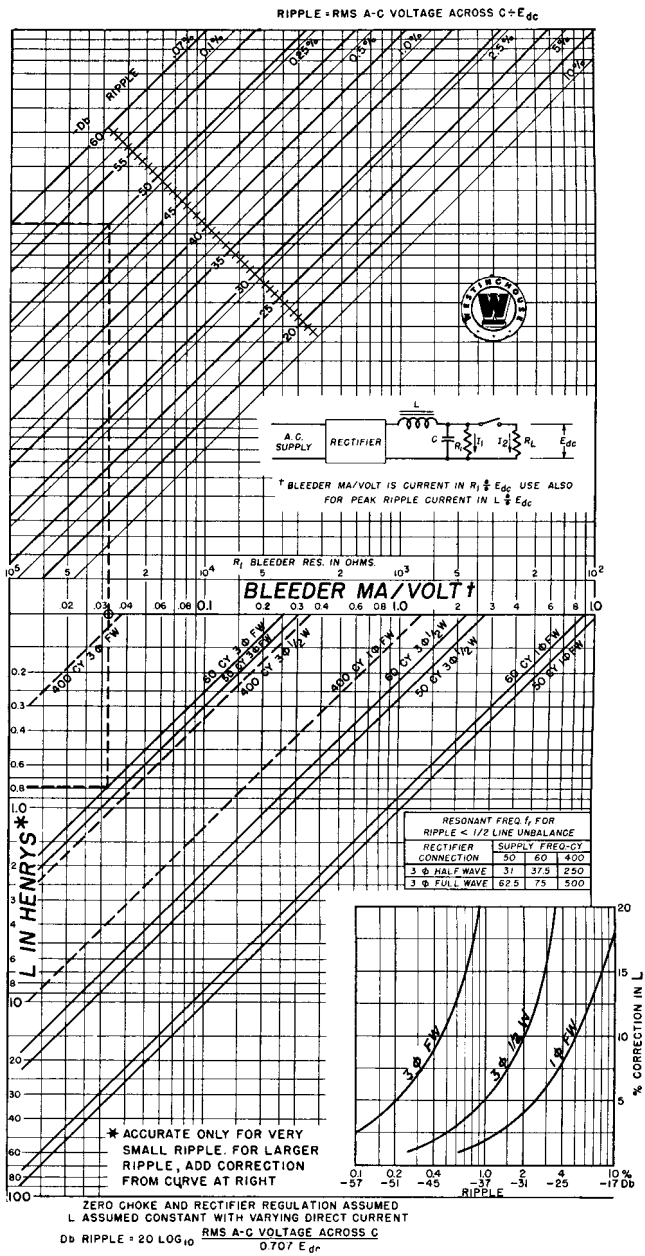

FIG. 100. *(Continued)*

value of L obtained by projecting the bleeder current downwards is the maximum or swinging value. It must be divided by S to obtain the full-load value. Transient conditions then may be approximated by using capacitance C_n and the full-load value of henrys.

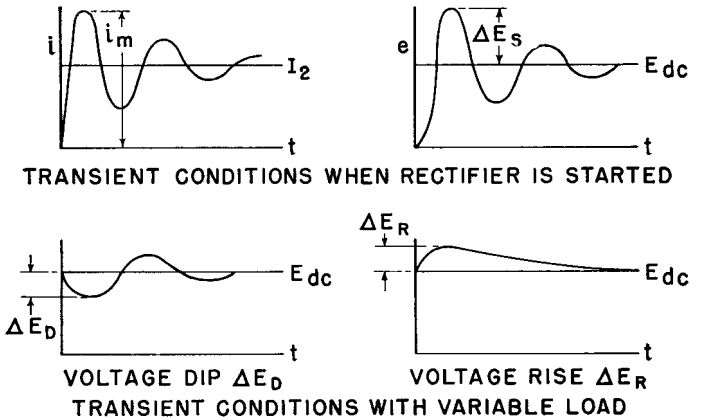

FIG. 101. Four transient conditions in choke-input filter circuit and curves.

(*c*) *Two-Stage Filters.* In a filter with two identical stages, Fig. 84(*b*), the chart can be used if it is recognized that the ripple is that on the load side of the first choke. For example, if the filter consists of two stages both equal to that in the example given for the single-stage filter, the ripple would not be −100 db but −75 db, because of the fact that the rectifier output has (per Table VII) only 4 per cent ripple, which is −25 db.

The regulation in a two-stage filter, as far as capacitor effect is concerned, depends upon the inductance of the first choke as in the single-stage filter. Therefore the chart applies directly to the inductance and capacitance of one stage. The peak ripple current likewise depends upon the inductance of the first choke, regardless of the location of the bleeder resistor. Transients, however, are more complicated, owing to the fact that the two stages interact under transient conditions.[1]

57. Rectifier Efficiency. Losses in a rectifier consist of transformer, tube, and filter losses. Filament power should be counted as loss, especially when a tube rectifier is compared with a rotating machine

[1] See *Proc. I.R.E., 22,* 213 (February, 1934).

or metal disk rectifier. In spite of this loss, a high-voltage polyphase rectifier of the mercury-vapor or pool type may have 95 per cent efficiency at full load. In contrast, the rectifier for a radio receiver rarely has more than 60 per cent efficiency. Reasons for this low figure are the high tube and reactor *IR* drops and low transformer efficiency. The filament power, too, is a greater portion of the total.

58. Rectifier Tests. Even though the transformers, chokes, tubes, and capacitors have been tested before assembly of the rectifier, performance tests of the rectifier are desirable. These generally include tests of output, regulation, efficiency, ripple, and input kilovolt-amperes or power factor. Accurate meters should be used, and polyphase rectifiers should have balanced supply voltages. Wiring is tested at some voltage higher than normal, preferably with transformers, tubes, and capacitors disconnected to avoid damage during the test. Ordinary care in testing is sufficient except for regulation tests. If the regulation is low, the difference in meter readings at no load and full load may be inaccurate. Differential measurements are sometimes used, such as a voltmeter connected between the rectifier and a fixed source of the same polarity and voltage. Artificial loading of a high-voltage rectifier is often a problem. Water rheostats have been used for this purpose. Load tests, preferably in combination with the transmitter or other apparatus which the rectifier is to supply, are safeguards against field troubles. Operating tests are essential when the load is keyed or modulated, so that overheating or inadequate transformer operation may be detected.

Ripple is measured either with a special hum-measuring instrument or with a capacitance-resistance network arranged to block the direct current from the measuring circuit. Capacitance and resistance values in the measuring circuit should be so chosen as to avoid influencing the ripple or loading the rectifier transformer. Sometimes capacitance dividers are used for this purpose. The problem of proper values becomes particularly critical with high-voltage low-current rectifiers. The effect of stray capacitance is especially important.

5. AMPLIFIER TRANSFORMERS

An amplifier is a device for increasing voltage, current, or power in a circuit. The original wave form may or may not be maintained; the frequency usually is. An amplifier may be mechanical, electromechanical, electromagnetic, or electronic in form, or it may be a combination of these. In this chapter the transformer-coupled electronic amplifier is considered. The amplifier consists of a vacuum tube, or similar device, with transformers, capacitors, and resistors. Input voltage or current is impressed on some element of the tube; this causes higher voltage or current to appear in the output circuit.

59. Amplifier Potentials. Electronic amplifiers are characterized by the use of tubes having three or more elements. In triodes or three-element tubes, the addition of the third element, the grid, alters the

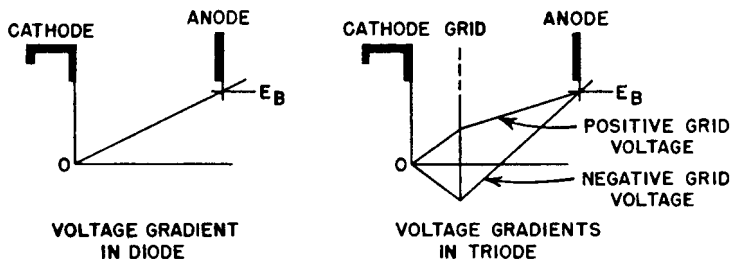

FIG. 102. Diode and triode voltage gradient.

voltage gradient between cathode and anode as shown in Fig. 102. The grid either aids or opposes the flow of electrons from cathode to anode, depending on whether the grid voltage is positive or negative respectively, compared to the cathode, which is shown at zero voltage in Fig. 102.

As the grid voltage is made more and more negative, electron flow is diminished and finally stops. At this point the anode current is zero; the condition is called *anode current cut-off*.

If the grid voltage is made more and more positive, eventually

further increase in grid voltage causes no additional anode current increase. This condition is called *grid saturation.*

Tetrodes and pentodes have respectively two and three grids. The voltage gradient between cathode and anode is more complex than that indicated in Fig. 102. The advantages to be gained from the additional grids are mentioned below.

60. Transformer-Coupled Amplifiers. Amplifier circuits in which transformers are used can be represented by a circuit similar to that of Fig. 103(*a*). Here a triode is shown with a voltage e_c impressed upon the grid, which comprises the grid bias (a constant negative direct voltage) and a superimposed alternating voltage e_g. Anode

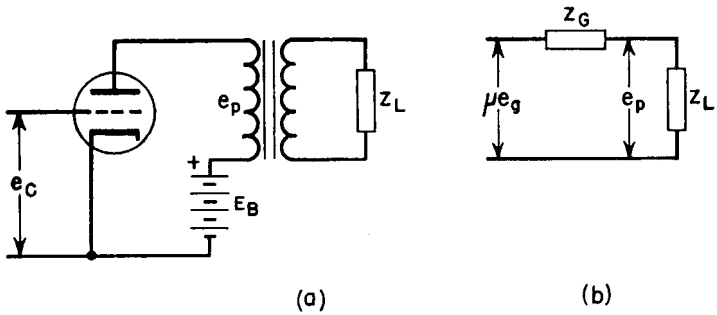

FIG. 103. (*a*) Transformer-coupled amplifier; (*b*) equivalent circuit.

voltage E_B is supplied from some source through the primary of the transformer, across which appears an alternating voltage e_p. The secondary of the transformer is connected to a load Z_L. Under certain conditions, which will be defined below, this circuit may be simplified to that of Fig. 103(*b*). A fictitious alternating voltage μe_g is impressed on the circuit, where μ is the tube amplification factor. Internal tube resistance Z_G is in series with the load Z_L, which is reflected by the transformer to the proper value in the primary circuit for tube operation. That is, Z_L in Fig. 103(*b*) is equal to that in Fig. 103(*a*) only if the transformer has a 1:1 ratio. For any turns ratio, the quotient of two Z's is equal to the (turns ratio)^2 as in equation 7 (p. 8). Note that the winding resistances are regarded as zero, so that, in the absence of a grid signal, full voltage E_B appears on the plate of the vacuum tube.

Alternating voltage μe_g causes voltage e_p to appear across the load Z_L. The voltage e_p is not μ times e_g but is related by the following equation:

$$e_p = \mu e_g \frac{Z_L}{Z_G + Z_L} \tag{58}$$

Although transformer-coupled amplifiers are used sometimes for voltage amplification, they are used mostly where power output is required of the amplifier and where a good reproduction of the grid voltage is required in the plate circuit.

61. Tuned Amplifiers. Figure 104 shows the circuit for an amplifier in which the output voltage appears across a parallel-tuned circuit.

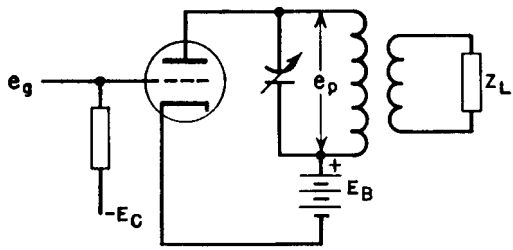

FIG. 104. Tuned amplifier.

This circuit is shown coupled to a load Z_L. This type of amplifier may be used where large outputs are required, but the voltage e_p is not necessarily a reproduction of e_g, and they are not related as in equation 58.

62. Amplifier Classification. Amplifiers can be divided into classes, depending upon the mode of operation. A class A amplifier is one in which the grid bias and alternating grid voltage are such that anode current flows continuously. In a class B amplifier the grid bias is almost equal to the cut-off value, so that plate current is nearly zero when no exciting grid voltage is applied. When full alternating grid voltage is applied, plate current flows for approximately one-half of each cycle. A class C amplifier has a grid bias greater than the cut-off value, so that the plate current is zero when no alternating grid voltage is applied and it flows for appreciably less than one-half of each cycle when an alternating grid voltage is applied. These classes are illustrated in Fig. 105, in which the alternating plate current, plate voltage, grid voltage, and grid current are shown with the steady or average values which are, respectively, I_B, E_B, E_C, and I_G. Relative plate and grid voltage amplitudes for these three types of amplifiers are shown in Fig. 105, and other properties are summarized in Table XI.

Class A amplifiers are characterized by comparatively high no-signal anode current. Usually the grid never swings positive. Anode cur-

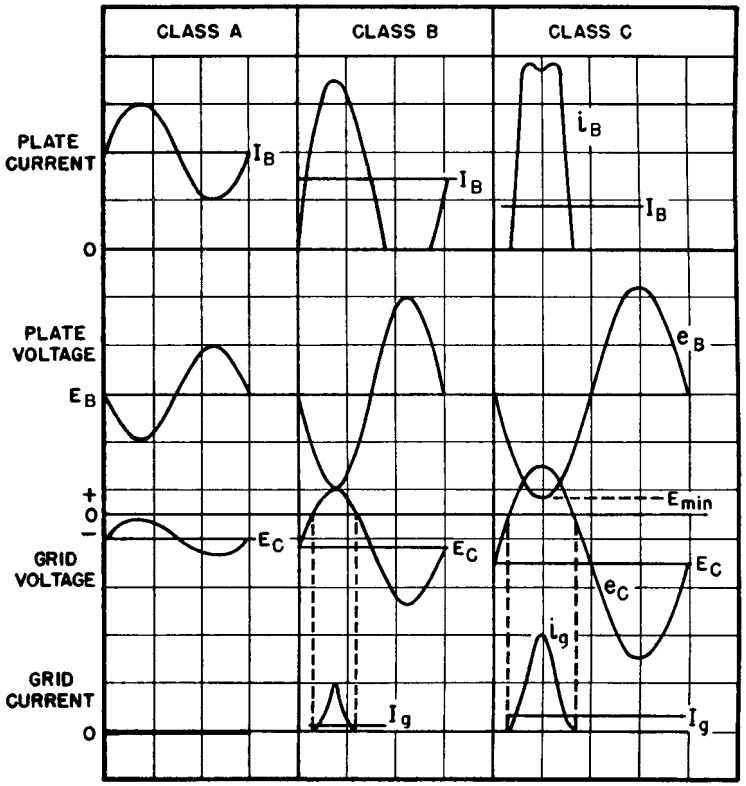

FIG. 105. Amplifier voltages and currents.

TABLE XI. AMPLIFIER CLASSES

Amplifier Class	A	B	C
Anode efficiency			
a. Theoretical maximum	50%	78.5% *	100%
b. Practical value for low distortion	Up to 30%	40–67% *	70–85% †
Output proportional to	e_g^2	e_g^2	E_B^2 (grid saturated)
Grid current I_g	None	Small	Large (may $\approx I_B$)
Anode current I_B	Fairly constant	$e_g = 0$, I_B low e_g = max, I_B high	$e_g = 0$, $I_B = 0$ e_g = max, I_B high

* These values are for push-pull amplifiers.

† With a high-Q tank circuit, the efficiency depends on excitation power.

rent remains comparatively constant, when averaged over a whole a-c cycle. In class B amplifiers, the grid is biased at a greater negative potential so that current is nearly cut off in the absence of a signal. Positive swings of grid voltage result in anode current being drawn; this causes a dip in the residual voltage on the plate of the amplifier. Negative grid swings cause no plate current to flow but do cause a positive plate voltage swing. In class C amplifiers, the grid is biased more negatively still, with the result that plate current flows for less than half a cycle, and mostly when the plate voltage on the tube is at a relatively low value. Grid current in this class of amplifier reaches values comparable to the plate current. Output voltage wave form is maintained by a tuned plate circuit.

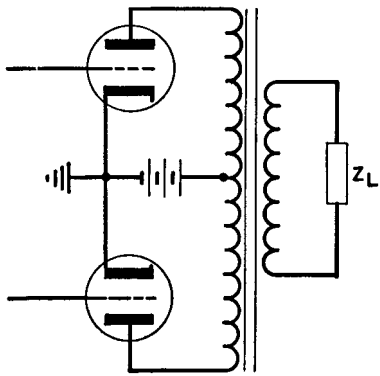

FIG. 106. Push-pull amplifier.

Operation may sometimes be improved by the use of two tubes connected push-pull, as shown in Fig. 106. This is the most common connection for class B amplifiers; also, it is frequently used in class A amplifiers. Intermediate between class A and class B amplifiers are those known as class AB with grid bias and efficiency intermediate between class A and class B amplifiers. Such amplifiers are further subdivided into class AB_1 and class AB_2. Class AB_1 amplifiers draw no grid current, but the bias voltage is somewhat higher than the class A value and the plate current may be discontinuous during the cycle when grid signal is applied. Class AB_2 amplifiers draw grid current but are not biased as close to cut-off as class B amplifiers. Both class AB_1 and AB_2 amplifiers are commonly used with the push-pull connection.

Tube properties such as plate resistance r_p, amplification factor μ, and mutual conductance g_m may be calculated from data published for each tube in the form of characteristic curves. Operating conditions such as plate- and grid-voltage swings, power output, plate dissipation, and efficiency also are found from these curves. Theoretical discussions of such data may be found in books on amplifiers.

63. Decibels; Impedance Matching. In amplifier work, the ratio of two voltages E_1 and E_2 at the same impedance level is often stated in decibels (db) according to the definition

$$\text{db} = 20 \log_{10} (E_1/E_2) \tag{59}$$

Amplifier voltage gain, transformer ratio, frequency response, and noise levels all may be expressed in decibels. Volume, voltage, or power in decibels must be compared to a reference level; otherwise the term is meaningless. A standard reference level is 1 milliwatt. This is expressed as zero dbm. Across 600 ohms, the voltage for zero dbm is $\sqrt{0.001 \times 600} = 0.775$ volt; for 20 dbm the voltage is 7.75 volts.

Transmission lines at audio and higher frequencies exhibit properties commonly ignored at 60 cycles. Line wavelength, characteristic impedance, and attenuation are important at audio frequencies; so is the matter of matching impedance. If a long transmission line has no attenuation, its characteristic impedance is given by

$$Z_0 = \sqrt{\frac{L}{C}} \tag{60}$$

where L and C are the inductance and capacitance per unit length. If such a line terminates in a pure resistance load equal in ohmic value to Z_0, all the power fed into the line appears in the load without attenuation or reflection. This is called matching the impedance of the line. It is very desirable to save audio power and avoid reflections; therefore impedance matching of lines is the usual practice wherever possible. The notion has been extended to include the loading of vacuum tubes, but this is stretching the meaning of the term matching. A vacuum tube has its optimum load impedance, but the value depends upon the conditions of tube operation and is not necessarily the same as the tube internal impedance.

Power transmission lines operating at 60 cycles are rarely long enough to act as appreciable source impedances. When a short-circuit or low-impedance fault occurs on the load side of a power transformer, the load current is limited mainly by the transformer short-circuit impedance. In a vacuum-tube amplifier, the load current delivered into a short-circuited load is limited mainly by the vacuum-tube internal resistance rather than by the transformer. At certain frequencies the transformer itself may contribute to low load impedance. But the greatest difference between power and amplifier transformers is the difference in source impedance. Even the use of the word impedance in the two fields of application reflects this difference. In power work, transformer impedance denotes the short-circuit im-

pedance; in amplifier work, the same term refers to the load or source impedance.

64. Amplifier Transformers. The major problem of amplifier transformer design is obtaining proper output when the transformer is operated in conjunction with the apparatus for which it is intended. Several factors external to the transformer affect its performance, namely, (1) impedance of the source; (2) linearity of this impedance; (3) impedance of the load; and (4) frequency.

The simplest method of dealing with amplifier transformers is an adaptation of the so-called equivalent network which has long been used for power transformers. The transformer that connects the source to its load in Fig. 103(*a*) may be represented more fully by the diagram of Fig. 107(*a*).

65. Low-Frequency Response. At low frequencies, the leakage reactances are negligibly small. Resistance R_P may then be combined with Z_g to form R_1 for a pure resistance source, and R_S with Z_L to form R_2 for a resistance load. At low frequencies both source and load are pure resistance, and the circuit may be simplified to that of Fig. 107(*b*). Here the a^2 has been dropped; in other words, a transformer with a 1:1 ratio is shown, referred to the primary side. X_N is the primary open-circuit reactance, or $2\pi f$ times the primary open-circuit inductance (*OCL*) as measured at low frequencies.

If shunt resistance R_N is included in load resistance R_2, the circuit becomes like that of Fig. 107(*c*). Winding resistances are small compared with source and load resistances in well-designed transformers. Likewise, R_N is high compared with load resistance, especially if core material of good quality is used.

Therefore, *to a good approximation,* in Fig. 107(*c*), R_1 may represent the source impedance and R_2 the load impedance. On a 1:1 turns-ratio basis, the voltages E_2 and E_1 are proportional to the impedances across which they appear or

$$\frac{E_2}{E_1} = \frac{\dfrac{jX_N R_2}{jX_N + R_2}}{R_1 + \dfrac{jX_N R_2}{jX_N + R_2}} \tag{61}$$

The scalar value of this ratio is found by taking the square root of the sum of quadrature terms:

$$\frac{E_2}{E_1} = \frac{1}{\sqrt{\left(1 + \frac{R_1}{R_2}\right)^2 + \left(\frac{R_1}{X_N}\right)^2}} \tag{62}$$

Equation 62 holds for any values of R_1, R_2, and X_N whatsoever, but there are three cases that deserve particular attention: (*a*) $R_2 = R_1$; (*b*) $R_2 = 2R_1$; and (*c*) $R_2 = \infty$. Of these, (*a*) corresponds to the usual line-matching transformer with the source and load impedances equal; (*b*) is often recommended for maximum undistorted output of triodes; (*c*) is realized practically when the load is the grid of a class A

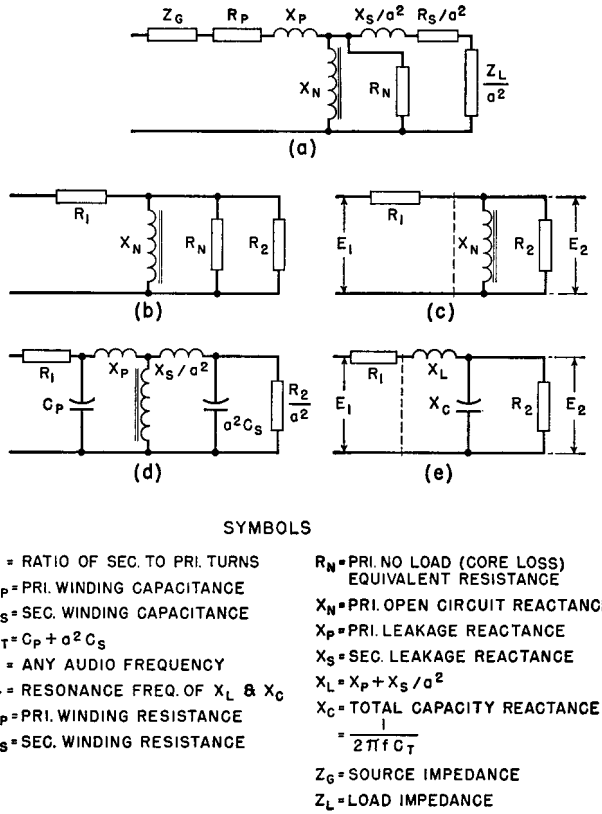

SYMBOLS

a = RATIO OF SEC. TO PRI. TURNS
C_P = PRI. WINDING CAPACITANCE
C_S = SEC. WINDING CAPACITANCE
$C_T = C_P + a^2 C_S$
f = ANY AUDIO FREQUENCY
f_r = RESONANCE FREQ. OF X_L & X_C
R_P = PRI. WINDING RESISTANCE
R_S = SEC. WINDING RESISTANCE
R_N = PRI. NO LOAD (CORE LOSS) EQUIVALENT RESISTANCE
X_N = PRI. OPEN CIRCUIT REACTANCE
X_P = PRI. LEAKAGE REACTANCE
X_S = SEC. LEAKAGE REACTANCE
$X_L = X_P + X_S/a^2$
X_C = TOTAL CAPACITY REACTANCE $= \frac{1}{2\pi f C_T}$
Z_G = SOURCE IMPEDANCE
Z_L = LOAD IMPEDANCE

FIG. 107. (*a*) Transformer equivalent circuit; (*b*) low-frequency equivalent circuit; (*c*) simplified low-frequency circuit; (*d*) high-frequency equivalent circuit; (*e*) simplified high-frequency circuit.

amplifier. For these cases, equation 62 becomes

$$\frac{E_2}{E_1} = \frac{1}{\sqrt{4 + \left(\frac{R_1}{X_N}\right)^2}} \tag{62a}$$

$$\frac{E_2}{E_1} = \frac{1}{\sqrt{2.25 + \left(\frac{R_1}{X_N}\right)^2}} \tag{62b}$$

$$\frac{E_2}{E_1} = \frac{1}{\sqrt{1 + \left(\frac{R_1}{X_N}\right)^2}} \tag{62c}$$

These three equations are plotted in Fig. 108 to show low-frequency response as "db down" from median. The median frequency in an audio transformer is the geometric mean of the audio range; for other transformers it is a frequency at which the ratio X_N/R_1 is very large. At median frequency the circuit is properly represented by Fig. 103(*b*).

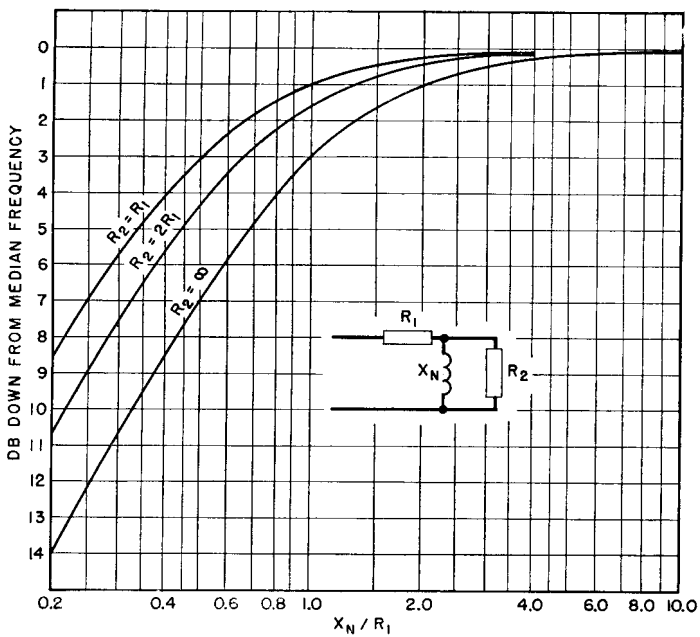

FIG. 108. Transformer characteristics at low frequencies.

The equivalent voltage ratio E_2/E_1 has maxima of 0.5, 0.667, and 1.0 for cases (a), (b), and (c), respectively, at the median frequency, or for $X_N/R_1 = \infty$ in Fig. 108. The higher OCL, the nearer the transformer voltage ratio approaches median-frequency value. The lower the value of loading resistance R_2, the lower the equivalent voltage ratio is. The factors 0.5, 0.667, and 1.0 multiplied by the turns ratio, a, give the actual voltage ratio at median frequency. At lower frequencies, the factors diminish.

The transformer loaded by the lowest resistance has the best low-frequency characteristic. A transformer having an open-circuit secondary has twice the voltage ratio and gives the same response at twice the "low end" frequency of a line-matching transformer of the same turns ratio.

Figure 108 is of direct use in determining the proper value of primary OCL. Permissible response deviation at the lowest operating frequency fixes X_N/R_1 and therefore X_N. At the corresponding frequency, this represents a certain value of primary OCL. As this inductance determines the size and weight of the transformer, the importance of Fig. 108 is evident.

If the primary and equivalent (1:1) secondary winding resistance each are 5 per cent of R_1, the total effect will be a decrease of 10 per cent in the median-frequency voltage ratio, in the case of the line-matching transformer, with corresponding decreases at lower frequencies. On the other hand, the primary resistance of an open secondary transformer has no effect upon the median-frequency voltage ratio but has some effect at lower frequencies, whereas the secondary resistance has no effect either at median or at lower frequencies. Hence it is important in the open secondary case, for the sake of low-frequency response, to keep the primary winding resistance low, but the secondary winding resistance may be any value. The maximum number of secondary turns may be determined by the smallest practicable wire size rather than by winding resistance.

As the frequency increases, the primary inductive reactance X_N also increases until it has almost no effect upon frequency response. This is true for median frequency in Fig. 108. It is also true for higher frequencies; in other words, the OCL has an influence only on the low-frequency end of the frequency response curve. The ratio of R_2 to R_1 still limits the voltage ratio, however. If the amplifier works at one frequency only, OCL is determined by the deficiency in voltage gain that can be tolerated in the amplifier design. This can be found in Fig. 108.

In an amplifier with a band of operating frequencies, e.g., the audio band, a well-designed transformer has uniform voltage ratio for a frequency range extending from the frequency at which X_N ceases to exert any appreciable influence, upward to a zone designated as the high-frequency end of the transformer frequency range.

66. High-Frequency Response. The factors that influence the high-frequency response of a transformer are leakage inductance, winding capacitance, source impedance, and load impedance. Hence a new equivalent diagram, Fig. 107(*d*), is necessary for the high-frequency end. Winding resistances are omitted or combined as in Fig. 107(*b*). Winding capacitances are shown across the windings. If primary and secondary leakage inductances and capacitances are combined, X_N is omitted as if it were infinitely large, and a^2 is dropped as before, the circuit becomes that shown in Fig. 107(*e*). X_L is the leakage reactance of both windings, X_C the capacitive reactance of both windings, and R_2 the load resistance, all referred to the primary side on a 1:1 turns-ratio basis.

At any frequency, the equivalent voltage ratio in the circuit of Fig. 107(*e*) can be found by the ratio of impedances, as for the low-frequency response. The scalar value is

$$\frac{E_2}{E_1} = \frac{1}{\sqrt{\left(\frac{R_1}{X_C} + \frac{X_L}{R_2}\right)^2 + \left(\frac{X_L}{X_C} - \frac{R_1}{R_2} - 1\right)^2}} \tag{63}$$

In equation 63 the term X_L/X_C may be written $4\pi^2 f^2 LC = f^2/{f_r}^2$, where $1/(2\pi\sqrt{LC}) = f_r$, the resonance frequency of the leakage inductance and winding capacitance, considered as lumped and without resistance. Also $X_L/R_2 = X_C f^2/R_2 {f_r}^2$. Assign to the ratio X_C/R_1 a value B at frequency f_r. Then at any frequency f, $X_C/R_1 = Bf_r/f$. In the three cases considered at the low frequencies,

$R_2 = R_1$,

$$\frac{E_2}{E_1} = \frac{1}{\sqrt{\left(\frac{f}{Bf_r} + \frac{Bf}{f_r}\right)^2 + \left(\frac{f^2}{{f_r}^2} - 2.0\right)^2}} \tag{63a}$$

$R_2 = 2R_1$,

$$\frac{E_2}{E_1} = \frac{1}{\sqrt{\left(\frac{f}{Bf_r} + \frac{Bf}{2f_r}\right)^2 + \left(\frac{f^2}{{f_r}^2} - 1.5\right)^2}} \tag{63b}$$

$R_2 = \infty$,

$$\frac{E_2}{E_1} = \frac{1}{\sqrt{\left(\frac{f}{Bf_r}\right)^2 + \left(\frac{f^2}{f_r^2} - 1\right)^2}} \tag{63c}$$

Equations 63*a*, *b*, and *c* are plotted in Figs. 109, 110, and 111. If X_C/R_1 has certain values at frequency f_r, the frequency characteristic is relatively flat up to frequencies approaching f_r. In particular, performance is good at $B = 1.0$ in all three figures.

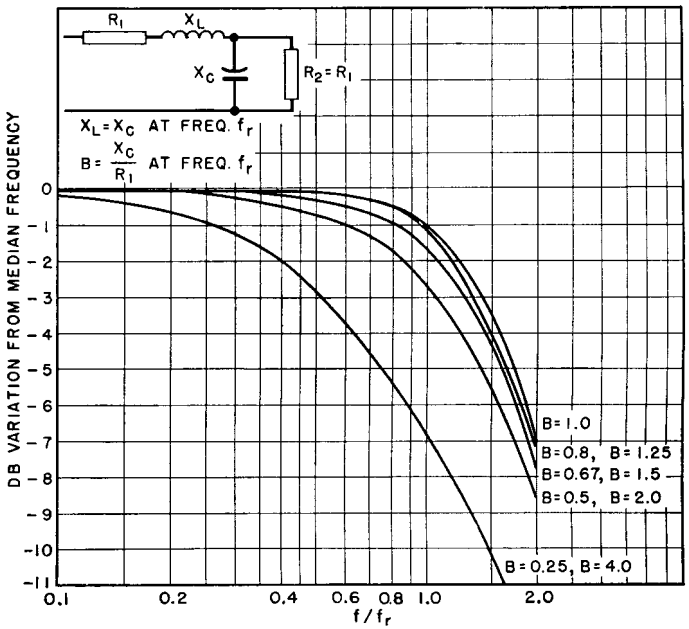

FIG. 109. Transformer characteristics at high frequencies (line matching).

When leakage inductance and winding capacitance are regarded as "lumped" quantities, current distribution in the windings is assumed to be uniform throughout the range of frequencies considered. As shown in Chapter 7 (Section 97), this assumption is valid up to the resonance frequency f_r. At frequencies higher than f_r, there may be appreciable error in Figs. 109, 110, and 111. But good frequency characteristics lie mainly below the frequency f_r, where the curves are correct within the assumed limits.

To use these curves in design work, choose the most desirable

characteristic curve and, from a knowledge of the source impedance, find the proper value of capacitive reactance X_C at frequency f_r. The value of f_r should be such that the highest frequency to be covered lies on the flat part of the curve. X_C and f_r determine the values of wind-

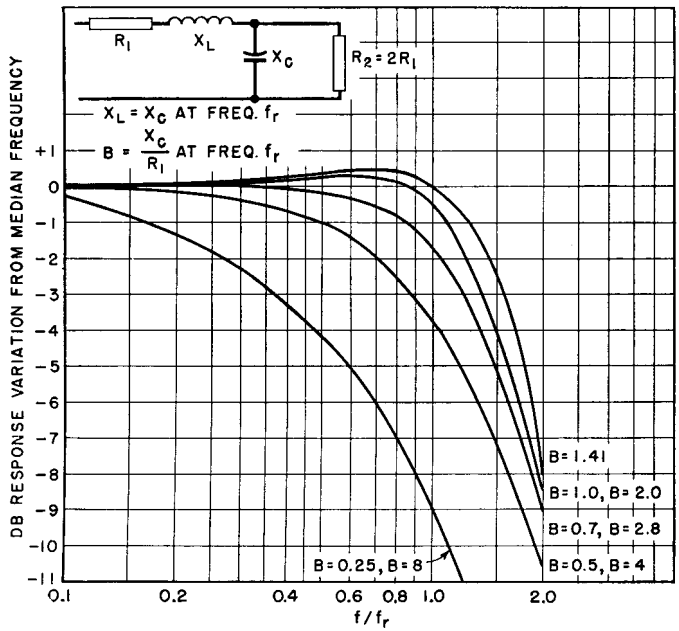

FIG. 110. Transformer characteristics at high frequencies (triode output).

ing capacitance and leakage inductance that must not be exceeded in order to give the required performance.

In Fig. 107(*e*) the capacitance is shown across the load. This is correct if the main body of capacitance is greater on the secondary than on the primary side. Normally this is true if the secondary winding has the greater number of turns. Figures 109, 110, and 111 are thus plotted specifically for *step-up* transformers. Modifications are necessary for *step-down* transformers, the equivalent circuit for which is shown in Fig. 113. Analysis shows the scalar voltage ratio to be

$$\frac{E_2}{E_1} = \frac{1}{\sqrt{\left(\frac{R_1}{X_C} + \frac{X_L}{R_2}\right)^2 + \left(\frac{R_1}{R_2} \cdot \frac{X_L}{X_C} - \frac{R_1}{R_2} - 1\right)^2}} \tag{64}$$

Notice the similarity to equation 63. In fact, if $R_1 = R_2$, equation 64 reduces to equation 63; for this case the response is the same for step-down and step-up transformers, and is given by Fig. 109.

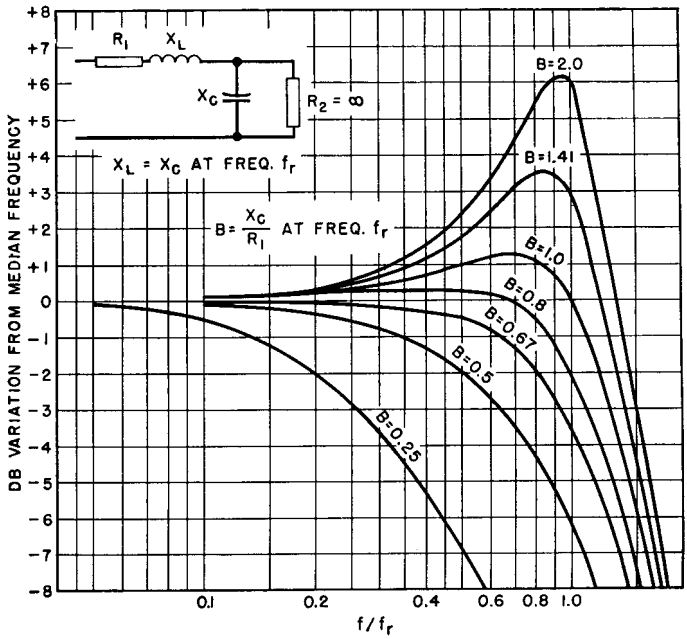

FIG. 111. Transformer characteristics at high frequencies (class A grid).

For $R_2 = 2R_1$, equation 64 becomes, after substitution in terms of frequency,

$$\frac{E_2}{E_1} = \frac{1}{\sqrt{\left(\frac{f}{Bf_r} + \frac{Bf}{2f_r}\right)^2 + \left(\frac{f^2}{2f_r{}^2} - 1.5\right)^2}} \tag{65}$$

which is plotted in Fig. 113. Non-uniform response comes at somewhat lower frequency than in Fig. 110.

The case of $R_2 = \infty$ for step-down transformers is not important. By inspection it can be seen to be the response of R_1 and X_C in series, because X_L carries no current. This case rarely occurs in practice.

67. Harmonic Distortion. Audio response may be good according to Figs. 109, 110, 111, and 113, but at the same time the output may be badly distorted because of changes in load impedance or phase angle.

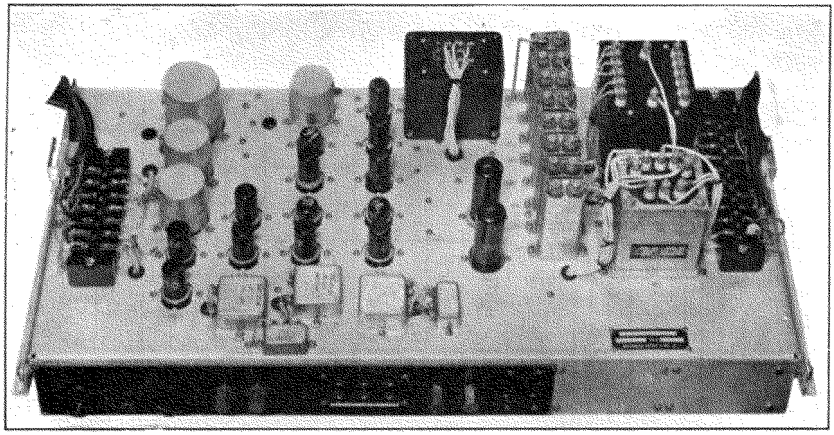

FIG. 112. Audio amplifier. Audio transformers are inverted on chassis at left. Power supply is at right.

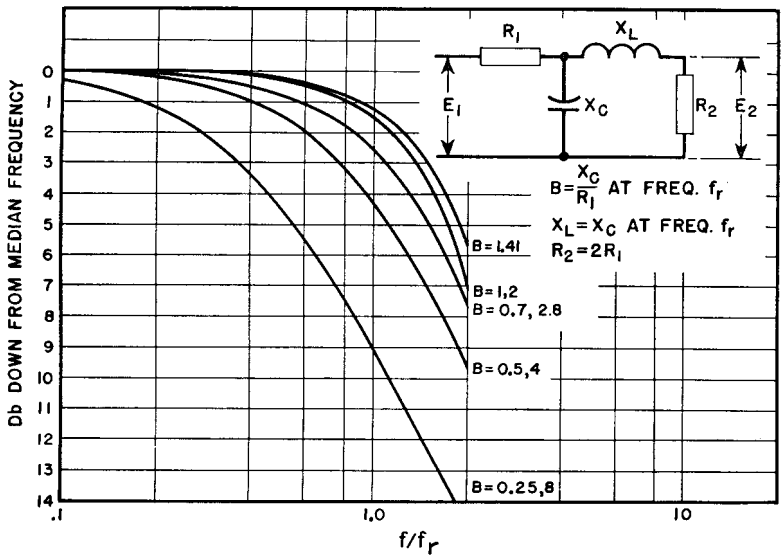

FIG. 113. High-frequency response of step-down transformers.

This possibility is considered here for the case in which the load impedance is twice the source impedance.

The phase angle of the equivalent circuits of Figs. 107(*a*) and (*e*) is found by taking the angle whose tangent is the ratio of imaginary to real components of the total circuit impedance in each case. This

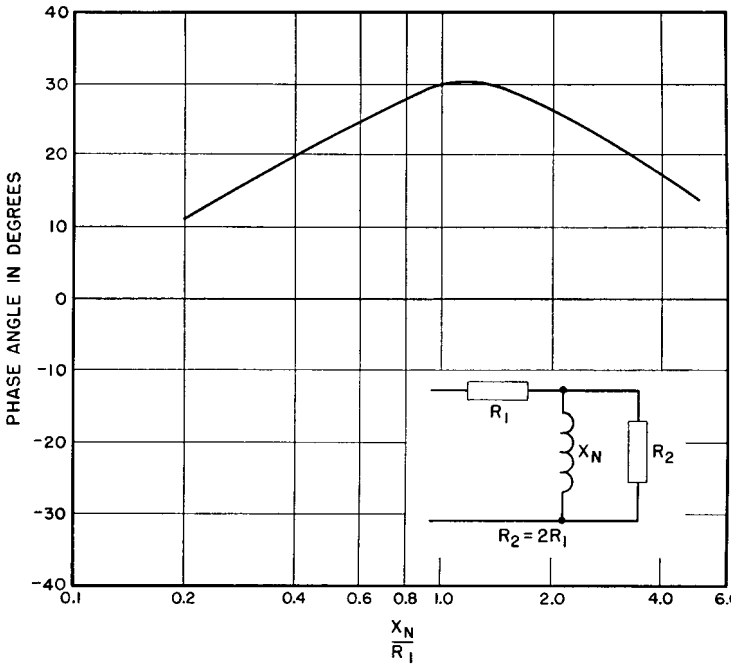

FIG. 114. Variation of amplifier phase angle at low frequencies.

angle is plotted in Figs. 114 and 115 for the low- and high-frequency ranges, respectively, with the same abscissas as in Figs. 108 and 110. It is the angle between the voltage E_1 and the current entering the equivalent circuits of Figs. 107(*c*) and (*e*) and therefore represents the angle between a-c grid voltage and plate current. Positive angle indicates lagging plate current.

The phase angle exhibited by a transformer over the range considered in Figs. 114 and 115 does not exceed 30°, whereas for the most favorable curve in Fig. 115 ($B = 1.0$) it does not exceed 15°. To study the effect of phase angle alone upon distortion, the light load of 8,800 ohms is plotted upon the plate characteristics of triode type 851 in Fig. 116. The result is a sine wave of plate voltage. If the phase angle

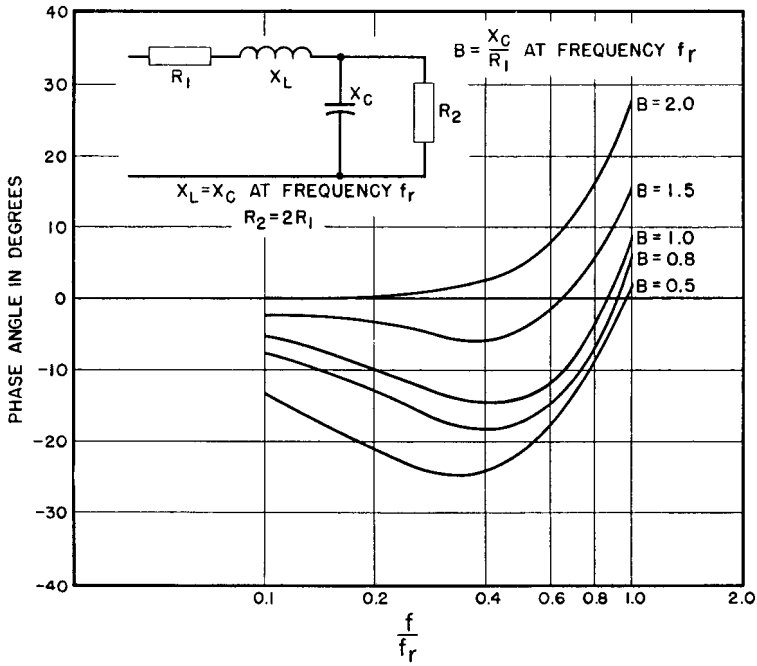

FIG. 115. Variation of amplifier phase angle at high frequencies.

between grid voltage and plate current waves is then arbitrarily made 30°, as in Table XII, the elliptical load curve obtains. The wave of

TABLE XII. 851 TRIODE OPERATION WITH 8,800-OHM 30° PHASE ANGLE LOAD

θ (deg)	e_c	i_B	e_B
0	− 60	0.245	1850
30	− 33	0.300	1400
60	− 13	0.355	1080
90	− 6	0.395	960
120	− 13	0.410	1150
150	− 33	0.395	1520
180	− 60	0.355	2000
210	− 87	0.300	2460
240	−107	0.245	2790
270	−114	0.205	2880
300	−107	0.190	2720
330	− 87	0.205	2350
360	− 60	0.245	1850

plate voltage is plotted for both zero and 30° phase angle in Fig. 117. These wave forms indicate that the phase angle encountered in audio

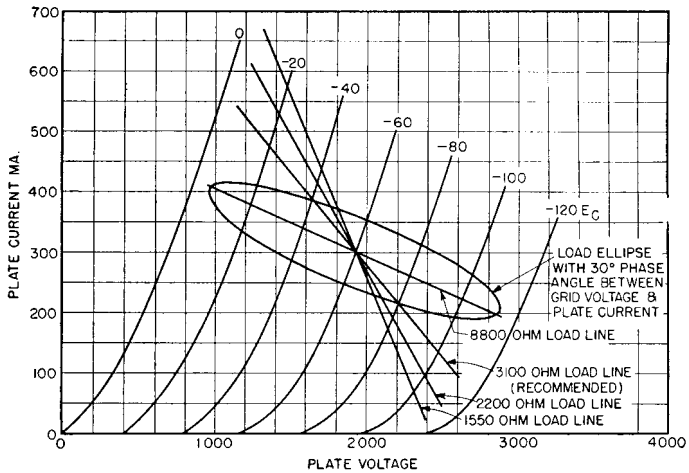

FIG. 116. Triode type 851 with reactive load.

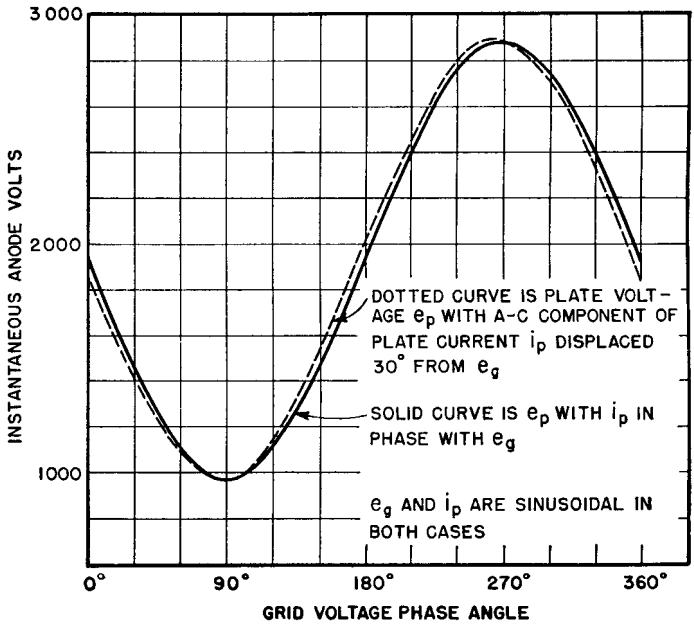

FIG. 117. Plate voltage wave forms with zero and 30° phase angles.

transformers does not of itself introduce much distortion in a lightly loaded triode.

The influence of load impedance on distortion will be considered next. In Fig. 107(*c*) the load impedance, to the right of the dotted line, is

$$Z = \frac{jR_2X_N}{R_2 + jX_N}$$

Hence

$$\frac{Z}{R_2} = \frac{\sqrt{1 + \left(\frac{X_N}{R_2}\right)^2}}{\frac{R_2}{X_N} + \frac{X_N}{R_2}} \tag{66}$$

Equation 66 is plotted in Fig. 118. It shows the change in load Z from its median-frequency value R_2, as the frequency is lowered. Abscissas are X_N/R_2 instead of X_N/R_1 as in Fig. 108.

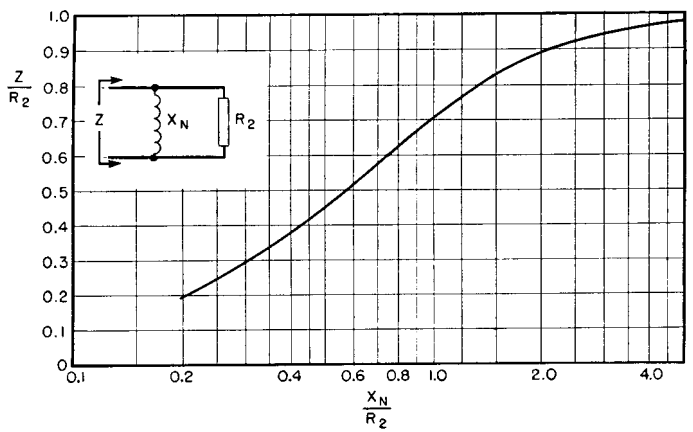

FIG. 118. Variation of load impedance with transformer characteristics at low frequencies.

For the higher audio frequencies, the load impedance at the right of the dotted line in Fig. 107(*e*) is

$$Z = \frac{jX_LR_2 + X_LX_C - jX_CR_2}{R_2 - jX_C}$$

$$\frac{Z}{R_2} = \frac{\sqrt{\left(\frac{X_C}{R_2}\right)^2 + \left(\frac{X_LX_C}{R_2^2} + \frac{X_L}{X_C} - 1\right)^2}}{\frac{R_2}{X_C} + \frac{X_C}{R_2}} \tag{67}$$

If we let $X_C/R_2 = D$ at frequency f_r, then, at any frequency f, $X_C/R_2 = Df_r/f$. If this substitution is made in equation 67 and also if $X_L/X_C = f^2/f_r^2$,

$$\frac{Z}{R_2} = \frac{\sqrt{\frac{D^2f_r^2}{f^2} + \left(D^2 + \frac{f^2}{f_r^2} - 1\right)^2}}{\frac{f}{Df_r} + \frac{Df_r}{f}} \tag{67a}$$

Equation 67*a* is plotted in Fig. 119 for several values of D. The impedance varies widely from its median-frequency value, especially at lower values of D.

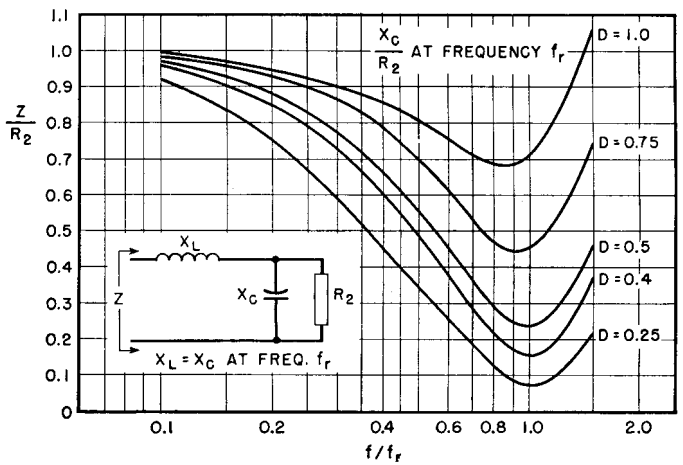

FIG. 119. Variation of load impedance with transformer characteristics at high frequencies.

From Figs. 118 and 119 it is possible to compare the change in impedance with the frequency response curves in Figs. 108 and 110. When this comparison is made it should be remembered that $B = 2D$ for the triode conditions assumed here. If the amplifier response is allowed to fall off 1.0 db at the lowest frequency, the corresponding value of X_N/R_1 from Fig. 108 is 1.3. This means that X_N/R_2 is 0.65. The corresponding load impedance in Fig. 118 is only 0.55 of its median-frequency value. Likewise, for 0.5-db droop of the frequency characteristic, the load impedance falls to $0.7R_2$, whereas for a good load impedance of $0.9R_2$ the frequency characteristic can fall off only 0.1 db. It is thus evident that load impedance may vary widely even with comparatively flat frequency characteristics.

At high audio frequencies the divergences are still greater. Suppose, for example, that a transformer has been designed so that X_C/R_1 is 1.0 at f_r (that is, $B = 1.0$ in Fig. 110). Suppose further that the highest audio frequency at which the transformer operates is $0.75f_r$. The amplifier then has a relatively flat characteristic, with a slight rise near its upper limit of frequency. In Fig. 119, the curve corresponding to $B = 1.0$ is marked $D = 0.5$, for which at $0.75f_r$ the load impedance has dropped to 32 per cent of R_2, an extremely poor match for the tube.

It might be thought that, since $0.75f_r$ is the upper frequency limit, the harmonics resulting from the low value of load impedance would not be amplified, and no harm would be done. But at the frequency $0.375f_r$, whose second harmonic would be amplified, the load impedance is only $0.69R_2$.

Between $0.375f_r$ and $0.75f_r$ (over half of the amplifier frequency range) the load impedance gradually drops from $0.69R_2$ to $0.32R_2$. Thus distortion is large over a wide frequency range. It would be much better to design the transformer so that $B = 2.0$; the change in impedance is much less, and the rise in response is slight.

To ascertain how much distortion these low load impedances produce, a series of loads was plotted in Fig. 116 on 851 plate characteristics: 100, 70, and 50 per cent of the class A *UPO* value of twice the plate resistance (3,100, 2,200, and 1,550 ohms, respectively). The distortion is tabulated below for 54 volts grid swing.

Load	Percentage of 2nd Harmonic	Percentage of 3rd Harmonic	Plate Voltage Swing (Peak to Peak)
3100 ohms	4	1	1500
2200 ohms	10	4	1270
1550 ohms	19	6	1100

The plate voltage amplitude decrease with low impedance loads means that the combination of tube and transformer has a characteristic which droops instead of remaining flat as indicated by the curve $B = 1.0$ in Fig. 110.

This droop modifies the upper ends of the curves of Fig. 110. Although these curves were intended specifically for vacuum tubes, they were derived on the basis of a constant sinusoidal voltage in the source. Figure 119 demonstrates one important fact: For vacuum tubes operating into loads of twice the tube plate resistance, it is better to design transformers so that $B = 2$ or more. Then the output voltage and distortion are less affected by impedance variations at high frequencies. The actual frequency characteristics for triodes lie somewhere between the curves of Fig. 110 and the corresponding curves of Fig. 119.

Designing transformers for $B \geqq 2.0$ means keeping the effective capacitance lower, but the leakage inductance may be proportionately greater than for transformers having $B = 1.0$.

Variations of load impedance at high frequency shown in Fig. 119 are for step-up transformers. Similar variations for step-down transformers may be found from equation 68.

$$\frac{Z}{R_2} = \frac{1 + (D^2 f^2 / f_r^2)}{\sqrt{\left(\frac{f}{Df_r} + \frac{Df^3}{f_r^3} - \frac{Df}{f_r}\right)^2 + 1}} \tag{68}$$

Equation 68 is plotted in Fig. 120. Impedance rises to peaks in the vicinity of f_r, in contrast to the valleys in Fig. 119. For the same variation of impedance, the frequency range is greater for step-down transformers, especially with values of $D = 0.5$ and 0.7.

Besides the harmonic distortion caused by variations in load impedance, at low frequencies additional distortion is caused by nonlinear magnetizing current. If a transformer is connected to a 60-cycle supply line, the no-load current contains large harmonics, but the voltage wave form remains sinusoidal because the line impedance is low. But if distorted magnetizing current is drawn from an amplifier tube, the plate resistance is high enough to produce a distorted voltage wave form across the transformer primary winding, caused mainly by the third harmonic. If the harmonic current amplitude I_H in the magnetizing current is found by connecting the transformer across a low-impedance source, the amplitude of harmonic voltage appearing in the output with a higher-impedance source is

$$\frac{E_H}{E_f} = \frac{I_H R}{I_f X_N}\left(1 - \frac{R}{4X_N}\right) \tag{69}$$

where E_H = harmonic voltage amplitude
E_f = fundamental voltage amplitude
I_H = harmonic current amplitude
I_f = fundamental current amplitude
$R = R_1R_2/(R_1 + R_2)$. R_1, R_2, and X_N are as shown in Fig. 107(*c*).[1]

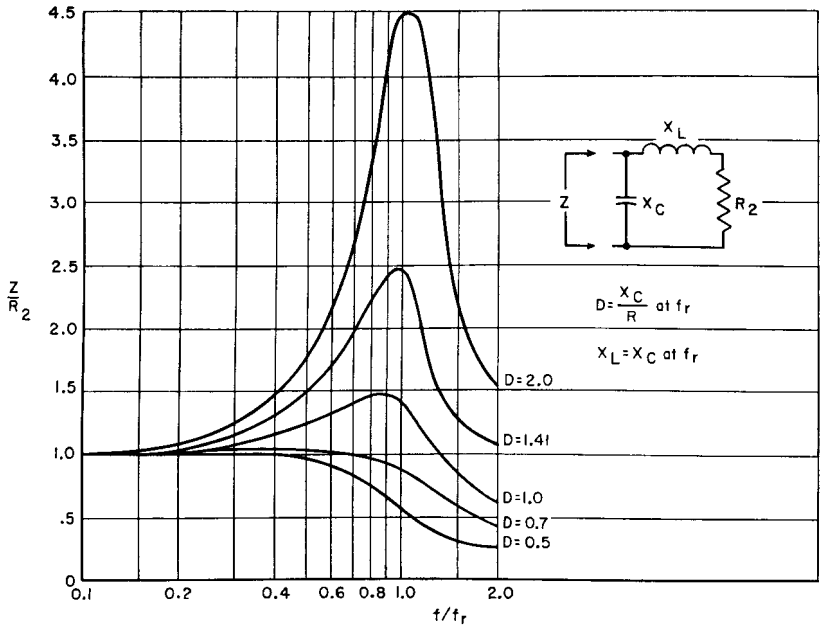

FIG. 120. Step-down transformer impedance at high frequencies.

If flux density is below the knee of the saturation curve, and if $X_N = 3R_2$ at the lowest operating frequency, the harmonic amplitude is less than 5 per cent. An air gap in the core reduces this figure. Table XIII gives typical harmonic currents for silicon steel.

Output voltage distortion may be analyzed to find harmonic content by the usual Fourier method. Several simplifications have been de-

[1] For a discussion of equation 69 and magnetizing currents in general, see "Harmonic Distortion in Audio-Frequency Transformers," by N. Partridge, *Wireless Engr., 19* (September, October, and November, 1942).

TABLE XIII. TYPICAL SILICON-STEEL MAGNETIZING CURRENT HARMONIC COMPONENTS WITH ZERO IMPEDANCE SOURCE

B_m Gauss	Percentage of 3rd Harmonic	Percentage of 5th Harmonic
100	4	1
500	7	1.5
1,000	9	2.0
3,000	15	2.5
5,000	20	3.0
10,000	30	5.0

vised to reduce the labor and increase accuracy.[1] In general, if the recommended tube load impedances are maintained, harmonic percentages will be as given in the tube manuals. If other load impedances obtain at some frequencies, to predict the harmonic output requires harmonic analysis.

68. Push-Pull Amplifier Transformers. The analysis of single-side amplifiers in Section 67 applies to class A push-pull, except that the second-harmonic components in the amplifier output are due to unlike tubes rather than to low-impedance distortion.

The internal tube resistance of a class B amplifier varies so much with the instantaneous signal voltage on the grids, power output, and plate voltage that it is not practicable to draw curves similar to Figs. 110 and 113 for class B operation. Qualitatively, the characteristic curves may be expected to follow the same general trend as for class A amplifiers. A basis for class B amplifier design is to make the transformer constants such that the load impedance does not fall below a given percentage of the load resistance R_2. This is discussed below.

Usually the decline with frequency response is greater for class B than for class A amplifiers, because the effect of internal plate impedance is greater. In the extreme, frequency response falls off proportionately with load impedance.

A change in mode of operation occurs in a class B amplifier as the output passes from one tube to the other in the region of cut-off. This change-over may cause transient voltages in the amplifier which distort the output voltage wave form. If the two halves of the transformer primary winding are not tightly coupled, primary-to-primary leakage inductance causes nicks in the output voltage wave, in somewhat the same way as leakage inductance in a rectifier plate trans-

[1] For example, "Graphical Harmonic Analysis," by J. A. Hutcheson, *Electronics*, *9*, 16 (January, 1936).

former. In a class B amplifier, the change from one tube to the other is less abrupt than in a rectifier, but in triode amplifiers perceptible nicks in the voltage wave occur if the ratio of primary-to-primary leakage reactance to average plate resistance is 4 or more.[1]

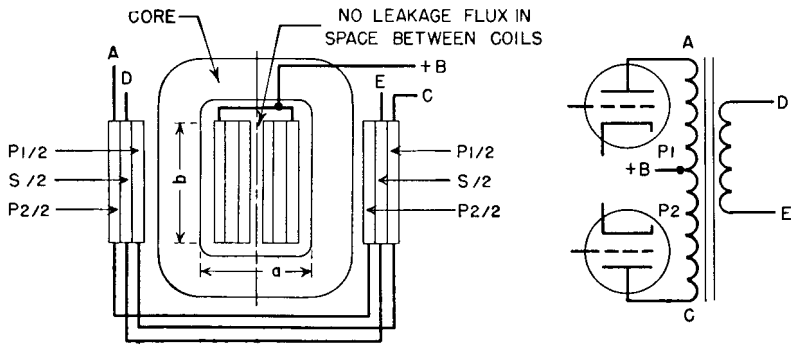

FIG. 121. Core-type push-pull balanced windings.

Balanced operation in a push-pull amplifier, i.e., equal plate current and voltage swing on both sides, is possible only if the tubes are alike and if transformer winding turns and resistances per side are equal. Shell-type concentric windings do not fulfill this condition because the half of the primary nearer to the core tongue has lower resistance than the other half. Balance is easier to achieve in the core type of arrangement shown in Fig. 121. In class A amplifiers close primary-primary coupling is not essential, and balance may be attained by arranging part coils as in Fig. 122.

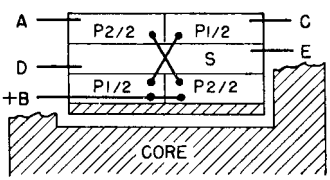

FIG. 122. Shell-type push-pull balanced windings.

Because only half of the primary winding of a class B amplifier carries current during a half-cycle, the leakage flux and therefore the primary-to-secondary leakage inductance have approximately half the values with both windings active all the time. With capacitive currents, both windings *are* active, at least partially. Transformers with $D > 1.0$ have low capacitive currents, low leakage inductance, high resonance frequency, and extended frequency range, in addition to the

[1] See "Quasi Transients in Class B Audio-Frequency Push-Pull Amplifiers," by A. Pen-Tung Sah, *Proc. I.R.E.*, *24*, 1522 (November, 1936).

load-impedance advantages given in Section 67. At high frequencies a class B amplifier transformer presents a circuit to the tubes like that in Fig. 123. Let L_1 be leakage inductance between the halves of the

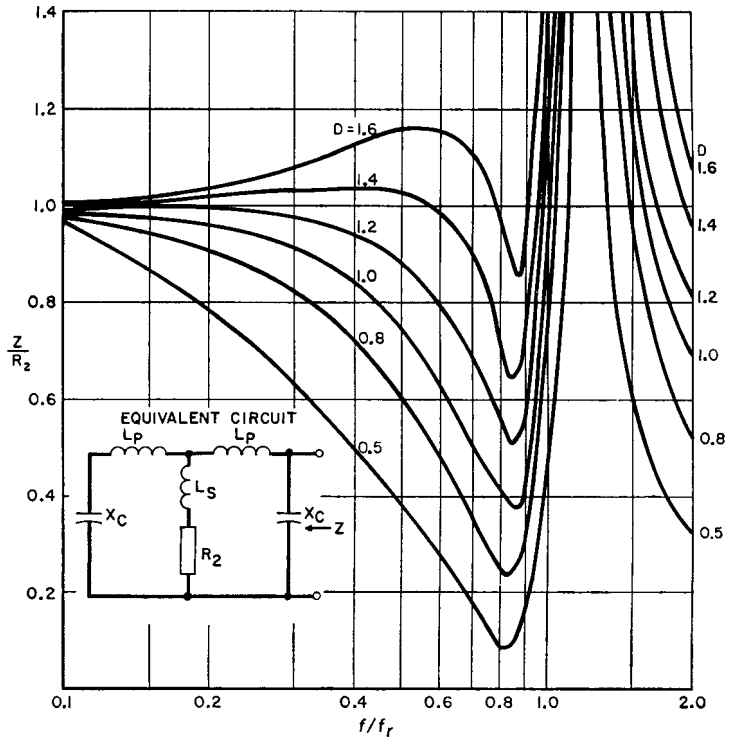

FIG. 123. High-frequency load impedance of class B amplifiers.

primary winding, and L_2 between each half of the primary and the secondary. L_1 is the inductance of one half of the primary winding, measured with the other half-primary short-circuited and the secondary open. L_2 is the inductance of one half of the primary winding, measured with the other half-primary open and the secondary short-circuited. In Fig. 123, $L_1 = 2L_P$ and $L_2 = L_P + L_S$. Resonant frequency f_r is determined by X_C and $X_{L1} = 2\pi f L_1$. In this figure $D = X_C/R_2$ at f_r.

First one tube delivers power into the equivalent circuit at one end; then, during the next half-cycle, this tube is cut off and the other tube delivers power into the circuit at the other end. Thus the transformer equivalent impedance Z seen looking into the circuit, first at the end

shown and then at the other end, is fed by one of the tubes at all times. Impedance ratio Z/R_2 varies with frequency as in Fig. 123. For some values of parameter D, impedance falls more rapidly than for class A amplifiers (Fig. 119), but frequency f_r in Fig. 123 is determined by L and C having approximately half the values of these elements in class A amplifiers. Hence class B *impedance* stays flat at higher frequencies, although *response* may droop at lower frequencies, than for class A.

Figure 123 is drawn for a ratio of $L_1/L_2 = 1.5$, which is a practical design ratio. Lower ratio L_1/L_2 results in deeper valleys in the impedance curve; higher L_1/L_2 is more likely to cause nicks in the voltage wave. Good practice consists in designing class B amplifier transformers so that the highest operating frequency is less than $f_r/2$ and $L_1/L_2 \leqq 1.5$. Then harmonic distortion at *high frequencies* should not exceed 5 per cent.[1] Class B modulation transformer impedance is influenced by circuit elements, so that maintenance of constant impedance over a wide frequency band becomes an overall amplifier problem. This is discussed further in Chapter 6.

Capacitive currents also cause unbalance at high frequencies, even with winding arrangements like Figs. 121 and 122. This is evident if the secondary winding in these figures is grounded at one end; the effective capacitances to the two primary windings are then unequal. This problem may be solved by keeping the capacitances small with liberal spacing, but this practice increases leakage inductance and cannot be carried very far. Coil mean turn length should be kept as small as possible by the use of the most suitable core steel. Core-type designs have smaller mean turns than shell-type. Also, the two outer coil sections have low capacitance to each other and to the case if liberal spacing is used, *without* an increase in leakage inductance. Flux in the space between the outer sections links all the windings on one leg and hence is not leakage flux. Consequently, this space is not part of the term a in equation 33 (p. 76). In push-pull amplifiers the winding arrangement of Fig. 121 is advantageous because of the low capacitance between the points of greatest potential difference, A and C.

69. Plate Current Increase. In a lightly loaded amplifier the frequency characteristic stays flat at high frequencies, even with a droop in load impedance, but the plate current rises in inverse proportion to the impedance. If the plate current can rise enough to maintain constant output voltage, this plate current rise may be objectionable from

[1] See "The Design of Broad-Band Transformers for Linear Electronic Circuits," by H. W. Lord, *Trans. AIEE, 69,* 1005.

the standpoint of tube heating or plate supply regulation. Values of plate current rise calculated on the basis of constant output for low and high frequencies are shown in Figs. 124 and 125. Many satisfactory audio amplifiers have plate currents which would be excessive at the extremes of the range if high or low notes were amplified continu-

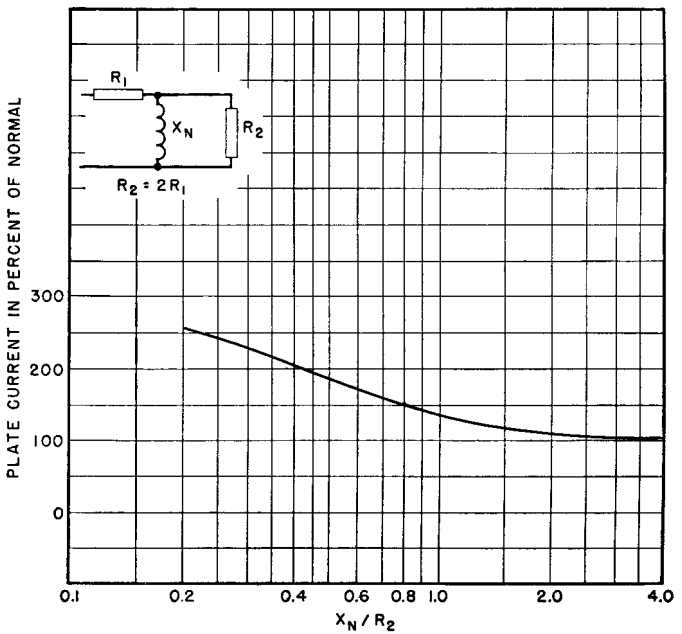

FIG. 124. Rise in plate current due to transformer impedance change at low frequencies.

ously. They are not damaged because these tones are of short duration.

70. Pentode Amplifiers. Tetrode tubes have an additional grid between anode and control grid to reduce the grid-to-anode capacitance. This additional grid is known as the screen grid and is operated at a positive potential with a-c bypass to reduce the grid-to-anode capacitance. The chief drawback to this type of tube is that the anode voltage swing is limited to the difference between the anode voltage and screen voltage. This disadvantage is overcome by the addition of a third grid known as the suppressor, which removes this limitation and allows large anode voltage swings down to the diode line of the tube. Sometimes the third electrode is connected internally to the cathode.

Similar characteristics are obtained with the so-called beam tubes, which are tetrodes with special screen-grid spacings. Figure 126 shows 6L6 beam tube plate characteristics, with a typical load line of 2,500 ohms. As a single-side amplifier, such a tube is likely to have large distortion because of the uneven spacing of constant-grid-voltage lines. Distortion is reduced in a push-pull amplifier, especially for

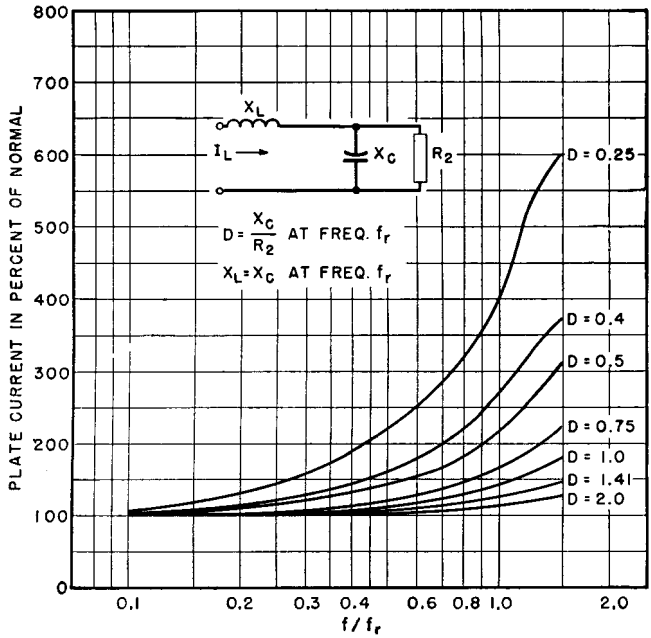

FIG. 125. Rise in plate current due to transformer impedance change at high frequencies.

high power output. Plate resistance r_p is very high in pentodes and beam tubes, of the order of 10 times the load resistance.

Pentodes are essentially constant-current devices. The value of load impedance is thus an indication of the output voltage, at least for low frequencies. Response of a low-frequency transformer-coupled pentode amplifier can be taken from Fig. 118.

At high frequencies, leakage inductance of the transformer intervenes between the pentode and its load, so that the primary voltage and secondary or load voltage are not identical. In Fig. 127 the change of output voltage for a constant grid voltage at high frequencies is shown. In this figure, the equivalent circuit is a pi-filter, which is

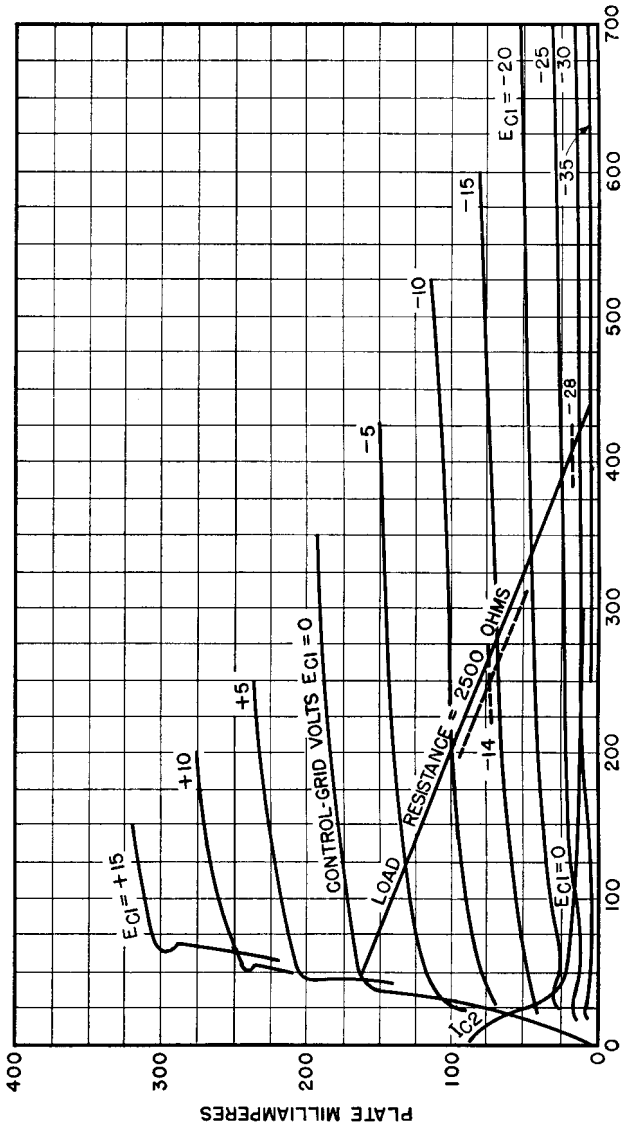

FIG. 126. Plate characteristics of type 6L6 beam tube.

desirable for pentode transformers, and is approximated when the transformer ratio is 1:1. Harmonic content of pentodes is high, especially in single-side amplifiers. Large phase angle and low load impedance produce undesirable distortion. It is best to use values of X_N/R_2 greater than 2 in Fig. 118 at the lowest frequency to avoid distortion.

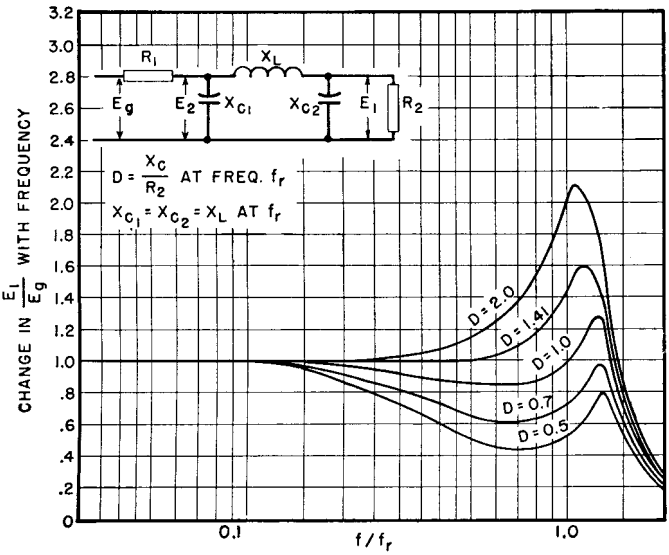

FIG. 127. Pentode frequency response with pi-filter output circuit.

Semiconductor amplifiers known as *transistors* have emitter, collector, and base electrodes; these are analogous, respectively, to grid, plate, and cathode in a vacuum tube. Emitter and collector currents are of the same order of magnitude in grounded-base transistors, but collector impedance is much larger than emitter impedance. To match impedances, transformer coupling is often used between stages of transistor amplifiers. Junction transistors resemble pentode amplifiers in having nearly constant collector current over a large range of collector voltage. Hence junction transistor transformer operation closely resembles that of pentode vacuum-tube transformers, and the foregoing discussion is generally applicable to both.

71. Calculation of Inductance and Capacitance. Transformer-coupled amplifier performance is dependent at low frequencies upon transformer *OCL*, and at high frequencies upon leakage inductance

and winding capacitance. Calculation of these quantities is essential in design and useful in tests for proper operation. Inductance formulas are repeated here for convenience, along with capacitance calculations.

$$OCL = \frac{3.2N^2A_c}{10^8\left(l_g + \frac{l_c}{\mu}\right)} \quad \text{(henrys)} \tag{38}$$

where N = turns in winding
A_c = core area in square inches
l_g = total length of air gap in inches
l_c = core length in inches
μ = permeability of core (if there is unbalanced direct current in the winding, this is the incremental permeability).

For concentric shell- or core-type windings the total leakage inductance referred to any winding is

$$L_S = \frac{10.6N^2MT(2nc + a)}{n^2b \times 10^9} \quad \text{(henrys)} \tag{33}$$

where N = turns in that winding
MT = mean length of turn for whole coil
a = total winding height
b = winding width
c = insulation space
n = number of insulation spaces
= number of primary-secondary interleavings (see Fig. 57, p. 75).

Winding capacitance is not expressible in terms of a single formula. The effective value of winding capacitance is almost never measurable, because it depends upon the voltages at the various points of the winding. The capacitance current at any point is equal to the voltage across the capacitance divided by the capacitive reactance. Since many capacitances occur at different voltages, in even the simplest transformer, no one general formula can suffice. The major components of capacitance are from

1. Turn to turn.
2. Layer to layer.
3. Winding to winding.
4. Windings to core.

5. Stray (including terminals, leads, and case).
6. External capacitors.
7. Vacuum-tube electrode capacitance.

These components have different relative values in different types of windings. Turn-to-turn capacitance is seldom preponderant because the capacitances are in series when referred to the whole winding. Layer-to-layer capacitance may be the major portion in high-voltage single-section windings, where thick winding insulation keeps the winding-to-winding and winding-to-core components small. Items 5, 6, and 7 need to be watched carefully lest they spoil otherwise low-capacitance transformers and circuits.

If a capacitance C with E_1 volts across it is to be referred to some other voltage E_2, the effective value at reference voltage E_2 is

$$C_e = C(E_1^2/E_2^2) \tag{70}$$

By use of equation 70 all capacitances in the transformer may be referred to the primary or secondary winding; the sum of these capacitances is then the transformer capacitance which is used in the various formulas and curves of preceding sections.

In an element of winding across which voltage is substantially uniform throughout, capacitance to a surface beneath is

$$C = (0.225A\epsilon/t) \quad (\mu\mu f) \tag{71}$$

where A = area of winding element in square inches
ϵ = dielectric constant of insulation under winding = 3 to 4 for organic materials
t = thickness in inches of insulation under winding. This includes wire insulation and space factor.

If the winding element has uniformly varying voltage across it, as in Fig. 128, the effective capacitance is the sum of all the incremental

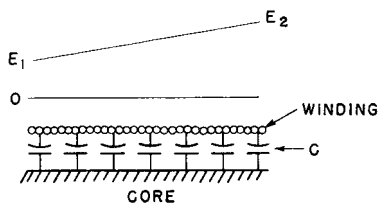

FIG. 128. Transformer winding with uniform voltage distribution.

effective capacitances. This summation is

$$C_e = \frac{C(E_1^2 + E_2^2 + E_1E_2)}{3E^2} \tag{72}$$

where C = capacitance of winding element as found by equation 71
E_1 = minimum voltage across C
E_2 = maximum voltage across C
E = reference voltage for C_e.

If E_1 is zero and $E_2 = E$, equation 72 becomes

$$C_e = C/3 \tag{73}$$

or the capacitance, say, to ground of a single-layer winding with its low-voltage end grounded is one-third of the measured capacitance of the winding to ground. Measurement should be made with the winding ungrounded and both ends short-circuited together, to form one electrode, and ground to form the other.

In a multilayer winding, E_1 is zero at one end of each layer and $E_2 = 2E/N_L$ at the other, where E is the winding voltage and N_L is the number of layers. The effective layer-to-layer capacitance of the whole winding is

$$C_e = \frac{4C_L}{3N_L}\left(1 - \frac{1}{N_L}\right) \tag{74}$$

where C_L is the measurable capacitance of one layer to another. The first and last layers have capacitance to other layers on one side only, and this is accounted for by the term in parentheses in equation 74.

Because the turns per layer and volts per layer are greater in windings with many turns of small wire, such windings have higher effective capacitance than windings with few turns. In a transformer with large turns ratio, whether step-up or step-down, this effective capacitance is often the barrier to further increase of turns ratio. With a given load impedance across the low impedance winding, there is a maximum effective capacitance C_m which can be tolerated for a given frequency response. If layer and winding capacitances have been reduced to the lowest practicable figure C_l, the maximum turns ratio is $\sqrt{C_m/C_l}$. Appreciable amounts of capacitance across which large voltages exist must be eliminated by careful design.

Since effective capacitance is greater at higher voltages, in step-down transformers the capacitance may be regarded as existing mainly across the primary winding, in step-up transformers across the secondary winding. The effect of this on frequency response has been discussed in Section 66.

The input capacitance of a triode amplifier is given by [1]

$$C_{\text{input}} = C_{G-F} + (\alpha + 1)C_{G-P} \tag{75}$$

where C_{G-F} = grid-to-cathode capacitance
C_{G-P} = grid-to-anode capacitance
α = voltage gain of the stage.

C_{G-F} and C_{G-P} are given for many tubes in the tube handbooks. They can be measured in any tube by means of a capacitance bridge.

72. Amplifier Transformer Design. In amplifiers which operate at a single frequency, transformers are similar in design to rectifier plate transformers. Size of core is determined by the required value of OCL. See Section 65. If the winding carries unbalanced direct current, an air gap must be provided to keep B_m within the limits discussed in Section 38 (Chapter 3). Winding resistances are limited by permissible loss in output, or in larger units by heating.

If the amplifier operates over a frequency range, the start of the design is with OCL to insure proper low-frequency performance. After ample core area and turns have been chosen, attention must be given to the winding configuration. Leakage inductance and winding capacitance are calculated and, from them, f_r and B. If the high-frequency response does not meet the requirements, measures must be taken to increase f_r or change B to a value nearer optimum. Sometimes these considerations increase size appreciably.

Below frequency f_r, the leakage inductance per turn is constant and equal to the total coil inductance divided by the number of turns. Capacitance per turn is constant and may be large because of the close turn-to-turn spacing. But the LC product per turn is smaller than the LC product per layer, because the layer *effective* capacitance is greater. Therefore the frequency at which the turns become resonant is higher than that at which the layers become resonant. Likewise, if there is appreciable coil-to-coil capacitance, the layer resonant frequency is higher than the coil resonant frequency f_r. If the coil design is such

[1] See *Principles of Radio Communications*, by J. H. Morecroft, John Wiley & Sons, 2nd ed., New York, 1927, p. 511.

that resonance of part of a coil occurs at a lower frequency than f_r, the transformer frequency response is limited by the partial resonance. This condition is especially undesirable in wide range designs, but with reasonable care it can be avoided.

It is helpful in amplifier transformer design work to use a reactance chart, especially at the higher frequencies where resonance frequency f_r must be known in order to determine high-frequency properties. Several reactance charts have appeared in the literature.[1]

Two examples of audio transformer design are given here to illustrate low- and high-frequency response calculations.

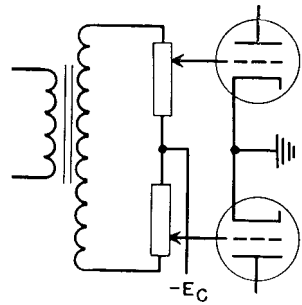

FIG. 129. Input transformer driving push-pull grids.

Example (a). Input Transformer. To terminate a 500-ohm line and apply input to push-pull class A grids as in Fig. 129. Primary voltage is 2.0 volts. Frequency range 100 to 5,000 cycles. Step-up ratio 1:20. No direct current flows in either primary or secondary winding. Nickel-iron laminations are used. Refer to Fig. 57 for dimension symbols and winding arrangement.

$A_c = 0.5$ sq in.
$l_c = 4.5$ in.
Permeability (initial value) = 5,000.
Coil mean turn 4.5 in.
Window 0.578 in.
Primary 400 turns No. 30 single enamel wire.
Secondary 8,000 turns No. 40 single enamel wire (total).
Primary layers 7; layer paper 0.0015 in.
Secondary layers 44; layer paper 0.0007 in.
Vertical space factor 0.9.
$b = 0.75$ in.
$c = 0.008$ in.

$$\text{Secondary } OCL = \frac{3.2 \times (8{,}000)^2 \times 0.5 \times 10^{-8}}{0.0005 + \dfrac{4.5}{5{,}000}} = 730 \text{ henrys with smallest possible air gap (per Table IX, p. 99).}$$

= 540 henrys with average gap = 0.001 in.

$$\text{Secondary leakage inductance} = \frac{10.6 \times (8{,}000)^2 \times 4.5 \times (4 \times 0.008 + 0.578)}{4 \times 0.75 \times 10^9} = 0.62 \text{ henry}$$

[1] See "Reactance Chart," by H. A. Wheeler, *Proc. I.R.E., 38,* 1395 (December, 1950).

Capacitances:

$$\text{Secondary layer-to-layer} = \frac{0.225 \times 4.5 \times 0.75 \times 3 \times 0.9}{0.0007 + 0.0005} = 1{,}700$$

Ditto referred to whole secondary $= \frac{1700}{44} \times 1.33 \times 0.977 =$		51 $\mu\mu$f
Primary layer-to-layer, referred to secondary	$<$	1
Tube input capacitance	$=$	25
Winding-to-core capacitance	$=$	40
Stray capacitance	$=$	10
Total secondary capacitance $=$		127 $\mu\mu$f

With the primary winding located at audio ground on the secondary, there is virtually zero winding-to-winding capacitance. Secondary-to-core capacitance is based on a coil form $\frac{1}{16}$ in. thick.

Total secondary load resistance $= 500 \times (20)^2 = 200{,}000$ ohms.

Based on inductance with 0.001-in. gap, $X_N = 339{,}000$ ohms and $X_N/R_1 = 1.7$.

Response is 0.3 db down, in Fig. 108.

Resonance frequency of 0.62 henry and 127 $\mu\mu$f is 18,000 cycles and $X_c = 70{,}000$ ohms. $B = X_c/R_1 = 0.35$. $f/f_r = 5{,}000/18{,}000 = 0.28$. Response is 0.6 db down at 5,000 cycles (from Fig. 109).

Example (b). Interstage Transformer. In interstage coupling the impedance level is high, to maintain both high load impedance and high grid excitation in the following stage. The limit on the secondary side is the highest resistance which affords grid circuit stability. There is no impedance limit on the primary side except that imposed by transformer design. Usually a 1:1 ratio is about optimum. A step-down ratio gives less voltage on the following grid. A step-up ratio reflects the secondary load into the plate circuit as a lower impedance. This reduces the voltage gain, especially with pentodes which have high plate resistance compared to load resistance. Under this condition, equation 58 becomes

$$e_p/e_g = \mu Z_L/r_p = g_m Z_L \tag{76}$$

or the voltage gain is proportional to load impedance. Interstage transformers commonly have many turns and high *OCL*.

Suppose that a transformer is required to connect a 6SK7 tube to a 6L6 operating class A with 10 volts rms on the grid over a frequency range of 300 to 3,000 cycles. 6L6 grid resistance is 90,000 ohms, which is to be reflected into the 6SK7 plate circuit as a 90,000-ohm load. Hence a 1:1 turns ratio is used. 6SK7 plate current is 10 ma. The same core as in Example (*a*) is used, except that here it is made of silicon steel, and the stacking is reduced so that A_c is 0.32 sq in. Primary and secondary windings are single sections; with the primary start lead connected to 6SK7 plate and secondary finish lead connected to 6L6 grid. This leaves adjacent turns in both these windings at zero audio potential, and effective primary-secondary capacitance is zero.

Primary turns = secondary turns = 6,600 turns No. 40 enamel wire.
Primary and secondary layers = 37.
Primary mean turn = 3.3 in.
Secondary mean turn = 4.2 in., $l_g = 0.005$ in.

$$B_{dc} = \frac{0.6 \times 6{,}600 \times 0.010}{0.005} = 7{,}750 \text{ gauss.}$$

$$B_{ac} = \frac{3.49 \times 10 \times 10^6}{300 \times 0.32 \times 6{,}600} = \quad 55 \text{ gauss.}$$

$$B_m = \overline{7{,}805} \text{ gauss.}$$

From Fig. 70, $\mu_\Delta = 1{,}100$.

$$OCL = \frac{3.2 \times (6{,}600)^2 \times 0.36 \times 10^{-8}}{0.005 + \dfrac{4.5}{1{,}100}} = 55 \text{ henrys.}$$

$$\text{Leakage } L = \frac{10.6 \times (6{,}600)^2 \times 3.8(2 \times 0.008 + 0.578)}{0.75 \times 10^9} = 1.4 \text{ henrys.}$$

Capacitances:

$$\text{Primary layer-to-layer} = \frac{0.225 \times 3.3 \times 0.75 \times 3}{0.0015} = 1{,}120\ \mu\mu\text{f.}$$

$$\text{Secondary layer-to-layer} = \frac{0.225 \times 4.2 \times 0.75 \times 3}{0.0015} = 1{,}415\ \mu\mu\text{f.}$$

Referred to the whole winding, the capacitances are

$$\frac{1{,}120 \times 4 \times 0.973}{37 \times 3} = 40\ \mu\mu$$

and

$$\frac{1{,}415 \times 4 \times 0.973}{37 \times 3} = 50$$

Primary—core C	= 44
Secondary—core C	= 14
Tube capacitances	= 17
Stray capacitances	= 10
Total capacitance	= 175 $\mu\mu$f

$f_r = 10$ kc. $X = 90{,}000$, $D = 1$, and response is 1 db down at 3,000 cycles (from Fig. 127). $X_N/R_2 = 6.28 \times 300 \times (55/90{,}000) = 1.04$. Figure 118 shows a Z/R_2 of 0.72; therefore the response is 3 db down at 300 cycles.

6. AMPLIFIER CIRCUITS

Amplifier applications may require control of hum, distortion, or frequency response beyond the limits of practical transformer design. Sometimes the additional performance is obtained by designing extra large transformers; this is usually an expensive procedure. Sometimes extra features can be incorporated into the transformers without marked increase in size. At other times additional circuits are used either preceding or in conjunction with the amplifier.

In this chapter several devices for obtaining special performance are considered. Transformer and amplifier design both are affected by them to a marked degree.

73. Inverse Feedback. If part of the output of an amplifier is fed back to the input in such a way as to oppose it, the ripple, distortion, and frequency response deviations in output are reduced. The amplifier gain is reduced also, but with the availability of high-gain tubes an extra stage or two compensates for the reduction in gain caused by inverse feedback, and the improvement in performance usually justifies it. In the amplifier of Fig. 130, a network is shown connected to out-

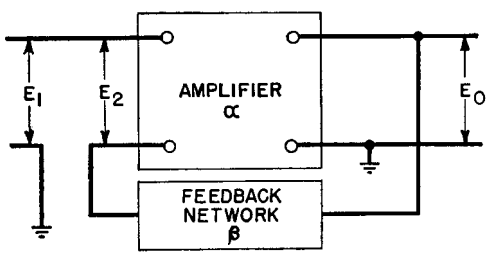

FIG. 130. Voltage feedback.

put voltage E_0; part of this output is fed back so that the input to the amplifier is

$$E_2 = E_1 - \beta E_0 \tag{77}$$

Here β is the portion of E_0 which is fed back. If α is the voltage ampli-

fication of the amplifier and E_R and E_H are the ripple and harmonic distortion in the output without feedback, and α', E'_R, and E'_H are the same properties with feedback, the following equations hold, if α, E_R, and E_H are assumed to be independent:

Without feedback,

$$E_0 = \alpha E_2 + E_R + E_H \tag{78}$$

With feedback,

$$E_0 = \alpha' E_1 + E'_R + E'_H \tag{79}$$

From these equations it can be shown that

$$\alpha' = \frac{\alpha}{1 + \alpha\beta} \approx \frac{1}{\beta} \tag{80}$$

$$E'_R = \frac{E_R}{1 + \alpha\beta} \approx \frac{E_R}{\alpha\beta} \tag{81}$$

$$E'_H = \frac{E_H}{1 + \alpha\beta} \approx \frac{E_H}{\alpha\beta} \tag{82}$$

With high-gain amplifiers and large amounts of feedback, the output ripple and harmonic distortion can be made astonishingly small. Likewise the frequency response can be made flat, even with mediocre transformers. Inverse feedback is not used in class C amplifiers, because the output and input are not linearly related.

Incidental effects in the amplifier, like distributed capacitance and leakage inductance, have to be carefully matched in the inverse feedback network so that the phase shift around the loop does not become too large. If it reaches 180°, feedback is regenerative, so that the amplifier may become an oscillator with a frequency determined by the circuit constants. Nyquist has shown [1] that oscillation does not take place so long as the gain $\times$ feedback product $\alpha\beta$ is less than unity at the frequencies for which the phase shift is 180°. In a plot of $\alpha\beta$ made on the complex plane, the requirement for stability is that the curve of $\alpha\beta$ must not enclose the point 1, 0, with the sign of β considered opposite to that of α. Both gain α and feedback β are ratios of voltages. Therefore, both may be expressed in decibels and both are complex quantities at some frequencies. Proper care in application is required so that amplifiers with 180° or more phase shift do not oscil-

[1] See "Regeneration Theory," by H. Nyquist, *Bell System Tech. J., 11,* 126 (January, 1932).

late at some frequency outside the pass band. If it is desired to correct for distortion or hum over a frequency range of 30 to 10,000 cycles, the amplifier should have low phase shift over a much wider range, say 10 to 30,000 cycles. In the frequency intervals of 10 to 30 cycles and 10,000 to 30,000 cycles, both the amplification and the feedback should taper off gradually to prevent oscillations.

Low phase-shift amplifiers benefit most from inverse feedback. Feedback in such amplifiers reduces size or improves performance, including phase shift. Transformer phase shift, therefore, is a vital

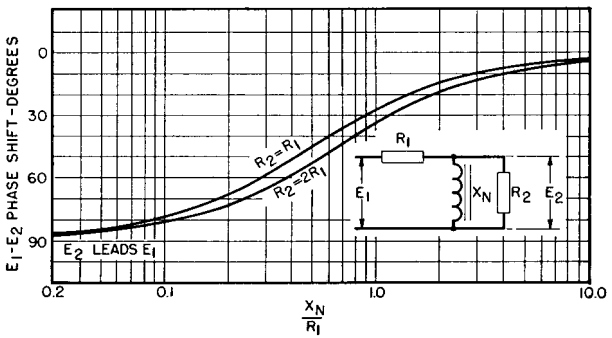

FIG. 131. Transformer-coupled amplifier low-frequency phase shift.

property in feedback amplifiers and may take precedence over frequency response in some instances.

Phase shift at low and high frequencies is shown in Figs. 131 and 132 for transformer-coupled stages. At high frequencies, 180° phase shift is possible whereas at low frequencies but 90° is possible. In a resistance-coupled amplifier, only 90° phase shift occurs at either low or high frequencies. Partly for this reason, partly because less capacitance is incidental to resistors than to transformers and good response is maintained up to higher frequencies, it is in resistance-coupled amplifiers that inverse feedback is generally employed. But if the distortion of a final stage is to be reduced, transformer coupling is involved. It is preferable to derive the feedback voltage from the primary side of the output transformer. This is equivalent to tapping between R_1 and X_L in Fig. 132, where the phase shift is much less. The transformer must still present a fairly high impedance load to the output tube throughout the marginal frequency intervals to permit gradual decrease of both amplification and feedback.

Current feedback is effected in the circuit of Fig. 133 by removing capacitor C. This introduces degeneration in the cathode resistor circuit, which accomplishes the same thing as the bucking action of

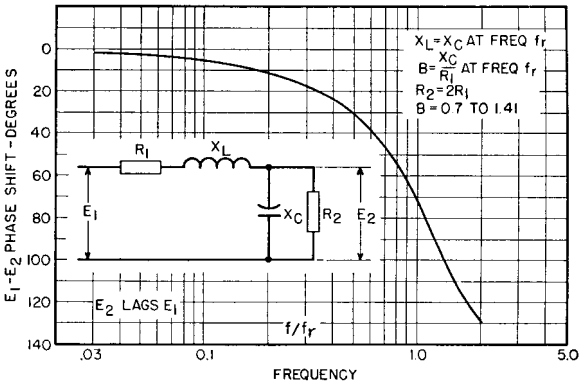

FIG. 132. Transformer-coupled amplifier high-frequency phase shift.

voltage feedback. It is less affected by phase shift and consequently is used with transformer-coupled amplifiers.

74. Cathode Follower. The circuit of Fig. 134 is known as a cathode follower. Here the anode is connected to the high-voltage supply E_B without any intervening impedance, so that for alternating currents it

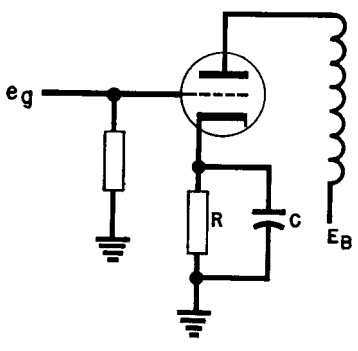

FIG. 133. Cathode bias.

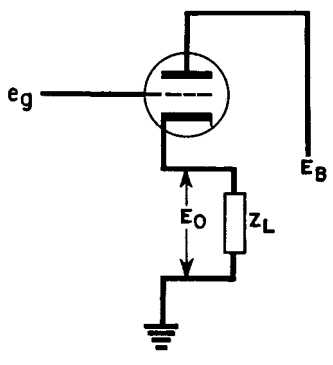

FIG. 134. Cathode follower.

is essentially grounded. Grid voltage e_g must be great enough to include the output E_0 in addition to the normal grid-to-cathode voltage at E_{min}. However, the grid power is still the same as it would be

were the cathode grounded. This circuit is used when the output impedance Z_L is variable or of low power factor so that normally it would be difficult to produce in it full output from the tube. The circuit has a low internal effective impedance as far as the output is concerned. It is approximately equal to the normal plate resistance r_p divided by the amplification factor μ of the tube. This is equivalent to saying that the effective internal impedance is approximately the reciprocal of the mutual conductance g_m [1] for class A or B amplifiers. Cathode followers have been used to drive grids of class B modulator tubes, which are highly variable loads. The circuit produces nearly constant output voltage but at the expense of increased grid swing.

If the tube feeds a low impedance load, output may be increased by coupling the load through a transformer. Frequency response in cathode output transformers is usually flat over a very wide range because of the low effective source impedance.

75. Wave Filter Principles. In preceding sections dealing with transformer frequency response, means for extending frequency range have been considered. In broadcast transmitters this is a vital problem. But in other applications amplifiers are used over a *limited* frequency range. It is sometimes desirable to allow certain frequencies which are present to pass through the amplifier at full amplitude but to suppress as nearly as possible certain other frequencies. The means usually employed to accomplish this result is a wave filter. In any such filter, the band of frequencies which it is desired to transmit is known as the transmission band, and that which it is desired to suppress is known as the attenuation band. At some frequency, known as the cut-off frequency, the filter starts to attenuate. Transition between attenuation and transmission bands may be gradual or sharp; the filter is said to have gradual or sharp cut-off accordingly. When a filter is used in conjunction with a transformer-coupled amplifier, the frequency response of both filter and amplifier must be coordinated. In a later section it will be shown how transformer response may be improved through the use of wave filter principles.

To avoid introducing losses and attenuation in the transmission bands, reactances as nearly pure as practicable are used in the elements of a wave filter. For example, in the "low-pass" filter T-section of Fig. 135, the inductance arms shown as $L/2$ and the capacitance C are made with losses as low as possible. Capacitors ordinarily used in filters have low losses, but it is a problem to make inductors which

[1] See "Feedback," by E. K. Sandeman, *Wireless Engr., 17,* 350 (August, 1940).

have low losses. Values of inductor Q ranging from 10 to 200 are common, depending upon the value of inductance and the frequency of transmission. Therefore in wave filters the loss is mostly in the

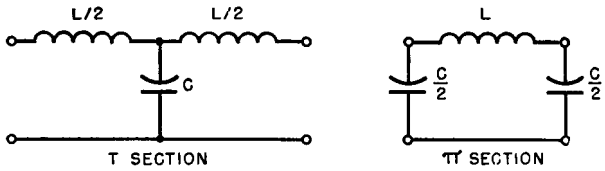

FIG. 135. Low-pass filter sections.

inductors. It can be shown [1] that for pure reactance arms the values of reactance are such that in the transmission band

$$0 > \frac{Z_1}{4Z_2} > -1 \tag{83}$$

where Z_1 is the reactance of the series arm and Z_2 is the reactance of the shunt arm. In the T-section of Fig. 135, Z_1 is $2\pi f[(L/2) + (L/2)]$

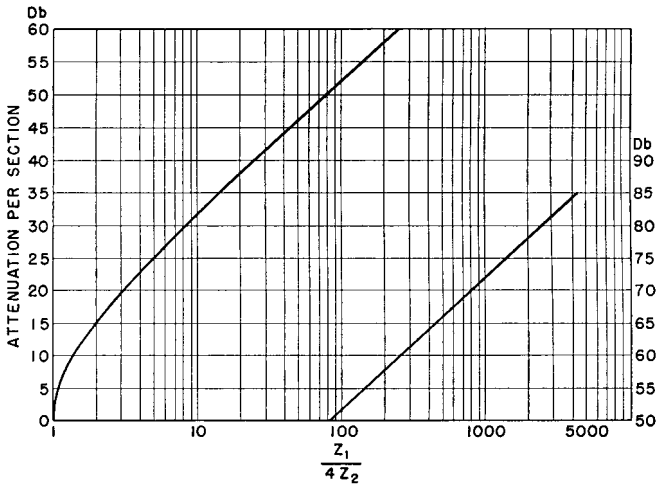

FIG. 136. Attenuation per section with pure reactance arms.

$= 2\pi fL$ and Z_2 is the reactance of C. The attenuation for sections of filter like Fig. 135 is shown in Fig. 136, for a pure reactance network

[1] See *Transmission Networks and Wave Filters,* by T. E. Shea, D. Van Nostrand Co., New York, 1929, p. 187.

starting at the cut-off frequency. The attenuation is shown in decibels, and the abscissas are one-fourth of the ratio of series to shunt reactance in a full section.

It is important, in the transmission band, to terminate the sections of filter in the proper impedance. Like a transmission line, a wave filter will deliver its full energy only into an impedance which is equal to its characteristic impedance. Many wave filters are composed of several sections which simulate transmission lines. A properly constructed filter exhibits the same impedance at either end when terminated at the opposite end with an impedance equal to its characteristic impedance. The impedance seen at any one point in the filter is called its image impedance; it will be the same in either direction provided that the source and terminating impedances are equal. In general, however, the image impedance will not be the same for all points in the filter. For example, the impedance looking into the left or T-section of Fig. 135 (if it is assumed to be terminated properly) will not be the same as that seen across the capacitor C. For that reason, another half-series arm is added between C and the termination to keep equal input and output impedances. The terminating sections at both the sending and receiving ends of a filter network are half-sections, whereas the intermediate sections are full sections. A full T-section of the type shown in Fig. 135 includes an inductance L equal to $L/2 + L/2$. The image impedance seen at the input terminals of the T-section of Fig. 135 is known as the mid-series impedance, and that seen across capacitor C is known as the mid-shunt impedance.

Likewise, in the pi-section shown at the right in Fig. 135, the mid-shunt image impedance is seen at the input or output terminals. The mid-series impedance is seen at a point in the middle of coil L. This section terminates properly in its characteristic impedance at either end. Note that adjacent sections have $C/2$ for the shunt arm, so that a full section would again be composed of a capacitor C and an inductance L. The choice of T- or pi-sections is determined by convenience in termination, or by the kind of image impedance variation with frequency that is desired.

If these precautions are not observed, wave reflections are likely to cause a loss of power transfer in the transmission band.

76. Limitations of Wave Filters. Several factors modify the performance of wave filters, shown in Fig. 136, especially in the cut-off region. One is the reflection due to mismatch of the characteristic

impedance.[1] The load resistor is usually of constant value, whereas the image impedance changes to zero or infinity at cut-off for lossless filters. The resulting reflections cause rounding of the attenuation curve in the cut-off region instead of the sharp cut-off of Fig. 136.

Another cause of gradual slope at cut-off is the Q of the filter chokes, or ratio of reactance to resistance. Figure 137 gives the attenuation

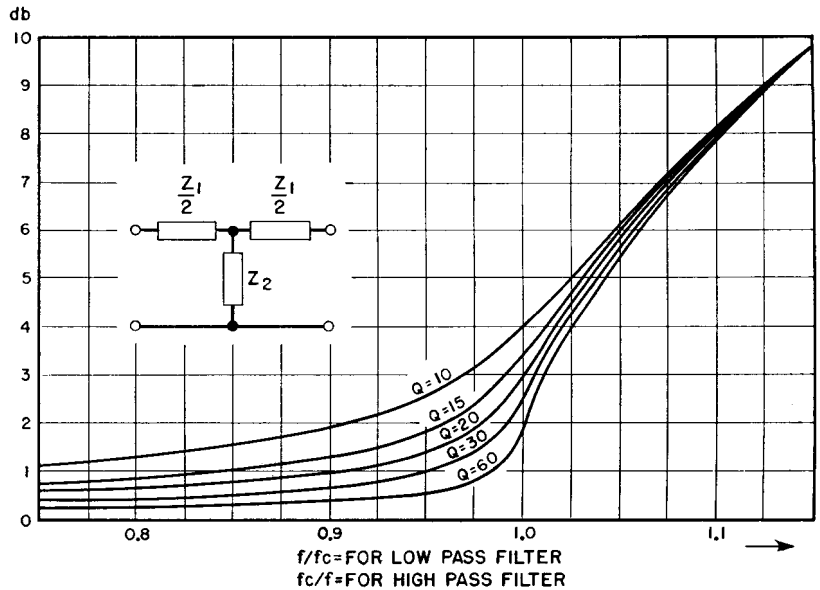

FIG. 137. Insertion loss near cut-off of a constant-K filter section.

at cut-off in terms of Q for a section of the so-called constant-K filter (e.g., Fig. 135).

Still another cause of the gradual slope of cut-off is the practice of inserting a resistor to simulate the source impedance in attenuation tests. In typical cases the source and terminating resistances are equal. The correct prediction of filter response near cut-off requires a good deal of care. It cannot be taken directly from the usual attenuation charts.

Phase shift is nearly linear with frequency up to approximately 50

[1] See "An Analysis of Constant-K Low- and High-Pass Filters," by O. S. Meixell, *RCA Rev., 5,* 337 (January, 1941); also "Single-Section m-Derived Filters," by C. W. Miller, *Wireless Engr., 21,* 4 (January, 1944).

per cent of cut-off frequency for constant-K filters in the transmission band. This fact is important in connection with networks used for the transmission of steep wave fronts, as in video amplifiers. It is proved in books on network theory [1] that, when a non-sinusoidal voltage wave is applied to the input of a network, it appears at the output without distortion of its original shape if the phase shift of the network is proportional to frequency and if the amplitude response is flat for all frequencies. In no actual network are these conditions fulfilled completely, but the closer a network approximates them the smaller the distortion it causes in irregular wave forms. Linearity of phase shift is usually more essential to good wave form than flatness of response. For this reason, when a non-sinusoidal wave passes through a filter, distortion is minimized if the major frequency components of the wave all lie in the linear region of the phase shift curve. Considerable judgment must be exercised in the choice of cut-off frequencies. Higher-order harmonics are usually of smaller amplitude, and the natural tendency is to include too few of them in the pass band; then the output wave form is a poor reproduction of the input.

In band-pass filters, the effects just noticed are present, with the additional complication of band width. The filter designer must choose a band width of transmission such that high attenuation is afforded at unwanted frequencies and low attenuation at desired frequencies. This is often not a simple choice. For a given frequency separation from the mid-frequency, attenuation decreases as the filter band width is made wider. Impedance variation is much less with a wider band width. Therefore, choosing a narrow band width attenuates frequencies in the transmission band because of reflections.

77. Artificial Lines. Sometimes a certain amount of time delay must be interposed between one circuit and another. Or, if the length of a transmission line is not an exact multiple of 90°, some means must be found to increase its length to the next higher multiple of 90°. For either of these purposes, artificial lines are used. They may operate at a single frequency or over a range of frequencies. They may be tapped for adjustment to suit any frequency in a given range, so that impedance and line length are correct. The configuration may be either T or π, high- or low-pass. Figure 138 shows these four combinations for any electrical length θ of line section in degrees. It

[1] See *Communication Networks,* by E. A. Guillemin, John Wiley & Sons, New York, 1935, Vol. II, p. 474.

is assumed in this figure that the line operates at a single frequency and is terminated in a pure resistance equal in value to the line characteristic impedance Z_0. Figure 139 is the vector diagram for a leading

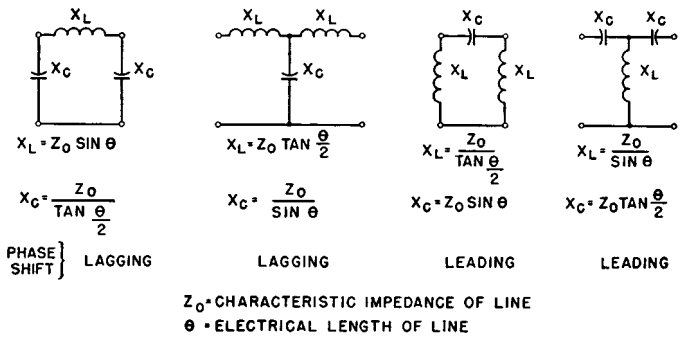

FIG. 138. Artificial line relations.

phase shift pi-section line of 90° electrical length. Proportions of L and C are somewhat different in these line sections than in wave filters.

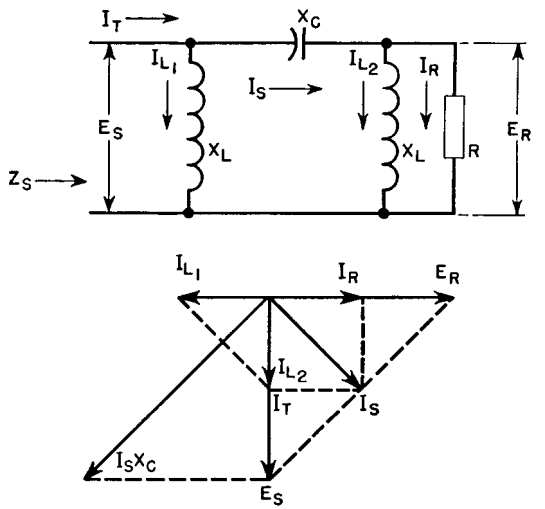

FIG. 139. Vector diagram for 90-degree line length.

To obtain approximately constant time delay over a range of frequencies, several constant-K low-pass filter sections may be used, each having a cut-off frequency high enough so that the phase shift is pro-

portional to frequency. The time delay per section is then $\theta/2\pi f$ at any frequency in the range, and $\theta = 2\pi f\sqrt{LC}$, where θ is the phase shift in radians, L is the inductance per section, and C is the capacitance per section. In Fig. 139, $E_R = E_S$. If the section were terminated in impedance higher than Z_0, $E_R > E_S$. The line section is then a kind of transformer, although the ratio E_R/E_S varies with frequency. Ninety-degree line sections are often used at high frequencies to obtain transformation of voltage.

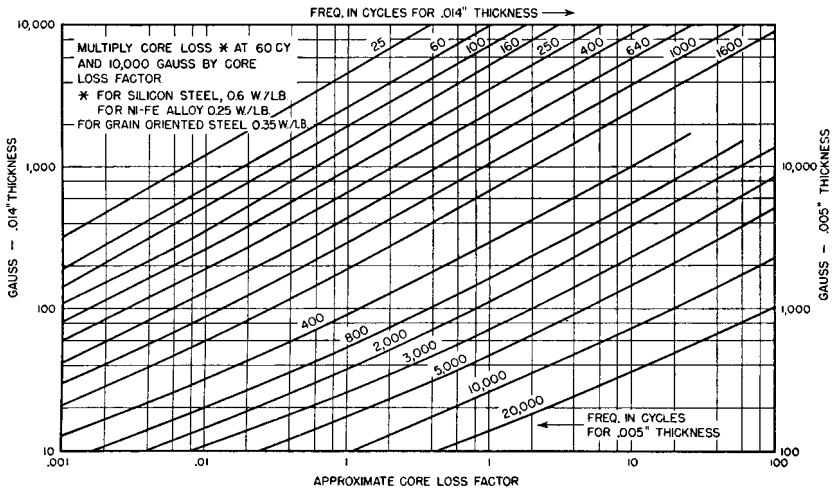

FIG. 140. Core loss in laminations 0.014 and 0.005 in. thick.

78. Filter Inductor Design. In Sections 75 and 76, it was pointed out that inductors for wave filters must have Q great enough to provide low attenuation in the pass band. In design, attention must be given as much to Q as to inductance.

Low-loss core material is essential for high Q. Nickel-iron alloys are widely used; the lamination thickness depends on frequency. At frequencies up to 400 cycles, 0.014-in.-thick laminations are used, and at frequencies higher than 400 cycles, 0.005 in. thick. This is an approximate practical guide. Figure 140 shows how loss varies with thickness, frequency, and flux density. At frequencies higher than 1,000 cycles, flux density must be quite small for low core loss. In the majority of audio applications, low flux density conditions prevail. Under such conditions, core loss is largely eddy-current loss and may be treated as a linear resistance.

Core gaps are used in filter reactors to obtain better Q. For any core, inductance per turn, and frequency, there is a maximum value of Q. The reason for this is that the a-c resistance is composed of at least two elements: the winding resistance and the equivalent core loss. In previous chapters the core loss has been regarded as an equivalent resistance *across* a winding. But it can also be regarded as an equivalent resistance *in series* with the winding. Figure 141 shows this equivalence, which may be stated:

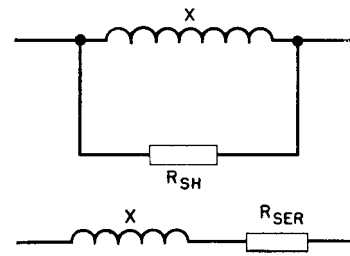

FIG. 141. Shunt and series equivalent core-loss resistance.

$$R_{ser} + jX = \frac{jR_{sh}X}{R_{sh} + jX}$$

For values of $Q > 5$,

$$R_{sh} \approx \frac{X^2}{R_{ser}} \tag{84}$$

where R_{sh} = equivalent shunt resistance
R_{ser} = equivalent series resistance
X = winding reactance = $2\pi fL$.

The equivalence depends upon frequency. The formula for large Q may then be changed to

$$Q = \frac{R_{sh}}{X} = \frac{R_{sh}}{2\pi fL} \tag{85}$$

or Q is proportional to shunt resistance, the winding resistance being neglected. Thus Q can be increased by lowering L, and L is lowered by increasing core gap, but there are limits on the increase of Q that can be obtained in this way.

First, the winding resistance is not negligible. With small gaps, maximum Q is obtained when winding resistance and equivalent series core-loss resistance are equal. For a given air gap there is a certain frequency f_m at which this maximum Q holds. At higher and lower frequencies, the manner in which Q falls below the maximum is found as follows: Let R_c be the coil winding resistance. Then

$$Q = \frac{X}{R_c + R_{ser}}$$

If for R_{ser} we substitute the value obtained from equation 84, we have, approximately,

$$Q = \frac{X}{R_c + \frac{X^2}{R_{sh}}} = \frac{1}{\frac{R_c}{X} + \frac{X}{R_{sh}}} \tag{86}$$

Equation 86 therefore gives the relation of Q to frequency. When it is plotted on log-log coordinates with frequency as the independent variable,[1] it is symmetrical about the frequency f_m for which Q is a

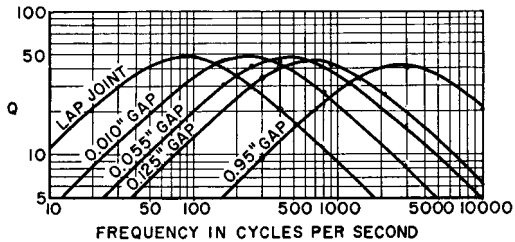

FIG. 142. Frequency variation of Q for an iron-core coil with air gaps.

maximum. If the core gap is changed, frequency f_m changes. Figure 142 shows how the Q of a small inductor varies with frequency for several values of air gap in the core. All these curves have the same shape, a fact which suggests the use of a template for interpolating such curves.

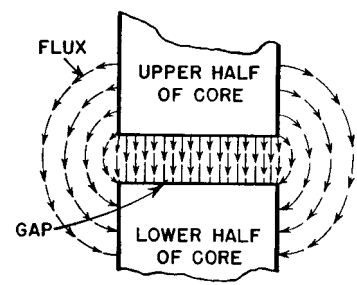

FIG. 143. Magnetic flux fringe at core gap.

Another phenomenon that limits Q is the *flux fringing at the core gap,* the influence of which on inductance was discussed in Chapter 3. As the air gap increases, the flux across it fringes more and more, like that shown in Fig. 143, and L ceases to be inversely proportional to the gap. Some of the fringing flux strikes the core perpendicular to the laminations and sets up eddy currents which cause additional loss. Accurate prediction of gap loss depends on the amount of fringing flux. For laminated cores it can be estimated from

[1] See "How Good Is an Iron-Cored Coil?" by P. K. McElroy and R. F. Field, *General Radio Experimenter, XVI* (March, 1942). This article also discusses choke design from the standpoint of similitude.

$$W_g = Gl_g d\mu t_e \sqrt{f}\, B_m^2 \quad \text{watts} \tag{87}$$

where G = a constant (17×10^{-10} for silicon steel)
d = lamination tongue width in inches
μ = permeability
t_e = lamination tks. in inches
f = frequency in cycles
B_m = peak core induction in gauss
l_g = gap length in inches.

In Section 33, Chapter 3, it was shown that under certain conditions maximum transformer rating for a given size is obtained when core and winding losses are equal. The same would be true for inductors with zero core gap. Similarly it may be shown that, if the core gap is large enough to cause appreciable gap loss, maximum Q is obtained with core, winding, and gap losses equal. In a given design, if this triple equality does not result in the required Q, size must be increased. Losses may be compared by finding either the equivalent series resistances or the equivalent shunt resistances.

79. Powdered Iron Cores. As frequency increases above a few thousand cycles, gap loss becomes predominantly large. At such frequencies, cores of powdered iron are preferable for large Q. Powdered-iron cores are made from several grades of iron and nickel-iron alloys. Proportions of insulating bond and iron powder are varied to obtain permeabilities ranging from 10 to 125. Permeability in such cores is only *apparent;* it is far less than the inherent permeability of the iron used because of the many small gaps throughout the core structure. Finely divided iron has low eddy-current loss and virtually zero gap loss. Equation 85 indicates how Q varies with frequency; that is, low-permeability cores should be used to reduce inductance and maintain large Q at high frequencies. At frequencies higher than audio, coil eddy-current losses make stranded wire necessary. This is discussed further in Chapter 7.

One of the problems of filter design is the maintenance of cut-off and attenuation frequencies under conditions of varying temperature. This may be so important as to dictate the choice of core material. Powdered cores are available which have very low temperature coefficients. Usually these cores have less than the maximum Q for a given kind of iron powder. With low-temperature-coefficient cores, attention also must be paid to filter capacitors in order to obtain the requisite overall frequency stability.

TABLE XIV. SHAPES OF POWDERED-IRON CORES

Core Shape	Use
Shell	Low-voltage r-f transformers and inductors.
Cup	Adjustable low and medium r-f inductors.
Slug	Adjustable r-f inductors. Also used to adjust cup-core inductance.
Toroid	Audio and low r-f inductors.
C	High-voltage audio and r-f transformers and inductors.

Powdered cores are made in several forms. Table XIV indicates the main areas of usefulness of such forms. Figure 144 illustrates the core shapes in this table. A study of available molds and materials is worthy of the designer's time.

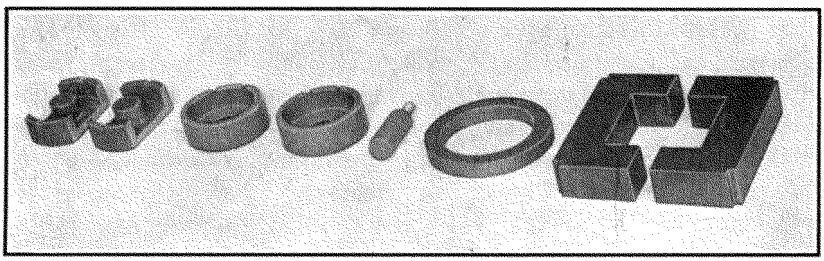

FIG. 144. Powdered iron-core shapes.

80. Modulation Transformers. Wave-filter principles are applied in many circuits other than filters. An example is the design of modulation transformers for high-level amplitude-modulated radio transmitters. Some of these transformers are large. In plate-modulated power amplifiers, the modulator power required to produce 100 per cent modulation is half of the power amplifier input. Improved audio quality and reduction in size of components are achieved through the use of what may be called the pi-filter method.

For low modulation frequencies, this method may be illustrated by means of the circuit diagram of Fig. 145(*a*). The modulator usually is a class B amplifier. Output transformer *OCL*, coupling capacitor, and modulation reactor combine to form a pi-section high-pass filter, Fig. 145(*b*). The elements are proportioned for characteristic impedance equal to the equivalent plate input resistance E_B/I_B of the modulated power amplifier.

Formerly these components were made as large as was considered practical. Transformer secondary and reactor reactances were each

3 to 4 times the power amplifier plate input resistance, and the coupling capacitor reactance was a fraction of this resistance, at the lowest modulation frequency. Advantages of the pi-filter are a reduc-

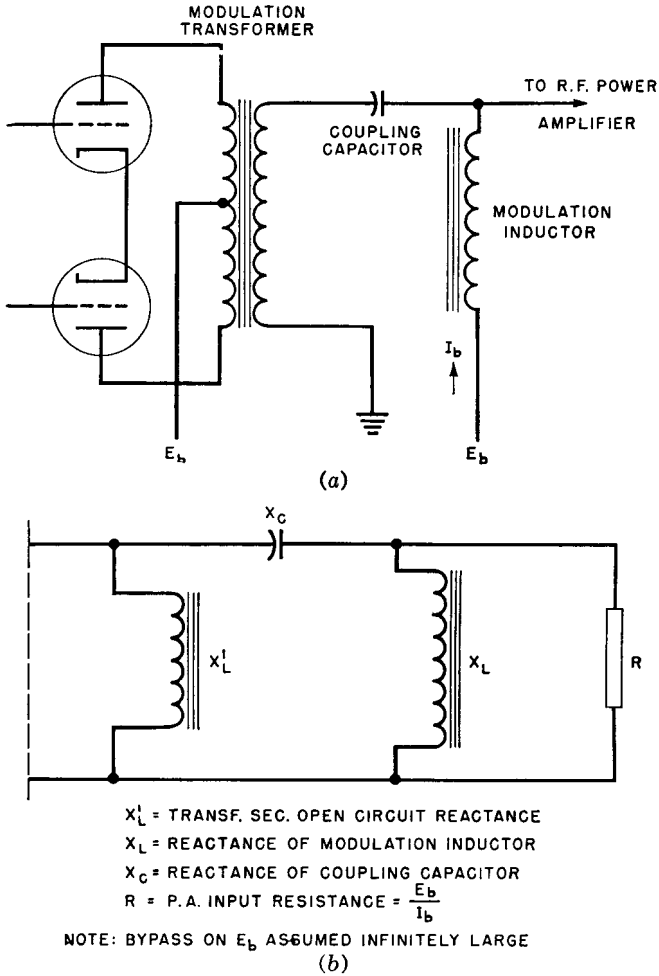

FIG. 145. (*a*) Circuit diagram of anode modulation system; (*b*) equivalent pi-filter modulator tube load.

tion of the two inductive reactances to 1.41 times the terminating load resistance, and increase in capacitive reactance to the same value, at a low frequency f_1, which is 1.41 times cut-off frequency of the filter.

Down to f_1 the filter maintains a tube load of almost 100 per cent

power factor, although the ohmic value rises to 190 per cent of the terminating load resistance at f_1. The voltage required for constant output rises to 138 per cent of normal. Partly compensating for this defect is the tendency of class B amplifier tubes to deliver higher voltages with higher tube load impedances. Thus, in a certain radio transmitter, the type 805 modulator tubes deliver 1,035 peak volts per side into a normal tube load of 1,860 ohms. At 30 cycles, the lowest audio frequency, the load impedance rises to 3,600 ohms, and the voltage required for full output is 1,440 volts. Plotting a 3,600-ohm load line on the tube curves shows that 1,275 volts will be delivered at 30 cycles, which is 1 db down from normal.

To obtain the same frequency response with the older "brute force" method, at least twice the values of transformer and reactor inductance and much more coupling capacitance would have been necessary. The voltage across the capacitor increases as the capacitance decreases, but surge voltages often exist across the coupling capacitor in service. The voltage rating was formerly determined more by these surges than by normal voltage. With the pi-filter method, the normal voltage at low frequencies cannot be greatly exceeded in service, owing to the limitation in voltage output of the tubes. Hence, the reduction in coupling capacitance is a real one and is offset very little by increases in voltage rating.

These points are made clearer by reference to Fig. 146. Phase shift between transformer and load voltages is 90° at f_1. At cut-off ($= 70$ per cent of f_1) the tube voltage for constant output is 224 per cent of the load voltage. A tube would not deliver so much voltage with this type of load, especially when the power factor is so low. The corresponding capacitor voltage at cut-off frequency is 284 per cent of E_R; it would not be delivered either, for the same reason. The useful frequency range is higher than f_1.

Another advantage of the pi-filter over the older method is the high power factor load down to frequency f_1. The maximum tube load phase angle above f_1 is 8°, and at frequencies above $3f_1$ the phase angle is zero. At $3f_1$ the tube load impedance is equal to R. Hence the tube works into a unity power-factor load of constant value at frequencies above $3f_1$. For the same size of inductive components, the "brute force" system would have been very much poorer. If these elements had been made twice as large in order to give the same frequency response at 30 cycles, the load phase angle at 30 cycles would be 35° and the load impedance 80 per cent of R. Hence the possibilities of low-frequency distortion and low efficiency are reduced by the pi-filter method.

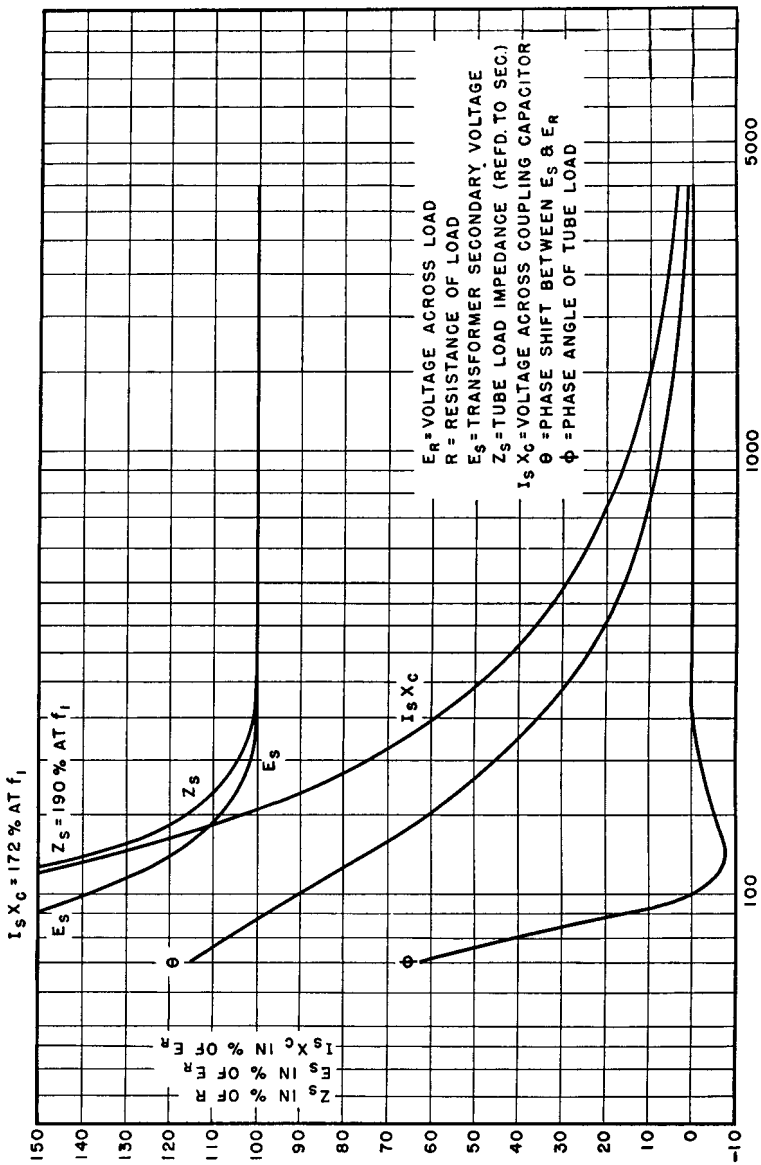

FIG. 146. Pi-filter basis of transformer design.

In very high fidelity modulators the lowest frequency is 2 to 3 times f_1 to reduce phase shift in connection with the inverse feedback.

The pi-filter just discussed conforms with the usual high-pass filter in regard to values of L and C. These elements can be proportioned on another basis such that the ohmic values of all the reactive elements are made equal to the load resistance at frequency f_1. These values are those of a 90° artificial line at frequency f_1. They give a unity power-factor tube load equal to the modulated power amplifier plate input resistance at frequency f_1, and thus represent 41 per cent increase in capacitor and 41 per cent reduction in transformer and reactor size. The disadvantages of the artificial line are that the tube load impedance drops to a minimum of 74 per cent R at the frequency $1.5f_1$, the maximum tube load phase angle is 16°, and it persists up to frequencies much higher than $3f_1$, which was the frequency where the response of the pi-filter became virtually perfect. This appreciable phase angle spread over a portion of the audio frequency range, together with the lower load impedance, causes distortion. The artificial line basis of design is used where larger amounts of distortion are not objectionable, or in fixed-frequency modulators.

No matter what method of design is used, it is important that the modulator be loaded properly. If the power amplifier input should be interrupted while the modulator is fully excited, the voltages on the various elements are likely to rise to dangerous values, because the load impedance becomes high and causes indefinitely high voltages in the positive e_B direction. The transformer and reactor in high-voltage modulators are equipped with spark gaps like those in Fig. 147 to prevent insulation breakdown due to accidental removal of load.

The pi-filter or artificial line method of design can be applied also at the higher modulation frequencies. Figure 148 shows how the usual properties of winding capacitance and leakage inductance are arranged to give a low-pass filter circuit. Preferably the internal capacitance and inductance should be so low that external L and C can be added to the transformer terminals to produce the required proportions at the highest modulator frequency.[1] Figure 149 shows how both high- and low-pass pi-filter performance can be combined in a modulator to obtain wide-range high-fidelity performance. Although these methods apply chiefly to modulation transformers, they may be used in the design of loaded interstage transformers.

[1] See "An Analysis of Distortion in Class B Audio Amplifiers," by True McLean, *Proc. I.R.E., 24,* 487 (March, 1936); also see Section 81.

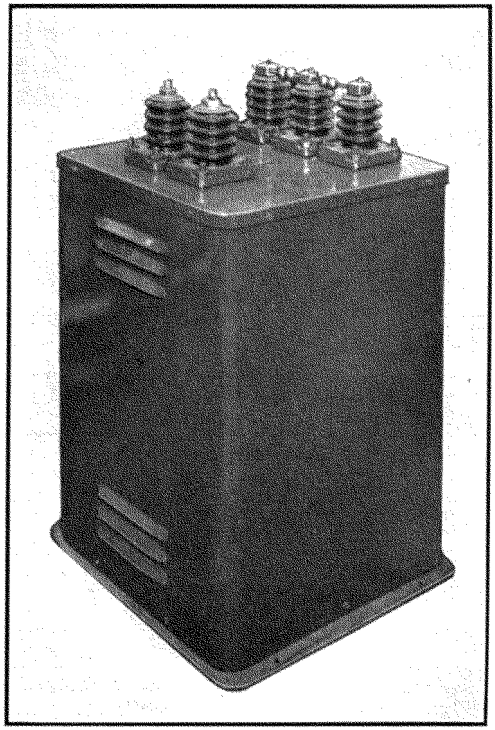

FIG. 147. Broadcast station modulation transformer.

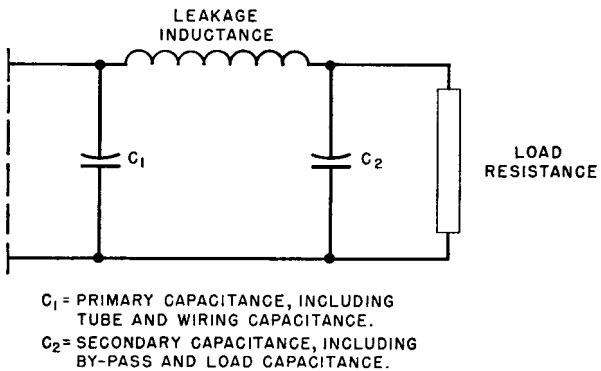

FIG. 148. Equivalent transformer diagram at high audio frequencies.

In high power modulation transformers, it is necessary to make the core larger in order to reduce the number of turns and obtain good high-frequency response. But, as the core becomes larger, so do the leakage inductance and winding capacitance. The core must grow very large to overcome this difficulty, and high power audio transformers are much larger than commercial power transformers of the same rating. One advantage of grain-oriented steel is that it permits this process to be reversed. High induction at low frequencies means

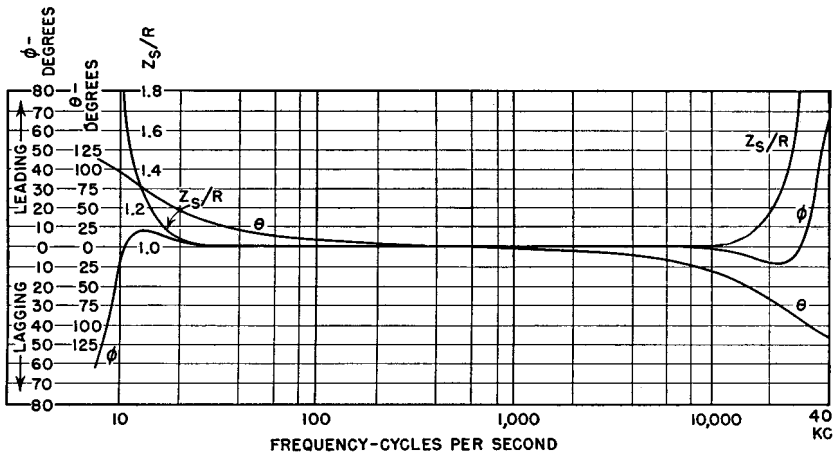

FIG. 149. High- and low-pass pi-filter performance in a modulator.

a smaller core area, smaller mean turn, and better high-frequency performance, or, for the same high-frequency performance, more turns and a still smaller transformer. Weight savings of 60 to 75 per cent have been made in this way.

Advantages of the pi-filter and artificial line methods are realized in transformers for 30 to 10,000 cycles; some advantage can be gained in the 100- to 5,000-cycle range, but not below 100 watts. Below this size, or for a narrower frequency range, the transformer becomes so small that combination with the modulation reactor into one unit is feasible and economical. The secondary current wave shape is like the first wave of Table I (p. 16). In such a transformer the core gap must be large enough to prevent saturation by the power amplifier plate current.

81. Driver Tansformers. Requirements for class B modulator driver transformers are unusually difficult to satisfy. The transformer load is non-linear, for grid current is far from sinusoidal. Although the average load is low, the driver tube must deliver instantaneous current peaks; otherwise distortion will appear in the modulator audio

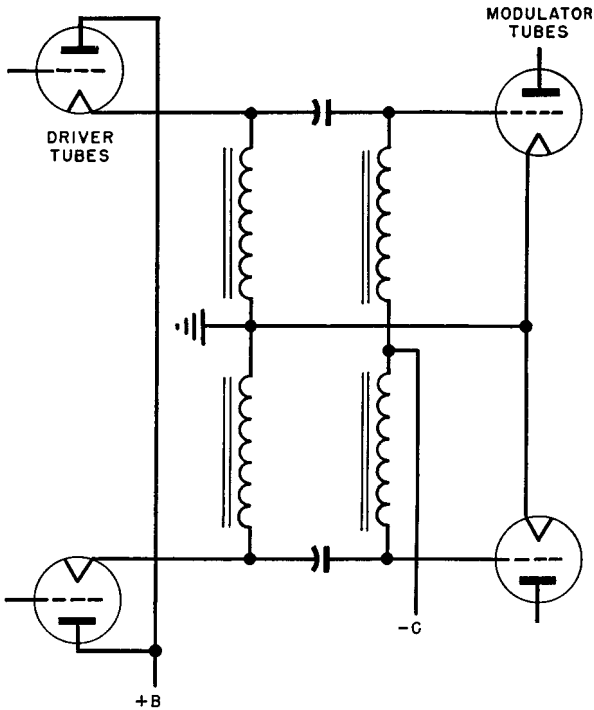

FIG. 150. Cathode follower driver circuit.

output and therefore in the r-f envelope. The grid current peaks contain harmonic currents of higher order, and to insure their appearance in the modulator grid current an extension of the driver transformer frequency range at both ends is required: on the high-frequency end because of the decreased leakage inductance necessary to allow the higher currents to flow, and on the low-frequency end to prevent transformer magnetizing current, itself non-linear, from loading the driver tube so that it does not deliver the peak grid power. If the driver tube is a pentode or beam tube, it is usually loaded with resistance to minimize current variations. Driver transformers are usually step-down because the grid potentials are relatively low.

These conditions require transformers of exceptionally large size. For low (1 to 2 per cent) overall harmonic distortion, driver transformer design becomes impractical, and it is advantageous to dispense with driver transformers entirely. This is accomplished by the cathode follower circuit (Fig. 150), which for a push-pull amplifier takes the form of a symmetrical pi-filter. The two input chokes connect the driver tube cathodes to ground and carry their plate current. Coupling capacitors connect these chokes to the modulator tube grid chokes, which carry modulator grid current. Sizes of chokes and coupling capacitors are chosen to give approximately constant impedance from the lowest modulation frequency up to the higher harmonics of the highest frequency, and choke capacitance is reduced to preclude pronounced resonance effects throughout the frequency range. In Fig. 151, the filter components are mounted in the exciter cubicle; a transformer for this purpose would be too large to locate internally.

The cathode follower circuit is advantageous in another way. Leakage inductance in a driver transformer causes high-frequency phase shift between driver and grid voltage, which does not exist in the coupling capacitor scheme. Since inverse feedback is often applied to audio amplifiers to reduce distortion, the absence of phase shift is a great advantage. The *low* frequency at which phase shift appears must be kept below the audio band, but this can be done without excessively large components.

82. Transformer-Coupled Oscillators. These have circuits similar to that of Fig. 152. Transformer OCL and capacitor C_1 form a tank circuit, to which are coupled sufficient turns to drive the grid in the lower left-hand winding. The output circuit is coupled by a separate winding. For good wave shape in such an oscillator, triodes and class B operation are preferable. The ratio of turns between anode and grid circuits is determined by the voltage required for class B operation of the tube as if it were driven by a separate amplifier stage. Single tubes may be used, because the tank circuit maintains sinusoidal wave shape over the half-cycle during which the tube is not operating. Grid bias is obtained from the RC_2 circuit connected to the grid.

In such an oscillator, tube load equals transformer loss plus grid load plus output. In small oscillators, transformer loss may be an appreciable part of the total output. This loss consists of core, gap, and copper loss. Copper loss is large because of the relatively large tank current, and the wire size in the anode winding is larger than would be normally used for an ordinary amplifier. The gap is neces-

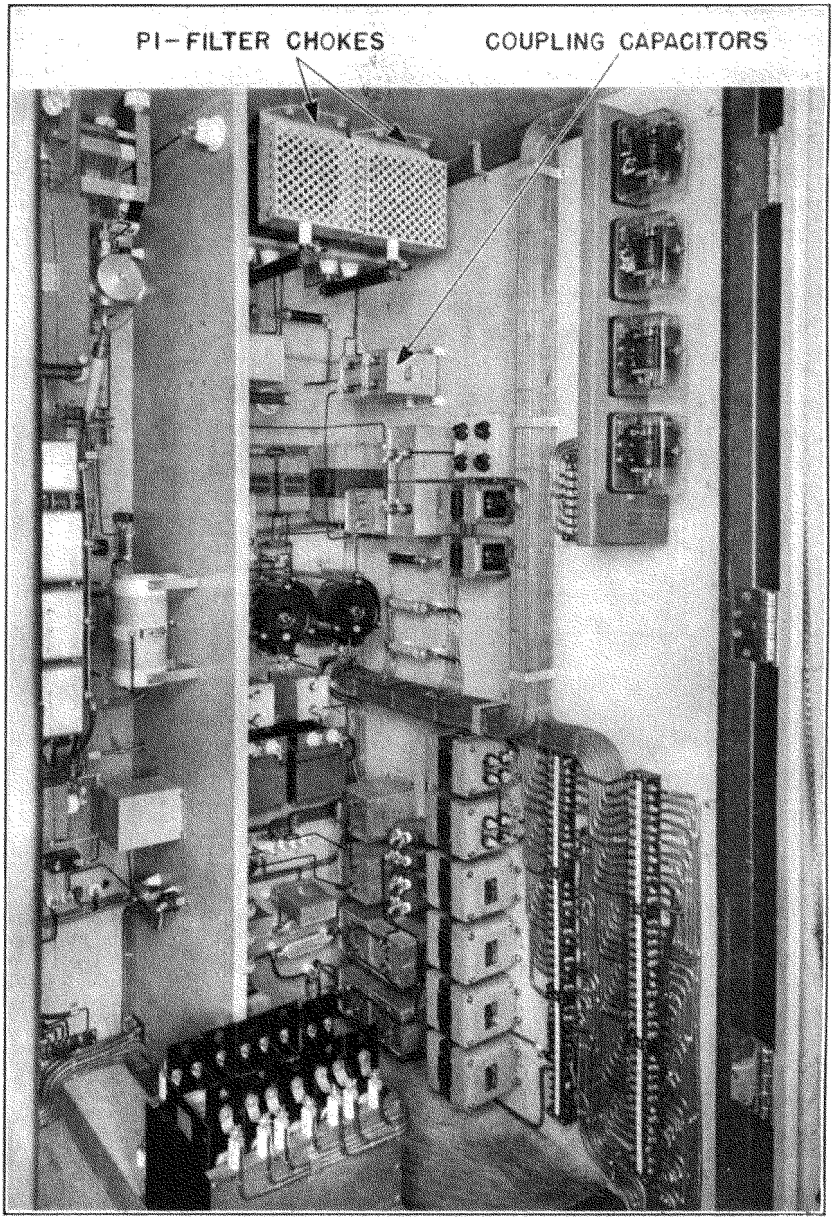

FIG. 151. Rear view of exciter cubicle for 50-kw broadcast transmitter.

sary to keep the inductance down to a value determined by the tank circuit Q or volt-amperes. This in turn is dictated by the required harmonic content. The use and selection of core materials are approximately the same as those indicated in Sections 78 and 79.

Class C oscillators are less desirable for very low harmonic requirements, because of the difficulty of designing tank circuits with sufficiently high Q. Where large harmonic values can be tolerated, the transformer can be designed for low Q, but the wave form becomes non-

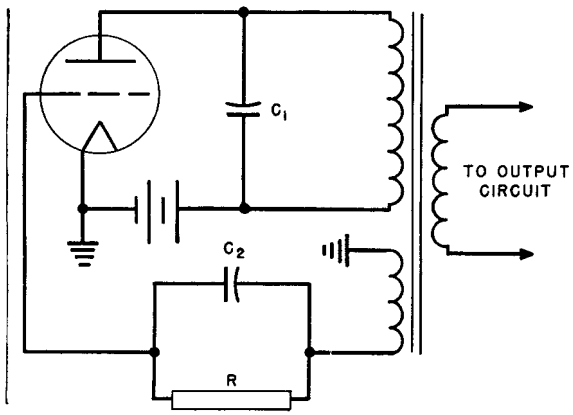

FIG. 152. Transformer-coupled audio oscillator.

sinusoidal. Transformer grid circuit turns are large, approximately the same as plate turns, and the grid voltage would be high if grid current did not limit the positive voltage swing. During the half-cycle when the tube is operating, the voltage wave has a roughly rectangular shape, and during the rest of the cycle it peaks sharply to a high amplitude in the opposite direction. Core losses are difficult to predict because loss data are not normally available for such wave forms. Consequently, designs of this type are usually cut-and-try. The frequency of oscillation varies with changes in load; hence low Q class C oscillators are to be avoided if good frequency stability is required.

83. Shielding. Gain of 80 to 100 db is often reached in high-gain amplifiers. It is important in these amplifiers that only the signal be amplified. Small amounts of extraneous voltage introduced at the amplifier input may spoil the quality or even make the received signal unintelligible. One source of extraneous voltage or hum is in stray magnetic fields emanating from power transformers in or near the amplifier. The stray fields enter the magnetic cores of input trans-

formers and induce small voltages in the windings, which may be amplified to objectionably high values by the amplifier. Several devices are used to reduce this hum pick-up:

1. The input transformer is located away from the power transformer.
2. The coil is oriented for minimum pick-up.
3. Magnetic shielding is employed.
4. Core-type construction is used.

The first expedient is limited by the space available for the amplifier, but, since the field varies as the inverse cube of the distance from the

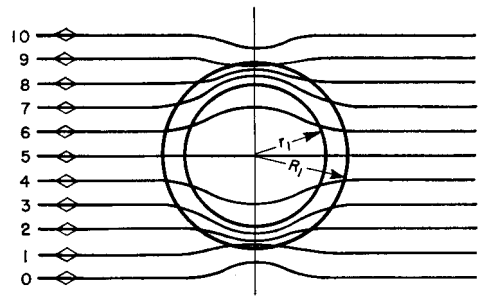

FIG. 153. Refraction of magnetic field by iron shield.

source, it is obviously helpful to locate the input transformer as far away from the power transformer as possible. The second method is to orient the coil so that its axis is perpendicular to the field. It requires extra care in testing. Magnetic shielding is the "brute force" method of keeping out stray fields; core-type construction is effective and does not materially increase the size. Of course, any of these methods increases manufacturing difficulties to a certain extent.

Magnetic shielding is ordinarily accomplished by a thick wall of ferrous metal or a series of thin, nesting boxes of high permeability material encasing the windings and core of the input transformer. Neither type of shield is applied to the power transformer because the flux lines originate at the power transformer and fan out in all directions from it. A large percentage of the flux would strike the shield at right angles and pass through it. On the other hand, the stray field near the input transformer is relatively uniform, and very few flux lines strike the shield at right angles. Thus more flux is bypassed by it. The action of a thick shield in keeping stray flux out of its interior is roughly illustrated in Fig. 153.

Multiple shields increase the action just mentioned because eddy currents induced in the shields set up fluxes opposing the stray field. Sometimes alternate layers of copper and magnetic material are used for this purpose, when hum pick-up 50 or 60 db below the no-shield value is required.[1]

In core-type transformers the flux normally is in opposite directions in the two core legs, as shown in Fig. 154. A uniform external field, however, travels in the same direction in both legs, and induced voltages caused by it cancel each other in the two coils.

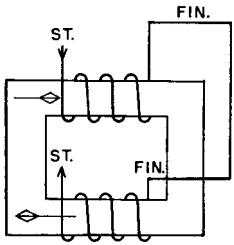

FIG. 154. Flux directions in a core-type transformer.

The relative effectiveness of these expedients is shown in Fig. 155. Hum pick-up is given in decibels with zero decibel equal to 1.7 volts across 500 ohms, and distance from a typical small power transformer as abscissas. All curves are for 500-ohm windings working into their proper impedances, and with no orientation for minimizing hum. Using impedances much less than 500 ohms reduces the hum picked up. Orientation of coil position also reduces hum. For all types of units there is a position of minimum hum. With the unshielded shell type the angle between the transformer coil and the field is almost 90° and is extremely critical. With shielding, this angle is less critical, but the minimum amount of hum picked up in this position is not noticeably reduced. The core type is less critical, especially with a shield. The minimum amount of hum picked up is from 10 to 20 db less than the shielded shell type in its minimum position. Removing the shields from the core type may change its position of minimum pick-up. This is because the shields reduce hum by a process different from that of the two bucking coils.

It is advantageous to have power transformers of the core type. Leakage fluxes from like coils on the two legs approximately cancel at a distant point. The U-and-I shape of lamination is better than the L shape because of its symmetry. A type C core has the advantage that gaps are inside the coils. Thus fringing is reduced, and stray flux from the core gap is minimized.

Static shielding does not prevent normal voltage on a primary winding from being transferred inductively into a secondary winding. It is

[1] See S. L. Gokhale, *J. AIEE, 48,* 770 (October, 1929); also, "Magnetic Shielding of Transformers at Audio Frequencies," by W. G. Gustafson, *Bell System Tech. J., 17,* 416 (July, 1938).

effective only against voltage transfer by interwinding capacitance. High-frequency currents from vacuum tube circuits are thus prevented from flowing back into the 60-cycle power circuits via filament and

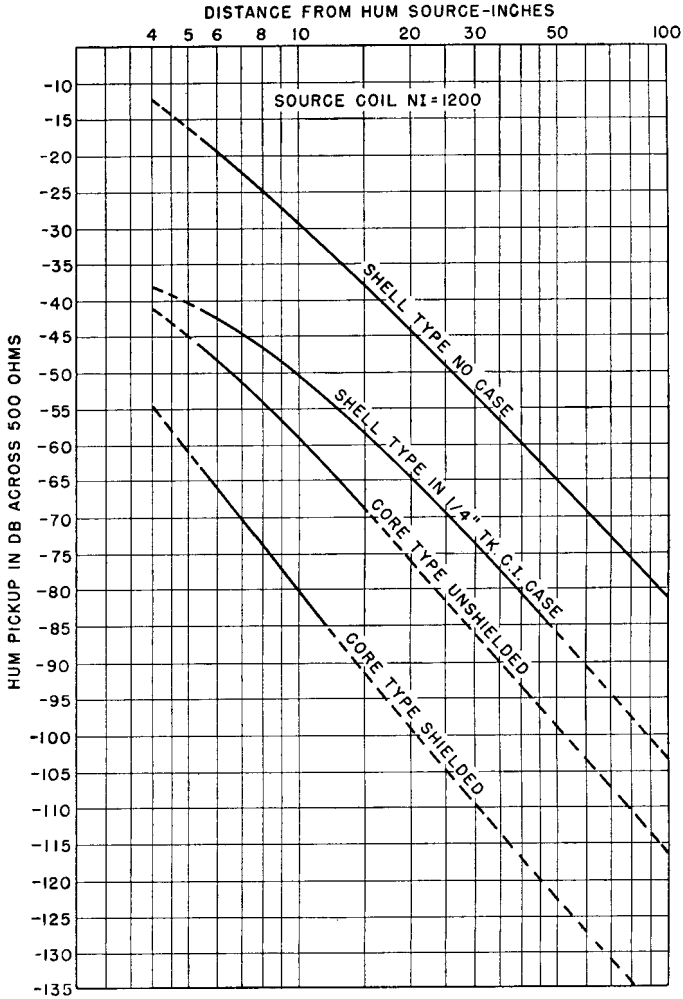

FIG. 155. Hum pick-up in input transformers.

plate transformers. Without shielding, such currents may interfere with operation of nearby receivers. Likewise, voltages to ground on telephone lines are kept from interfering with normal voice frequency voltages between lines. The extent of static shielding depends upon

the amount of discrimination required. Usually a single, thin, grounded strip of metal between windings is sufficient, with ends insulated to prevent a short circuit. Magnetic flux in the interwinding space causes eddy currents to flow in such shields, and even shields with insulated ends indicate a partial short circuit on test. This effect reduces the *OCL* of the transformer. If volts per layer are small compared to total winding voltage, a layer of wire is an effective shield.

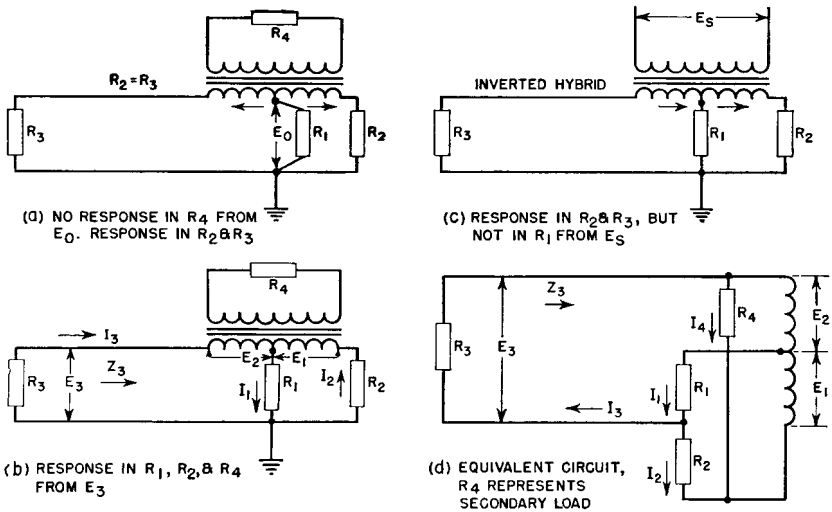

FIG. 156. Hybrid coil operation.

The start turn is grounded and the finish left free, or vice versa. A wire shield has none of the short-circuit effect of a wide strip shield.

Usually a transformer that requires static shielding has a low-voltage winding; the shield can be placed close to this winding, needs little additional insulation, and occupies but a small fraction of the total coil space. If shields are placed between high-voltage windings, as in modulation transformers, the shields must be insulated from each winding with thick insulation. This materially increases the coil mean turn length, transformer size, and difficulty in obtaining good high-frequency response. Shields have questionable value in such transformers and usually are omitted.

84. Hybrid Coils. Hybrid coils are used to isolate an unwanted signal from certain parts of a circuit, and allow the signal to be used in other parts of the circuit. In the hybrid coil shown in Fig. 156(*a*) the lower windings or primary sections are balanced with respect to each

other, and the two resistors R_2 and R_3 are equal. Voltage E_0 applied between the primary center tap and ground causes equal currents to flow in opposite directions through the two halves of the primary winding, and therefore produces zero voltage in the secondary winding. By this means, signal E_0 arrives at resistors R_2 and R_3 undiminished, but there is no voltage in R_4 connected across the secondary coil. Figure 156(*b*) shows what happens in this circuit if the voltage is applied across R_3 instead of across R_1. In this case, the voltage E_3 appears across resistors R_1, R_2, and R_4, that is, in all parts of the circuit.

An inverted hybrid coil is shown in Fig. 156(*c*). Here voltage E_s is applied across the upper coil, which is now the primary. The secondary sections are assumed to be balanced. Therefore, there is zero voltage between the center point of the secondary winding and ground, and though a signal appears at R_2 or R_3 there is no signal across R_1. Thus a hybrid coil works in both directions.

It has been assumed that R_2 and R_3 are equal and that the two primary half-windings are of equal number of turns. This is not necessarily true, for, if the resistance of R_2 is twice that of R_3, the number of turns connected to R_2 should be twice those connected to R_3. However, it is important that, through the range of frequency in which the hybrid coil is desired to function, the balance between the two halves be maintained closely. The most exact balance is achieved for $R_2 = R_3$ by winding the two halves simultaneously with two different wires. This method gives good isolation of the undesired signal. Other methods introduce some ratio error which reduces the isolation. For the same reason, it is necessary to balance the circuit with regard to capacitance and leakage inductance. That is, if a capacitance exists across R_3, such as line capacitance for example, an additional equivalent amount should be added across R_2 in order to achieve the balance desired. Likewise, any inductive apparatus, adding either series or parallel inductance in one circuit, should be compensated for by inductance of like character in the other circuit. Adding series inductance, for example, in series with R_3 will not compensate for shunt inductance across R_2, or vice versa, as the two have opposite effects with regard to frequency and therefore balance is attained only at one frequency.

Assume a perfect transformer having no exciting current and no leakage inductance between the two halves, and a transformer with equal turns in the two halves of the primary winding. Assume currents in the directions shown in Fig. 156(*d*). Then

$$I_1 = I_2 + I_3 \tag{88}$$

$$E_1 = I_2R_2 + I_1R_1 \tag{89}$$

$$E_3 = I_1R_1 + E_2 \tag{90}$$

On the assumption of equal turns in the two half-windings, $E_1 = E_2$. If the magnetizing current is assumed to be zero, the ampere-turns and hence the volt-amperes in the two primary halves are equal. The secondary load can be considered as reflected into the primary winding as resistor R_4.

$$I_4 = (E_1 + E_2)/R_4 \tag{91}$$

$$(I_3 - I_4)E_2 = (I_2 + I_4)E_1 \tag{92}$$

If equations 88 to 92 are combined, an expression for Z_3 can be found:

$$Z_3 = \frac{E_3}{I_3} = \frac{4R_1R_2 + 4R_1R_4 + R_2R_4}{4R_1 + 4R_2 + R_4} \tag{93}$$

If the secondary circuit is open, $R_4 = \infty$, and equation 93 becomes

$$Z_3 = 4R_1 + R_2 \tag{94}$$

85. Amplifier Tests. Tests for hum, distortion, linearity, and frequency response can be made with meters in the output circuit when voltage of a known frequency and wave form is applied to the input. Hum and distortion are conveniently measured by instruments specially made for the purpose. Linearity is measured by varying the input voltage and measuring corresponding output voltage. Frequency response is measured at a fixed input or output voltage, but frequency is varied. Normal production testing of amplifiers requires no more than such overall tests. But, in the development of the amplifier, excessive hum, distortion, or other defects may be indicated, and tests must be applied stage by stage to locate the trouble. Voltage is usually measured by a tube voltmeter, one terminal of which is grounded. In a push-pull amplifier, it is therefore necessary to block the direct voltage and measure the alternating voltage on each side. A cathode-ray oscilloscope is helpful in checking phase shift and wave form at various points.

Before being assembled in the amplifier, transformers are tested for turns ratio, balance, polarity, *OCL*, winding resistance, core loss, and insulation strength. Although with new designs it is desirable to check leakage inductance, winding capacitance, and shielding, these properties vary less in a given design than the others. Methods for

making most of these tests are the same as those described in Chapter 3. Tests for capacitance are limited to winding-to-winding and winding-to-core capacitance. These tests are made on a capacitance bridge. Evaluation of capacitance measurements is made as in Section 71.

Balance (an important property of push-pull amplifiers) and shielding tests are described in Standard TR-121 of the Radio-Electronics-Television Manufacturers Association.

Reactor Q is measured either on an inductance bridge (which also measures a-c resistance as in Fig. 75) or on a special Q meter. In either method, rated voltage and frequency should be used. Modulation reactors are usually measured for inductance with full direct current in the winding; great care should be exercised to prevent sudden interruption of this current and consequent dangerous high voltage. Such reactors are often surge-tested to guard against breakdown in service under conditions of overmodulation.

In the diagram of Fig. 157, the first two stages have current feedback, and so initial tests were made with the circuit shown. But overall voltage feedback from the modulator plates back to the 6J7 grids was not applied until the amplifier was first tested without it. Then resistors from which feedback is derived were adjusted to produce the feedback voltage necessary to give the required performance. The carrier power amplifier was completely adjusted before modulation was applied. Percentage of modulation was measured by the increase of carrier output current when modulation was applied. Inductance RFC and capacitor C_1 maintain the modulator load constant at high frequencies. C_2 in this circuit is the audio coupling capacitor. Separate meters are provided to measure the plate current of each driver and modulator tube, so that bias may be adjusted for the same plate current on each side.

Proper operation is predicated on amplifier stability, which often is not obtained when power is first turned on. Local or parasitic oscillations may easily occur as a result of natural resonance of circuit elements or even in connections and tube electrodes. These must be detected and eliminated by corrective measures which apply to the trouble. Some of these troubles may be caused by long leads, especially in the grid circuit. Tubes may require resistors in the plate and grid leads to damp out parasitic oscillations. Resistors are used in this manner in the amplifier shown in Fig. 157. Coils in circuits with widely different voltages should not be coupled closely, because regeneration may result. In circuits with high voltage, and therefore large capacitive currents, it may be necessary to add shielding to

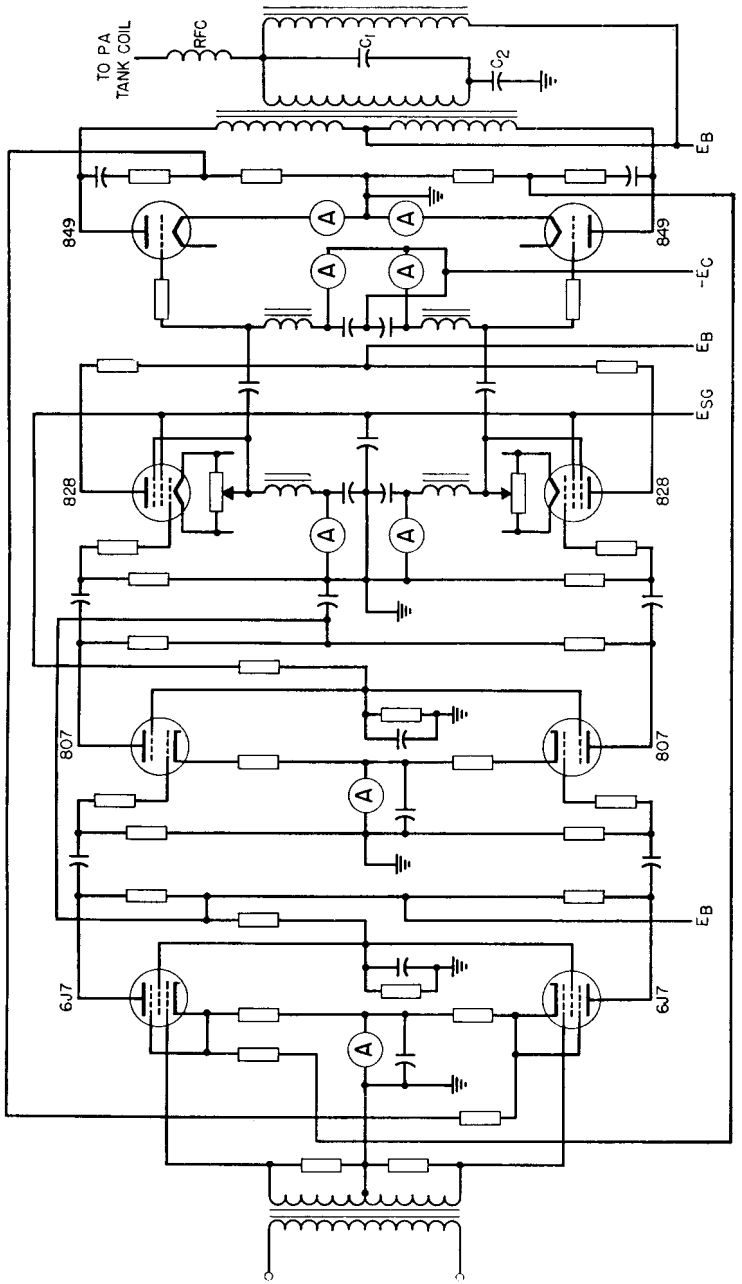

FIG. 157. Amplifier schematic diagram.

prevent stray pick-up from one stage to another. In push-pull amplifiers, if some circuit element is unbalanced, it may give rise to a push-push oscillation which can be eliminated by better balance, or by decoupling the tube plates at the unwanted frequency. If insufficient bypass capacity is used on plate or bias supplies, interstage coupling may occur at low frequencies. The frequency may be less than 1 cycle per second. This kind of instability is known as "motor-boating." Operating tubes so that some electrode becomes a negative resistance during a portion of the cycle may give rise to oscillations which cannot be prevented except by avoidance of the cause, or by some power-absorbing circuit which does not affect normal operation. The elimination of such trouble requires much testing time and skill, but it must be done before performance tests are made.

86. Design Examples.

Example (a). Transformer for Pi-Filter Modulator.
Frequency range 100 to 5,000 cycles.
Audio output 400 watts.
Power amplifier E_B/I_B = 10,000 ohms.
Voltage ratio primary/secondary (1,180 + 1,180)/2,000.
f_1 = 60 cycles.
Core: 4-in. stack of silicon-steel lamination *B*, Fig. 44 (p. 55).
Turns primary/secondary (800 + 800)/1,380 No. 26 wire.

A_c = 7.2 sq in. net; 8.0 sq in. gross.
l_c = 12.75 in.
l_g = 0.012 in.

Possible tube current unbalance = 0.032 amp.

$$B_{dc} = \frac{0.6 \times 800 \times 0.032}{0.012} = 1{,}260 \text{ gauss.}$$

$$B_{ac} = \frac{3.49 \times 2{,}000 \times 10^6}{100 \times 7.2 \times 1{,}380} = 7{,}000 \text{ gauss.}$$

$B_m = \overline{8{,}260}$ gauss. From Fig. 70 (p. 98), μ_Δ = 9,000+

$$\text{Secondary } OCL = \frac{3.2 \times (1{,}380)^2 \times 8 \times 10^{-8}}{0.012 + (12.75/9{,}000)} = 36.5 \text{ henrys.}$$

X_L at $f_1 = 6.28 \times 60 \times 36.5$ = 13,800 ohms. Z_s = 115 per cent R at 100 cycles from Fig. 146. Winding arrangement as in Fig. 158, to reduce layer voltage and capacitance.

Winding resistances: Total primary 90 ohms.
Secondary 80 ohms.
Secondary leakage inductance = 53 millihenrys.
Capacitances (referred to secondary):

$P_1 - S_1$(at A)	=	292 $\mu\mu$f
$P_1 - S_2$(at B)	=	0
$P_2 - S_1$(at C)	=	112
$P_2 - S_2$(at D)	=	58
Secondary layer to layer	=	140
Primary layer to layer	=	170
Stray and tube	=	50
Power amplifier r-f bypass	=	500
	Total =	1,322 $\mu\mu$f

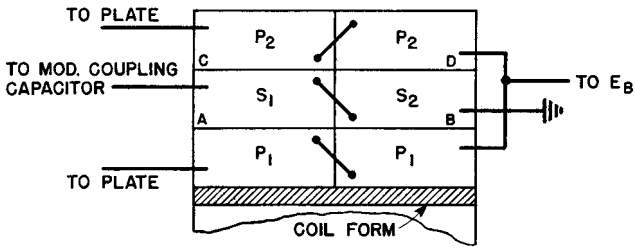

FIG. 158. Section of transformer coil wound for low layer voltage.

At high audio frequencies $f_r = 19{,}000$, $D = 0.6$, and Z/R_2 from Fig. 119 (p. 159) is 87 per cent at 5,000 cycles.

Example (*b*). *Audio Oscillator.*
Circuit of Fig. 152, with 6C5 tube, $E_B = 150$ volts, $E_C = -10$ volts.
Frequency 800 cycles.
Plate load impedance = 20,000 ohms.
Class B operation; grid swings to +2 volts.

$\Delta e_g = -12$ volts
$\Delta e_p = 150 - 35 = 115$ volts } during positive half-cycle.
$\Delta i_p = 5.6$ ma

Average power output = $(115 \times 5.6)/4 = 160$ mw.
Transformer voltage ratio $P/G = 115/12 = 81/8.5$ rms.
For low harmonic distortion, volt-amperes = 10 × tube output = 1.6 v-a.

$$X_c = \frac{(115 \times 0.707)^2}{1.6} = 4{,}140 \text{ ohms.}$$

$$C = \frac{1}{6.28 \times 800 \times 4{,}140} = 0.048 \ \mu\text{f.}$$

Plate $OCL = \dfrac{4{,}140}{6.28 \times 800} = 0.823$ henry.

Current in plate winding $= \frac{81}{4140} = 0.02$ amp.
Core is the same as in Example (*b*), Section 72.
Primary 2,100 turns No. 32 enamel. Winding resistance = 125 ohms.
Grid 250 turns No. 42 enamel. Winding resistance = 180 ohms.
$l_g = 0.060$ in., $l_c = 4.5$ in., $A_c = 0.32$ sq in., core weight = 0.4 lb.

$$B_{dc} = \frac{0.6 \times 2{,}100 \times 0.0056}{0.060 \times \pi} = 35 \text{ gauss.}$$

$$B_{ac} = \frac{3.49 \times 81 \times 10^6}{800 \times 0.32 \times 2{,}100} = 525 \text{ gauss.}$$

$$B_m = 560 \text{ gauss.} \quad (\text{From Fig. 70, } \mu_\Delta = 2{,}000.)$$

$$\text{Primary } OCL = \frac{3.2 \times (2{,}100)^2 \times 0.36 \times 10^{-2}}{0.060 + (4.5/2{,}000)} = 0.815 \text{ henry.}$$

From Fig. 140 core loss $= 0.2 \times 0.6 \times 0.4 = 0.048$ watt.
Gap loss $= 0.030$ watt.
Primary copper loss $= (0.02)^2 \times 125 = 0.05$ watt.
This leaves 32 mw available for secondary output.

Example (*c*). *Cathode Follower.* Assume that tubes 828 and 849 in Fig. 157 operate at $E_B = 1{,}700$ volts. With $E_c = -75$ and 700 watts output, 849 plate swing is 1,200, $E_{\min} = 500$, peak grid voltage $= +105$, and peak grid current is 0.090 amp. This is peak load for the 828 tube which can operate class AB1. The 828 tube plate swing is $1{,}200 + 180 = 1{,}380$, or $E_{\min} = 1{,}700 - 1{,}380 = 320$ volts, and the 828 peak load is $105/0.090 = 1{,}170$ ohms. The cathode choke of 828 and the grid chokes and capacitors of 849 should have $1.41 \times 1{,}170 = 1{,}650$ ohms reactance for 100 per cent modulation at frequency f_1. At 10 cycles this would be 27 henrys. Peak voltage across these chokes is the 828 plate swing.

7. HIGHER-FREQUENCY TRANSFORMERS

In Chapter 6 the influence of low-frequency performance on size was mentioned. If high transformer *OCL* is required to maintain good low-frequency response, many turns or a large core are necessary, either of which limits the high-frequency response. But if the amplifier frequency range is wholly composed of high frequencies, this limitation is in large part removed. For example, in a power-line carrier amplifier, the frequency range is 40 to 200 kc. It is then only necessary that *OCL* be high enough to effect good response at 40 kc. This is a great help in designing for proper response at 200 kc, and makes possible the use of laminated iron-core transformers for these and higher frequencies.

87. Iron-Core Transformers. At power-line carrier frequencies, the principles discussed in preceding sections for lower-frequency transformers apply. In terms of the mean frequency, the band is narrow,

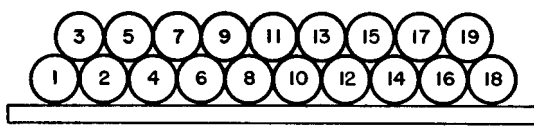

FIG. 159. Two-layer bank winding.

but at 40 kc the curves for low-frequency operation portray amplifier performance just as they do at 30 cycles. Likewise at 200 kc care must be used that the limiting factors of leakage inductance and winding capacitance do not interfere with proper operation.

In carrier frequency transmitters, transformers are normally used for coupling between stages and for coupling the output stage to the line. They sometimes transform a large amount of carrier power. Coils are usually wound in single layers, spaced well apart to reduce capacitance, and have but few turns. If the necessary turns cannot be wound in a single layer, a bank winding like that shown in Fig. 159 may be used. This winding has more capacitance than a single layer

but much less than two layers wound in the ordinary way. Since intrawinding layer-to-layer capacitance is zero in these transformers, the resonance frequency f_r is usually determined by winding-to-winding capacitance.

In high impedance circuits, the winding-to-winding capacitance may be reduced by winding "pies" or self-supporting vertical sections side by side. Pies are wound with one or more throws per turn and may be several turns wide. They have the general appearance of Fig. 160.[1] High, narrow core windows or several pies are desirable to re-

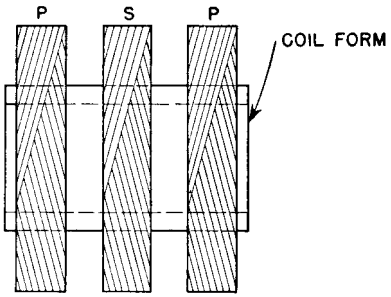

FIG. 160. Pie-section windings.

duce leakage inductance. Transformer loss is mostly core loss. Two-mil grain-oriented steel can be used advantageously in such transformers, because of its low losses and high permeability. In transmitter operation, class AB or class B amplifiers are commonly used, with or without modulation, which may be as high as 100 per cent. In a receiver, input and interstage transformers also are employed, mainly to obtain voltage gain or for isolation purposes. Similar transformers are used for line matching, especially where overhead lines are connected to underground cables. Line impedance changes abruptly, and transformers may be necessary for good power transfer.

Core data at these frequencies are usually not available except for a limited choice of materials and gages. Approximate loss for 2-mil oriented steel is given in Fig. 161. Interpolation or extrapolation from known data may be necessary to estimate core losses. In spite of this limitation, carrier frequency transformers are widely used. Some of the transformers in Fig. 16 operate in the carrier band. Core steel permeability decreases at high frequencies, depending on the

[1] See "Theory and Design of Progressive and Ordinary Universal Windings," by Myron Kantor, *Proc. I.R.E.*, December, 1947, p. 1563.

lamination thickness. Oriented steel and nickel alloys have high permeability at low frequencies, but, unless thin laminations are used, this advantage disappears at frequencies of 20 to 50 kc. The approximate decline for low induction is shown in Fig. 162. Decrease of permeability may be so rapid that *OCL* nearly decreases inversely as frequency with 0.014-in. and even 0.005-in. material.[1] Grain-oriented steel 0.002 in. thick is well suited to these frequencies.

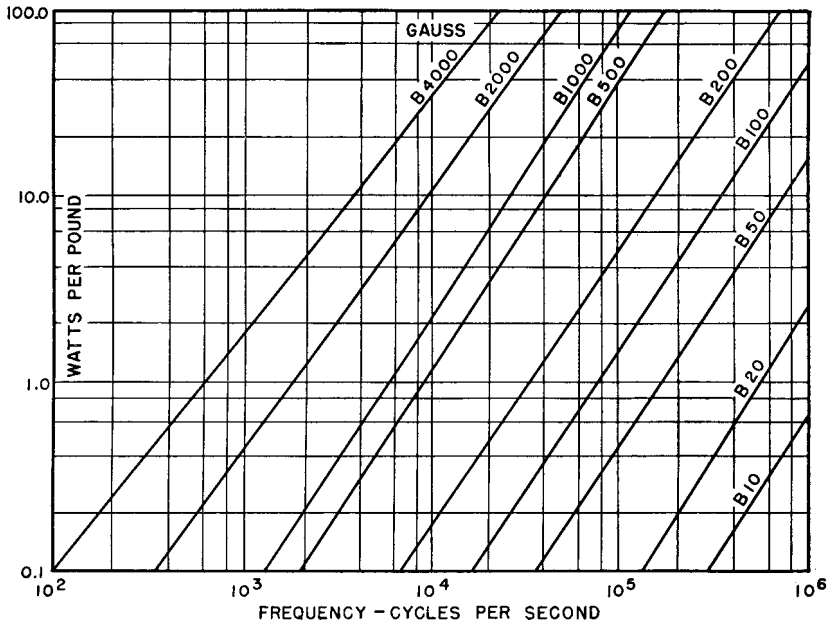

FIG. 161. Approximate loss for 2-mil steel at higher frequencies.

Transformers are used at still higher frequencies. Capacitance limits the upper frequency at which amplifier transformers may be operated. In a tuned circuit amplifier, the tuning includes the incidental and tube capacitance as well as the tank circuit capacitance. A transformer has no tuning to compensate for such capacitances. Even with zero winding capacitance there would be a frequency limit at which any tube could operate into an untuned transformer without

[1] For additional core-loss and permeability data at higher frequencies, see "The Variation of the Magnetic Properties of Ferromagnetic Laminae with Frequency," by C. Dannatt, *J.I.E.E., 79,* 667 (December, 1936).

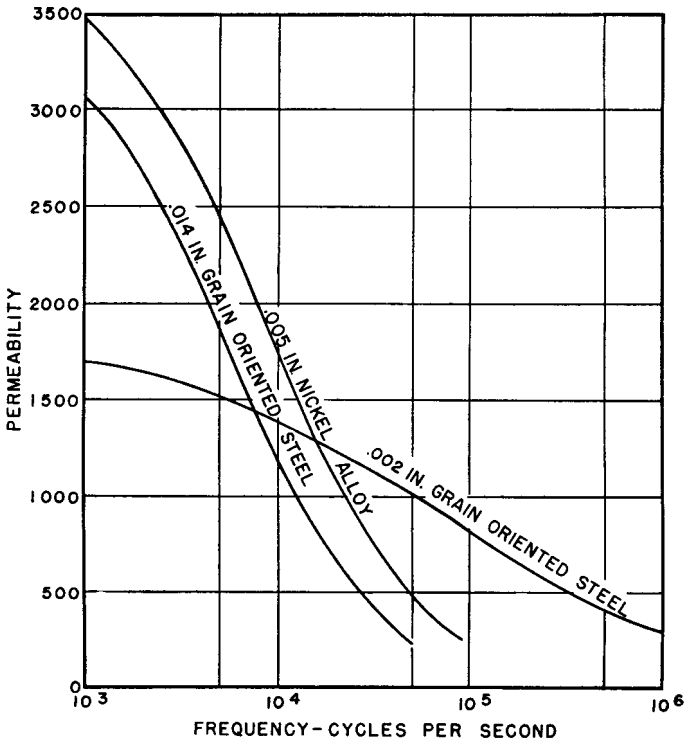

FIG. 162. Approximate permeabilities of core steels at higher frequencies.

spoiling its efficiency or other characteristics. The most favorable condition for the use of transformers at higher frequencies is low circuit impedance. With low leakage inductance and low impedance circuits, transformer operation is possible in the high- and very-high-frequency bands.

88. Other Core Materials. In the high radio-frequency bands, ferrite cores have the advantage of high resistivity and practically no eddy-current component of core loss. Several grades are manufactured commercially, usually mixtures of manganese, nickel, and zinc ferrites. Figure 163 is a set of normal permeability curves for different grades of ferrites, and Fig. 164 gives initial permeability. Usually the lower-permeability materials have lower loss at higher frequencies, so that permeability is an inverse indication of the relative frequencies at which ferrites are useful.

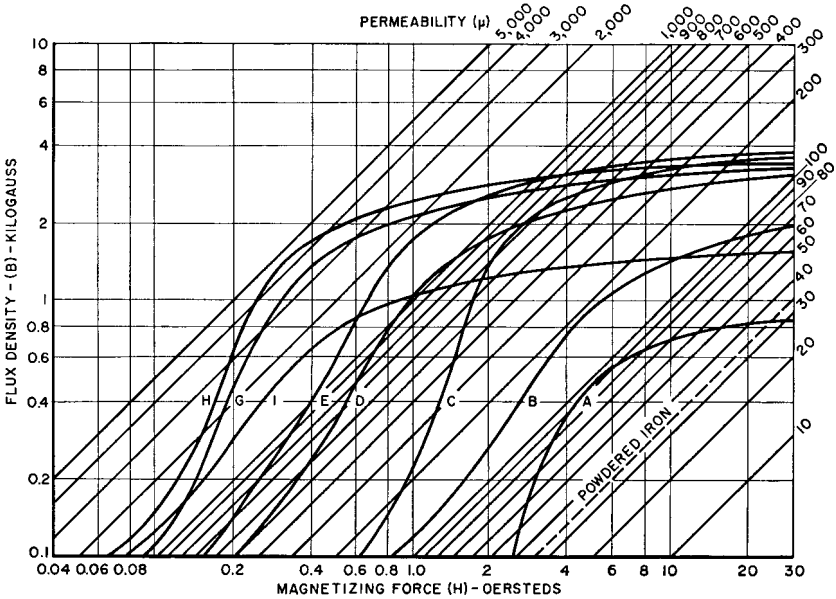

FIG. 163. Magnetic ferrite normal permeability.

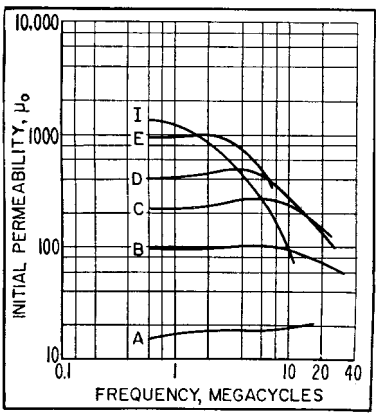

FIG. 164. Magnetic ferrite initial permeability.

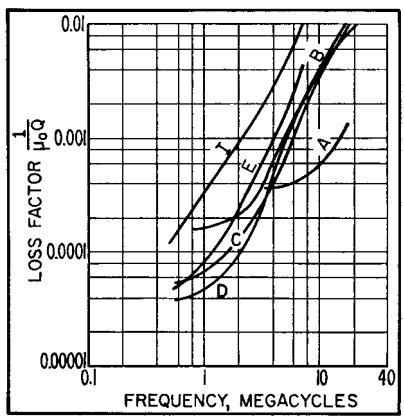

FIG. 165. Loss factor of ferrite cores.

Losses in ferrites are often related to the product $\mu_0 Q$. (See Fig. 165.) This relation is approximately as follows:

$$\frac{\text{Core loss}}{\text{in.}^3} = \frac{0.41 \times 10^{-6} f B^2}{\mu_0 Q} \tag{95}$$

Instead of $\mu_0 Q$, the quantity $R_{ser}/\mu f L$ is sometimes plotted, where R_{ser} is the equivalent *series* resistance corresponding to core loss. Equation 95 then becomes

$$\frac{\text{Core loss}}{\text{in.}^3} = 0.065 \times 10^{-6} f B^2 \left(\frac{R_{ser}}{\mu f L}\right) \tag{96}$$

At the lower radio frequencies, finely divided powdered iron has loss lower than some ferrites. Owens [1] gives 1.0 mc as the highest frequency for which this holds. Both ferrites and powdered iron have temperature limits far below that of strip-wound cores: ferrites because of low Curie temperature, and powdered iron because of possible damage to the bonding material. Powdered iron with certain bonds has the better temperature coefficient of permeability. Both materials are available in the forms shown in Fig. 144.

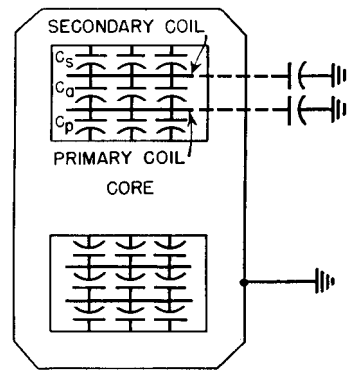

FIG. 166. Single-layer windings.

89. Capacitance Evaluation. In high-frequency transformers, the capacitances differ from those in audio transformers in that the windings are usually single layers, whose turn-to-turn capacitance is negligible compared to capacitance between windings and to the core. For example, in the transformer in Fig. 166, the primary and secondary are each wound in a single layer concentrically, in the same rotational direction, and in the same traverse direction (right to left). It will be assumed that the right ends of both windings are connected to ground (or core) through large capacitances, as shown dotted, so that the right ends are at substantially the same a-c potential. Primary capacitance C_1 is composed of many small incremental capacitances C_p, and secondary C_2 of many small incremental capacitances C_s, each of which has a different voltage across it. Likewise,

[1] See "Analysis of Measurements on Magnetic Ferrites," by C. D. Owens, *Proc. I.R.E., 41,* 360 (March, 1953).

many small incremental capacitances C_a exist between primary and secondary, which have different potentials across them. If the transformer is step-up,

$$C_1 = \frac{1}{3}\Sigma C_p \quad \text{and} \quad C_2 = \frac{1}{3}\left[\Sigma C_s + \frac{(N_s - N_p)^2}{N_s^2}\Sigma C_a\right] \tag{97}$$

If the transformer is step-down,

$$C_1 = \frac{1}{3}\left[\Sigma C_p + \frac{(N_p - N_s)^2}{N_p^2}\Sigma C_a\right] \quad \text{and} \quad C_2 = \frac{1}{3}\Sigma C_s \tag{98}$$

If the ratio is 1:1,

$$N_s = N_p, \quad C_1 = \tfrac{1}{3}\Sigma C_p \quad \text{and} \quad C_2 = \tfrac{1}{3}\Sigma C_s \tag{99}$$

For transformers with opposite angular rotations of primary and secondary windings, or with opposite traverse directions (but not both), minus signs in the factors $(N_p - N_s)^2/N_p^2$ and $(N_s - N_p)^2/N_s^2$ in equations 97 and 98 become positive; there is no other change. For transformers with both angular rotations and traverse directions opposite there is no change at all in these equations. If there is a shield between primary and secondary, omit terms containing C_a in these equations, and make ΣC_s and ΣC_p include the capacitance of secondary and primary to shield, respectively. ΣC_s is the measurable capacitance of the short-circuited secondary to core, and ΣC_p that of the short-circuited primary to core.

In push-pull amplifier transformers, the secondary winding is interleaved between two primary halves. The rotational directions of winding and traverse are important, as they affect not only effective capacitance but also plate-to-plate coupling. It is usually best to have all windings with the same rotational direction and traverse, and to connect the primary halves externally.

Winding resistance increases with frequency because of eddy currents in the larger wire sizes, and copper loss increases proportionately. Formulas for single-layer coils are given in handbooks.[1] Eddy-current resistance of layer-wound coils in deep open slots is plotted in Fig. 167 as a function of conductor thickness, frequency, and number of coil layers; it approximates the increase of winding resistance in a transformer.[2]

[1] See *Natl. Bur. Standards Circ.* 74, p. 304.

[2] See "Eddy-Current Resistance of Multilayer Coils," by T. H. Long, *Trans. AIEE, 64,* 716 (October, 1945).

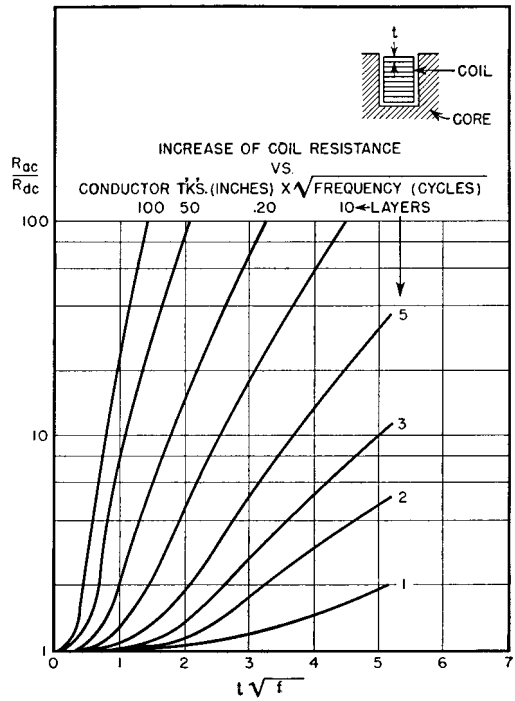

FIG. 167. Increase in coil resistance at high frequencies.

90. Example. *Line Matching Transformer 50 to 500 ohms.*

Frequency range 50 to 150 kc.
Power output 100 watts.
Primary voltage = $\sqrt{ZW} = \sqrt{50 \times 100} = 70.7$ volts.
Secondary voltage = $\sqrt{500 \times 100} = 224$ volts.
Core 2-mil oriented silicon steel.
$A_c = 0.45$ sq in., $l_c = 6$ in., $l_g = 0.002$ in. (incidental), core weight ¾ lb.
Window ⅝ in. × 1½ in.
Primary 31 turns No. 22 wire. Mean turn 3.8 in.
Secondary 100 turns No. 30 wire. Mean turn 4.6 in.
Windings arranged as in Fig. 166.
Insulation between primary and core, and between secondary and primary ⅛ in. of organic material.
Secondary effective capacitance 40 $\mu\mu$f.
$B_m = 350$ gauss.
Secondary $OCL = 20$ mh.
Secondary leakage inductance = 260 μh.

Core loss = 8 watts per lb $\times$ 0.75 = 6 watts. This is practically the only loss.

X_N/R_1 at 50 kc = (6.28 $\times$ 50,000 $\times$ 0.020)/500 = 12.56.

f_r = 1,560 kc. B = 5.00.

According to Figs. 108 and 109, this transformer has nearly flat response over the entire range.

91. Leakage Inductance at High Frequencies. Provided that a transformer is operated at frequencies below resonance, the leakage inductance measured at low frequencies governs response at high frequencies. Leakage inductance in concentric windings is lowest if the windings are symmetrically spaced in the traverse direction, as in Fig. 168(a). For a given number of turns, the leakage flux is least in Fig. 166, somewhat greater in Fig. 168(a), and much greater in Fig. 168(b). The increase in leakage flux is a function of core dimensions, winding-to-winding spacing, and margin inequality. Figure 169 shows typical increase of leakage inductance when one secondary margin is increased with respect to the other, as in Fig. 168(b).

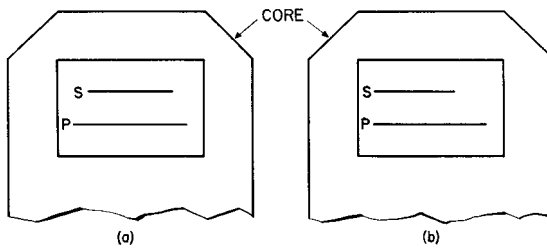

FIG. 168. (a) Symmetrical and (b) asymmetrical spacing of concentric windings.

Leakage inductance is very low in toroids with windings which cover the whole magnetic path. Toroids are wound on special machines which thread wire in and out of the core. Carefully wound toroidal transformers function at very high frequencies.[1] If part of the core is not covered by the windings, as indicated by dimension G in Fig. 170, leakage flux sprays out of the ends of the coils and reduces the frequency range.

92. Wide-Band Transformers. Untuned transformers operate in all frequency ranges from 0 to VHF. The lowest operating frequency is a

[1] See "Very-Wide Band Radio-Frequency Transformers," by D. Maurice and R. H. Minns, *Wireless Engr., 24,* 168 (June, 1947).

fraction of 1 cycle. The highest frequency is in the VHF band, somewhere around 150 megacycles. No known transformer covers this whole range at present. Television coaxial-line terminating trans-

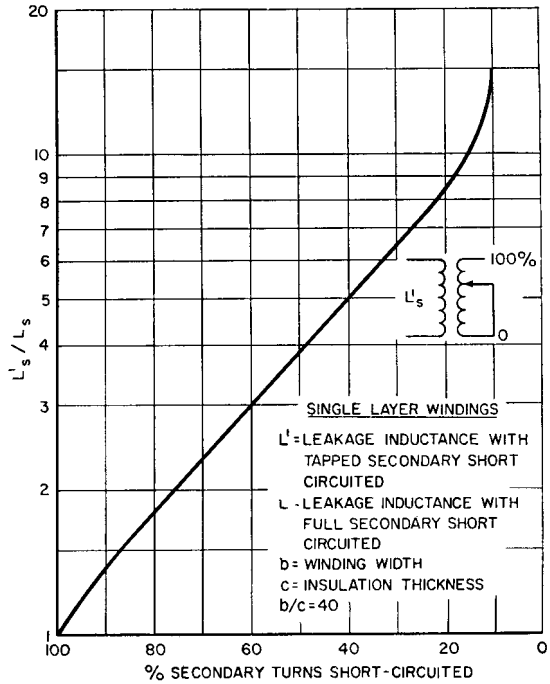

FIG. 169. Leakage inductance of asymmetrical windings.

formers have been made to cover the frequency range of 50 cycles to 6,000,000 cycles, or a ratio of highest to lowest frequency of over 100,000:1. This is an exceptionally wide band. More common wideband transformers are those in the audio band of 20 to 20,000 cycles, or 10 to 30,000 cycles, that is, with about a 3,000:1 frequency ratio. Often, transformers used at frequencies on the order of 100 megacycles are for relatively narrow bands, say 20 to 60 megacycles wide.

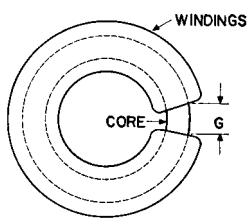

FIG. 170. Toroidal core and coil.

In low-impedance circuits, it is leakage inductance that determines transformer behavior, whereas at high impedance it is winding capacitance. In most audio transformers the coupling

coefficient is 0.9995 or higher. With bifilar windings, this figure may increase to 0.999995.[1] Such a high coefficient of coupling requires the use of good core materials. *For a given source impedance and transformer core material, the product of turns ratio and band width is a rough indication of size.* Quite generally, for low power the widest-band transformers are made of Permalloy or Supermalloy.

In high-impedance circuits the matter of size is not merely one of space for mounting; it also has a direct bearing on the upper frequency limit, since transformer capacitance is roughly proportional to size. If capacitance is low, the band-width ratio (highest/lowest frequency) is approximately equal to the ratio of OCL/leakage inductance. This may be verified by comparing Figs. 108 and 109. It is most nearly true for low-impedance transformers. With given primary impedance, core size, and material, there is a limit to the step-up turns ratio possible for any specified frequency response.

93. Air-Core Transformers. Transformers considered hitherto have had iron or ferrite cores. A class of transformers is widely used in radio-frequency circuits without cores or with small slugs of powdered iron. In a transformer with an iron core, the exciting current required for inducing the secondary voltage is a small percentage of the load component of current. In an air-core transformer *all* the current is exciting current and induces a secondary voltage proportional to the mutual inductance.

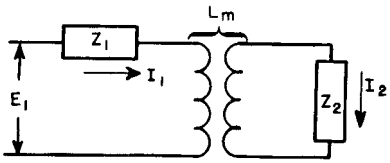

FIG. 171. General case of inductive coupling.

Consider the circuit of Fig. 171 in which Z_1 is complex and includes the self-inductance of the primary coil. Likewise, secondary impedance Z_2 is complex and includes the self-inductance of the secondary coil. With a sinusoidal voltage applied, Kirchhoff's laws give the following:

$$E_1 = Z_1 I_1 + j\omega L_m I_2 \tag{100}$$

$$0 = Z_2 I_2 + j\omega L_m I_1 \tag{101}$$

where $\omega = 2\pi$ times operating frequency, and L_m is the mutual inductance between the primary and secondary coils.

From equation 101 we see that the voltage in the secondary coil is

[1] See "New 50-Watt Amplifier Circuit," by F. H. McIntosh and Gordon J. Gow, *Audio Engineering,* December, 1949, p. 9.

numerically equal to $\omega L_m I_1$, the product of primary current and mutual reactance at the frequency of applied voltage E_1. The equivalent impedance of the circuit of Fig. 171 when referred to the primary side is given by

$$Z' = Z_1 + (X_M{}^2/Z_2) \tag{102}$$

where $X_M = j\omega L_m$.

In the above formulas, the impedances Z_1, Z_2, and Z' are complex quantities whose real and imaginary terms depend upon the values of resistance, inductance, and capacitance in the circuit. One common practical case arises when the primary resistance is zero, or virtually zero, and the secondary coil is tuned to resonance so that Z_2 is a pure resistance R_2. Under these conditions, equation 102 reduces to

$$R' = X_M{}^2/R_2 \tag{103}$$

where R' is the equivalent resistance in the primary.

Equation 103 gives the value of mutual inductance required for coupling a resistance R_2 so that it will appear like resistance R' with a maximum power transfer between the two coils, and states that the mutual reactance X_M is the geometric mean between the two values of resistance.

The ratio of mutual inductance to the geometric mean of the primary and secondary self-inductances is the coupling coefficient:

$$k = L_m/\sqrt{L_1 L_2} \tag{104}$$

The value of k is never greater than unity, even when coils are interleaved to the maximum possible extent. Values of k down to 0.01 or lower are common at high frequencies.

Coupling coefficient is related to untuned transformer open- and short-circuit reactance by means of the transformer equivalent circuit shown in Fig. 107(*a*), p. 147. Assume that the transformer has a 1:1 ratio, and leakage inductance is equally divided between primary and secondary windings. Then if L_1 and L_2 are the self-inductances of primary and secondary, respectively, L_s is the total leakage inductance (measured in the primary with secondary short-circuited), and L_m the mutual inductance,

$$L_1 = \frac{X_P + X_N}{2\pi f} = \frac{L_s}{2} + L_m$$

$$L_2 = \frac{X_S + X_N}{2\pi f} = \frac{L_s}{2} + L_m$$

From equation 104,

$$k = \frac{L_m}{\sqrt{L_1 L_2}} = \frac{L_m}{\sqrt{\left(L_m + \frac{L_s}{2}\right)^2}}$$

$$= \frac{1}{1 + (L_s/2L_m)} \tag{104a}$$

If $L_m \gg L_s$,

$$k \approx 1 - \frac{L_s}{2L_m} \tag{104b}$$

Equations 104(a) and (b) are useful in estimating approximate transformer band width.

A tuned air-core transformer often used in receivers is shown in Fig. 172. Here a sinusoidal voltage E_1 may be impressed on the pri-

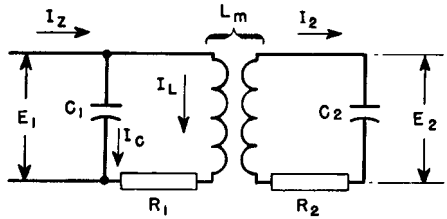

FIG. 172. Tuned air-core transformer.

mary circuit by a vacuum tube amplifier. Resistances R_1 and R_2 are usually the inevitable resistance of coils, but occasionally resistance is added to change the circuit response. The value of voltage E_2 obtained from this circuit depends on the impressed frequency; in Fig. 173 it is shown for resonance at three different values of coupling. If the value of coupling is such that

$$X_M = \sqrt{R_1 R_2}$$

we obtain a condition similar to that of equation 103, in which the maximum power or current is produced in the secondary circuit. Maximum current through condenser C_2 gives maximum voltage E_2. This value of coupling is known as the critical value. Smaller coefficient of coupling gives a smaller maximum value of E_2. Greater coefficient of coupling results in a "double hump" as shown in Fig. 173. The heights of resonant peaks and frequency distance between peaks de-

pend upon circuit Q and coefficient of coupling k. The double hump curve of Fig. 173 is desirable because, with modulated waves, frequencies in adjacent channels are rejected; yet very little attenuation is offered to audio frequencies which effectively add or subtract from the carrier frequency normally corresponding to resonance. Close tuning control and high Q are essential to good response and selectivity.

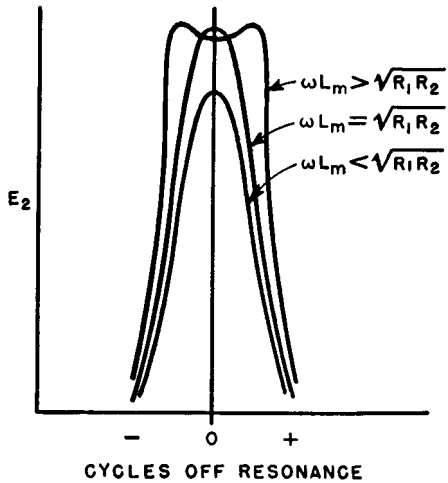

FIG. 173. Response curves for circuit of Fig. 172.

If the primary circuit is made to resonate at a different frequency from the secondary, audio response is much worse, and considerable distortion is likely. Moreover, the response at mean frequency is less than it would be if the circuits were properly tuned. Air-core transformers are usually made adjustable for tuning and coupling.

94. Multiple-Tuned Circuits. Double hump resonance was obtained with higher-than-critical coupling in the circuit of Fig. 172. Frequency response with more humps is obtainable if there are more than two coupled loops. Such circuits are more difficult to tune and adjust than the circuit of Fig. 172 because of the reaction of each coupled loop on the others. Easier adjustment can be made with successive "stagger-tuned" band-pass amplifiers. Each amplifier stage is tuned to a slightly different frequency. Because of the isolation of the stages by the associated tubes, tuning one stage does not influence the tuning of another.

Frequency response similar to that of multiple-tuned coupled cir-

cuits may be obtained by iterative ladder filter sections. In other words, it does not matter whether the coupling is inductive or capacitive; the same shape of response is obtained from the same number of circuits tuned in the same manner. Since similar results are obtained from coupled circuits and filters, the choice between them may be made on the basis of convenience or cost. Considerable literature has accumulated concerning the design and adjustment of multiple-tuned circuits, and special techniques have been developed for tuning them.[1]

95. Mutual Inductance. It is evident from equation 101 that the secondary voltage depends upon the mutual inductance between the coils. Mutual inductance can be calculated by formulas which depend upon the geometric configuration of the coils. If the coils are arranged

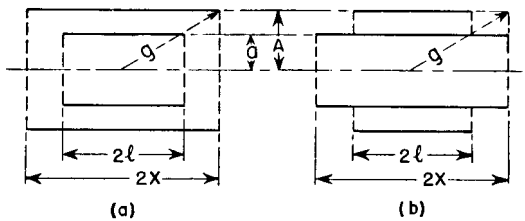

FIG. 174. Concentric coaxial coupled coils.

concentrically, as shown in either (*a*) or (*b*) of Fig. 174, the mutual inductance of the coils can be found from

$$L_m = \frac{0.05a^2N_1N_2}{g}\left[1 + \frac{A^2a^2}{8g^4}\left(3 - 4\frac{l^2}{a^2}\right)\right] \quad \mu\text{h} \qquad (105)$$

where N_1 = primary turns and N_2 = secondary turns. All dimensions are in inches. For most purposes, the bracketed portion of this formula is approximately unity, and it has been plotted in Fig. 175 for a single-turn secondary. To find the mutual inductance for any given number of secondary turns, multiply the mutual inductance found from this curve by the number of secondary turns. The range of ordinates and abscissas can be extended indefinitely.

If the coils are arranged coaxially as in Fig. 176, approximate values of mutual inductance are found as follows:

[1] See "Alignment and Adjustment of Synchronously Tuned Multiple Resonant Circuit Filters," by M. Dishal, *Proc. I.R.E., 39,* 1448 (November, 1951).

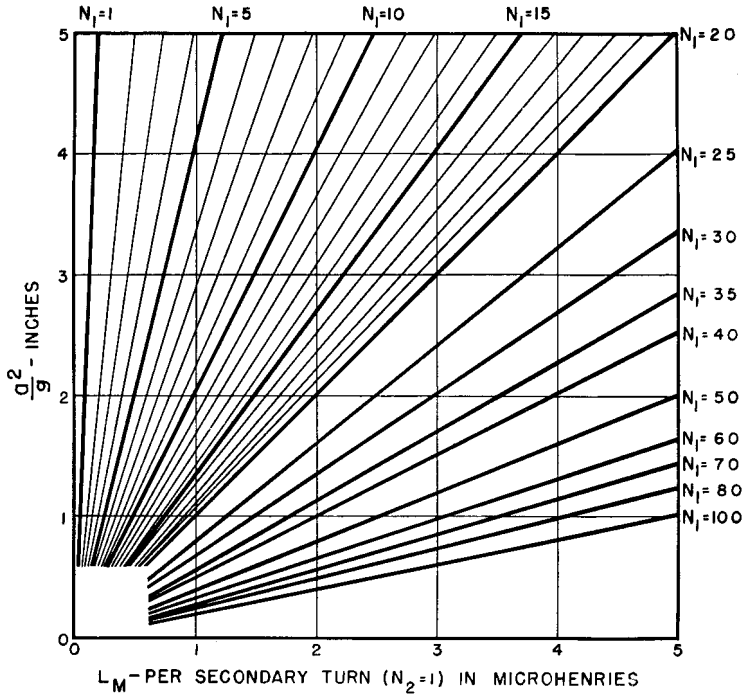

FIG. 175. Mutual inductance of coils in Fig. 174.

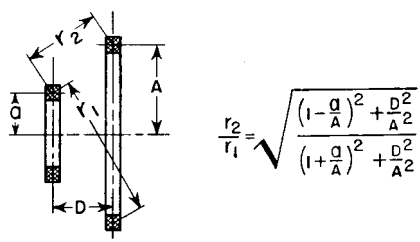

FIG. 176. Coaxial non-concentric coils with rectangular sections.

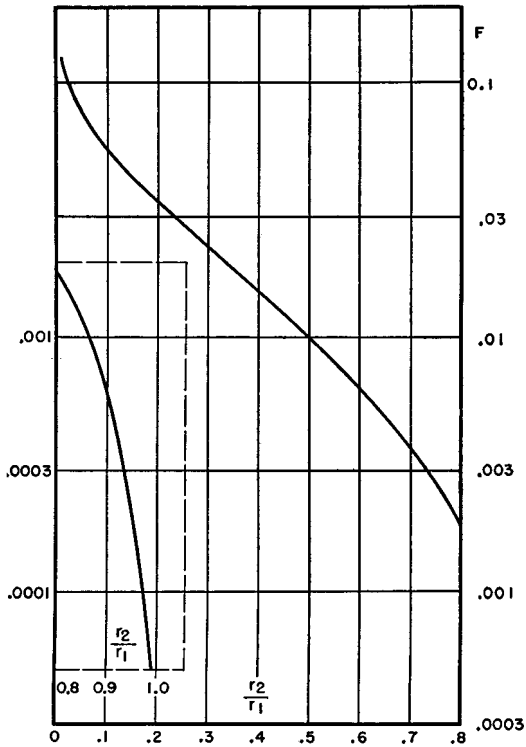

FIG. 177. Factor F in equation 106 as a function of r_2/r_1 (see Fig. 176).

$$L_m = FN_1N_2\sqrt{Aa} \tag{106}$$

In this formula all dimensions are in inches and the mutual inductance is in microhenrys. The factor F can be conveniently found in Fig. 177.

Self-inductance of single-layer coils is

$$L = \frac{0.1a^2N^2K}{l} \tag{107}$$

where a = mean coil radius in inches
N = number of turns
l = length of coil in inches
L = inductance in microhenrys
K may be found from Fig. 178.

Equations 105, 106, and 107 are based on equations 192, 187, and 153 in *Natl. Bur. Standards Circ.* 74.

Receiver intermediate-frequency tuned transformers generally have coaxial coils. If the wire is more than 0.005 in. in diameter, it is commonly subdivided into several strands in the type of cable known as Litzendraht, to reduce losses and increase Q. In transmitters, the size of the coils becomes much larger, and concentric coils are employed. The wire used is Litzendraht at 600 kc or lower frequency, and may

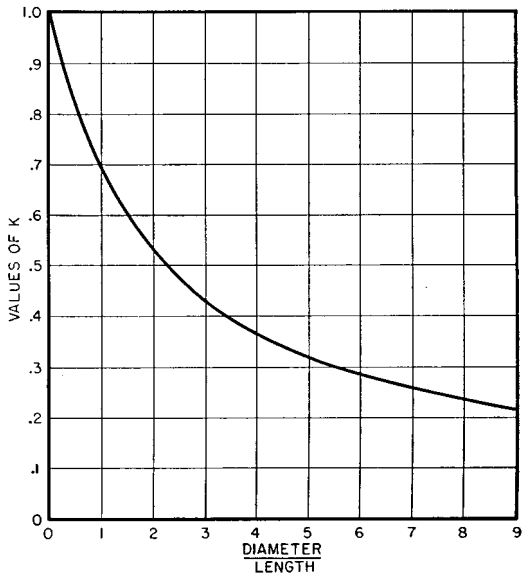

FIG. 178. Factor K in equation 107.

contain many strands for carrying heavy currents. At higher frequencies the wire is of solid or tubular section.

96. Powdered-Iron Slugs. Both self-inductances and mutual inductances of a coil may be increased by inserting a slug of powdered iron inside the coil tube. Tuning a coil to a given frequency is often effected in this manner with fixed capacitors instead of tuning with variable capacitors. Such a coil is shown in Fig. 179, with the powdered-iron core hidden by the coil form. At the left end is the screw and lock by which the inductance can be adjusted and maintained at a given value. The mutual inductance of a pair of coils can be changed similarly. This is preferable to attempting to vary the distance between the coils, since it requires no flexible connections. Powdered iron is available in several grades, from ordinary powdered iron to

powdered nickel alloy. Insulating compound reduces the permeability of the core to values ranging from 10 to 125, depending on the grade of iron and the frequency. In a given coil, the insertion of a powdered-iron slug raises the inductance from 2 to 3 times the value which it would have if no iron were present. Circuit Q increases similarly. Higher Q results from a powdered iron or ferrite magnetic path, closed except for small air gaps. For an untuned transformer, where high Q is not essential, the air gap may be zero to reduce magnetizing current.

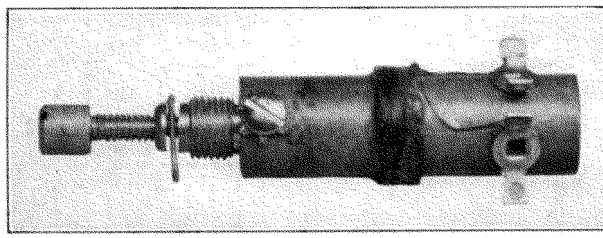

FIG. 179. Coil inductance is varied by powdered-iron slug.

97. R-F Chokes. When a choke is used to pass direct current and present high impedance to radio frequencies, it may have high r-f voltage across it. High choke impedance at operating frequency is necessary to avoid loss of r-f current which reduces the useful power and overheats the choke. If a single-layer choke is connected to an r-f generator at a given voltage, and if its current is measured as in Fig. 180, the choke impedance is the ratio of voltage to current measured.

By disconnecting the choke from the circuit, the tuning reaction may be noted, and from this whether the reactance of the choke is inductive or capacitive. The difference in watts input to the generator, when the coil is removed and the tank condenser is retuned for minimum plate current, is readily observable. This difference times the generator efficiency is the loss in the coil at a particular voltage and frequency.

The impedance of a typical coil, found as described above, is plotted in Fig. 180 against frequency. At low frequencies (a), the curve follows straight reactance line $X_L(=2\pi fL)$. At a frequency somewhat below natural frequency b (determined by the choke inductance and effective capacitance), the slope starts to increase and reaches a maximum point at a frequency c of $1.2b$ to $1.7b$. Above this frequency, the

impedance decreases until a minimum value is reached at *d*, which is from 2.2 to 3.0 times *b*. At higher frequencies, the increase and decrease are repeated in a series of peaks and valleys at approximately equal frequency intervals. The second, fourth, and sixth peaks are of

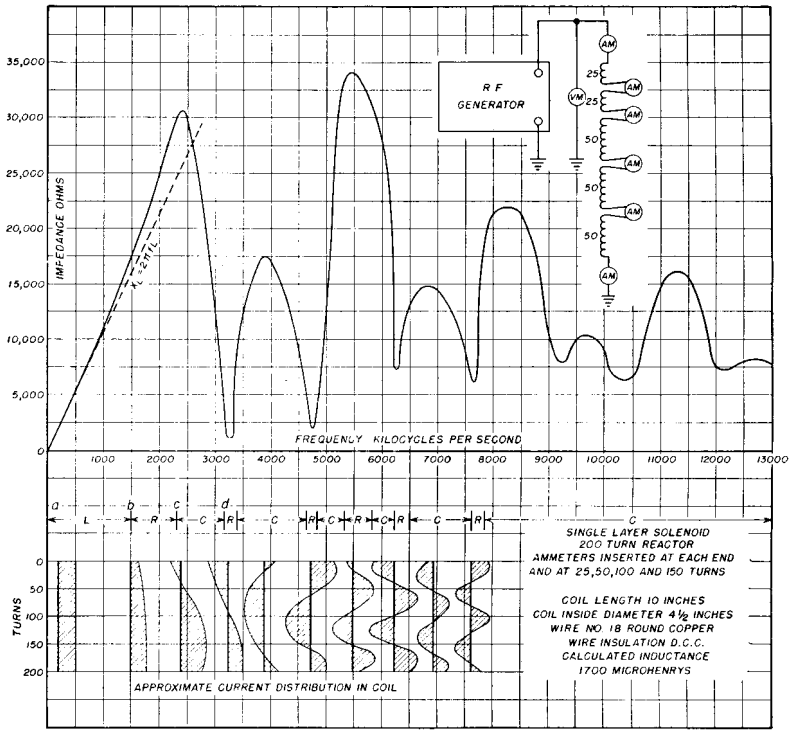

FIG. 180. R-f choke impedance.

lower value than the first, third, and fifth, respectively. The seventh peak is followed by a flattened slope which suggests a submerged eighth peak. The points of minimum impedance rise in value, so that at higher frequencies the valleys appear to be partly filled in and the peaks to be level off. The watts loss are high at points of low impedance, and they rise sharply at the frequency *d*.

The change in reactance is shown in Fig. 180. The coil is inductive up to frequency *b*. From *b* to *c* it has no noticeable effect on the tuning and hence is pure resistance, or nearly so. Above *c* it is capacitive up to a frequency slightly below *d*, where it again becomes of indefinite

reactance. Thereafter, it is capacitive, except for brief frequency intervals, where it is resistive, or only slightly inductive. At all frequencies higher than the fifth peak, the coil is capacitive.

Since a coil has distributed constants it is subject to standing waves at the higher frequencies. The character of these waves may be found by tapping the coil at various points and inserting thermogalvanometers in series with the coil at these points. The current distribution is plotted in Fig. 180 against coil length. These diagrams show the kind of standing waves as the frequency increases.

Current distribution is uniform at all frequencies below b. Most chokes are used within the first impedance peak. The useful range for choke impedance of 20,000 ohms in Fig. 180 is 1,700 to 2,800 kc. This choke could be operated at 5,500 kc safely also, but the frequency range is narrower. Also, the safe loss dissipation is less because it takes place over half of the coil surface. Pie-section chokes have similar impedance curves, but impedance peaks following the first are less pronounced.

98. Large Power Coupling Coils. In the tank circuits of large power amplifiers, the coupling coils are arranged to couple the antenna to the power amplifier, and the equivalent circuit is like that of Fig. 172. Optimum coupling between tank and antenna circuits is given by equation 103. The construction of the coupling coil itself is usually similar to that of Fig. 174(b), with the coupling coil on the outside and spaced from the main tank coil to reduce capacitive coupling. Taps are provided on the coupling coil for frequency and antenna resistance adjustments.

When the secondary circuit is untuned, and the secondary load is reactive, all the secondary volt-amperes (which may exceed the secondary watts many times) flow through the transformer windings. It is then necessary that tight coupling be used between primary and secondary in order to prevent loss of power, due to current circulating in the primary without corresponding current flowing in the load. If the load power factor is less than 20 per cent, currents and volt-amperes in the circuit may be considered independent of the winding and load resistances. In Fig. 171, let the load Z_2 be inductive, comprising L_3 and R_L. Also let

$R_1 = 0$
L_1 = primary self-inductance
L_2 = secondary self-inductance
L_m = mutual inductance
k = coefficient of coupling = $L_m/\sqrt{L_1 L_2}$

Then the secondary volt-amperes $= I_2^2 Z_2$, and primary volt-amperes $= E_1 I_1$. The ratio of maximum secondary volt-amperes transformed to the primary volt-amperes is related to k as follows:

$$\left(\frac{I_2^2 Z_2}{E_1 I_1}\right)_{\max} = \frac{k^2}{2(1 + \sqrt{1 - k^2}) - k^2} \tag{108}$$

This equation is plotted, together with values of ratio L_3/L_2 for maximum power transfer, in Fig. 181. If perfect coupling could be attained,

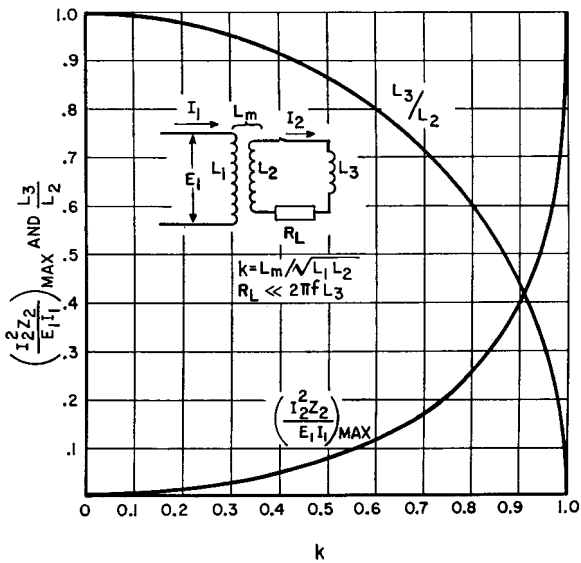

FIG. 181. Effect of coupling on maximum volt-amperes in untuned load.

all the primary volt-amperes could be transferred to the load. Iron-core transformers operate at the extreme right of Fig. 181. With air-core transformers it is often difficult to approach this condition, especially if voltages are high.

99. High-Frequency Power Supplies. In cathode-ray tubes for oscilloscopes or television receivers, high-voltage low-current sources of d-c power are needed for the accelerating anodes. Voltages range from 1 to 30 kv, and currents are on the order of 1 ma down to 1 μa.

Because of the many turns of wire required in high-voltage 60-cycle transformers, high-frequency power supplies are often used. A tetrode or pentode tube is used in a double-tuned circuit as shown in

Fig. 182. Here the plate circuit is tuned by means of elements $L_1 - C_1$, and the load circuit by means of $L_2 - C_2$. The grid winding is coupled from L_1. The coupling between L_1 and L_2 is usually higher than critical, so that changes in load do not affect the resonant frequencies, but instead vary the relative height of the two humps.

In general, the transformer represented by inductances L_1 and L_2

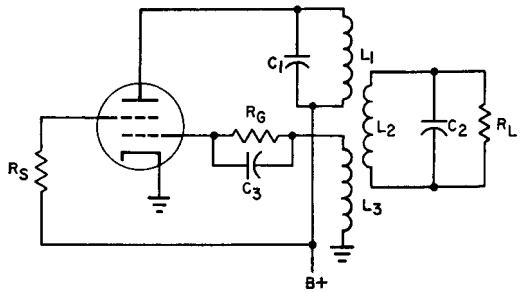

FIG. 182. R-f power supply.

is step-up. Load R_L may be a voltage doubler, tripler, or quadrupler, depending on the voltage needed from the oscillator.[1]

Frequencies used in such power supplies range from audio to medium high radio frequency. The oscillator is usually operated class B or C; loaded Q (or ratio of volt-amperes to watts) ranges from 10 to 20. Lower values of Q result in oscillator instability with load changes.

With ferrite cores, departures from the overcoupled case are feasible. Frequency is usually lower than with air-core transformers. The core itself affords a certain amount of load to the circuit and therefore results in better voltage regulation from load-on to load-off conditions. The single-tuned oscillator of Fig. 152 then becomes practical.

[1] See "Radio-Frequency-Operated High-Voltage Supplies for Cathode-Ray Tubes," by O. H. Schade, *Proc. I.R.E., 31,* 158 (April, 1943).

8. ELECTRONIC CONTROL TRANSFORMERS

Electronic devices are used to control speed, voltage, and current, or may require control of these quantities. Most of the circuits can be grouped into a few basic types. This chapter comprises typical circuits which use transformers and reactors.

100. Electronic Control Circuits. Vacuum-tube control circuits are used for amplification of the input voltage, not always at a single

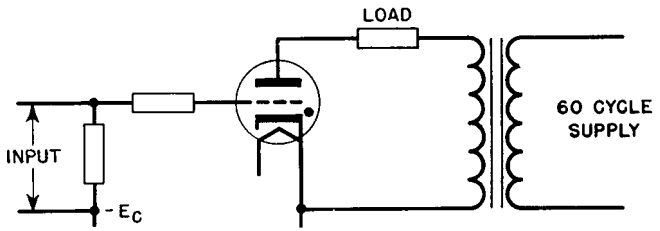

FIG. 183. Basic thyratron circuit.

frequency. With thyratrons the input voltage triggers the tube, which then allows current to flow into the controlled circuit, but the output wave may not resemble the input wave, as is described below.

A simple circuit for thyratrons operated with alternating anode supply and resistive load is shown in Fig. 183.[1] During that part of each cycle when the anode is positive with respect to the cathode, the tube conducts current which passes through the load, provided that the grid is at the right potential. In Fig. 184 is shown the positive anode voltage for a half-cycle, with the

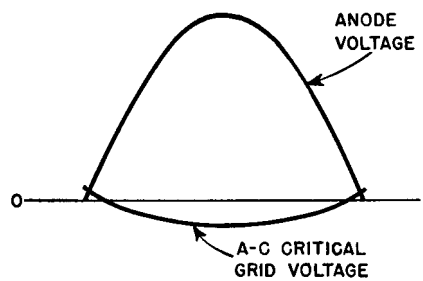

FIG. 184. Anode and critical voltages in basic thyratron circuit.

[1] See *Industrial Electronics,* by F. H. Gulliksen and E. H. Vedder, John Wiley & Sons, New York, 1935, p. 45.

corresponding critical grid voltage. Any value of grid voltage higher than this critical value will permit the tube to conduct. Once tube conduction is started, change of grid voltage to a value less than criti-

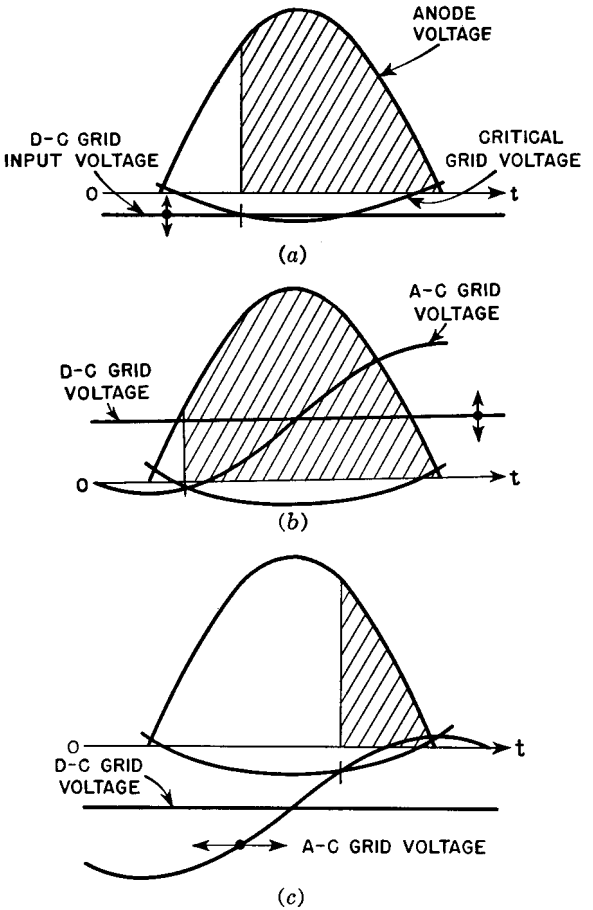

FIG. 185. Grid control of a thyratron tube with (*a*) variable d-c grid voltage, (*b*) variable d-c grid voltage with superposed a-c grid voltage, (*c*) fixed d-c grid voltage with superposed a-c grid voltage of variable phase position.

cal will not stop conduction. Conduction does stop, however, at the end of the half-cycle, or when the anode voltage falls to zero. Three methods of controlling the load current are shown in Fig. 185. Figure 185(*a*) shows how direct voltage applied to the grid permits conduction through the tube over the shaded portion of the cycle. Minimum con-

trollable current is half that which would flow if the tube were free to conduct over the entire positive half-cycle. This method of control is not precise, especially near the half-power point, because a small difference in d-c input control voltage produces a comparatively large change in conduction angle or may cause the tube to fail to fire altogether.

Figure 185(*b*) shows a more satisfactory method of amplitude control. The grid is maintained at a positive d-c potential, and an alternating voltage is superposed on it which lags the anode voltage by 90°. Varying the magnitude of the d-c grid voltage shifts the zero axis of the a-c wave up or down, and intersects the critical a-c grid voltage at different points of the cycle. Tube current can then be varied from zero to maximum. Close control of the tube current can be obtained because the grid voltage wave intersects the critical curve at a large angle.

In Fig. 185(*c*) another method is shown. The phase of a superposed alternating voltage is shifted upon a negative d-c bias which is more negative than the critical characteristic. Changing the phase position of the a-c grid voltage varies the tube current from zero to maximum. The phase position of the grid voltage can be shifted by several methods, one of which is discussed in Section 101.

The anode supply transformer carries load direct current. Core saturation may be prevented by an air gap; heating and regulation in the primary winding due to excitation current govern the length of air gap. Ordinarily, permissible maximum induction may be higher than in a single-side amplifier transformer because impedance or frequency response considerations are irrelevant with a 60-cycle supply line. Excitation current may be comparable in magnitude to load current. However, there is this difference: with a resistive load, current flows only during the positive half-cycle, whereas magnetizing current flows during the whole cycle. Secondary current is a series of pulses, the maximum width of which is 180°. The rms value of these pulses is half the peak amplitude, and this is the current which governs secondary wire size. Rms secondary voltage is 2.22 times maximum d-c load voltage, as in a single-phase half-wave rectifier. Design of the transformer is similar to the anode transformers in Chapter 3, except for the higher induction and current wave form.

Full-wave circuits [1] operate with two thyratrons and a center-tapped transformer in which the net d-c flux is zero. The design of the anode transformer is described in Section 102.

[1] See Gulliksen and Vedder, *op. cit.*, p. 54.

101. Grid-Controlled Rectifiers. The basic a-c grid control circuit described in the last section may be extended to more than one tube and may control large amounts of power. Any of the rectifier circuits of Table VII (p. 62) may be used with grid control of output voltage, which supplants the older practice of using induction regulators in the supply lines.

Smooth control of rectifier d-c voltage under load conditions is possible through the use of thyratrons or ignitrons with phase-shift control of the grid or igniter. Stable control of filtered output is possible only with choke input filters. In Chapter 4 the regulation of a rectifier is shown to be lowest if the input choke has inductance greater than critical value. With grid control, if the filter choke inductance is great enough, the tube conducts even after the anode reaches zero. The tendency of current to stop at voltage zero builds up voltage across the filter choke in such a direction that cathode potential is less than zero after the anode reaches zero. Thus conduction in the tube is maintained until the next tube fires. If the choke inductance is less than critical, tube current wave is discontinuous, regulation is poor, transient surges and oscillations in the output voltage occur, and control is unstable.

For a single-phase full-wave rectifier with grid control, the direct voltage output decreases as shown by curve I in Fig. 186. Critical value of inductance increases with firing angle and so does ripple voltage as shown by curves II and III in this figure. For a three-phase full-wave rectifier, the direct output voltage is approximately 41 per cent greater than the single-phase values shown in Fig. 186, and the critical value of choke reactance less filter capacitor reactance is approximately one-tenth of the single-phase values over the range of 20° to 90° firing angle. At 90° firing angle, the d-c output always is zero. Voltage across the choke reverses in sign but does not increase in magnitude even with the maximum angle of 90°. Therefore the maximum voltage from choke to ground is not changed, and the design of a reactor for this type of rectifier is the same as for a rectifier without grid control, except for the value of inductance.

Choke-input filters can be used to maintain continuous current flow in single-phase half-wave rectifiers. Although the output voltage is reduced, as mentioned in Chapter 3, this combination is occasionally useful.[1]

[1] For general calculation of discontinuous waves, see "Voltage and Current Relations for Controlled Rectification with Inductive and Generative Loads," by K. P. Puchlowski, *Trans. AIEE, 64,* 255 (May, 1945). For theory of controlled

Grid-controlled rectifiers have more irregular current wave forms and therefore more pronounced a-c line harmonics than ordinary rectifiers.[1]

Two methods of providing phase shift control of a constant amplitude a-c grid voltage for grid-controlled rectifiers are shown in Fig. 187. In

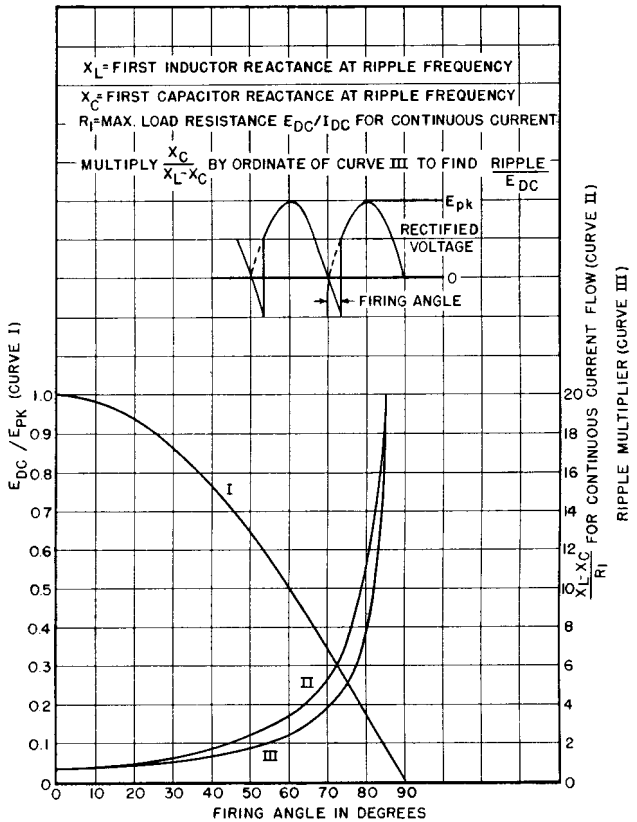

FIG. 186. Output voltage, ripple, and current continuity in single-phase full-wave grid-controlled rectifier.

(*a*) a small value of resistance R effectively connects the upper grid circuit terminal to the left-hand terminal of the supply transformer, and a large value of R shifts it nearer to the right-hand terminal of the

rectifiers, see "Critical Inductance and Control Rectifiers," by W. P. Overbeck, *Proc. I.R.E.*, *27*, 655 (October, 1939).

[1] See "Harmonics in A-C Circuits of Grid-Controlled Rectifiers and Inverters," by R. D. Evans and H. N. Muller, Jr., *Trans. AIEE*, *58*, 861 (1939).

supply transformer. If the supply transformer is center-tapped, the vector diagram of Fig. 188 shows the phase position of the grid voltage E_g in solid lines for a small value of R, and in dotted lines for a large value of R. Varying the rheostat R thus varies the rectifier output from full voltage to a low voltage.

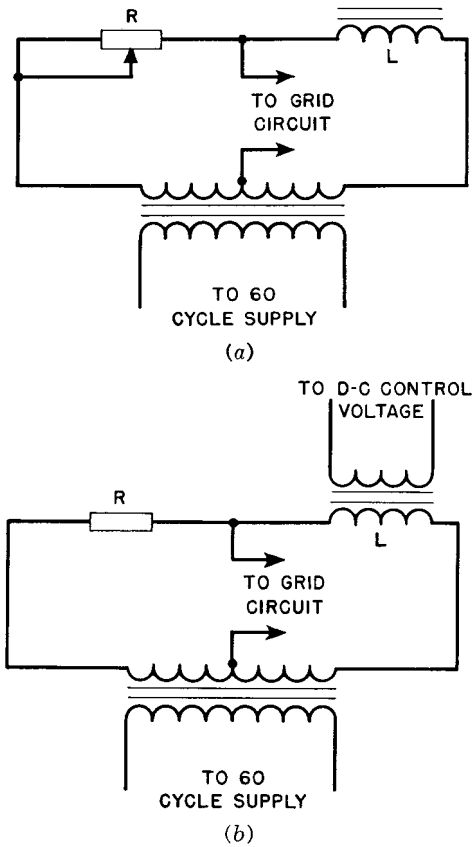

FIG. 187. Resistance-inductance phase shift circuits.

In Fig. 187(*b*) resistor R is fixed and inductance L is varied by means of direct current flowing in one of its windings. The vector diagram of Fig. 188 still applies; the solid lines are for high inductance and the dotted lines for low inductance. Direct current for varying the inductance may be obtained through a thyratron or a vacuum tube, especially when rectifier output voltage is automatically controlled. The reactor is usually of the saturable type.

The widest range of inductance is obtained with zero direct current at the higher inductance. In some vacuum-tube circuits, the minimum direct current is not zero, and a bias winding is added to the center leg to cancel the d-c ampere-turns with minimum current in the main d-c winding. Saturable reactors have many uses besides that described here, and are discussed more fully in Chapter 9.

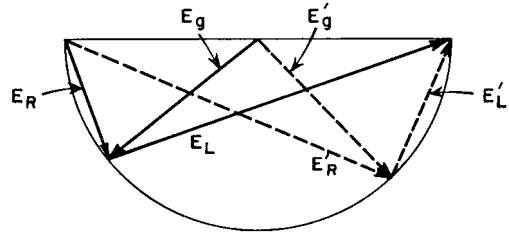

FIG. 188. Vector diagram for Fig. 187.

102. Thyratron Transformers. Anode transformers used for supplying thyratrons resemble rectifier anode transformers but generally have higher rms current for a given direct current in the load, and are more subject to voltage surges. With resistive loads, anode current has the same wave shape as the shaded portion of the anode voltage in Fig. 185. The relation of peak, rms, and average currents is shown in Fig. 189 as a function of firing angle θ for single-phase full-wave circuits. Voltage reduction as a function of θ is shown in Fig. 190. If a transformer is designed for operation with zero firing angle, maximum current flows in any given load; the transformer is then capable of carrying the current with greater firing angle, so long as the load impedance remains the same. If the load impedance is changed with $\theta > 0$ to keep the load current as high as possible, the limiting value may be found from Fig. 189. The average load current which may flow without overheating the transformer decreases as θ increases.

High-voltage surges occur when capacitance input filters are used with grid-controlled rectifiers. To a degree these surges are likely to occur even when the load is nominally resistive, because of incidental capacitance in the transformer, wiring, and other components. If the load is a radio-frequency generator, the r-f bypass capacitor adds to this effect. In Fig. 191(a) the total amount of external capacitance is designated C_1. A half-wave anode transformer is shown for simplicity, but each half of a full-wave transformer, or each phase of a three-phase transformer, behaves similarly. When the thyratron firing angle is

greater than zero, a steep voltage wave front occurs at the instant of firing t_θ, Fig. 191(*b*), as follows:

Normal voltage induced at point A in the secondary winding is e_1 volts above ground, just prior to t_θ. As soon as the thyratron fires,

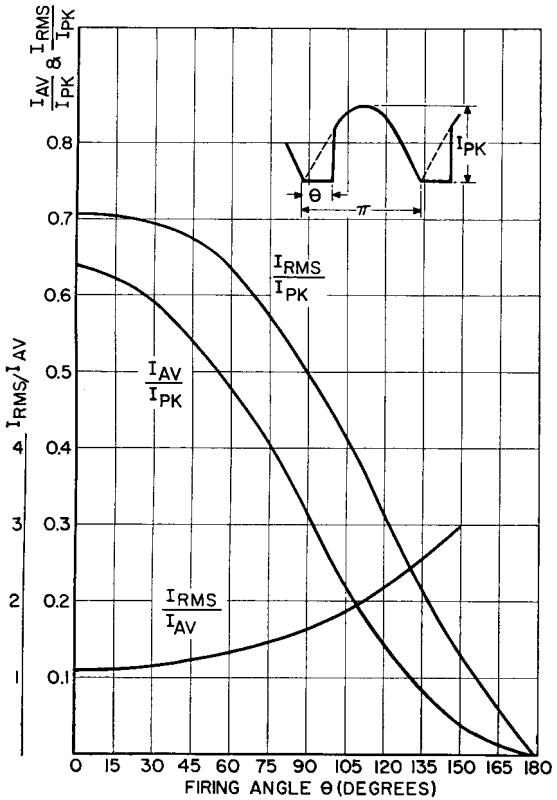

FIG. 189. Single-phase thyratron currents.

the external wiring and circuit capacitance C_1 momentarily forms an effective short circuit from A to ground. A large surge current flows into this short circuit, but initially this current cannot be drawn from the primary because of the inevitable inductance of the windings. The initial current is therefore supplied by the secondary winding capacitance. Since point A is momentarily short-circuited, a surge voltage, equal and opposite to e_1, is developed in the secondary winding. This voltage surge appears across the turns or layers of winding nearest to A. Unless precautions are taken in the design of the anode trans-

former the voltage may be high enough to damage the winding insulation.

As is shown in Chapter 10, with steep wave fronts in single-layer windings initial voltage distributes most equally between turns when ratio $\alpha = \sqrt{C_g/C_w}$ is small, C_g being the capacitance of the winding to ground and C_w the series capacitance across the winding. If the secondary of Fig. 191 were a single-layer winding of n turns, C_w would be C_s/n. In multilayer coils, ratio α is not so readily defined. In general, small effective layer-to-layer capacitance means small effective C_g in relation to C_w, small α, and more linear initial distribution of voltage. Many layers are better than few layers in keeping capacitance C_g small. In the limit, a one-turn-per-layer coil would have small α and good initial voltage distribution. In practice this extreme is not necessary to avoid layer insulation breakdown. It is usually sufficient to split the secondary into part coils, like S_1 and S_2 in Fig. 59. This reduces C_g to a quarter of the corresponding capacitance of full-width coils. Ratio α is reduced, and voltage distribution improved.

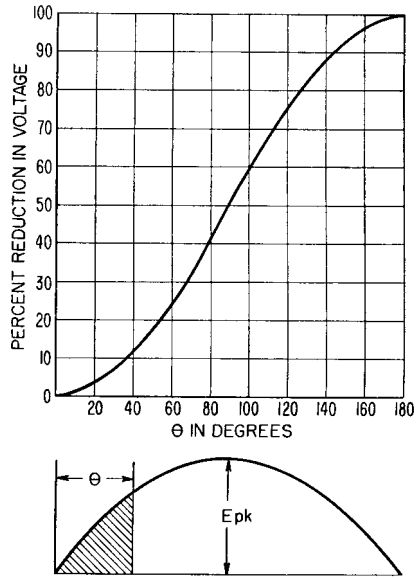

FIG. 190. Relation of firing angle to voltage output.

Even with part coils there is some non-linearity of voltage distribution, especially in the top layer. This non-linearity may be minimized by providing a static shield over the top layer and connecting it to point A, Fig. 191. The momentary voltage described above appears within the winding, and unless there are taps it may not be observable. If a surge suppressor circuit (usually a capacitor-resistor network across the secondary) is used, it does not appreciably diminish the internal winding voltage surge, but such a surge suppressor may be necessary to damp out oscillations in the external circuit due to firing of the thyratrons.

Secondary windings of control transformers in thyratron grid circuits, like those of Fig. 187, should be insulated for the anode voltage. When thyratrons arc-back the grids may be subjected to full anode potential, which would damage lesser amounts of insulation.

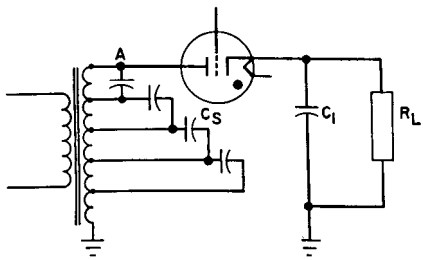

(a) SCHEMATIC CONNECTIONS FOR EACH PHASE

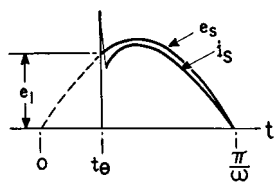

(b) SECONDARY VOLTAGE e_s AND CURRENT i_s WITH PHASE-BACK

FIG. 191. Thyratron plate transformer operation.

103. Peaking Transformers. It is stated in Section 100 that a large angle of intersection between the grid firing voltage wave and critical grid voltage is desirable for accurate control. A grid wave form with vertical front edge would be ideal. To produce a steep peaked wave form for firing thyratron tubes, sometimes special transformers are used. Usually the design depends on the non-linearity of the magnetizing current. Figure 192 shows a peaking transformer in which the magnetic core is made of special laminations. The primary is wound on the full-width left leg, and the secondary on the right leg which is made of a few laminations of small width. In the space between primary and secondary is a laminated shunt path with an air gap. In Fig. 193 are shown the core fluxes ϕ_m and ϕ_s, linking the primary and secondary coils, respectively. At low inductions, the same flux links both coils. As the flux rises from zero in each cycle, at first all the

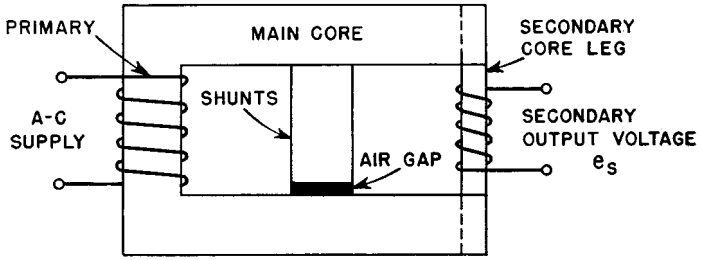

FIG. 192. Peaking transformer.

flux links the secondary coil, but because of the smaller cross section of the right leg it saturates at the value ϕ_s and the main flux ϕ_m flows through the shunt path. Thus there is a long interval in each cycle during which the flux change is substantially zero, and no voltage is induced in the secondary coil. During the short period θ_s, a voltage is induced in the secondary coil which has a very peaked wave form. This happens twice in each cycle.

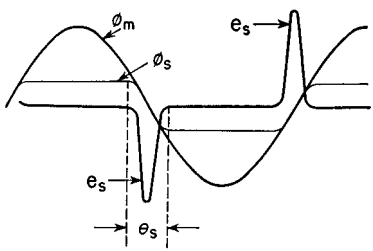

FIG. 193. Fluxes and secondary voltage in peaking transformer.

Because of the shorter time for the change in ϕ_s, $d\phi/dt$ would remain nearly constant over the angle θ_s if there were no leakage flux, and for 1:1 turns ratio there would be approximately equal volts in the primary and secondary coils. The secondary flux change takes place over a much shorter period of time, and the flux rises to only a fraction of its maximum value ϕ_m. Therefore less core area is needed in the secondary leg to obtain the desired voltage e_s. This leads to the following approximate ratio.

$$\frac{A_s}{A_p} = \frac{\theta_s}{\pi} \sin \frac{\theta_s}{2} \tag{109}$$

where A_s = core area in the secondary leg
A_p = core area in the primary leg.

Peaked secondary voltage may be made steeper by the use of nickel-iron laminations in the secondary leg, because these alloys have sharp saturation. The air gap in the center leg prevents it from shunting all the primary flux, which would reduce the secondary voltage to zero.

This air gap should be no more than 5 to 10 per cent of the window height, to keep leakage flux from threading through the secondary coil and giving a less peaked wave form. With this length of air gap and a total window length of twice the window height, the secondary turns are, for a 1:1 voltage ratio,

$$N_s \approx 2N_p \tag{110}$$

where N_p is the number of primary turns.

Transformers may be made to peak by the use of special circuits instead of special cores. Voltage wave forms like Fig. 193 are obtainable if the primary winding is operated at a voltage exceeding saturation but is connected in series with a large linear inductance or other high impedance. Grain-oriented core material, with its rectangular hysteresis loop, is well suited to peaking transformers. When primary and secondary windings are wound over the same magnetic path, the same volts per turn are induced in both windings, and equation 110 no longer applies. A peaking *reactor* circuit is shown in Chapter 11, Fig. 262.

104. Current-Limiting Transformers. Filaments of large vacuum tubes sometimes must be protected against the high initial current they draw at rated filament voltage. This is done by reducing the starting voltage automatically through the use of a current-limiting transformer, with magnetic shunts between primary and secondary windings. The shunts carry very little flux at no load; as the load increases, the secondary ampere-turns force more of the flux into the shunts until at current I_{sc}, Fig. 194(*B*), the output voltage is zero. The same principle is used to limit current in transformers for oil-burner ignition, precipitrons, and neon or other gas-filled tube signs.

Cross-sectional area through each shunt path is the same as that of the upper or lower leg of the shell laminations; then flux in the shunts does not exceed that in the core, shunt iron loss is not abnormal, and secondary voltage is sinusoidal. At short-circuit current I_{sc}, half the total flux flows through each set of shunts. The air-gap length in each shunt path can be found from equation 35:

$$l_g = \frac{0.6NI_{sc}}{B_m} \quad \text{(inches)}$$

where N = secondary turns

B_m = allowable induction in the shunts (in gauss).

The constant 0.6 is generally too small because of the flux fringing around the gap. The increase of gap made necessary by fringing may be found from Fig. 72 (p. 102). If the shunts are too short, the transformer does not limit the current properly. It is best to have slightly less air gap than necessary, and find by trial the right length of

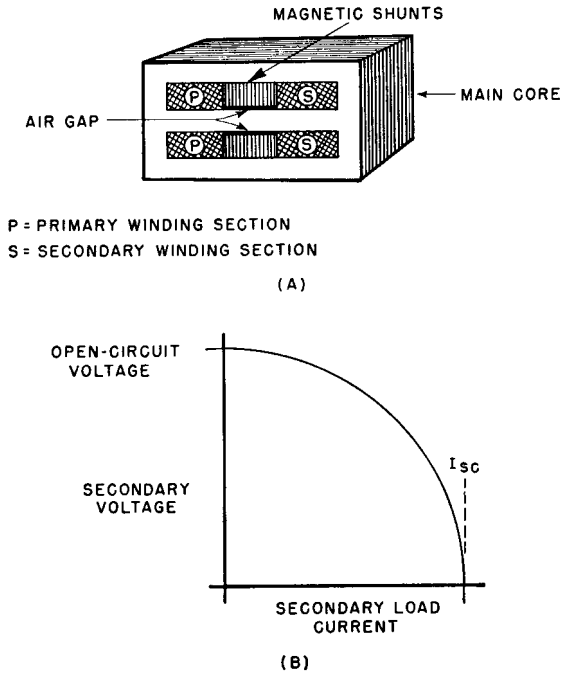

FIG. 194. (*A*) Current-limiting transformer; (*B*) output voltage versus current curve.

shunt. Fringing flux heats the coils and core somewhat more than in an ordinary transformer. If the secondary current is heavy, coils are wound pancake fashion and connected in parallel; they may have to be cross-connected for the coils to divide the load equally.

If the ordinate for open-circuit voltage and abscissa for short-circuit current in Fig. 194(*B*) are equal, the curve is a quarter-circle for a perfect transformer because the secondary current at short-circuit is all reactive. With core, shunt, and winding losses the curve for an actual transformer falls some 10 to 15 per cent less than the quarter-circle at currents 0.5 to 0.75 times I_{sc}.

105. Autotransformers. An autotransformer has a single winding which is tapped as shown in Fig. 195 to provide a fraction of the primary voltage across the secondary load. The connections may be reversed so that a step-up voltage is obtained. The regulation, leakage inductance, and size of an autotransformer for a given rating are all less than for a two-winding transformer handling the same power. Where the voltage difference is slight, the gain is large. Where the voltage difference is great, there is not much advantage in using an autotransformer, nor can it be used where isolation of the two circuits is required.

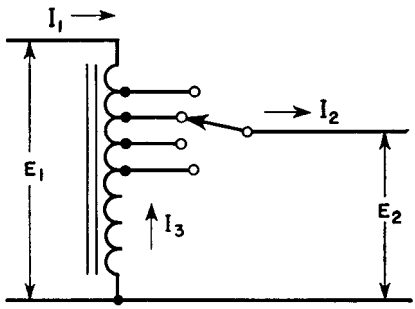

FIG. 195. Autotransformer voltages and currents.

Autotransformers are used in electronic applications chiefly for the adjustment of line voltage, either to change it or to keep it constant. Examples are the reduction of plate voltage for tuning an amplifier and the maintenance of constant filament voltage. Taps may be chosen by means of a tap switch to adjust the load voltage. The load voltage may be adjusted to within half the voltage increment between taps.

If the voltage is adjusted while load remains connected, bad switching arcs occur, either from breaking the circuit or from short-circuiting turns. To provide for adjustment under load conditions, a resistor may be momentarily connected in the circuit as the tap switch bridges from one tap to the next, and current is limited to full-load value. In large power tap changers, a reactor replaces the resistor to avoid heating and losses.

The v-a rating of an autotransformer depends on the ratio of input to output voltage. In Fig. 195 the output current $I_2 = I_1 + I_3$. Let p = per cent tap/100 $= E_2/E_1$. Neglecting losses, $I_2 = I_1/p$ and $I_3 = (1/p - 1)I_1$. Then

$$\text{Volt-amperes (in the upper portion)} = (1 - p)E_1I_1$$

$$\text{Volt-amperes (in the lower portion)} = pE_1I_3 = (1 - p)E_1I_1$$

which satisfies equality of volt-amperes in each section. For ratio p close to unity, the v-a rating and hence size for a given output can be made very small; for small values of p the size is not much less than

that of a two-winding transformer, but the autotransformer has much less regulation. Its effective winding reactance and resistance decrease as $(1 - p)^2$; that is, for a given unit,

$$\frac{X \text{ (or } R\text{) as autotransformer}}{X \text{ (or } R\text{) as two-winding transformer}} = (1 - p)^2 \qquad (111)$$

Appreciably less regulation is obtained in an autotransformer, even when size is not reduced much, because the right-hand term in equation 111 is squared.

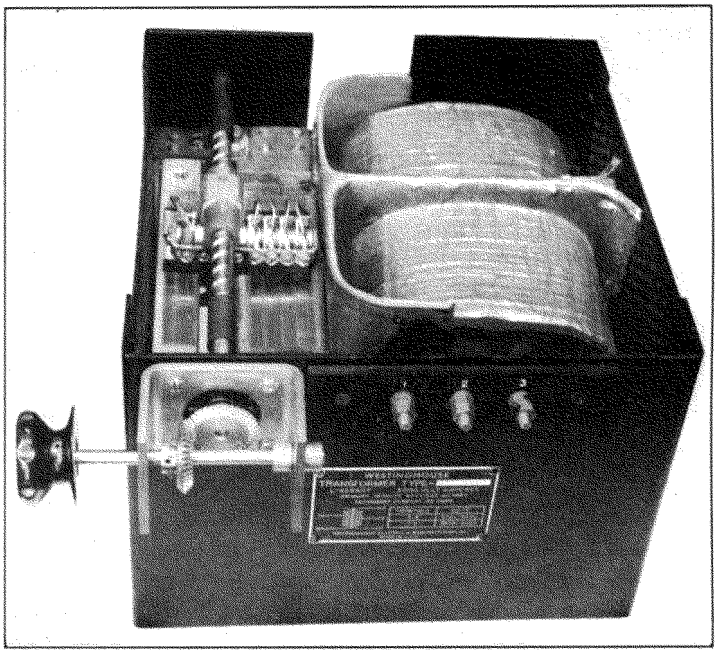

FIG. 196. Adjustable primary anode transformer.

When the power for electronic equipment is supplied by a 230-volt line, but auxiliary items such as relays and small motors are used at 115 volts, a convenient way of obtaining the latter voltage is to center-tap the primary of a large plate transformer, and use it as a 2:1 step-down autotransformer. The larger primary winding copper requires little extra space, and an additional transformer is thereby saved.

To improve the closeness of voltage control, a variable autotransformer has been developed in which the moving tap is a carbon brush

which slides over exposed turns of the winding. Brush resistance prevents excessive transition current and permits smooth voltage control; yet it offers little additional series resistance to the load. The same idea can be applied to two-winding transformers for secondary voltage adjustment. A typical unit of this kind is shown in Fig. 196.

When autotransformers are used on three-phase supply lines, they may be connected the same as two-winding transformers in star, delta, open-delta, or Scott connections. The last two connections are less subject to objectionably high regulation in autotransformers and, if they supply three-phase anode transformers, cause no serious primary voltage unbalance for voltage ratio p close to unity.

106. Static Voltage Regulators. Automatic regulators of various kinds have been devised for keeping comparatively small amounts of power at a constant voltage. Figure 197 shows one circuit for a res-

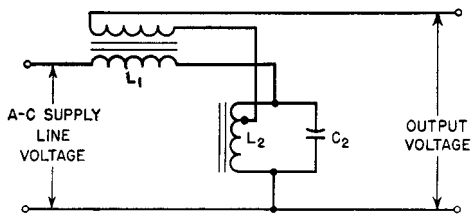

FIG. 197. Resonant-circuit voltage regulator.

onant-reactor voltage regulator. Inductance L_1 is linear. Inductance L_2 and capacitor C_2 are parallel-resonant at the supply line frequency and rated voltage. The pair draws very little current, so that the reactive voltage in L_1 is low. Output current flows through its secondary winding which is of such polarity as to maintain rated voltage. Inductance L_2 is partially saturated at this voltage. If line voltage falls below rated value, less current is drawn by L_2, and the L_2C_2 combination becomes untuned. Total current to the parallel circuit is then capacitive, and this capacitive current, drawn through L_1, raises the output voltage. Conversely, if line voltage rises above rated value, the L_2C_2 combination becomes untuned on the inductive side, and the output voltage falls below the line value. Output voltage variations of ± 1 per cent are obtained with ± 10 per cent line voltage variations in this manner, and with load changes from zero to full load.

Constant supply frequency is a condition for resonance at rated voltage; with the good frequency control of modern power systems this condition is generally fulfilled. Load power factor variations

cause output voltage to change. Some regulators are provided with taps to minimize this effect. Output wave form contains a noticeable third harmonic, because the large magnetizing current of L_2 must flow through appreciable impedance in L_1. Owing to the partial saturation of reactor L_2, it tends to operate at a high temperature and requires good ventilation. Practical regulators are in use with ratings from 25 v-a to several kva.

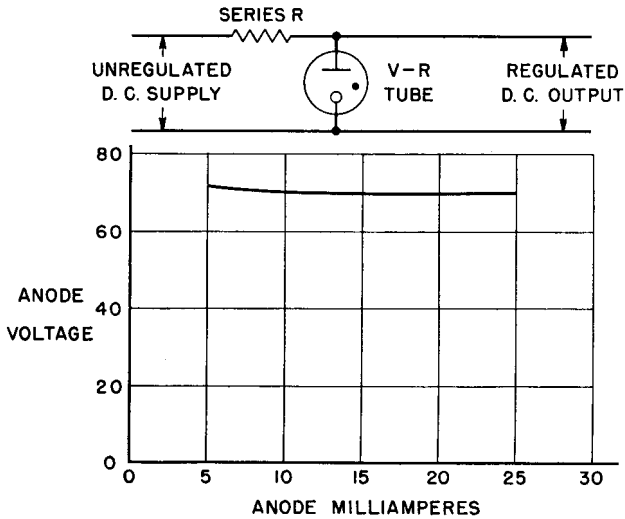

FIG. 198. Voltage regulator characteristic.

Electronic voltage regulators make use of a gas-filled regulator tube, which has a v-a characteristic such as that shown in Fig. 198. Current drawn by this tube changes between wide limits with virtually no change in voltage. A series resistor is ordinarily used to limit the current. When output current in excess of the "V-R" tube rating is desired, it may be used as a voltage reference for a current amplifier.

Some voltage regulators amplify the difference between a voltage reference and the output voltage of a rectifier or generator. This difference is called the *error* voltage. The amplifier output reduces the generator field if generator output voltage is high and increases the field if the output voltage is low. Likewise, motor speed may be regulated by the difference between tachometer output and a voltage reference. Or the angular position of a motor may be controlled electrically as desired by remote means. These means are discussed in

books on servomechanisms.[1] If a thyratron amplifier is used as part of a servo system, one thyratron may produce an effect opposite to that of the other, such as reversing current in the load. This amplifies the power controlled by error voltage.

In many modern regulator and servo systems, *magnetic* amplifiers are used. These devices are described in Chapter 9.

107. Demodulators. Demodulators or detectors measure phase or amplitude variations which are used to convey intelligence or control

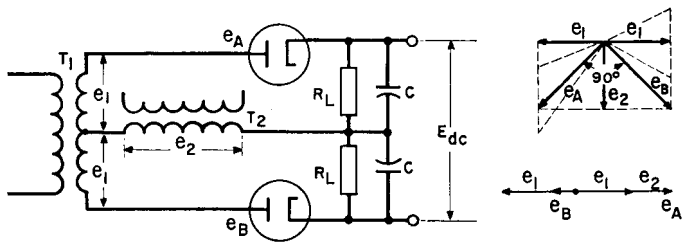

FIG. 199. Phase-difference demodulator.

another device. A circuit often used for phase detection is shown in Fig. 199. Transformer T_1 has a balanced secondary with e_1 volts per side. In frequency or phase demodulators, the circuit is called a discriminator, and uses air-core transformers. This circuit is used in phase demodulation to produce a d-c voltage proportional to phase shift. In this case e_2 leads e_1 by 90° for zero output. This condition is shown in the upper vector diagram. If e_2 should lead the upper e_1 by less than 90°, e_A would increase and e_B decrease, causing a net d-c voltage to appear across the output. If e_2 should lead the lower e_1 by less than 90° the d-c output voltage would change polarity. The plate voltage of one diode is the vector sum of e_1 and e_2, and is 90° out of phase with the plate voltage of the other diode (which is the vector difference of e_1 and e_2). If the phase angle ϕ between e_1 and e_2 changes either positively or negatively, output voltage E_{dc} is very nearly proportional to ϕ, up to $\phi = \pm 60°$. For positive phase shift, the output E_{dc} is negative; for negative phase shift, E_{dc} is positive. For good linearity, load resistances R_L should be large compared to the diode resistances.

Modifications of this circuit made to eliminate the vector difference

[1] See *Principles of Servomechanisms,* by G. S. Brown and D. P. Campbell, John Wiley & Sons, New York, 1948.

voltage or to reduce the degree of amplitude modulation are known as *balanced* and *ratio detectors.*[1]

As used in servo control, the demodulator produces d-c output which changes polarity when one voltage reverses with respect to the other; in this case e_2 adds directly to one voltage e_1 and subtracts from the other. The lower vector diagram shows how a voltage $e_2 - e_1$ causes a low difference voltage on diode A and a large sum voltage on B to produce a net d-c output voltage. Transformers in phase-reversal demodulators are usually iron-cored. Both transformers T_1 and T_2

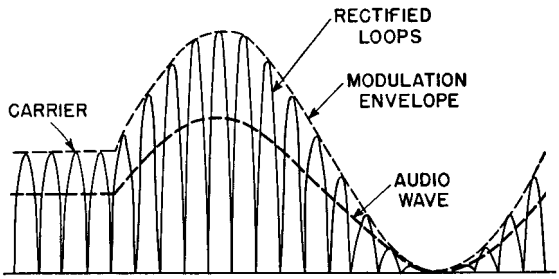

FIG. 200. Rectified amplitude-modulated wave.

should have low exciting current so that the phase angle between the voltages to be measured is not appreciably increased. For the same reason, the source impedances should be small; when this is not possible, the transformers should be matched. Figure 131 shows how necessary this is. With equal source and load resistances, several degrees of phase shift are introduced even if the ratio of transformer reactance to source resistance is 10:1. Variations in this reactance cause errors in the phase-demodulator output.

In a-m receivers, the received signal is modulated radio frequency. If 100 per cent amplitude modulation is used, the r-f amplitude is varied from 0 to 200 per cent at an audio-frequency rate. The detector, or demodulator, of the receiver first rectifies the r-f signal and then eliminates the r-f component, leaving only audio frequencies in the output. A rectified signal, before the r-f is eliminated, is shown in Fig. 200.

Demodulation is accomplished in the circuit of Fig. 201 by means of diode 6H6-2. Each half of the r-f cycle is rectified and the d-c

[1] See "Diode Phase-Discriminators," by R. H. Dishington, *Proc. I.R.E., 37,* 1401 (December, 1949); also, *Radiotron Designer's Handbook,* F. Langford-Smith, RCA Victor Division, Harrison, N. J., p. 1088.

power is absorbed in resistor R_3. Audio power is bypassed around R_3 by capacitor C_2, and the voltage is impressed upon the primary of transformer T_2. If an amplitude-modulated wave is used in this amplifier, the output voltage of winding S_1 on transformer T_1 has the form shown in Fig. 200. The first few cycles are shown as full-wave rectified loops with constant amplitude, that is, with no modulation. The audio output for this section of the wave is zero. A sine-wave envelope of 100

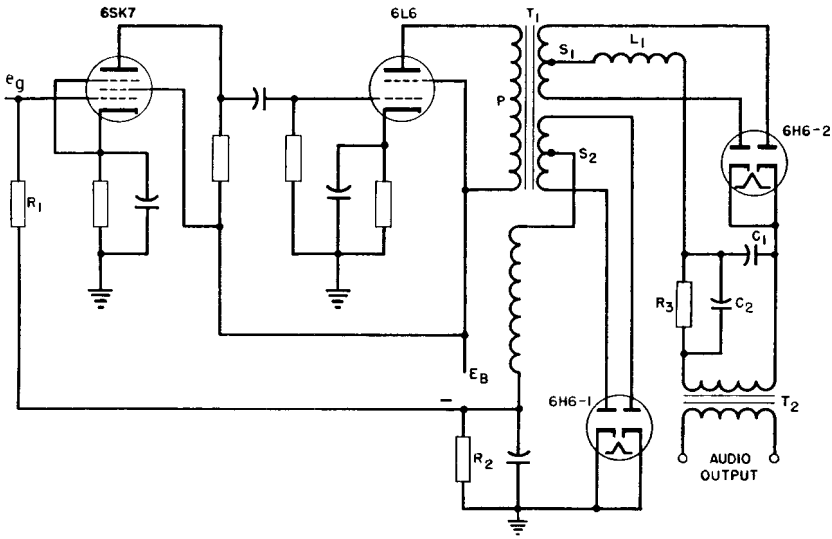

FIG. 201. Demodulator and automatic gain control circuits.

per cent modulation is shown in the rest of the figure. Average voltage left after the carrier frequency half-loops have been absorbed by the r-f filter L_1C_1 is the audio voltage impressed on transformer T_2.

The method of demodulation just described is known as diode demodulation. It is often accomplished by means of a single diode, and then every other lobe of the wave in Fig. 200 is omitted. Methods are in use also for demodulation with a triode, in which some amplification of the demodulated wave is obtained.

108. Automatic Gain Control. Vacuum-tube amplification factor is constant under certain conditions of operation. With high current operation the amplification factor in the region of high anode current and low anode voltage is no longer constant.

Some tubes are designed to have large variations in amplification factor. These are known as variable-mu, remote cut-off, or super-

control tubes. The mutual conductance of such tubes is highly variable with grid bias. Figure 202 is the curve of mutual conductance for a tube of this kind. Such a characteristic can be used to reduce gain at high amplitudes and thus prevent overmodulation in audio

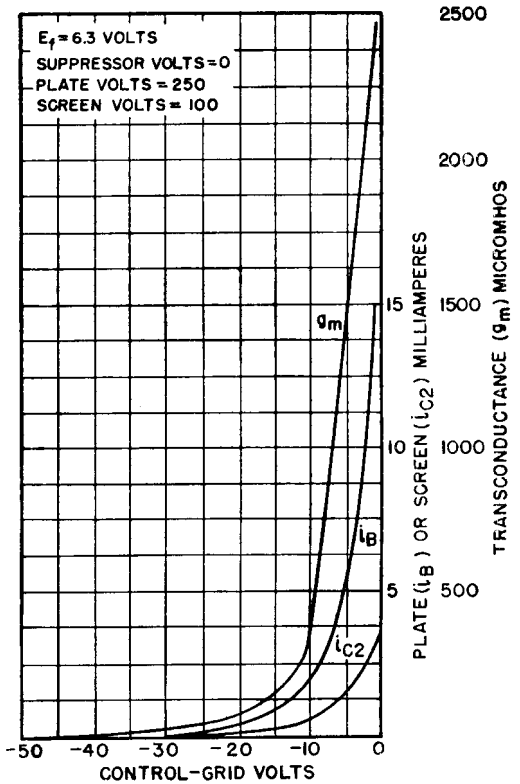

FIG. 202. Variable-mu tube (6SK7) mutual conductance curve.

systems. In Fig. 201 the circuit shown automatically reduces gain for excessive values of applied grid voltage e_g on the grid of the 6SK7 tube. This tube drives a 6L6 output tube through transformer T_1. On this transformer there is an auxiliary winding S_2 which is connected to rectifier tube 6H6-1 and produces the rectified output across resistance R_2 having a negative potential at the point shown. With large signals, the voltage rectified across R_2 is large and reduces the mutual conductance and plate voltage swing of the 6SK7 tube. Nearly constant output voltage is maintained in the 6L6 output.

If the power output of the 6L6 tube is delivered mainly into a linear

a-c impedance, the slight additional load imposed by the gain control makes little difference. But if all the output is delivered to rectifier loads, as it is in Fig. 201, the non-linearity of both tube and load causes output distortion. This is true particularly of beam or pentode output tubes. The normal class A output of a 6L6 beam tube is 6 watts but, if the output power is all rectified, only 50 mw can be drawn without excessive distortion. Half-wave rectifiers and capacitor-input filter outputs are worst in this respect, because of the current discontinuities. If the automatic gain control rectifier input is taken from a tuned amplifier, these difficulties decrease. The tuned circuit capacitor readily supplies irregular current wave forms, provided the amplifier has sufficient power output available.

Automatic volume control (AVC) is applied in receivers to either the r-f or audio stages, to maintain approximately constant volume in spite of fading or other causes of input voltage variations. It is applied in audio amplifiers to maintain better output volume with differing voice levels.

If the input grid resistor R_1 in Fig. 201 is connected to a fixed negative bias the AVC is inoperative below the value of bias voltage. This is called delayed AVC; with it, no AVC is applied until a certain output level is reached. In some receivers, more than one stage may be controlled, and the AVC action is amplified.

Circuits similar to this are used in power-line carrier receivers. The carrier frequency is 40 to 200 kc, and audio frequencies are employed for modulation. In transformer T_1 some special problems are encountered because the transformer operates over a range of 40 to 200 kc, delivers the correct amount of voltage to the automatic gain control tube 6H6-1 for proper AVC action, delivers the proper output to the audio load without distortion, and obtains these voltages from a nearly constant current source. The transformer ratio is obtained by estimating the r-f voltage swing obtained with a square primary input current wave, and dividing this by the voltage required to produce the necessary audio output after choke L_1 smooths the rectified lobes to the average value shown by the heavy dotted lines in Fig. 200. Transformer voltages and currents are calculated as in Table VII (p. 62) for a single-phase full-wave rectifier, but with peak audio current and voltage taking the place of d-c output.

9. MAGNETIC AMPLIFIERS

Amplifiers with saturable reactive elements are known as magnetic amplifiers. Such amplifiers have been built with power gains of over 1,000,000. Compared with electronic amplifiers, magnetic amplifiers have the advantage of long life. It is the purpose of this chapter to describe the operation and design of elementary magnetic amplifiers.

109. Saturable Reactors. From the fundamental theory of transformers, it will be recalled that the voltage induced in a winding usually far exceeds the resistance drop in that winding. In other words, winding open-circuit reactance usually is much greater than winding d-c resistance. Further, it will be recalled that a relatively small amount of direct current flowing into the winding of a transformer, in the core of which there is no air gap, causes the core to saturate. Thus, the reactance of the transformer may be varied by a small amount of d-c power. Now, if one winding of a transformer is connected between an a-c supply and a load, the amount of power delivered to the load may be controlled by a small amount of d-c power flowing in another winding. Because of the fact that open-circuit reactance ordinarily exceeds d-c resistance, the possibility of power amplification is inherent in a transformer. When one winding of a transformer is used for d-c control power and another for a-c output power, the transformer is called a saturable reactor.

110. Simple Magnetic Amplifiers. A single reactor, with a battery-fed d-c source controlling one winding and a-c power fed through the other winding, would have a-c voltage induced in the d-c winding. If this d-c winding were closed only on the battery, it would effectively short-circuit the a-c voltage in the power winding. This difficulty might be overcome by using a high impedance in the d-c control circuit. A more common solution is to use two reactors, one of the d-c windings of which is reversed, while the a-c windings add normally. Connections of this sort are shown in Fig. 203(*a*), with the a-c windings in series; it is possible to connect them in parallel as in Fig. 203(*b*) in order to allow more load current to flow at lower a-c voltage.

When there is zero direct current in the control windings of Fig. 203, both reactor impedances are large and prevent any load current except exciting current from flowing throughout the a-c voltage cycle. When direct current is applied to the control windings, impedance remains large for the first part of a cycle, until saturation flux density is reached. Then reactor impedance is reduced and a large load current may flow. With rectangular *B-H* loop core material, such as that shown in Fig. 22 (p. 26), the change from high to low impedance

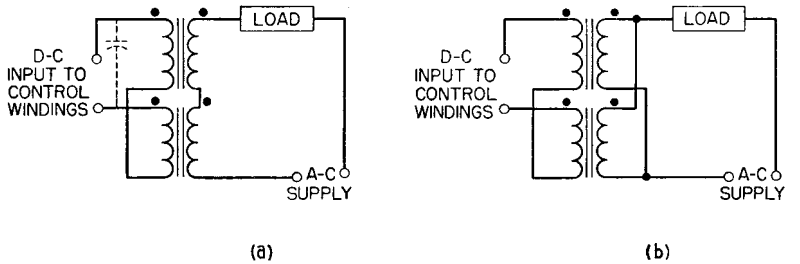

FIG. 203. (*a*) Series and (*b*) parallel-connected simple magnetic amplifiers.

is abrupt. If the loop were a true rectangle, the load current wave form would be as shown by i_L in Fig. 204(*a*). Only the exciting current flows in the load during the interval 0–θ_1. Then saturation is reached and load current suddenly rises to a large value. From θ_1 to π, i_L has sinusoidal shape. During the next half-cycle, this load current shape is repeated but in the reverse direction.

For a 1:1 turns ratio in each reactor, current i_c in each control winding equals i_L minus the exciting current. In one reactor, because of the reverse connection, current i_c flows in the opposite direction. Total current in the control circuit is as shown by the lower trace of Fig. 204(*a*), the average value of which is the input direct current I_c. Thus load current contains fundamental and odd harmonics, whereas control current contains only even harmonics. If sufficient control current flows to saturate the cores over the full cycle, load current also flows over the full cycle and is sinusoidal in wave form. For turns ratios other than unity, load and control currents are inversely proportional to turns ratio.

In the foregoing it was assumed that control current was free to assume the shape shown in Fig. 204(*a*). This is true, on a 1:1 turns-ratio basis only if the control circuit impedance is small. If total control circuit resistance is denoted by R_C and load resistance by R_L,

for $R_C \ll R_L$, load and control currents are sine waves, or portions thereof. If the opposite is true, namely $R_C \gg R_L$, control current wave shape is determined by R_C. For very large R_C, control current is continuous, and the current wave shapes approach those in Fig. 204(*b*). In this figure, d-c source impedance is large, even harmonics cannot flow, magnetization is "constrained," load current is flat-topped, and voltage across the reactor is distorted considerably. This distortion can be overcome by the use of a capacitor across the control coils as

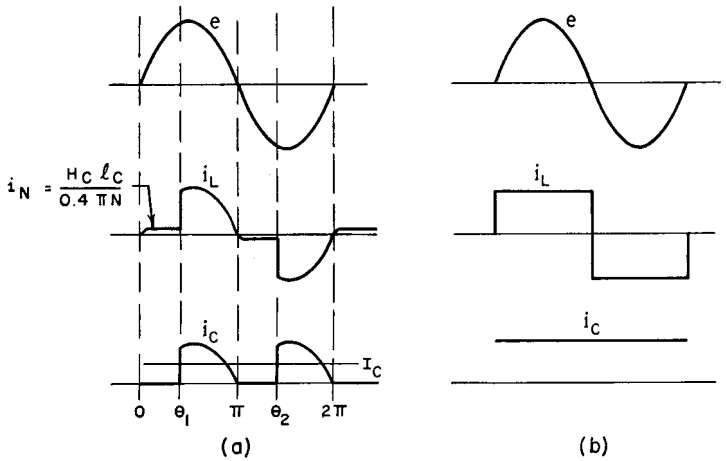

FIG. 204. Simple magnetic amplifier voltage and currents with (*a*) $R_C \ll R_L$, and (*b*) $R_C \gg R_L$.

shown dotted in Fig. 203(*a*). When the reactors are parallel-connected, as in Fig. 203(*b*), even harmonics may flow in the load coils, and capacitors are unnecessary for $R_C \gg R_L$.

Sometimes the two cores are combined into one, in the manner shown in Fig. 205. This is called a three-legged reactor, with one d-c coil and two a-c coils. Figure 205 shows the relative paths for the a-c and d-c fluxes. Equal turns in the a-c coils set up equal a-c magnetomotive forces which cancel in the center leg, and cause flux to flow as indicated by the solid line. No fundamental alternating voltage is induced in the d-c coil, but d-c flux flows in both outer legs as indicated by the dotted lines. A change of current in the d-c coil causes a change in total flux linking the a-c coils and hence a change of inductance. A-c coils may be connected in parallel instead of series, provided that equal turns in each coil and the flux polarity of Fig. 205 are maintained; for the same total number of turns the in-

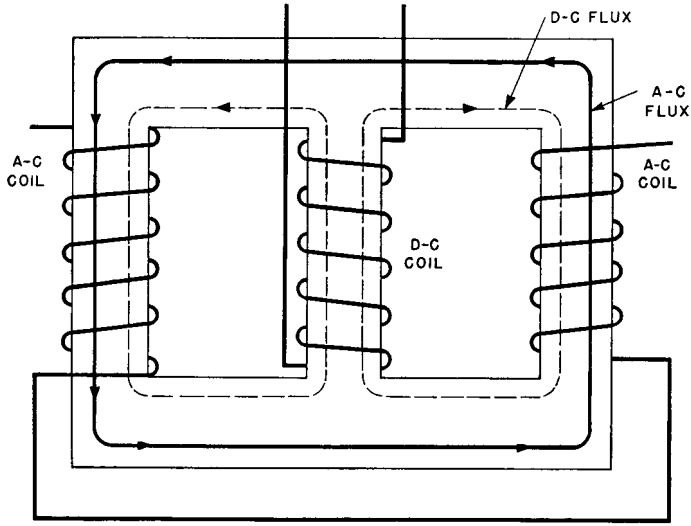

FIG. 205. Windings and core flux paths in a saturable reactor.

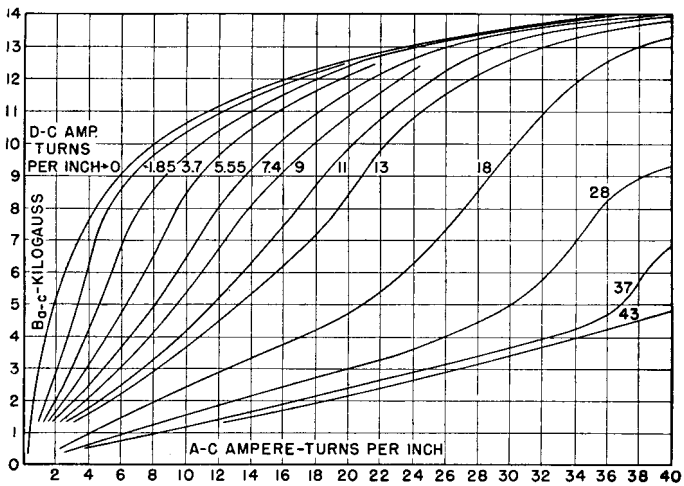

FIG. 206. Magnetization curves for 4% silicon steel.

ductance is halved and the alternating current doubled. The middle core leg shunts the even harmonics of a-c flux.

Rectangular *B-H* loops are obtained in grain-oriented core materials. It is only in these materials that the wave shapes of Fig. 204(*a*) are even approximated. In unoriented core steel, wave shape is much more rounded, and control current bears less resemblance to load current. Figures 206 and 207 indicate the contrast in saturation control afforded by unoriented silicon steel and oriented nickel steel. In

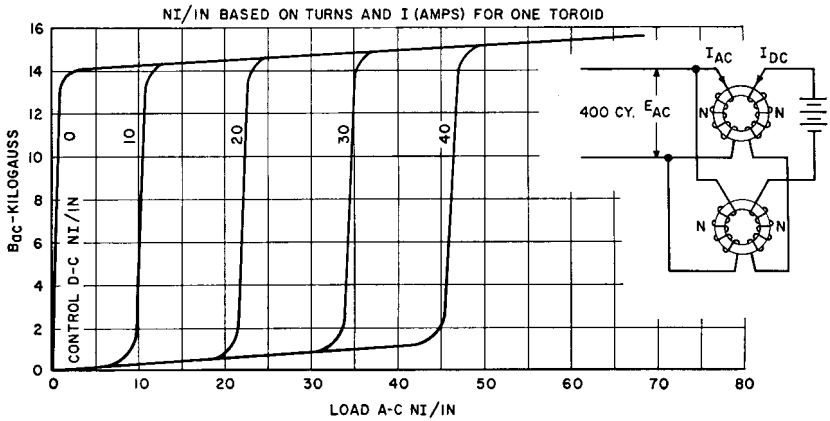

FIG. 207. Typical magnetization curves for 0.002-in. grain-oriented nickel-steel toroidal cores.

grain-oriented steel cores there is an approximately linear relationship between d-c ampere-turns per inch and a-c ampere-turns per inch over a large range of flux density. Moreover, the a-c *NI*/in. for a given d-c *NI*/in. change but little with a-c flux density over this range. In Fig. 207, each of the lines for a given value of control magnetizing force is nearly vertical. For a given value of control *NI*/in., load current is almost independent of flux density and therefore of a-c supply voltage. The sections following are based on the use of grain-oriented core steel.

111. Graphical Performance of Simple Magnetic Amplifiers. Since with a given core and supply frequency there corresponds a definite voltage for every flux density, and since for a given number of turns the ampere-turns per inch are proportional to current, the curves of Fig. 207 may be replotted in terms of voltage and current. We may then plot load lines on these curves in a manner similar to those in electronic

amplifiers, so that the operation, efficiency, control power, etc., may all be determined from a study of these load lines.

In Chapter 5 (p. 142) equation 58 indicates that the a-c voltage in a vacuum-tube circuit is divided between the load and the tube. If a resistive load is used, a straight line can be drawn on the characteristics of a vacuum tube which will form the locus of plate current and plate voltage for any given load and supply voltage. This line is called the load line, and by use of it the gain and power output of the amplifier can be determined.

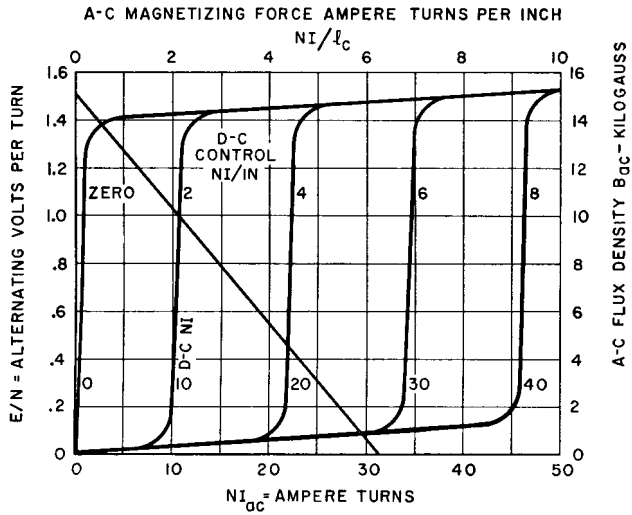

FIG. 208. Generalized magnetic amplifier characteristics and load line.

A similar method can be used with magnetic amplifiers. If a linear reactor were connected in series with the load, the voltage across the load and the voltage across the reactor would add at right angles. With rectangular loop core materials, currents are not reactive in the linear sense, so that the actual load line is neither a straight line nor an ellipse. For practical calculations the straight line is used, and the results obtained are correct within small percentages if the reactor voltage and current are measured on an average-reading voltmeter and ammeter.

Figure 208 shows similar information to Fig. 207, except that it is for a given core. The scale of abscissas is ampere-turns, and the scale of ordinates is volts per turn. These characteristics can be used for any amplifier which uses the same cores and the same supply voltage and frequency as the amplifier on which the measurements

were made to obtain these characteristics. These characteristics can be derived for a given core from the parameters of a-c flux density, a-c magnetizing force, and d-c magnetizing force as shown to the right and top of Fig. 208. These curves then give a set of characteristics for a given core rather than for a given core material. Some error is involved if these curves are used with a different supply frequency from the one used in making the original curves. Over a narrow range of frequency the curves of Fig. 208 using the scale at the top and to the right can be used to determine the operation of a magnetic amplifier for different loads. The curves of Fig. 207 may be used for magnetic amplifier calculations in this manner. For convenience of calculation, it is usually preferable to make a set of characteristic curves for several core sizes and for each supply frequency.

An example will show how these curves can be used in the design of magnetic amplifiers. Assume that it is necessary to design an amplifier with 30 watts output using cores with E/N and NI of Fig. 208. The supply voltage is 100 volts, the load is 200 ohms, and 0.01 amp is available for use in the control winding. The characteristics show the E/N can be varied from about 1.4 to 0.2 and still stay on the linear part of the characteristic curves. The power output is equal to $\Delta E \times \Delta I$ which is also equal to $\Delta(E/N) \times \Delta NI$, where E is the alternating voltage across the reactors, I is the alternating current through the reactors, and N is the number of turns in the load windings of the reactor. ΔNI needed for 30 watts $= 30/(1.4 - 0.2) = 25$ ampere-turns. Load impedance is $\Delta E/\Delta I$. A load line on Fig. 208 is $(\Delta E/N_L) \div \Delta NI = (\Delta E/\Delta I)(1/N_L^2)$, where N_L = turns in load winding. For 200 ohms, the load line passes through the points $E/N_L = 1.4$, $NI_{ac} = 2.5$, and through $E/N_L = 0.2$, $NI_{ac} = 27.5$. When this line is extended to the ordinate it intersects at 1.54. This is the point of zero alternating current or of infinite reactor inductance. At this point the total supply voltage would be across the reactor. Since the supply voltage is 100 volts, $100/N = 1.54$ and $N_L = 65$ turns. By interpolation of the d-c NI curves, we see that, for $E/N = 0.2$ and $NI_{ac} = 27.5$, 25 ampere-turns are necessary in the control winding. The turns in the control windings are $N_cI_c/I_c = 25/0.01 = 2{,}500$ turns. Here I_c is the current in the control winding, and N_c are the turns in the control winding. Control winding resistance is determined by the wire size. For the purpose of this example, assume that the resistance of the control winding is 500 ohms. Then the power in the control winding is $500 \times I_c^2 = 0.05$ watt. Power gain of the amplifier is power out/power in $= 30/0.05 = 600$. The impedance of either the input cir-

cuit or output circuit can be changed by changing the number of turns in the respective windings. Either impedance varies with the square of the number of turns used in the winding. For example, the load line which was used for 200 ohms in the preceding example could be used for 800 ohms. The load winding would then have $\sqrt{800/200} \times 65 = 130$ turns, and the supply voltage would be 200 volts instead of 100 for $E/N = 1.54$ at zero current.

Power output is proportional to the area of the rectangle of which the load line forms a diagonal. More power output can be obtained by using a load line with less slope, but gain may increase or decrease, depending upon the winding resistances and core material. In the

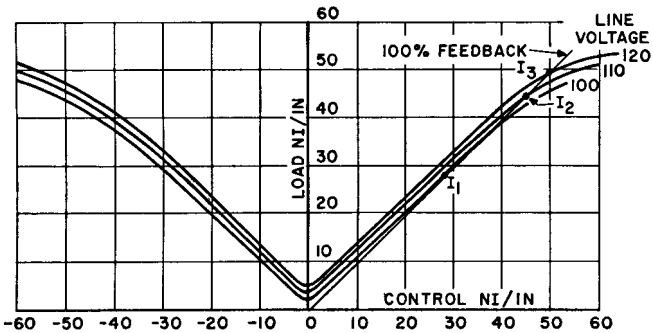

FIG. 209. Simple magnetic amplifier transfer curves with line-voltage variations.

preceding example, the load windings were assumed to be in series with the load, as in Fig. 203. This is the connection commonly used when the source is a 60-cycle a-c line. With a high impedance source, it is preferable to connect the load windings in shunt with the load. Then the ordinates of Figs. 207 and 208 correspond to load voltage at all times.

If we choose three line voltages corresponding to flux densities within the linear portions of Fig. 207, and plot the d-c control versus a-c load ampere-turns per inch, the curves of Fig. 209 result. If, instead of *NI*/in., average load current is plotted, Fig. 209 gives the transfer curves for a simple magnetic amplifier. The curves are symmetrical about zero ampere-turns. The difference between the transfer curve and a straight line indicates the degree of non-linearity in the amplifier for any load current. With grain-oriented core material the a-c load current is nearly independent of supply voltage for a-c inductions less than saturation. Provided that appropriate changes

in scale are made, transfer curves may be plotted between load voltage and control current, or between load ampere-turns and control ampere-turns, or between combinations of these.

Load current is the result of flux excursions beyond the knee of the normal magnetization curve. In Fig. 207 the curve for zero control *NI*/in. is normal magnetization for the material. When direct current flows in the control windings, it sets up a constant magnetizing force in the core. Then superposed a-c magnetizing force readily causes a flux excursion beyond the knee of the curve, permeability suddenly drops, and a large current flows through the load winding. The point in the voltage cycle at which this sudden increase in current occurs depends upon the amount of direct current in the control winding. Magnetic amplifiers with steep current curves like those of Fig. 207 can be used as control relays.

Load current is usually measured with an average-reading ammeter, such as a rectifier-type instrument. This kind of ammeter is generally marked to read the rms value of sinusoidal current but actually measures the average value. Thus the ammeter reading is $0.707/0.636 = 1.11$ times the average current over a half-cycle. When the meter is used to measure non-sinusoidal current, it still reads 1.11 times the average.

Except for the slight amount of non-linearity noted in Fig. 209, the *average* value of ampere-turns in the load winding of each reactor equals the d-c ampere-turns in the control winding. But since the a-c ammeter reads 1.11 times this value, the load a-c *NI*/in. are 1.11 times the control d-c *NI*/in., plus the differential due to core magnetizing current. Thus, if a core had infinite permeability up to the knee of the magnetization curve and zero permeability beyond the knee, the transfer curve would be exactly linear. Oriented nickel-iron alloy cores approach this ideal and therefore are more nearly linear than other materials.

112. Response Time. Because of the inductance of the reactor coils, when a change is made in the control winding direct current, load current does not change immediately to its final value. An interval of time, called *response time,* elapses between the change in control current and the establishment of a new steady value of load current. If the inductance were constant during the change, the response time constant would be the time required for a load current increase to rise to 63 per cent of the final value after a sudden control current increase. Magnetic amplifier response time cannot be evaluated as an

ordinary linear L/R time constant. Storm [1] shows that the time of response of simple magnetic amplifiers is independent of core permeability. An average or equivalent control circuit inductance may be found from the relation

$$T_d = \frac{L_C}{R_C} = \frac{R_L}{4fR_C}\left(\frac{N_C}{N_L}\right)^2 \tag{112}$$

where T_d = time for load current increment to reach 63 per cent of final value
L_C = equivalent total control coil inductance (henrys)
R_C = total control circuit resistance (ohms)
R_L = load resistance
f = line frequency
N_C = turns in control winding
N_L = turns in load winding.

An obvious method of decreasing magnetic amplifier response time is by increasing R_C, but this has the disadvantage of reducing overall power gain. Gain and response time are so related that the ratio of gain to time constant in a magnetic amplifier is usually given as a figure of merit.

113. Feedback in Magnetic Amplifiers. If a rectifier is interposed between the reactor and load, and a separate winding on the reactor is connected to this rectifier as in Fig. 210, it is possible to obtain

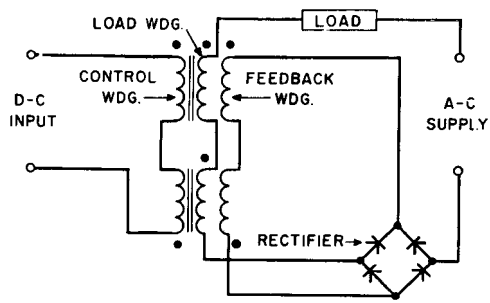

FIG. 210. Magnetic amplifier with external feedback.

sufficient power from the rectifier to supply most of the control power. If the control power from the rectifier furnishes the ampere-turns represented by the straight line in Fig. 209, the amplifier is said to

[1] "Transient Response of Saturable Reactors with Resistive Load," by H. F. Storm, *Trans. AIEE, 70,* Part I, p. 99 (1951).

have 100 per cent "feedback." It is then necessary for the control winding to supply only the amount represented by the horizontal difference between the transfer curve and the straight line. This greatly increases the amplification of a pair of reactors.

Typical transfer curves for a simple magnetic amplifier are plotted in Fig. 209 for three a-c supply voltages: 100, 110, and 120 volts. A 100 per cent feedback line intersects the transfer curves at I_1, I_2, and I_3, respectively. The control NI/in. are furnished by the feedback, except for the control current difference between the feedback line and

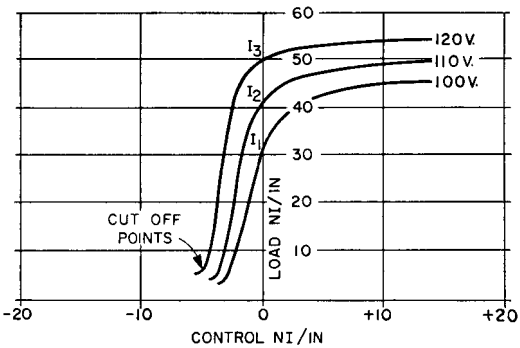

FIG. 211. Transfer curves for magnetic amplifier with feedback.

the transfer curve. Positive control current is required when the transfer curve is at the right, and negative current when it is at the left, of the feedback line. Net control NI/in. for the three voltages are plotted in Fig. 211 with expanded abscissa scale. Now the transfer curve is asymmetrical. Most of the amplifier gain occurs with negative control current changes. On the steep parts of the transfer curves, gain is fairly linear and greatly exceeds the gain of simple amplifiers. Below the steep parts, output current reaches a minimum but remains small with relatively large excursions of negative control current. These current minima are called *cut-off points*. Reference to Fig. 207 shows that cut-off current is I_N, the normal exciting current at supply voltage E. With positive control, current output levels off to a nearly constant value, depending on the voltage. Feedback causes output current to be quite dependent on variations in a-c supply voltage, because I_N has a greater effect than in simple amplifiers.

Computing control current for transfer curves with feedback as described in the preceding paragraph involves a small difference between two large quantities. Minor measurement errors in the original

data cause large inaccuracies in the feedback transfer curves of Fig. 211. A more accurate derivation of 100 per cent feedback transfer curves is given in Section 117.

To the left of the cut-off points, the transfer curve rises slowly toward the left along a straight line, as in Fig. 212(*a*). This line corresponds to 100 per cent *negative* feedback; it is practically linear, but gain is much reduced. The transfer curves of Fig. 211 would, if continued to the left, merge into such a line.

Polarities in Fig. 210 are for positive feedback with positive direct current entering the control winding at the top. Negative feedback is obtained if the control current is reversed. If series feedback is derived as shown in Fig. 210, the feedback current is E_L/R_L. It is possible to connect the feedback circuit across the load to obtain voltage feedback. To conserve power, the feedback resistance should be large relative to R_L.

114. Bistable Amplifiers. Positive feedback in a magnetic amplifier can be increased to more than 100 per cent by increasing turns in the feedback winding. Transfer curves may then become double-valued and give rise to abrupt load current changes with changing control current. Such amplifiers are called bistable. In Fig. 209, the effect of increasing feedback would be to *decrease* the slope of the feedback line. If the feedback were increased gradually, operation would remain stable until the feedback line had the same slope as the transfer curve. Then the load current would become some indefinite value along the transfer curve. If the feedback were increased further stable operation would be had at only one of two values of load current. Bistability is illustrated in Fig. 212(*a*). Here a transfer curve similar to those of Fig. 211 is shown except that it is with load voltage ordinates and expanded $N_C I_C$ abscissas. The amount of feedback in excess of 100 per cent is drawn as line AB with slope less than that of the main part of the 100 per cent feedback transfer curve. Another line, CD, is drawn parallel to the line AB. These lines are tangent to the transfer curve at points A and C. With feedback $>$ 100 per cent, let d-c control current be decreased from some negative value toward zero. Load voltage or current follows the transfer curve until it reaches point A; then it jumps to point B, and further increase of control current results in very little load voltage increase beyond point B. If control current is subsequently reduced, load voltage follows the top of the transfer curve until it reaches point C; then it drops abruptly to point D.

Bistable action is shown in Fig. 212(*b*) as a function of control *NI*/in., with points *A*, *B*, *C*, and *D* corresponding to those in Fig. 212(*a*). Line *AB* in Fig. 212(*a*) represents feedback ampere-turns $N_f I_f$ in excess of 100 per cent, which are proportional to E_L. Line *AB* extended intersects the axis of abscissas at *F'*, and *CD* extended intersects at *G*. Vertical lines erected at *A'* and *F'* intersect the transfer

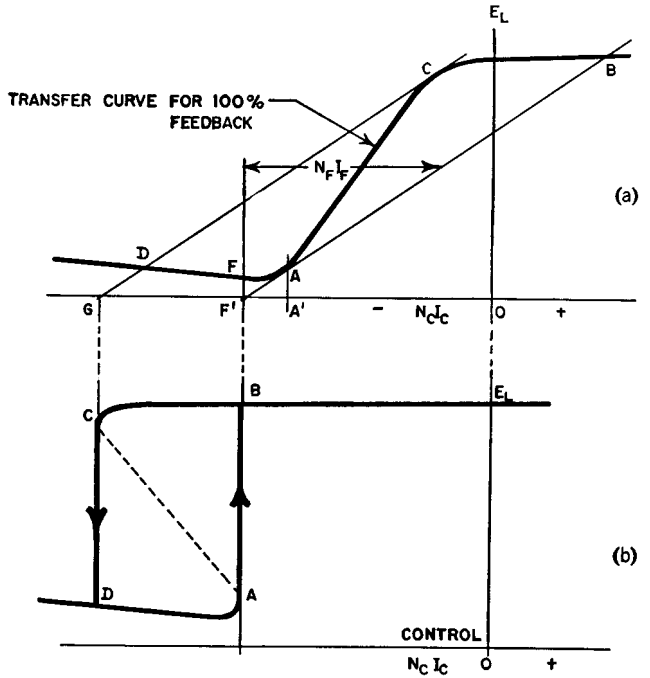

FIG. 212. (*a*) Typical transfer curve, and (*b*) bistable magnetic amplifier.

curve at *A* and *F*, respectively. *F'A'* represents ampere-turns $N_f I_f$ when control ampere-turns $N_C I_C$ are at point *F*. When decreasing negative $N_C I_C$ reach value *F*, the load voltage jumps from *A* to *B*. Points *F'* and *G* are projected downward to Fig. 212(*b*). In this figure the output jumps to final value *B*, but the increase actually takes place along the dotted line. Decreasing additional feedback $N_f I_f$ reduces the differential amount *F'G* of control $N_C I_C$ and reduces the width of the bistable loop. Conversely, increasing $N_f I_f$ widens the loop and provides a greater margin for variations in $N_f I_f$ due to voltage, temperature, etc. Bistable amplifiers are used in protective and control circuits to turn relays or indicators on or off when control

power varies between narrow limits and the inherent lock-in action is desirable.

115. Current Transductors. In some countries the term *transductor* is used to denote any magnetic amplifier. Here it denotes a saturable reactor circuit for measuring direct current. A current transductor is hardly an amplifier; it is a metering device. A transductor circuit is shown in Fig. 213. It is similar to that of Fig. 210 but with feed-

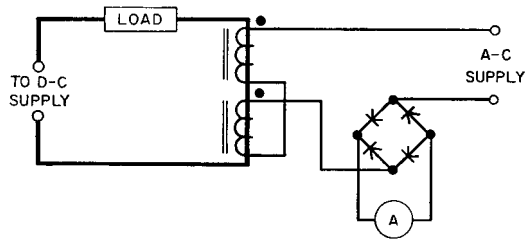

FIG. 213. Current transductor circuit.

back windings and a-c load removed. Operation is entirely different. Cores are circular or square, and are wound in-and-out toroidally in a manner resembling through-type current transformers. The heavy d-c bus then may be inserted through the toroid to form a single turn on each core. In Fig. 213 the d-c load windings are shown aiding, and the a-c windings bucking; this accomplishes the same core flux polarities as for Fig. 205. Load direct current is determined by the load resistance, which is large compared to the reactance of the transductor. Control circuit impedance multiplied by the turns ratio is large; magnetization is constrained. It will be recalled from Section 110 that, under this condition, even current harmonics cannot flow. Therefore a-c winding current is flat-topped. After this flat-topped current is rectified, it flows through the ammeter as smooth direct current.[1]

At any instant one reactor of the pair is saturated, and the other unsaturated. On each a-c half-cycle the unsaturated reactor maintains the output current constant. Total output d-c ampere-turns of course must equal twice the load direct current at all times. Transductors are like simple magnetic amplifiers as far as the relations of load and output currents are concerned. They have been built to measure currents of 10,000 amp or more, with good linearity.

[1] For a description of the current and flux conditions, see "Magnetic Amplifiers," by S. E. Tweedy, *Electronic Eng.*, February, 1948, p. 38.

116. Self-Saturated Magnetic Amplifiers. In Section 113 it was seen that the use of feedback windings greatly increases the gain of a magnetic amplifier. Several circuits have been devised to provide the feedback by means of the load circuit and thus eliminate the extra feedback winding. Such circuits are termed self-saturating. A "building-block" or elementary self-saturating component is the half-wave circuit of Fig. 214, from which several magnetic amplifiers may

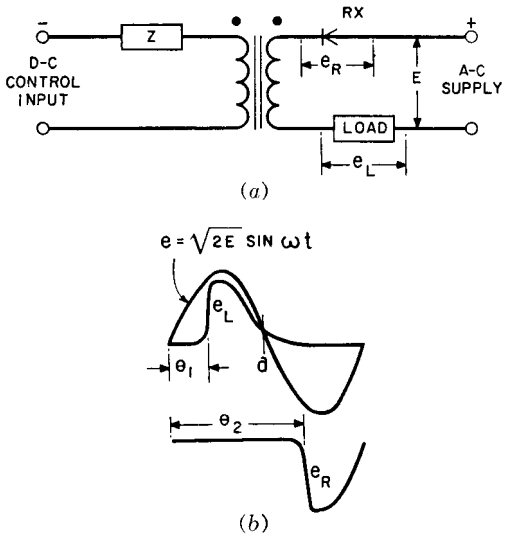

FIG. 214. (*a*) Half-wave self-saturated magnetic amplifier circuit and (*b*) load and rectifier voltage wave shapes.

be formed. Impedance Z in the control circuit prevents short-circuiting the reactor. It may be the control winding of another reactor in a practical amplifier. Rectifier RX prevents current flow into the load in one direction, so that the core tends to remain in a continually saturated condition. This condition is modified by negative control winding NI/in., which opposes the load winding NI/in. and permits the core to become unsaturated during the portion of the cycle when there is no load current flowing. The greater the control NI/in., the less the average output current. Transfer characteristics are similar to those of Fig. 211. Ideally the circuit has 100 per cent feedback.

Assuming the core to be saturated at all times with zero control current, current flows into the load throughout the whole positive half-cycle and is zero for the whole negative half-cycle. With a given

value of negative control current, reactor inductance is high at the start of the positive half-cycle and load current does not build up appreciably until an angle θ_1 is reached when the core saturates. Then it climbs rapidly and causes most of the supply voltage to appear across the load as shown by the curve marked e_L in Fig. 214(*b*) for the remainder of the positive half-cycle. As negative control current increases, so does angle θ_1. In the limit $\theta_1 = 180°$; that is, with large negative control current, virtually no load current flows. The similarity of load voltage wave shape to thyratron action is at once evident. It has led to the use of the same terminology. Angle θ_1 is often called the firing angle of a magnetic amplifier. Load voltage is reduced as θ_1 increases, approximately as in Fig. 190. There are some important differences, too:

(*a*) Reactor inductance is never infinite, and magnetizing current is therefore not zero. This means that during the interval 0–θ_1 a small current flows into the load. The change in reactor inductance at the firing instant is not instantaneous; the time required for the inductance to change limits the sharpness of load current rise.

(*b*) Even with tight coupling between control and load windings, the saturated reactor inductance is measurable. This saturated inductance causes the load current to rise with finite slope.

(*c*) After load voltage reaches its peak and starts to drop along with the alternating supply voltage e, core flux continues at saturation density. An instant a is reached when the load voltage exceeds the supply voltage. Beyond a, the reactor inductance increases and magnetizing current decreases, but at a rate slower than the supply voltage because of eddy currents in the core.

(*d*) After supply voltage e in Fig. 214(*b*) reaches zero, the reactor continues to absorb the voltage until the core flux is reset to a value dependent on the control current, that is, until angle θ_2 is reached. Then part of the negative supply voltage rises suddenly across rectifier RX as shown by the wave form of e_R.

During the interval 0–θ_1 the reactor inductance is high and virtually all the supply voltage appears across it. The voltage time integral $\int e\,dt$ represented by the reactor flux increase during this interval is equal to $\int e\,dt$ during π–θ_2. That is, the energy stored in the core before the firing instant is given up during the negative half-cycle of supply voltage.

Self-saturated magnetic amplifiers have transfer curves similar to that of Fig. 212(*a*). A small amount of additional positive feedback makes them bistable. Negative feedback makes the transfer curve more linear but reduces the gain. Ordinates and abscissas may be current, ampere-turns, or oersteds, as for simple magnetic amplifiers.

117. Hysteresis Loops and Transfer Curves. Several workers have observed [1] that the transfer curves of Fig. 211 are similar in shape to the left-hand or return trace of the hysteresis loop. There is a con-

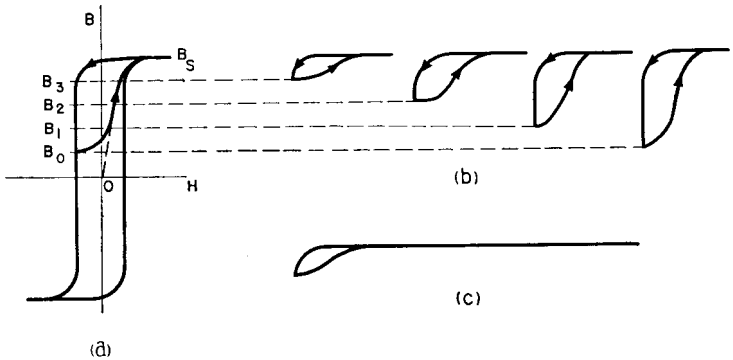

FIG. 215. Minor loops in rectangular hysteresis loop core material.

nection between the two. In Fig. 21, p. 25, it was shown that in a core with both a-c and d-c magnetization the minor hysteresis loop follows the back trace of the major loop in the negative or decreasing B direction, and proceeds along a line with less slope in the positive direction until it joins the normal permeability curve at B_m. Also, it was pointed out in connection with Fig. 69, p. 94, that, if ΔB has the maximum value B_m, the result is the banana-shaped figure OB_mD'. Here again the loop representing flux excursion O–B_m follows the left-hand side of the hysteresis loop in the downward or negative direction. In a rectangular hysteresis loop material with B-H loop shown in Fig. 215(*a*), the path traced over a flux excursion B_0B_s is more irregular in shape but still follows the left-hand trace of the loop. If magnetic amplifier cores are biased to a series of reset flux positions B_0 to B_3 the corresponding flux excursions and minor loops are those shown in Fig. 215(*b*). Usually, the load current far exceeds the control current necessary to reset the cores, so that these loops actually have a much longer region over which the loop width is practically

[1] See "Self-Saturation in Magnetic Amplifiers," by W. J. Dornhoefer, *Trans. AIEE, 68,* 835 (1949).

zero, as shown in Fig. 215(*c*). This is true of all the loops regardless of flux excursion.

The foregoing is true of a slowly varying flux excursion, so that the locus of the lower end points of the minor loops is the left-hand trace of the d-c hysteresis loop. Most magnetic materials, including rectangular loop materials, have a wider loop when the hysteresis loop is taken under a-c conditions, because of eddy currents. The difference between loops is as shown in Fig. 216. The locus of the end points of the minor loops under a-c flux excursions is neither the a-c nor the d-c loop but an intermediate line such as that drawn dot-dash in Fig. 216. The slope of this line is less than that of either the a-c or the d-c loop, and the gain of the magnetic amplifier is accordingly reduced.

An analysis for the self-saturated magnetic amplifier of Fig. 214(*a*) is given below. Load current is assumed to have the same shape as e_L in Fig. 214(*b*), and the following assumptions are made:

1. Sinusoidal supply voltage and negligible a-c source impedance.
2. Negligible reactor and rectifier forward voltage iR drops.
3. Negligible rectifier back leakage current.
4. Negligible magnetizing current compared to load current.
5. Negligible saturated inductance.
6. High control circuit impedance.
7. $E = 4.44fN\phi_s \times 10^{-8}$. (113)

This will be recognized as equation 4 (p. 6) with peak flux at saturation value ϕ_s. Other terms are listed as follows:

θ_1 = firing angle as in Fig. 214(*b*).
$t_1 = \theta_1/\omega$.
$\omega = 2\pi \times$ supply frequency f.
E = rms supply voltage.
ϕ_s = saturation flux = B_sA_c (for B_s see Fig. 215).
A_c = core section in cm^2.
ϕ_0 = reset core flux = B_0A_c (for B_0 see Fig. 215).
R_L = load resistance.
I_{av} = average load current.
i = instantaneous load current.
N = turns in load winding.

Under the assumptions, equation 1 becomes

$$\sqrt{2}\,E \sin \omega t = \frac{N}{10^8}\frac{d\phi}{dt} \qquad \text{for } 0 < \omega t < \omega t_1 \tag{114}$$

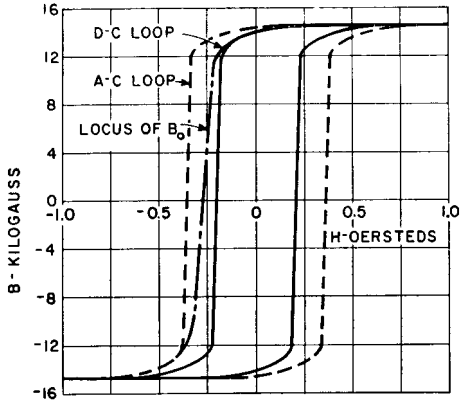

FIG. 216. D-c and a-c *B-H* loops for grain-oriented nickel steel.

Integrating equation 114 gives

$$10^{-8}\int_{\phi_0}^{\phi_s} N\,d\phi = \int_0^{t_1} \sqrt{2}\,E \sin \omega t\,dt \tag{115}$$

and

$$\frac{\omega N(\phi_s - \phi_0)}{\sqrt{2}\,E \times 10^8} = 1 - \cos \omega t_1 \tag{116}$$

During the interval $\theta_1 < \omega t < \pi$, load voltage is

$$\sqrt{2}\,E \sin \omega t = iR_L \tag{117}$$

where R_L is the load resistance. This may be integrated to give

$$\frac{\omega R_L}{\sqrt{2}E}\int_{t_1}^{\pi/\omega} i\,dt = 1 + \cos \omega t_1 \tag{118}$$

Combining equations 116 and 118 and substituting equation 113,

$$\int_{t_1}^{\pi/\omega} i\,dt = \frac{N}{R_L}(\phi_s + \phi_0) \times 10^{-8} \tag{119}$$

The left side of equation 119 is the average load current over the conducting interval $\pi/\omega - t_1$. Average load current over the whole cycle is

$$I_{\text{av}} = \frac{fN(\phi_s + \phi_0)}{R_L \times 10^8} \tag{120}$$

Equation 120 has two flux terms: ϕ_s, which is a fixed quantity for a given core material; and ϕ_0. The relation between ϕ_0 and control

current is, as indicated in Fig. 215, the return trace of the major hysteresis loop. Thus equation 120 states that the average load current is the sum of a constant term and a term which has the same shape as the return trace of the hysteresis loop. Quantitatively, a self-saturated half-wave magnetic amplifier has a *current* transfer curve the same as the return trace of the core hysteresis loop, except that ordinates are multiplied by $fA_cN/10^8R_L$ and are displaced vertically by an amount $fB_sA_cN/10^8R_L$.

Comparison with equation 113 reveals that the ordinate multiplier and vertical displacement are $E/4.44R_LB_s$ and $E/4.44R_L$, respectively. As noted above, the return trace should be modified to mean the dot-dash line of Fig. 216.

118. Self-Saturated Magnetic Amplifier Circuits. In Fig. 217 three single-phase circuits are diagrammed which comprise two of the half-

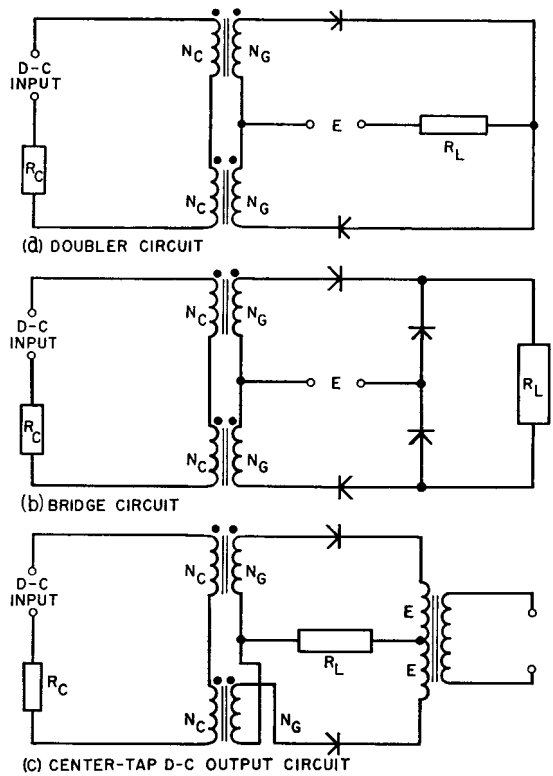

FIG. 217. Self-saturated magnetic amplifier circuits.

wave elements described in the preceding sections. These circuits are discussed briefly below.

(*a*) *Doubler Circuit.* This is really two half-wave circuits working into a common load. Rectifier polarities are such as to cause a-c voltage to appear across the load, as in Fig. 218(*a*). The wave shape departs somewhat from alternately reversed half-waves. In the doubler, the reactor which is carrying load current during a given half-cycle causes a reduction in the resetting voltage, and therefore in the time rate of resetting flux change of the other reactor. This increases the output and gain for a given control current compared to the half-wave circuit but has no effect on current minima at the cut-off points (see Fig. 211).

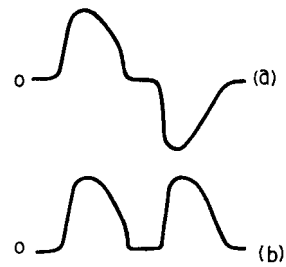

FIG. 218. Single-phase magnetic amplifier output; (*a*) a-c voltage across load; (*b*) d-c voltage across load.

When control circuit resistance R_C is large, the control current and associated magnetizing force are fixed, but, when R_C is small, even harmonic currents flow freely in the control circuit and influence the wave shape for a given control current further. Generally, low values of resistance R_C cause a slight increase in the control oersteds for a given output but virtually no change in slope. In other words, the whole transfer curve is displaced slightly to the right.

(*b*) *Single-Phase Bridge Circuit.* Here two extra rectifiers isolate the two reactors at all times, and the wave form is like that of the half-wave rectifier, except that it occurs twice each cycle. Load current is d-c; that is, both reactors produce load current of the same polarity, as in Fig. 218(*b*). Because of the isolation of the two reactors, the transfer curve closely follows a dot-dash line like that in Fig. 216 if the core is grain-oriented nickel steel, or a similar line between a-c and d-c loops for other core material. Control resistance R_c affects output in a manner similar to that mentioned for the doubler.

(*c*) *Center-Tap D-C Circuit.* Although the reactors are not isolated in this circuit, load and resetting currents are still the same as for the bridge circuit, and hence the transfer curve has the same shape, unless the rectifier reverse currents are appreciable. Then gain is appreciably reduced.

In all these single-phase circuits, the load current is twice that of

the half-wave circuit. Therefore transfer curves may be predicted from B-H loops as in Section 117, but ordinates are multiplied by $E/2.22R_LB_s$, and the vertical displacement is $E/2.22R_L$. From these multipliers it can be seen that output current is proportional to supply voltage E, and therefore power gain is proportional to E^2. In this respect, a self-saturated amplifier contrasts with a simple magnetic amplifier, the output current of which is nearly independent of E, for rectangular B-H loop core material. At least this is true below maximum current, or current flow over a complete half-cycle.

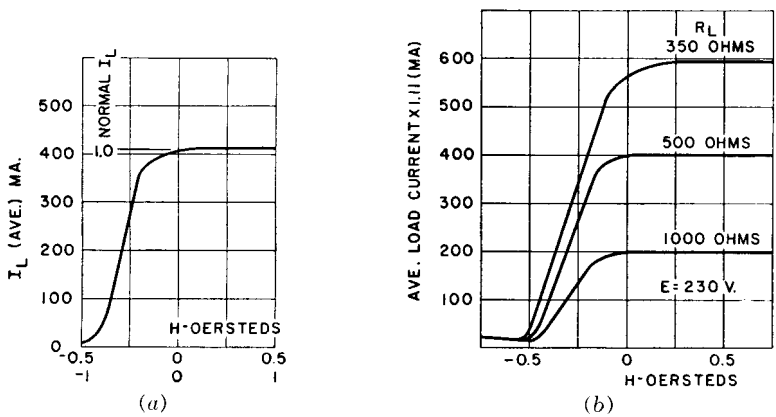

FIG. 219. Self-saturated magnetic amplifier output; (a) calculated for 500 ohms from Fig. 216; (b) in actual amplifier.

As an example of the manner in which a transfer curve is found from the B-H loop, suppose that, in a given self-saturated amplifier, Fig. 216 is the B-H loop, supply voltage $E = 230$ v, $R_L = 500$ ohms, $B_s = 14.7$ kilogauss. The ordinate multiplier is $230/(2.22 \times 500 \times 14.7) = 0.0141$, and displacement is $230/(2.22 \times 500) = 0.207$.

Table XV indicates the change in ordinates. The last two columns of the table are plotted in Fig. 219(a) as load current in milliamperes. Also indicated is the "normalized" value of unity for maximum output current. For any load impedance the same calculated transfer curve can be used, and all ordinates multiplied by $E/1.11R_L$. Abscissas may be normalized likewise, with cut-off $H = -1.0$.

Normalized output current at cut-off is $\Delta_N = I_N R_L/E$. Cut-off control current is most accurately found from H corresponding to $-B_r$. This is $H = -0.5$ in Fig. 216. These relations are, of course, idealized, but they are still very useful in practical work. For example, winding

TABLE XV. DERIVATION OF TRANSFER CURVE FROM *B-H* LOOP (FIG. 216)

H (oersteds)	B (kilogauss)	$0.0141B$ amp (av)	Vertical Displacement (amp)	Load Current, Fig. 219(*a*) (av)	
				Amp	Normalized
−0.5	−14.3	−0.202	+0.207	0.005	0.012
−0.4	−14.0	−0.197	0.207	0.010	0.024
−0.3	0	0	0.207	0.207	0.500
−0.15	13.0	0.183	0.207	0.390	0.943
0	14.0	0.197	0.207	0.404	0.975
0.5	14.7	0.207	0.207	0.414	1.000

resistance R_G and rectifier forward resistance R_F reduce load current and output power, but these resistances may be added to the actual R_L arithmetically to obtain total resistance $R_T = R_G + R_F + R_L$. Then the transfer curve ordinates are

$$I_{\text{av}} = \frac{E(B\text{-}H \text{ loop ordinates})}{2.22R_TB_s} \tag{121}$$

displaced vertically by

$$E/2.22R_T \tag{122}$$

Output current and power are reduced somewhat by these inevitable resistances. This can be verified in Fig. 219(*b*) which is a plot of transfer curves for an actual doubler amplifier with $E = 230$ v, with 350-, 500-, and 1,000-ohm load resistances, and with average load current $\times$ 1.11 as read directly on the output meter. The 500-ohm load resistance curve is approximately the same as Fig. 219(*a*); this means that $R_F + R_G \approx 0.11R_L$ in this particular amplifier. The accuracy of Fig. 219(*a*) is evidently poorest at cut-off. Upward slope at control currents more negative than cut-off is not shown at all. For the most practical region, i.e., to the right of cut-off, the calculated curve is eminently useful.

Additional windings are often used on the reactors for control purposes. One common winding, called a *bias* winding, carries negative control current. The function of this winding is to maintain low output in the absence of control current. Thus in Fig. 211, with $E = 120$, $-5NI$/in. of bias magnetizing force keeps the amplifier load NI/in. at 5. Then positive control current raises the load current to the desired value. Most of the gain is obtained with less than $+5NI$/in. control magnetizing force.

Additional control windings are used for adding or subtracting input signals. This provides a simple means of combining several control functions in one magnetic amplifier.

Response time in a self-saturated amplifier is longer than in a simple amplifier, but the gain per second is much greater. The time constant is

$$T_d = \alpha_v/2f \quad \text{(seconds)} \tag{123}$$

where T_d = time for 63 per cent response to step input
α_v = amplifier voltage gain for 1:1 turns ratio
= $(\Delta E_L/\Delta E_C) \times (N_C/N_L)$ for any turns ratio
f = supply frequency
ΔE_L = change in load voltage
ΔE_C = change in control voltage
N_C = turns in control winding
N_L = turns in load winding.

Equation 123 is valid for T_d down to approximately 4 cycles minimum. Although smaller T_d may be obtained, it does not follow equation 123.

Push-pull amplifiers are used to provide a-c or d-c output, with the output polarity dependent on input polarity. A d-c push-pull circuit which senses input polarity is shown in Fig. 220. Bias windings on each reactor carry current in such directions that amplifier outputs cancel for $E_C = 0$. For positive E_C, amplifier 1 produces positive E_L, and for negative E_C, amplifier 2 produces negative E_L. This circuit has low efficiency, owing to the power dissipated in the balance resistances R_1 and R_2 but has linear output.

It is important, wherever two or more reactors are used together in magnetic amplifiers, that the reactors be alike in turns and in cores. Cores are generally selected to "match," with closely duplicated B-H characteristics. It is not feasible to compensate core differences in balanced amplifiers by bias adjustments and still obtain linear output.

119. Half-Wave Control of Magnetic Amplifiers. Through attention to a-c voltages present in the control circuit, Dr. R. A. Ramey analyzes magnetic amplifiers in a manner which gives rise to new circuits with desirable properties.[1] A half-wave building block of such circuits is shown in Fig. 221 (*a*) for a 1:1 turns-ratio reactor. The load circuit is the same as in the half-wave amplifier of Fig. 214. The con-

[1] See "On the Mechanics of Magnetic Amplifier Operation" and "On the Control of Magnetic Amplifiers," by R. A. Ramey, *Trans. AIEE, 70,* 1214 and 2124, respectively.

trol circuit comprises a-c voltage E and rectifier RX_C in addition to variable rectified control voltage e_C of polarity indicated. A-c voltage polarities are for the positive or conducting half-cycle in the load

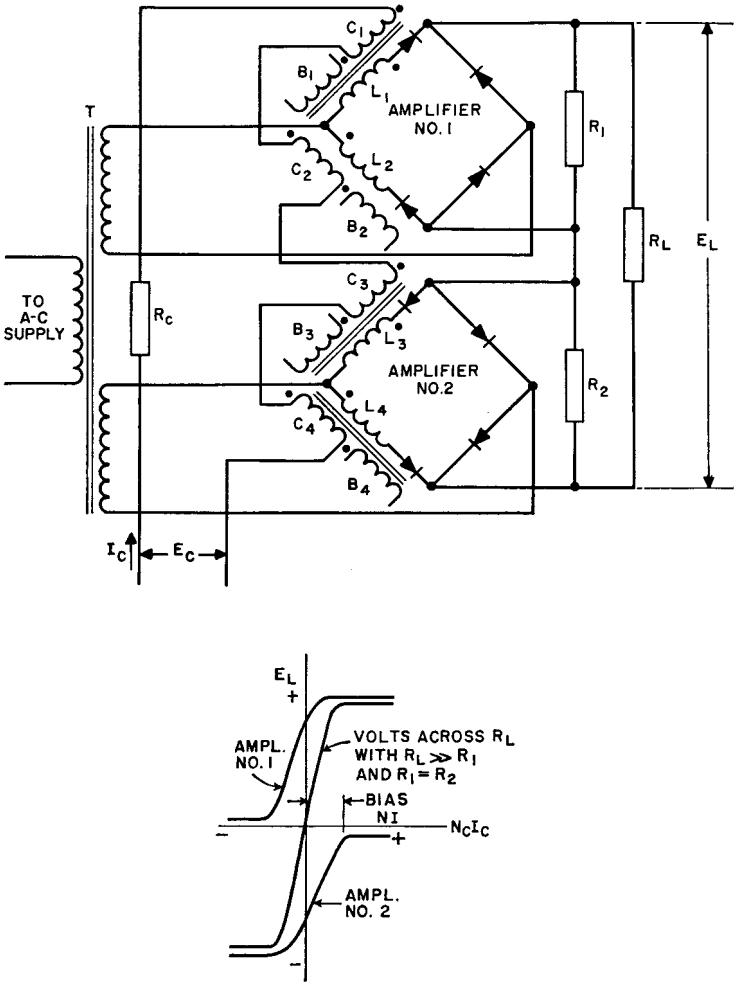

FIG. 220. D-c push-pull magnetic amplifier.

circuit. During this half-cycle, RX_C blocks and the control voltage is zero. During the next half-cycle, a-c line voltage $E - e_C$ appears across the reactor control coil. If e_C is zero, the core is not magnetized by control current flowing during the positive half-cycle, and

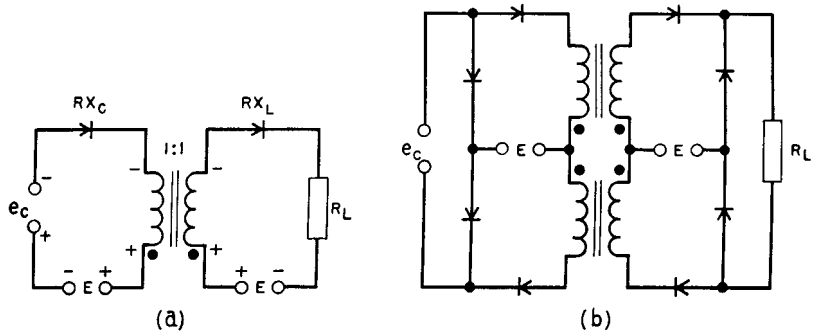

FIG. 221. Half-wave controlled magnetic amplifiers.

the core is completely reset by E during the negative half-cycle. If the peak value of e_C is equal to $\sqrt{2}E$, it appears across the reactor in opposite phase to the line voltage and completely cancels it during the resetting half-cycle. This is shown dotted in Fig. 222, with both voltage waves designated by capital letters. This cancellation results in zero resetting; therefore full output current flows over 180° of the positive half-cycle. If $E_C = E/2$ it subtracts from E, resulting in the lower dot-dash line of Fig. 222. The area under $E - E_C$ (shown hatched) is just half of the area under E and therefore equals the hatched area under E during the interval 0 to $\pi/2$ of the positive half-cycle. That is, the reactor absorbs voltage E during the interval 0 to $\pi/2$ and allows current to flow from $\pi/2$ to π. But this is half of full or maximum output. Thus the output current is:

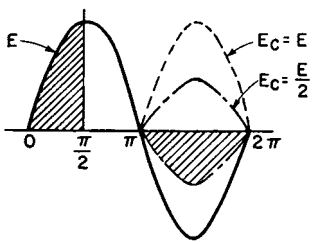

FIG. 222. Resetting voltages with half-wave control.

$$\text{zero for } E_C = 0$$

$$\tfrac{1}{2} \text{ max for } E_C = E/2$$

$$\text{max for } E_C = E$$

Several advantages accrue from this type of control:

1. Output is proportional to control voltage.
2. Output depends only on control voltage and is independent of variations in line voltage or frequency.

3. Time of response is short (2 cycles or less).
4. Filtered d-c source of control power is not necessary.

Proportionality of output to input voltage is strictly true only for zero control circuit resistance or zero reactor exciting current. The lower the control circuit resistance and reactor exciting current, the more nearly is output proportional to input. Rectangular *B-H* loop core material is necessary for linearity. Control circuit resistance can be made small without causing slow response in this circuit. Exciting current and control circuit resistance give rise to load voltage output with zero control voltage. Raising control voltage e_C restores linearity of output. With half-wave control, voltage gain is more important than power gain; voltage gain is approximately equal to turns ratio. Mixing is not so readily accomplished in half-wave control circuits. Figure 221(*b*) shows how two half-wave sections are combined to form a full-wave bridge circuit with d-c output. This circuit differs from the circuit of Fig. 217(*b*) in that the control windings are isolated from each other by the control circuit rectifiers. Voltage E in the control circuit is an a-c bias voltage, and e_C is rectified a-c signal voltage. Zero output voltage appears across R_L with $e_C = 0$. When e_C is increased, full-wave rectified voltage appears across R_L. The fundamental a-c component of this voltage is zero.

120. Magnetic Amplifier Design. Of first concern in design is the reactor core material. Supermalloy or other high-percentage nickel alloys are best suited as core material for the low power input stage. Grain-oriented nickel steel is used in the stages where output power is appreciable, and grain-oriented silicon steel where power is large. Figure 223 shows the d-c loops of two grain-oriented core materials, Hipersil and Orthonik. Although both materials have approximately rectangular *B-H* loops, the difference in rectangularity is marked. Grain-oriented nickel-steel strip such as Orthonik is usually wound into toroids, to insure that the flux flows in the preferred direction. The toroidal cores are protected from mechanical damage and strain by encasing them, as in Fig. 224, after the core material is annealed to preserve the magnetic properties. Grain-oriented silicon-steel cores are much less sensitive to damage; type C cores may be used, with coils wound as described in Chapter 2.

In either type of core there is a small inevitable air gap. In a toroid, the flux must change from one lamination to the next as it flows around the core. If the insulating space between laminations is 0.0005 in. and the average core length is 5 in., the effective core gap

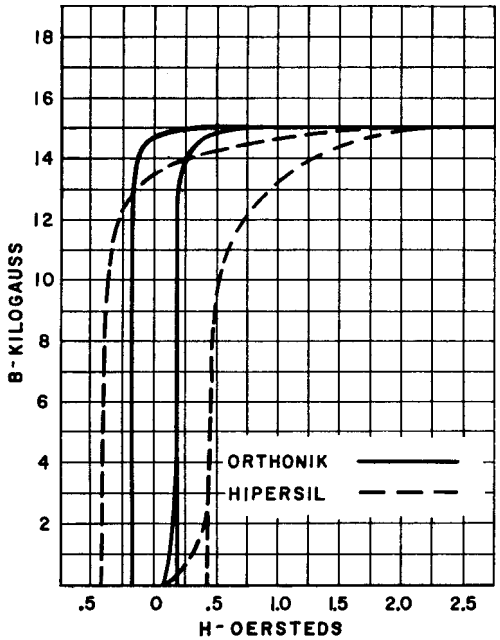

FIG. 223. Typical d-c magnetization curves and hysteresis loops for 2-mil Hipersil and 2-mil Orthonik toroidal cores.

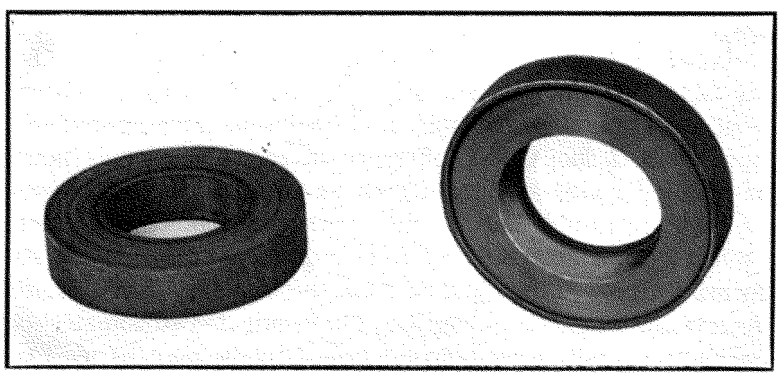

FIG. 224. Toroidal core of grain-oriented nickel steel in case, and with top of case removed.

is $0.0005/5 = 0.0001$ in. This gap is not negligible in high-permeability core material, but it is about one-tenth of the gap that manufacturers allow in type C cores. Effective core gap requires more control NI/in. and reduces gain because the gap causes a more sloping B-H loop. See Fig. 242 (p. 310). Special U-shaped punchings of grain-oriented steel are sometimes used with alternate stacking to reduce the effective core gap.

Another effect that reduces gain is rectifier "back" resistance, or current flow during the part of the negative half-cycle when inverse voltage exists across the diode. The peak value of inverse voltage divided by the corresponding reverse current is the rectifier back resistance. For a given peak source voltage $\sqrt{2}\,E$, the inverse peak rectifier voltage is $2\sqrt{2}\,E$ in the center-tap d-c circuit, and it is $\sqrt{2}\,E$ in the bridge circuit, for zero winding and rectifier forward IR drops. In a doubler amplifier with zero forward drop, inverse peak voltage is zero, and increases with forward drop up to a maximum of $\sqrt{2}\,E$. The reverse current corresponding to these voltages resets the core more than control circuit current with no rectifier reverse current. This causes transfer characteristic slope to decrease; the unity ordinate of the normalized transfer curve is displaced to the right by the ratio of reverse current to cut-off control current I_C. Normal cut-off control current I_C and cut-off output current I_N are not affected, because I_C operates to reduce *load* current during the positive half-cycle. Good-quality rectifiers are as important as good core material. This applies equally well to leakage current and forward current IR drop. Losses may limit output in rectifiers as well as in reactors. Most of the I^2R loss in windings of self-saturated amplifiers is usually in the load windings. This loss occurs during the part of the cycle in which load current flows, or while the core is saturated and core loss is zero. I^2R loss is a maximum when $\theta_1 = 0$ in Fig. 214(b). When $\theta_1 = 180°$, I^2R loss is negligible and core loss is a maximum.

When the supply frequency is high, choice of rectifiers is limited to those with good high-frequency properties. At radio frequencies this may mean that suitable rectifiers are not available; simple magnetic amplifiers must then be used. To reduce core loss at high frequencies, ferrites are used.

Insulation of toroidal coils is difficult to apply. Insulation between concentric windings is taped in and out like the wire. If voltage is low, the wire enamel is sufficient insulation. For 115- or 230-volt circuits, windings are laid on the core progressively, that is, with turns bunched

so that adjacent turns have but a small a-c voltage difference. Insulation difficulties increase with voltage, and high-voltage reactors are preferably layer wound, with type C or stacked cores.

Induced voltage in control windings requires careful attention, especially when control current is limited and many control turns are required. Although fundamental a-c voltage cancels in the control circuit, the full magnitude of this voltage is induced in the control windings. In the example of simple magnetic amplifier given in Section 111, the voltage induced in the control windings is $2{,}500/65 \times 100 = 3{,}850$ volts. With layer-wound coils and solventless resin coil impregnation the insulation is readily provided, but it would be difficult with toroidal coils.

Winding space in a toroid is limited by the minimum practicable hole size in the finished coil. This varies with the kind of winding machine and also with the size of toroid. If

d_1 = hole diameter
d_2 = core case inside diameter
d_3 = core case outside diameter
A_w = total winding area,

then

$$A_w = (\pi/4)(d_2^2 - d_1^2) \tag{124}$$

On the outside of the toroid, the winding builds to a smaller height than on the inside. Since A_w is fixed by the minimum hole size, the coil outside diameter is

$$d_4 = \sqrt{d_3^2 + (4A_w/\pi)} \tag{125}$$

$$\text{Coil axial length} = \text{Core case height} + 2A_w/l_c \tag{126}$$

$$\text{Mean turn of first winding} = \text{Case periphery} + \pi A_{w1}/l_c \tag{127}$$

where A_{w1} is area occupied by first winding. Equation 127 is approximate because wire turns tend to become circular after several layers are wound on the core.

Example. Control Reactors for Single-Phase Rectifier. Assume the following conditions:

Power supply 400 cycles.
Center-tap d-c circuit per Fig. 217(*c*).
Control current available = 40 ma d-c.
Plate transformer E = 125 volts per side.

At full output $I_{dc} = 2$ amp in R_L.

Per cent reduction in $E_{dc} = 33$ per cent at minimum output.

Assume grain-oriented nickel-steel core with $A_c = 0.1$ sq in., $l_c = 5.5$ in., and $B_s = 14{,}700$ gauss.

Core-case dimensions 1¼ in. I.D., 2^3⁄$_{16}$ in. O.D., 1^5⁄$_{32}$ in. high.

Each reactor must be capable of absorbing the voltage-time integral corresponding to 33 per cent voltage reduction, or $0.33 \times 125 = 41$ volts. From equation 34 (p. 83),

$$N_L = \frac{3.49 \times 41 \times 10^6}{400 \times 0.1 \times 14{,}700} = 244 \text{ turns}$$

With full output, load winding current $= 2\pi/(2 \times 2) = 1.57$ amp rms. From Fig. 219(a) this can be controlled with $H = 0.5$ oersted

$$0.5 = 0.5 N_C I_C / l_c$$

$$N_C = l_c / I_C = 5.5/0.04 = 138 \text{ turns}$$

This will be increased to 276 turns to allow for rectifier reverse current, variations in slope of the core B-H loop, and effective core gap. Using 650 cir mils per ampere, and single enameled wire, yields $1.57 \times 650 = 1{,}020$ cir mils or No. 20 wire for N_L, and $0.040 \times 650 = 26$ cir mils or No. 35 wire for N_C. With an average winding area space factor of 60 per cent, the coil winding areas required are, from Table V (p. 37), $244/(860 \times 0.60) = 0.48$ in.^{2} for N_L and $276/(24{,}500 \times 0.60) = 0.019$ in.^{2} for N_C. If N_C turns are wound concentrically over N_L, the load winding inside diameter is, from equation 124,

$$d_1 = \sqrt{d_2^2 - (4A_w/\pi)}$$

$$= \sqrt{(1.25)^2 - (4 \times 0.48/\pi)} = 0.975 \text{ in.}$$

N_C turns occupy but a single layer. Then, for N_C, $d_1 = 0.955 - 2(0.0064) = 0.94$ in. With 10-mil insulation over N_C, the hole diameter becomes $0.94 - 0.02 = 0.92$ in. Space required to insulate the ends of the windings and space for additional control windings reduce the hole diameter further.

Winding mean turn lengths are, for a core-case periphery of 1.88 in.,

$$MT_L = 1.88 + \frac{\pi \times 0.48}{5.5} = 2.16 \text{ in.}$$

$$MT_C = 2.16 + \pi([0.48/5.5] + 0.0064 + 0.020) = 2.44 \text{ in.}$$

$$\text{Resistance of load winding} = \frac{244 \times 2.16 \times 10.3}{12{,}000} = 0.45 \text{ ohms}$$

$$\text{Resistance of control winding} = \frac{276 \times 2.44 \times 338}{12{,}000} = 19 \text{ ohms}$$

Load winding $IR = 0.71$ volt. $I^2R = 1.12$ watt.
Control winding $IR = 0.76$ volt. $I^2R = 0.0305$ watt.

$$\text{Power gain} = \frac{\frac{125}{1.11} \times [1 - (0.67)^2]}{0.0305} = 2{,}050$$

$$\text{Time constant} = \frac{41 \times 276}{1.11 \times 0.76 \times 244 \times 800} = 0.07 \text{ sec}$$

with no external series resistance in the control circuit. With feedback applied to the control winding, this rectifier can be made self-regulating. If the feedback is further refined by comparison with a voltage reference, a stable voltage regulator results.

121. Magnetic-Amplifier Limitations. Several limitations may affect the practical usefulness of magnetic amplifiers. Some of these limitations are beneficial in certain applications:

1. Residual output with zero input.
2. When more than one reactor is used in a circuit, reactor cores must often be matched.
3. Zero drift. At low input levels (of the order of 10^{-13} watt for toroids of rectangular loop core material) magnetic amplifiers do not track because of hysteresis.
4. Amplifiers with feedback or high-gain self-saturated amplifiers are subject to instability when biased to cut-off and may change linear amplifiers into bistable amplifiers.
5. When the amplifier operates over a wide range of ambient temperature, variations in resistance of the reactors and rectifiers, and hysteresis loop width, cause changes in gain, output, and balance.
6. Response time of a magnetic amplifier is a limitation in comparison with an electronic amplifier.
7. Variations in supply frequency and voltage cause variations in gain and output, especially with self-saturated amplifiers.
8. Whereas the vacuum tube is a relatively high-impedance device, the magnetic amplifier is better adapted to low impedances, where the turns are fewer.
9. Saturation inductance is greater than the leakage inductance of the reactor, measured as in a transformer. The B-H curve slope at B_s, even with rectangular loop core materials, always gives μ greater than unity at the top. This effect reduces output and gain, and causes a sloping wave front at the instant of firing.

Many ingenious circuits have been devised to overcome one or more of these limitations. For descriptions of these circuits, for refinements of operation, and for fields of application, the reader is referred to the bibliography on magnetic amplifiers.

10. PULSE AND VIDEO TRANSFORMERS

122. Square Waves. Square waves or pulses differ from sine waves in that the front and back sides of the wave are very steep and the top flat. Such pulses are used in the television and allied techniques to produce sharp definition of images or signals. A square wave can be thought of as made up of sine waves of a large number of frequencies starting with, say, audio frequencies and extending into the medium r-f range. The response of a transformer to these frequencies determines the fidelity with which the square wave is reproduced by the transformer. Some pulses are not square, but have sloping sides and a round top, like a half-wave rectifier voltage. Such pulses will not be discussed here, because if a transformer or circuit is capable of reproducing a square wave, it will reproduce a rounded wave at least as well.

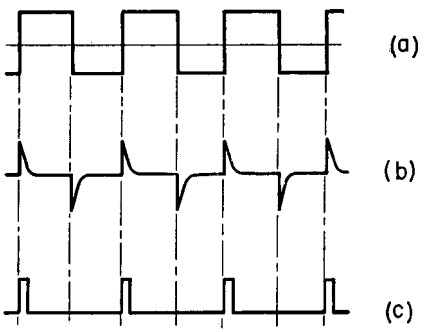

FIG. 225. Square waves differentiated and clipped.

Square waves can be generated in several ways: sometimes from sine waves by driving a tube into the diode region each cycle. The plate circuit voltage wave form is then different from that of the grid voltage because the round top of the sine wave has been removed. By repeating this process (called clipping) in several stages, it is possible to produce very square waves, alternately plus and minus, like those of Fig. 225(*a*). If a voltage having such a wave form is applied across a capacitor, it causes current to flow in the capacitor only at the vertical edges, as in Fig. 225(*b*). If a voltage proportional to this current is then successively amplified and clipped at the base, it results in the wave form of Fig. 225(*c*). Here the negative loops are assumed to be missing, as they could be after single-side amplification. The wave is

again square but of much shorter duration than in Fig. 225(*a*), and the interval between pulses greatly exceeds the pulse duration. The pulse duration is usually referred to as the pulse width, and the frequency at which the pulses occur is called the repetition rate and is expressed as pulses per second (pps). Common pulse widths lie between 0.5 and 10 microseconds; the intervals between pulses may be between 10 and 1,000 times as long as the pulse width. These values are representative only, and in special cases may be exceeded several-fold. The general wave shape of Fig. 225(*c*), with short pulse duration compared to the interval between pulses, is the main subject of this chapter. The ratio of peak to average voltage or current may be very high, and the rms values appreciably exceed average in such pulses.

There are two ways in which the response of any circuit to a square wave can be found. The first of these consists in resolving the pulse into a large number of sine waves of different frequencies, finding the response of the circuit to each frequency and summing up these responses to obtain the total response. This can be formulated by a Fourier integral, but for most circuits the formulation is easier than the solution. An approximation to this method is the arbitrary omission of frequency components having negligible amplitude, and calculation of the circuit response to the relevant frequencies. This approximation has two subjective criteria: the number of frequencies to be retained, and the evaluation of the frequency components for which the circuit has poor response.

The second method, which will be used here, consists in finding the transient circuit response to the discontinuities at the front and trailing edges of the square wave. It is possible to reduce the transformer to a circuit amenable to transient analysis, without making any more assumptions than would be necessary for practical design work with the Fourier method. The transient method has the advantage of giving the total response directly, and it can be plotted as a set of curves which are of great convenience to the designer. The major assumption is that one transient disappears before another begins. If good square wave response is obtained, this assumption is justified.

Analyses are given of the influence of iron-core transformer and choke characteristics on pulse wave forms. In all these analyses the transformer or choke is reduced to an equivalent circuit; this circuit changes for different wave forms, portions of a wave form, and modes of operation.

Initial conditions, resulting formulas, and plots of the formulas for

design convenience are given for each case. Formulas may be verified by the methods of operational calculus.

123. Transformer-Coupled Pulse Amplifiers. The analysis here given is for a square- or flat-topped pulse impressed upon the transformer by some source such as a vacuum tube, a transmission line, or

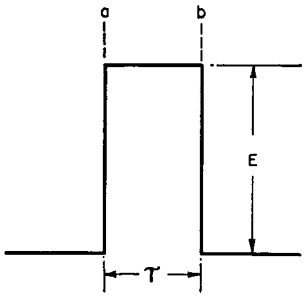

FIG. 226. Flat-topped pulse.

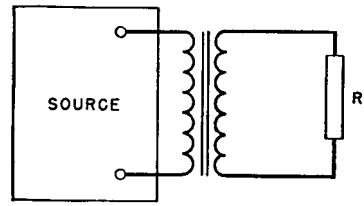

FIG. 227. Transformer coupling.

even a switch and battery. Such a pulse is shown in Fig. 226, and a generalized circuit for the amplifier is shown in Fig. 227. The equivalent circuit for such an amplifier is given in Fig. 228. At least this is the circuit which applies to the front edge a of the pulse shown in Fig. 226 as rising abruptly from zero to some steady value E. This change is sudden, so that the transformer OCL can be considered as presenting infinite impedance to such a change, and is omitted in Fig. 228. Transformer leakage inductance, though, has an appreciable influence and is shown as inductance L_s in Fig. 228. Resistor R_1 of Fig. 228 repre-

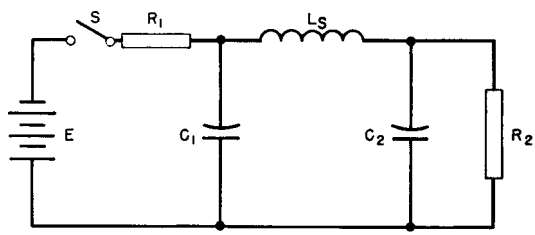

FIG. 228. Equivalent circuit.

sents the source impedance; transformer winding resistances are generally negligible compared to the source impedance. Winding capacitances are shown as C_1 and C_2 for the primary and secondary windings, respectively. The transformer load resistance, or the load resistance into which the amplifier works, is shown as R_2. All these values are

referred to the same side of the transformer. Since there are two capacitance terms C_1 and C_2, it follows that, for any deviation of the transformer turns ratio from unity, one or the other of these becomes predominant. Turns ratio and therefore voltage ratio affect these capacitances, as discussed in Chapter 5; for a step-up transformer, C_1 may be neglected, and, for a step-down transformer, C_2 may be neglected. The discussion here will be confined first to the step-up case.

124. Front-Edge Response. The step-up transformer is illustrated by Fig. 229. When the front of the wave (Fig. 226) is suddenly im-

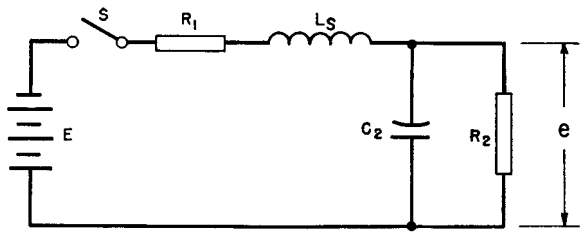

FIG. 229. Circuit for step-up transformer.

pressed on the transformer, it is simulated by the closing of switch S. At this initial instant, voltage e across R_2 is zero, and the current from battery E is also zero. This furnishes two initial conditions for equation 128, which expresses the rate of rise of voltage e from zero to its final steady value $E_a = ER_2/(R_1 + R_2)$:

$$e = \frac{ER_2}{R_1 + R_2}\left[1 + \frac{m_2\epsilon^{m_1 t}}{m_1 - m_2} - \left(1 + \frac{m_2}{m_1 - m_2}\right)\epsilon^{m_2 t}\right] \qquad (128)$$

where $m_1, m_2 = -m(1 \pm \sqrt{1 - 1/k_1^2})$.

Figure 230 shows the rate of rise of the transformed pulse for $R_1 = 0$ and Fig. 231 for $R_1 = R_2$. In hard-tube modulators, source resistance is comparatively small and approaches $R_1 = 0$. Line-type modulators are usually designed so that $R_1 = R_2$.

The scale of abscissas for these curves is not time but percentage of the time constant T of the transformer. The equation for this time constant is given in Figs. 230 and 231. It is a function of leakage inductance and of capacitance C_2. The rate of voltage rise is governed by another factor k_1, which is a measure of the extent to which the circuit is damped. The relation of this factor k_1 and the various con-

stants of the transformer is given directly in Figs. 230 and 231. The greater the transformer leakage inductance and distributed capacitance, the slower is the rate of rise, although the effect of R_1 and R_2 is important, for they affect the damping factor k_1. If a slight amount of

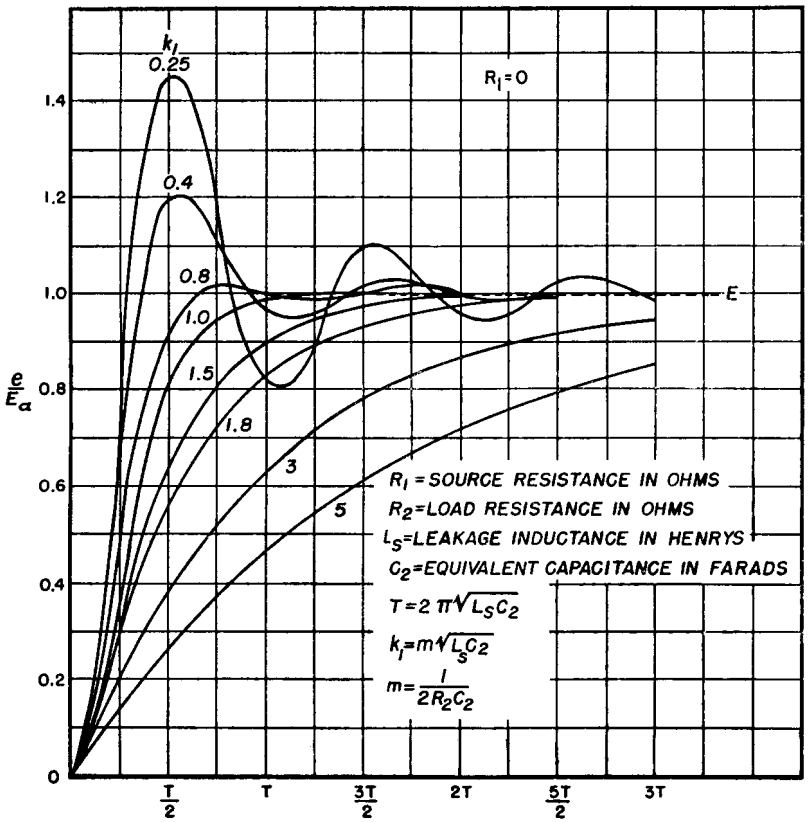

FIG. 230. Influence of transformer constants on front edge of pulse ($R_1 = 0$). For equivalent circuit see Fig. 229.

oscillation can be tolerated, the wave rises up faster than if no oscillation is present. Yet, if the circuit is damped very little, the oscillation may reach a maximum initial voltage of twice steady-state voltage E_a, and usually such high peaks are objectionable. The values for k_1 given in these figures are those which fall within the most practicable range. Time required for pulse voltage to reach 90 per cent of E_a is given in Fig. 232.

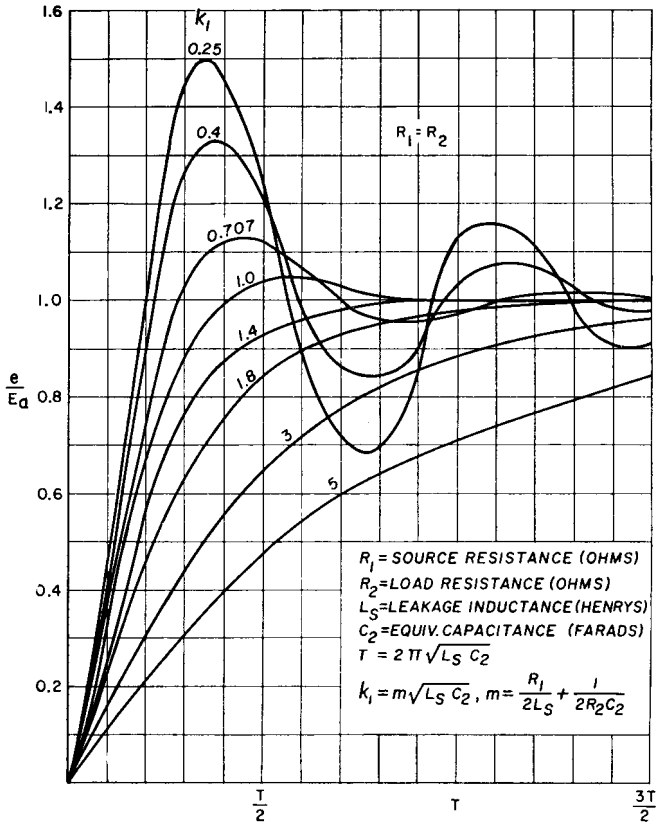

FIG. 231. Influence of transformer constants on front edge of pulse ($R_1 = R_2$).

125. Response at the Top of the Pulse. Once the pulse top is reached, E_a is dependent on the transformer OCL for its maintenance at this value. If the pulse stayed on indefinitely at the value E_a, an infinite inductance would be required to maintain it so, and of course this is not practical. There is always a droop at the top of such a pulse. The equivalent circuit during this time is shown in Fig. 233. Here the inductance L is the OCL of the transformer, and R_1 and R_2 remain the same as before. Since the rate of voltage change is relatively small during this period, capacitances C_1 and C_2 disappear. Also, since leakage inductance usually is small compared with the OCL, it is neglected. At the beginning of the pulse, the voltage e across R_2 is assumed to be at steady value E_a which is true if the voltage rise is rapid. Curves for the top of the wave are shown by Fig. 234. Several curves

are given; they represent several types of pulse amplifiers ranging from a pentode in which R_2 is one-tenth of R_1, to an amplifier in which load resistance is infinite and output power is zero. In the latter curve, the

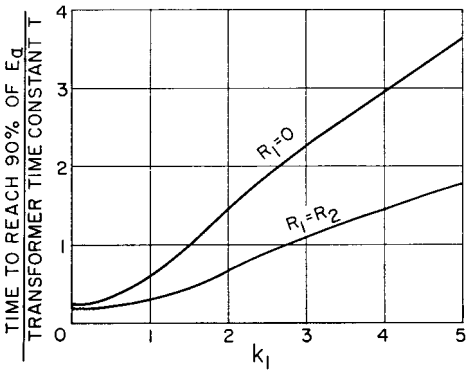

FIG. 232. Time required to reach 90 per cent of final voltage.

voltage e has for its initial value the voltage of the source. All the curves are exponential, having a common point at 0, 1. Abscissas are the product of time τ and R_1/L_e, time τ being the duration of the pulse between points a and b in Fig. 226. The greater the inductance L_e the less the deviation from constant voltage during the pulse.

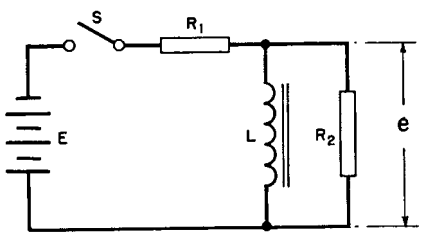

FIG. 233. Circuit for top of pulse.

126. Trailing-Edge Response. At instant b in Fig. 226, it is assumed that the switch S in Fig. 233 is opened suddenly. The equivalent circuit now reverts to that shown in Fig. 235, in which L_e is the OCL, and C_D is total capacitance referred to the primary. Figure 235 illustrates the decline of pulse voltage after instant b (Fig. 226), the equation for which is:

$$e = \frac{E_a}{m_1 - m_2}[(m_1 + 2\Delta m)\epsilon^{-m_1 t} - (m_2 + 2\Delta m)\epsilon^{m_2 t}] \qquad (129)$$

where $m_1, m_2 = -m(1 \pm \sqrt{1 - 1/k_3^2})$, $m = \frac{1}{2}R_I C_D$, and other terms are defined in Fig. 235. Abscissas are time in terms of the time constant determined by OCL and capacitance C_D. Ratio k_3 on these curves has

a different meaning, and time constant T is greater than in Fig. 230, but with low capacitance k_3 is high and the curves with higher values of k_3 drop rapidly. The slope of the trailing edge can be kept within tolerable limits, provided that the capacitance of the transformer is small enough. Accurate knowledge of this capacitance is therefore important. Measurement and evaluation of transformer capacitance should be made as in Chapters 5 and 7.

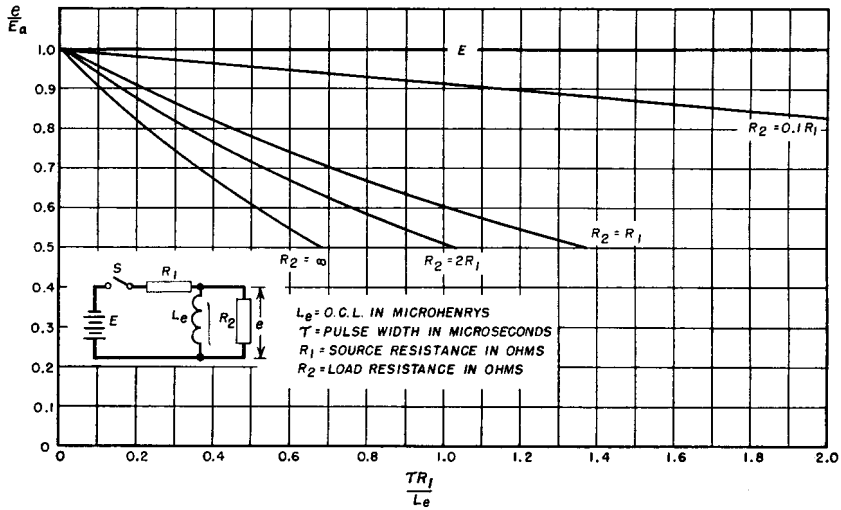

FIG. 234. Droop at top of pulse transformer output voltage.

If the transformer has appreciable magnetizing current, the shape of the trailing edge is changed. The greater the magnetizing current, the more pronounced the negative voltage backswing. The ordinates at the left of Fig. 235 are given in terms of the voltage E_a, at instant a, as if there were no droop at the top of the pulse. These curves apply when there is droop, but then the ordinates should be multiplied by the fraction of E_a to which the voltage has fallen at the end of the pulse.

Magnetizing current at the end of the pulse is

$$i_M = (E_a/mL)(1 - \epsilon^{-m\tau}) \tag{130}$$

where $m = R_1R_2/(R_1 + R_2)L$ (see Fig. 233)
τ = pulse duration in seconds
L = primary OCL in henrys

Magnetizing current can be expressed as a fraction Δ of the primary load current I, or $\Delta = i_M/I$. For any R_1/R_2 ratio, $\Delta = [(R_1 + R_2)/R_1]$

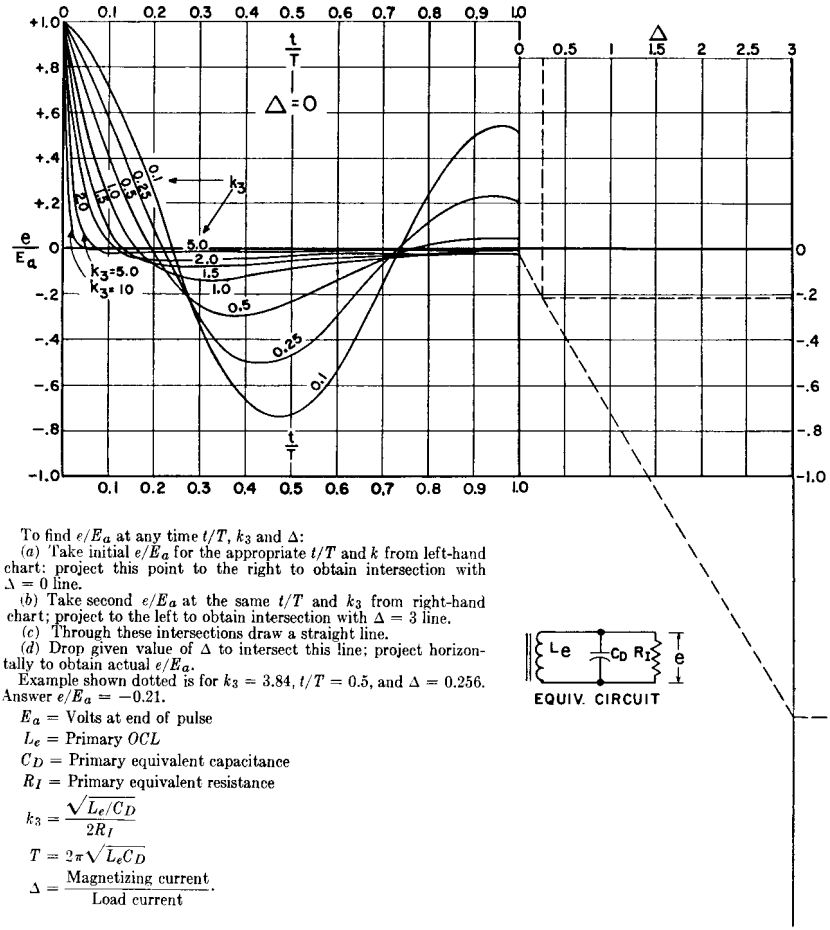

To find e/E_a at any time t/T, k_3 and Δ:
(*a*) Take initial e/E_a for the appropriate t/T and k from left-hand chart: project this point to the right to obtain intersection with $\Delta = 0$ line.
(*b*) Take second e/E_a at the same t/T and k_3 from right-hand chart; project to the left to obtain intersection with $\Delta = 3$ line.
(*c*) Through these intersections draw a straight line.
(*d*) Drop given value of Δ to intersect this line; project horizontally to obtain actual e/E_a.
Example shown dotted is for $k_3 = 3.84$, $t/T = 0.5$, and $\Delta = 0.256$. Answer $e/E_a = -0.21$.

E_a = Volts at end of pulse
L_e = Primary *OCL*
C_D = Primary equivalent capacitance
R_I = Primary equivalent resistance

$$k_3 = \frac{\sqrt{L_e/C_D}}{2R_I}$$

$$T = 2\pi\sqrt{L_eC_D}$$

$$\Delta = \frac{\text{Magnetizing current}}{\text{Load current}}.$$

FIG. 235. Interpolation chart for

× voltage droop at point *b* (Fig. 226), or

$$E'/E_a = 1 - R_1\Delta/(R_1 + R_2) \qquad (131)$$

where E_a = voltage at point *a* (Fig. 226), and E' = voltage at point *b*.

This equation gives the multiplier for finding the actual trailing-edge voltage from the backswing curve parameters in Fig. 235. With increasing values of Δ the backswing is increased, especially for the damped circuits corresponding to values of $k_3 \geqq 1.0$. The same is also true for lower values of k_3, but with diminishing emphasis, so that in Fig. 235 exciting current has less influence on the oscillatory

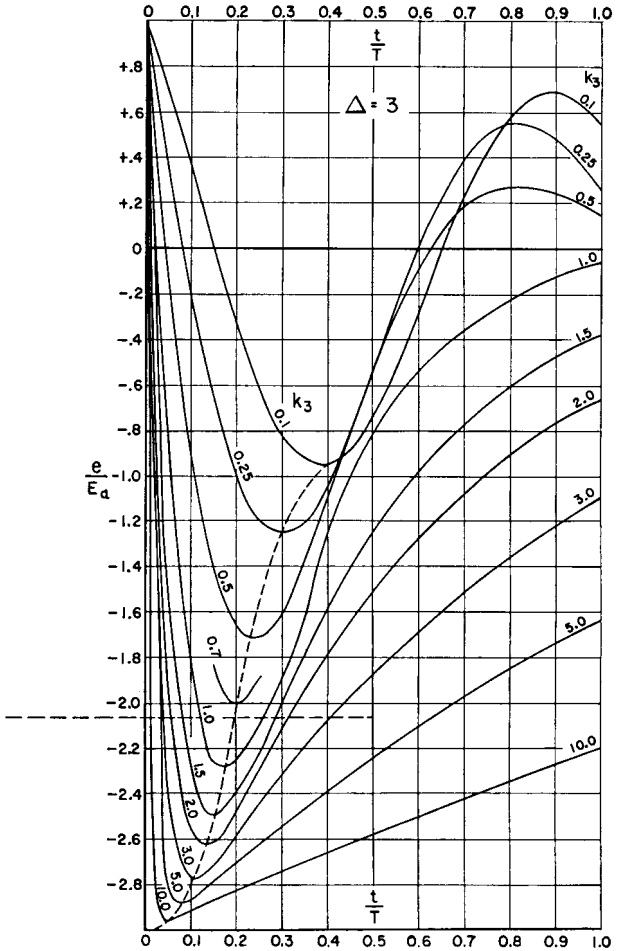

pulse transformer backswing.

backswings. These afford poor reproduction of the original pulse shape, but occasionally large backswing amplitudes are useful, as mentioned in Section 137.

Equation 129 is plotted at the left of Fig. 235 for $\Delta = 0$, and at the right of Fig. 235 for $\Delta = 3$. Instructions are given under Fig. 235 for finding the backswing in terms of E_a by interpolation for $0 < \Delta < 3$, and for given values of k_3 and t/T. This chart eliminates the labor of solving equation 129 for a given set of circuit conditions. Elements L_e, C_D, and R_I in Fig. 235 sometimes include circuit components in addi-

tion to the transformer, as will be explained later. For linear resistive loads, the terms are interchangeable with L and R_2 of Fig. 233, and with C_2 of Fig. 229, all referred to the primary winding.

In transformers with oscillatory constants the backswing becomes positive again on the first oscillation. In some applications this would appear as a false and undesirable indication of another pulse. The conditions for no oscillations are all included in the real values of the equivalent circuit angular frequency, i.e., by the inequality

$$\frac{1}{4R_I^2C_D^2} > \frac{1}{L_eC_D}$$

or

$$\sqrt{L_e/C_D} > 2R_I \tag{132}$$

Terms are defined in Fig. 235.

The quantity $\sqrt{L_e/C_D}$ may be regarded as the open-circuit impedance of the transformer. Its value must be more than twice the load resistance (on a 1:1 ratio basis) to prevent oscillations after the trailing edge. This requires low distributed capacitance.

Likewise the negative backswing may prove objectionable in certain apparatus. Certain conditions for avoiding all backswing are those represented in Fig. 235 by $k = 5$ and $\Delta = 0$; these require good core material, low exciting current, low distributed capacitance, and a loaded transformer.

127. Total Response. By means of the curves we can now construct the pulse shape delivered to load R_2. Suppose that a transformer with the following properties is required to deliver a flat top pulse of 15 microseconds' duration.

Primary leakage inductance (secondary short-circuited)	$= 1.89 \times 10^{-4}$ henry
Primary open-circuit inductance	= 0.1 henry
Primary/secondary turns ratio N_p/N_s	= 1:3
Source resistance R_1	= 800 ohms
Load resistance (primary equivalent) R_2	= 5,000 ohms
Primary effective capacitance C_2	= 448 $\mu\mu$f

From the expressions given in Fig. 230

$$m = 2.34 \times 10^6$$

$$T = 1.8 \text{ microseconds}$$

$$k_1 = 0.68$$

The front of the wave follows a curve between those marked $k_1 = 0.4$ and $k_1 = 0.8$ in Fig. 230. Value E_a is reached in $0.5T$ or 0.85 microsecond, and an overshoot of about 10 per cent occurs in 1.2 microseconds.

The top of the wave slopes down to a voltage determined by the product $\tau R_1/L_c = 0.12$, and by a curve between those for $R_2 = \infty$ and $R_2 = 2R_1$ in Fig. 234. Voltage E' at b is evidently $0.9E_a$.

The trailing edge is found from Fig. 235. Here

$$T = 42.2 \times 10^{-6}$$

$$k_3 = \frac{\sqrt{0.1/448 \times 10^{-12}}}{2 \times 5{,}000} = 1.5$$

$$\Delta = \frac{5{,}800}{800} \times 0.09 = 0.65$$

Load voltage reaches zero in $0.05T$ or 2.11 microseconds. The negative loop has maximum amplitude of 33 per cent E' at $0.2T$ or 8.44 microseconds beyond the pulse edge b. The pulse delivered to load R_2 is shown in Fig. 236, in terms of E instead of E_a.

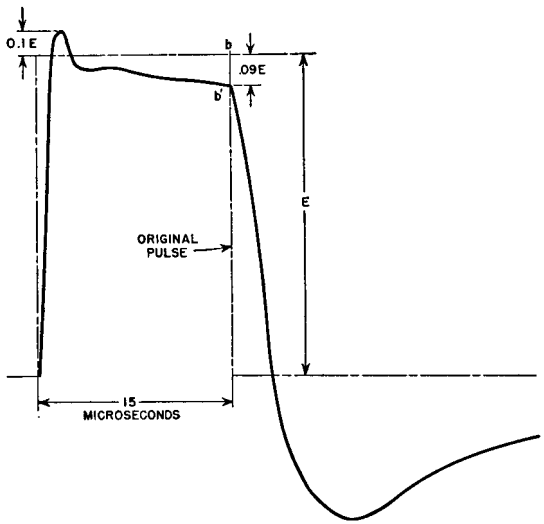

FIG. 236. Output voltage of pulse transformer.

So far we have assumed that the pulse source is disconnected at the end of the pulse. In some applications the source remains connected.

This would result if switch S (Fig. 233) were left closed, and battery E were short-circuited. Under these conditions the leakage inductance remains in the circuit, and an additional transient occurs. The transient has a shape similar to one of the curves of Fig. 231 but is inverted and superposed on the backswing voltage due to OCL. In the example just given, this superposed oscillation has an amplitude of 10 per cent of E, with a total result similar to the oscillogram of Fig. 237. Superposed backswing oscillations are discussed more fully in Section 134. Because of the distributed nature of leakage inductance and

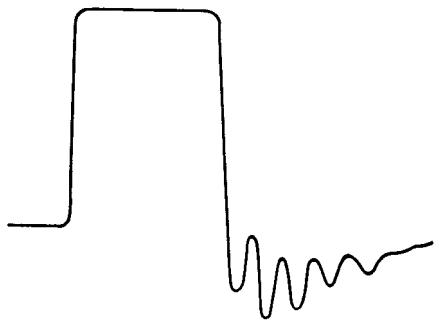

FIG. 237. Oscillogram of voltage pulse.

capacitance, higher-frequency superposed oscillations may sometimes occur even when the load is disconnected at the end of a pulse. By their very nature, the conditions for these oscillations are difficult to state with certainty, but if oscillations occur on the front edge they are likely to appear on the trailing edge, superposed on the voltage backswing.

128. Step-Down Transformers. The circuits of Figs. 229 and 233 for step-up pulse transformers are essentially the same as those of Figs. 107(e) and 107(c), respectively, for audio transformers. Low-frequency response corresponds to the top of the pulse and high-frequency response to the front edge. In step-down pulse transformers the top is unchanged, but the front edge corresponds to Fig. 113. Step-down transformer analysis shows that the form of equation is similar to that for step-up transformers, except that the damping factor for the sine term is greater by the quantity $R_2/L_s\beta$. Also, the decrement, although still composed of two terms, has the resistances R_1 and R_2 in these two terms reversed with respect to the corresponding terms for the step-up transformer. Except for this, the front-edge curves are little different in shape from those of step-up transformers. Where

$R_1 = R_2$ the curves are virtually the same as in Fig. 231. Pentode amplifiers, with their constant-current characteristics, can be represented by the circuit of Fig. 238. Here I is the current entering the primary winding from the tube, and is constant over most of the voltage range. The transformer is usually step-down for the reasons of impedance mentioned in Section 70 (Chapter 5). Front-edge response of these transformers is the same as in Fig. 230 if the rise in load current is expressed as a fraction of final current I, and the decrement is changed to $R_2/2L_s$. It is reproduced in Fig. 239 with this change in constants. Flatness of top is approximately that of the curve $R_2 = 0.1R_1$ in Fig. 234. Trailing edge is the same as in Fig. 235.

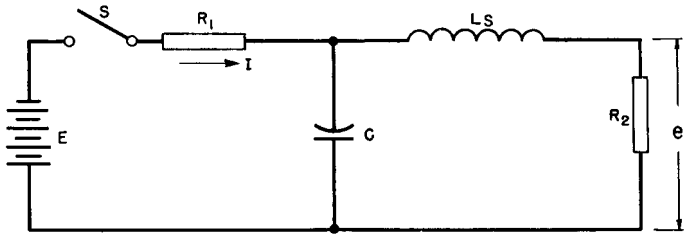

FIG. 238. Step-down transformer equivalent circuit.

It is evident that many practical cases are represented by the figures. If transformer constants are outside the curve values, the pertinent equation should be plotted to obtain the response.

129. Frequency Response and Wave Shape. Because of the prevalent thinking of engineers in terms of frequency response rather than wave shape, it is sometimes necessary to correlate the two concepts. The matter of phase shift enters, for the reason that the relative phase of the different frequency components affects wave shape. It is sometimes convenient to know whether a transformer, whose frequency response is known, can deliver a given wave shape. Starting with the low-frequency response, assume equal source and load resistances; the upper curve of Fig. 108 (p. 148) applies. This curve shows 90 per cent of maximum response at the frequency for which $X_N/R_1 = 1$. How does this frequency compare with the reciprocal of the pulse width at the end of which there is 10 per cent droop in the top of the pulse? X_N/R_1 can be written

$$2\pi fL/R_1 = 1 \quad \text{or} \quad f = R_1/2\pi L \tag{133}$$

Likewise, from the proper curve of Fig. 234, for 10 per cent droop,

$$\tau R_1/L = 0.2 \tag{134}$$

Combining equations 133 and 134 gives $f = 0.0318\ (1/\tau)$, or the transformer should be not over 1 db down at a frequency about $\frac{1}{30}$ of the reciprocal of the pulse width. For example, if a maximum of 10 per cent droop is desired at 2 microseconds the response should be not

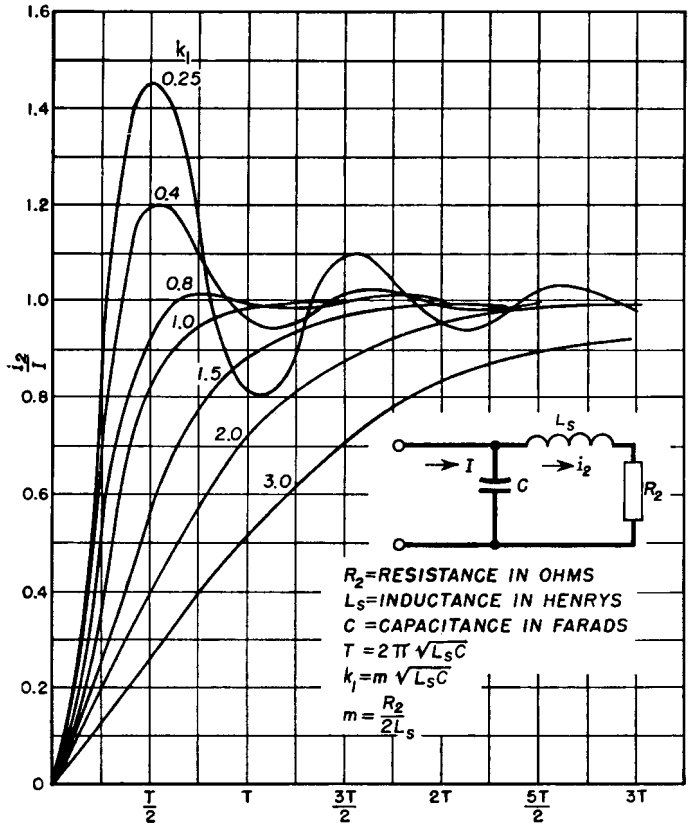

FIG. 239. Pentode amplifier front-edge response.

more than -1 db at $0.0318 \times 0.5 \times 10^6 = 16$ kc. Maximum phase shift is 27 degrees (from Fig. 131, p. 180), but this is taken into account in Fig. 234.

Similarly, front-edge steepness can be related to transformer high-frequency response, which for the case of $R_1 = R_2$ is found in Fig. 109. The corresponding front-edge curves are found in Fig. 231. Parameter k_1 of these curves is related to B in Fig. 109 as follows.

$$k_1 = m\sqrt{LC} = \frac{R_1\sqrt{LC}}{2L} + \frac{\sqrt{LC}}{2R_1C} \quad \text{(for } R_1 = R_2\text{)}$$

$$B = \frac{X_C}{R_1} = \frac{X_L}{R_1} \quad \text{at frequency } f_r$$

$$= \frac{2\pi f_r L}{R_1} = \frac{L}{R_1\sqrt{LC}}$$

$$k_1 = \frac{1}{2B} + \frac{B}{2} \tag{135}$$

From equation 135 we can prepare Table XVI.

TABLE XVI. PARAMETERS FOR FREQUENCY RESPONSE AND WAVE SHAPE

B	k_1
1.0	1.0
0.8, 1.25	1.025
0.67, 1.5	1.08
0.5, 2	1.25
0.25, 4	2.125

If a transformer has frequency response according to the curve for $B = \frac{1}{2}$, 2 in Fig. 109, its front edge will rise somewhere between curves for $k_1 = 1$ and $k_1 = 1.4$ in Fig. 231.

Transformer OCL, leakage inductance, and effective capacitance must be known to make this comparison, but these quantities are already known if it is established that the frequency response is given by Figs. 108 and 109, or the wave shape by Figs. 231 and 234. If conditions other than $R_1 = R_2$ prevail, another set of response curves can be used, and corresponding approximate relations can be found in the manner here outlined.

Pulse transformer windings are similar to those in the high-frequency transformers described in Section 87 (Chapter 7). Resonance frequency f_r is determined largely by leakage inductance and winding-to-winding capacitance. With pulse operation, partial resonances of sections of a coil, and even turn-to-turn resonance, may appear because of the steep front edge of voltage impressed on the transformer. If these resonances cause pronounced oscillations in the output wave form, larger coil or turn spacings or fewer turns may be necessary to reduce them.

130. Core Material. In Chapter 7 it was shown that core permeability decreases with frequency, especially at frequencies higher than audio. This decrease also occurs with short pulse widths. When a pulse is first applied to the transformer, there is initially very little penetration of flux into the core laminations because of eddy currents. Hence initially only a fraction of the total core is effective, and the apparent permeability is less than later in the pulse, or after the flux density becomes uniform throughout the laminations.

A typical *B-H* curve for pulse transformers is shown in Fig. 240. Flux density builds up in the core in the direction shown by the arrows.

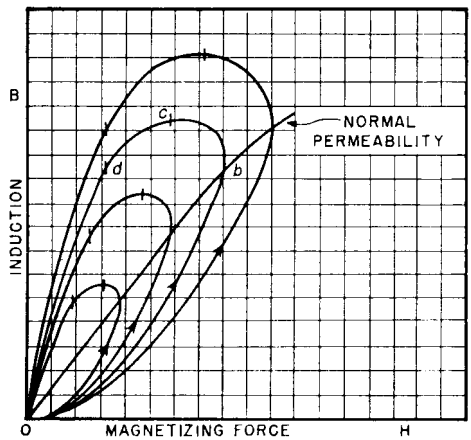

FIG. 240. Pulse *B-H* loops.

For a typical loop such as *obcd*, the slope of the loop (and hence the permeability) rises gradually to the end of the pulse *b* which corresponds to point *b'* in Fig. 236. Since magnetizing current starts decreasing at this point, *H* also starts decreasing. Current in the windings does not decay to zero immediately but persists because of winding capacitance, and sufficient time elapses for permeability to increase. Therefore, flux density *B* may also increase during a short interval after point *b*. The trailing edge of the pulse voltage soon reaches zero, and this corresponds to point *c* on the loop. At some interval later, the maximum backswing amplitude is reached, which corresponds to point *d* on the loop. At this point the slope or permeability is several times as great as at point *b*.

For any number of pulses of varying amplitudes but of the same width, there are corresponding loops having respective amplitudes *c*.

A curve drawn through point b of each loop is called the normal permeability curve, and this is ordinarily given as the permeability curve for the material. The permeability μ for a short pulse width is less than the 60-cycle or d-c permeability for the same material. Values of pulse permeability for 2-mil grain-oriented steel are given in Fig. 241. The permeability values include the irreducible small gap which exists in type C cores; the cores on which the measurements were made had a ratio of gap to core length $l_g/l_c \approx 0.0003$, but the data are not criti-

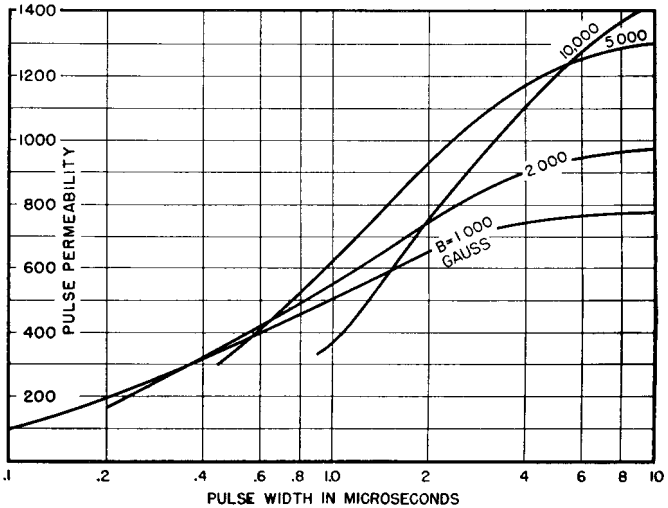

FIG. 241. Effective permeability versus pulse width.

cally dependent on this ratio. The effect of penetration time is clear.

Flux densities attained in pulse transformers may be low for small units where very little source power is available, or they may be high (several thousand gauss) in high power units. This is true whether the pulse width is a few microseconds or 1,000 microseconds.

The nickel-iron alloys in general have lower saturation densities, but higher permeabilities below saturation than either grain-oriented or ordinary silicon steel. Depending on the flux density chosen, the increase of permeability with the use of a nickel-iron alloy may vary from zero to 300 per cent. This increase holds also for long-time pulses, during which permeability may approach the 60-cycle value.

In order to overcome the net d-c pulse magnetization which is in the same direction throughout each pulse, an air gap may be inserted in the core to prevent it from returning only to the residual magnetism

value B_r at the end of each pulse, and thereby limiting its useful pulse flux density range ΔB to the difference between maximum flux density B_m and residual B_r (see Fig. 242). This gap increases the effective length of the magnetic path and reduces OCL from the value it has with symmetrical magnetization. The reduction is less with core materials of low permeability. To maintain the advantage of high permeability in nickel-iron alloys, the core is "reset." This is done by

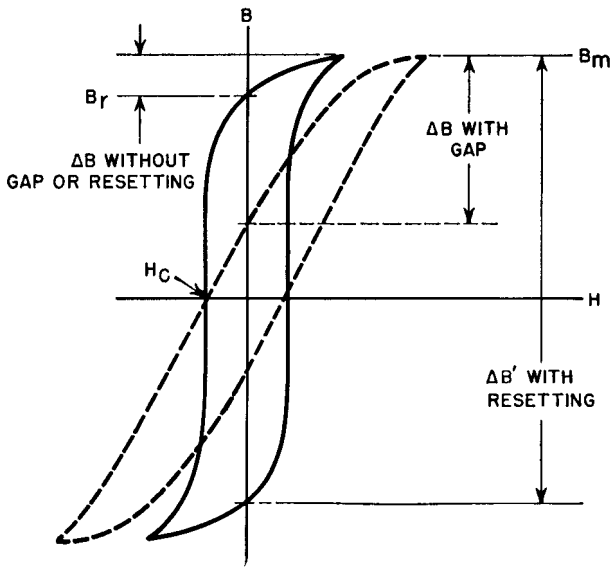

FIG. 242. Flux density range in pulse transformer cores.

arranging the circuit so that, during the period of backswing, sufficient negative current flows through the windings to overcome coercive force H_c and drop the flux density to the negative value of residual magnetism. Then nearly twice the previous maximum flux density ($\Delta B'$ in Fig. 242) is available for the pulse. Where resetting is possible, it is advantageous to use nickel-iron alloys; where resetting is not practicable, grain-oriented silicon steel is preferable.

131. Windings and Insulation. Pulse transformers generally have single-layer concentric windings with solid insulation between sections. For high load impedance, a single section each for primary and secondary as in Fig. 166 is favorable, as the effective capacitance is lowest. For low load impedance, more interleaving is used to reduce leakage inductance. To reduce capacitance to a minimum, pie-section co-

axial windings may be used. In these, coil capacitance is kept low by the use of universal windings, and intersection capacitance between windings is low because the dielectric is air. Such coils are more difficult to wind, require more space, and therefore are used only when necessary.

Coil sections can be wound with the same polarity as in Fig. 166 (p. 219) or with one winding reversed. Effective capacitance between P and S is given below for three turns ratios. Capacitance is based on 100 $\mu\mu$f measurable capacitance.

Turns Ratio	Effective Capacitance Referred to Primary	
N_1/N_2	Same Polarity	Reversed Polarity
1:5	533	1200
1:1	0	133
5:1	21	48

From this it can be seen that the polarity exemplified in Fig. 166 is preferable for reducing effective capacitance, but that the percentage difference is greatest for turns ratios near unity and less as the ratio increases.

Attention to the insulation so far has centered around capacitance. The insulation also must withstand the voltage stress to which it is subjected. It can be graded to reduce the space required. Low-frequency practice is adequate for both insulation thickness and end-turn clearances.

Small size is achieved by the use of solventless varnish. Small size with consequent low capacitance and low loss results in higher practicable impedance values and shorter pulses.

In order to utilize space as much as possible, or to reduce space for a given rating, core-type construction is often used. Low capacitance between high-voltage coils is possible in such designs. It is advantageous in reducing space to split the secondary winding into non-symmetrical sections. Although the leakage inductance is higher with non-symmetrical windings, there is less distributed capacitance when the high-voltage winding has the smaller length. Lower capacitance obtains with two coils than with a shell-type transformer of the same interleaving. In core-type transformers high-voltage windings are the outer sections. It is preferable to locate terminals or leads in the coil directly over the windings in order to maintain margins. Insulating barriers may be located at the ends of the windings to increase creepage paths.

Autotransformers, when they can be used, afford opportunity for space saving, because there are fewer total turns and less winding space is needed. Less leakage inductance results, but not necessarily less capacitance; this always depends on the voltage gradients.

Initial distribution of voltage at the front edge of a pulse is not uniform because of turn-to-turn and winding-to-winding capacitance. In a single-layer coil the total turn-to-turn capacitance is small compared to the winding-to-ground capacitance, because the turn capacitances add in series but the ground or core capacitances add in shunt. Therefore a steep wave of voltage impressed across the winding sends current to ground from the first few turns, leaving less voltage and less current for the remaining turns. Initially, most of the pulse voltage appears across the first few turns.

After a short interval of time, some of the current flows into the remaining turns inductively. Before long the capacitive voltage distribution disappears, all the current flows through all the turns, and the voltage per turn becomes uniform. This condition applies to most of the top of a pulse. Between initial and final current distribution, oscillations due to leakage inductance and winding capacitance may appear which extend the initially high voltage per turn from the first few turns into some of the remaining turns.

Winding capacitance to ground is evenly distributed along the winding of a single coil, and so is the turn-to-turn capacitance. If a rectangular pulse E is applied to one end of such a winding, and the other end is grounded, the maximum initial voltage gradient is [1]

$$\frac{\alpha E}{N} \coth \alpha$$

where N = number of turns in winding
$\alpha = \sqrt{C_g/C_w}$
C_g = capacitance of winding to ground
C_w = capacitance across winding
= turn-to-turn capacitance/N.

Practical values of α are large, and coth α approaches unity. Then

$$\text{Maximum gradient} \approx \alpha E/N \qquad (136)$$

[1] For the development of this expression see "Surge Phenomena," British Electrical and Allied Industries Research Association, 1941, pp. 223–226.

or the maximum initial voltage per turn is approximately α times the final or average voltage per turn.

If the other end of the winding is open instead of grounded, equation 136 still governs. This means that maximum gradient is independent of load. If there is a winding N_1 between the pulsed winding N_2 and ground, α depends on C_{1-2} and C_1 in series. The initial voltage in winding N_1 is [1]

$$E_1 = \frac{EC_{1-2}}{C_{1-2} + C_1} \tag{137}$$

where E_1 = initial voltage in winding N_1
E = pulse voltage applied across N_2
C_{1-2} = capacitance between N_1 and N_2
C_1 = capacitance between N_1 and core.

Thus the initial voltage in winding N_1 is independent of the transformer turns ratio. It is higher than the voltage which would appear in N_2 if N_1 were pulsed, because then current would flow from N_1 to ground without any intervening winding. If winding N_1 is the low-voltage winding (usually true), applying pulses to it stresses turn insulation less than if N_2 is pulsed.

Reinforcing the end turns of a pulsed winding to withstand better the pulse voltages is of doubtful value, because the additional insulation increases α and the initial gradient in the end turns. Increasing insulation throughout the winding is more beneficial, for although α is increased the remaining turns can withstand the oscillations better as inductance becomes effective. Decreasing winding-to-core capacitance is better yet, for then α decreases and initial voltage gradient is more uniform.

132. Efficiency. Circuit efficiency should be distinguished from transformer efficiency. Magnetization current represents a loss in efficiency, but it may be returned to the circuit after the pulse. Circuit efficiency may be estimated by comparing the area of the actual wave shape across the load to that impressed upon the transformer; it includes the loss in source resistor R_1 (Fig. 233). Except for this loss, the circuit and transformer efficiency are the same when the source is cut off at the end of the pulse. It is important in testing for losses to use the proper circuit.

Core loss can be expressed in watt-seconds per pound per pulse. A convenient way to measure core loss is to use a calorimeter. The trans-

[1] See "Surge Phenomena," pp. 227–281.

former is located in the calorimeter, and the necessary connections are made by through-type insulators. Dielectric loss is included in such a measurement. It is appreciable only in high-voltage transformers, and may be separated from the iron loss by first measuring the loss of the complete transformer and then repeating the test with the high-voltage winding removed. At 6,000 gauss and 2 microseconds pulse width, the loss for 2-mil grain-oriented steel is approximately 6,000 watts per pound, or 0.012 watt-second per pound per pulse. For square pulses, core loss varies (*a*) as B^2 or E^2 for constant pulse width and (*b*) as pulse width, for constant voltage and duty τf, where τ is the pulse width and f is the repetition rate. Dielectric loss is independent of pulse width and varies (*a*) as the repetition rate, for constant voltage, and (*b*) as E^2 for constant repetition rate.

Copper loss is usually negligible because of the comparatively few turns required for a given rating if a wire size somewhere near normal for the rms current is used. If the windings are used to carry other current, such as magnetron filament current, the copper loss may be appreciable but this is a circuit loss.

Efficiencies of over 90 per cent are common in pulse transformers, and with high-permeability materials over 95 per cent may be obtained. These figures are for pulse power of 100 kw or more. Maximum efficiency occurs when the iron and dielectric losses are equal.

133. Non-Linear Loads. The role played by leakage inductance and distributed capacitance in determining pulse shape has been mentioned in Sections 124 and 126. It has been shown that the first effect is a more or less gradual slope on the front edge of the pulse, and that the second effect consists of oscillations superposed upon the voltage backswing following the cessation of the pulse. Consider the additional influence of non-linear loads upon the first effect, that is, upon the pulse front edge.

Figure 230 is based on the following assumptions:

(*a*) Load and source impedances are linear.
(*b*) Leakage inductance can be regarded as "lumped."
(*c*) Winding capacitance can be regarded as "lumped."

Assumptions (*b*) and (*c*) are approximately justified. Pulses effectively cause the coils to operate beyond natural resonance, like the higher-frequency operation of r-f coils in Section 97 (Chapter 7). The distributed nature of capacitance and leakage inductance, as well as partial coil resonance, may cause superposed oscillations which re-

quire correction. But the general outline of output pulse shape is determined by low-frequency leakage inductance and capacitance.

Assumption (*a*) may be a serious source of error, for load impedances are often non-linear. Examples are triodes, magnetrons, or grid circuits driven by pulse transformers. In a non-linear load with current flowing into the load at a comparatively constant voltage, the problem is chiefly that of current pulse shape. First assume that no current flows into this load for such time as it takes to reach steady voltage E. During this first interval, the transformer is unloaded except for its own losses, and is oscillatory. After voltage E is reached, the current rises rapidly at first and then more slowly, as determined by the new load R_2. The sudden application of load at voltage E damps out the oscillations which would exist without this load, and furnishes two conditions for finding the initial current. A rigorous solution of the problem involves overlapping transients and is complicated.

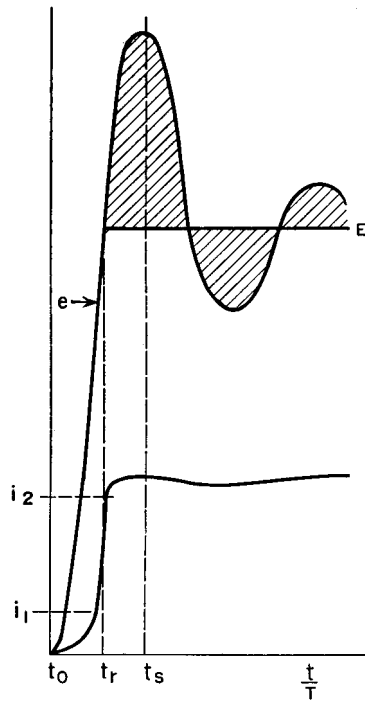

FIG. 243. Non-linear load voltage and current pulse shapes.

The problem can be simplified by assuming that the voltage pulse has a flat top E. When the pulse voltage reaches E, capacitance C_2 ceases to draw current. At the instant t_r (Fig. 243) when voltage E is first reached, the current in L_s which was drawn by capacitance C_2 flows immediately into the load. Also since the voltage was rising rapidly at instant t_r, the energy which would have resulted in the first positive voltage loop (shown shaded in Fig. 243) must be dissipated in the load. The remaining oscillations also are damped. Prior to the time t_r, all the current through L_s flowed into C_2. The value of this current is $C_2\, de/dt$. Therefore we may find the slope of the appropriate front-edge voltage curve and multiply by the transformer capacitance to obtain the initial current. Unloaded transformer front edge means small k_1 in Figs. 230 and 231. The front-edge slope at

voltage E is given in Fig. 244, the ordinates of which are $(T\ de/E)/dt$, with E corresponding to the E_a of Fig. 230. Ordinates of Fig. 244 are multiplied by C_2E/T to find the initial load current.

Few non-linear loads have absolutely zero current up to the time that voltage E is reached, and the foregoing assumptions are thus

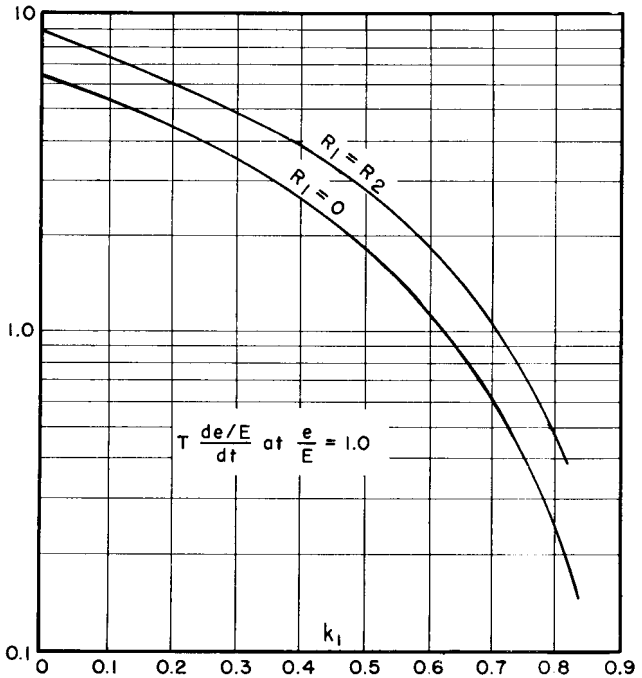

FIG. 244. Front-edge slope of pulse transformer.

approximate. In spite of this, the following procedure gives fair accuracy.

(*a*) Find the initial capacitance current as just outlined.

(*b*) Estimate the current at which the load e-i curve departs from a straight line (i_1, in Fig. 243).

(*c*) Add currents (*a*) and (*b*). This gives i_2 (Fig. 243), as the total initial current.

Pulse current continues to rise beyond the value i_2 if the initial current value just found is less than the final operating current corresponding to the voltage E; it will droop if the initial current is higher than

the load current at voltage E. To obtain constant current over the greater part of the pulse width, i_2 should equal the load current at voltage E. When this equality does not exist, the rate of rise or droop is determined by transformer leakage inductance, source impedance, and load resistance. Where the mode of operation depends upon the rate of voltage rise, as it does in some magnetrons, the initial current may drop off to nearly zero before the main current pulse starts. When there is negligible initial current i_1, the condition for a good current pulse is $E/i_2 \approx \sqrt{L_s/C_2}$, where L_s is the leakage inductance.

At the end of the pulse, when the source voltage is reduced to zero (point b, Fig. 226), the circuit reverts to that shown on Fig. 235, but the transformer loses all the load except its own losses. Since by this time it has drawn exciting current, the higher values of Δ in the backswing curves apply. Backswing amplitudes with non-linear loads are complicated and can be predicted only approximately. A procedure for line-type pulsers is given in Chapter 11.

134. Design of Pulse Transformers. (*A*) *Requirements.* The performance of a pulse transformer is usually specified by the following:

(*a*) Pulse voltage.
(*b*) Voltage ratio.
(*c*) Pulse duration.
(*d*) Repetition rate.
(*e*) Power or impedance level.
(*f*) Slope of front.
(*g*) Droop on top.
(*h*) Amount of backswing permissible.
(*i*) Type of load.

Design data for insuring that these requirements are met are provided in the foregoing sections, in several sets of curves. Below are outlined the steps followed in utilizing these curves for design purposes.

(*B*) *Start of Design.* The first step in beginning a design is to choose a core. It is helpful if some previous design exists which is close in rating to the transformer about to be designed.

After choosing the core to be used, the designer must next figure the number of turns. In pulse transformers intended for high voltages, the limiting factor is usually flux density. If so, the number of turns may be derived as follows, for unidirectional pulses:

$$e = \frac{N\,d\phi}{dt} \times 10^{-8} = NA_c \frac{dB}{dt} \times 10^{-8}$$

$$\int e\,dt = NA_c \int dB \times 10^{-8} \tag{138}$$

For a square wave, $e = E$ and

$$E\tau = NA_cB \times 10^{-8}$$

or

$$N = \frac{E\tau \times 10^8}{6.45BA_c} \tag{139}$$

where E = pulse voltage
τ = pulse duration in seconds
B = allowable flux density in gauss
A_c = core section in square inches
N = number of turns.

In many designs, the amount of droop or the backswing which can be tolerated at the end of the pulse determines the number of turns, because of their relation to the OCL of the transformer.

After the turns are determined, appropriate winding interleaving should be estimated and the leakage inductance and capacitance calculated.

With the leakage inductance and winding capacitance estimated, the front-end performance for linear loads can be found from Figs. 230 and 231. Likewise, from OCL and winding capacitance, the shapes of the top and trailing edge are found in Figs. 234 and 235. If performance from these curves is satisfactory and the coil fits the core, the design is completed.

(*C*) *Final Calculations.* Preliminary calculations may show too much slope on the front edge of the pulse (as often happens with new designs). Two damping factors $R_1/2L_s$ and $1/2R_2C_2$ contribute to the front-edge slope, and the preliminary calculations show which one is preponderant. Sometimes it is possible to increase leakage inductance or capacitance without increasing time constant T greatly, and this may be utilized in decreasing the slope.

If the front-edge slope is still too much after these adjustments, the core chosen is probably inadequate. Small core dimensions are desirable for low leakage inductance and winding capacitance. Small core area A_c may require too many turns to fit the core. These two considerations work against each other, so that the right choice of core is a problem in any design.

If the calculated front-edge slope is nearly good enough it may be improved by one of the following means:

(*a*) Change number of turns.
(*b*) Reduce core size.
(*c*) Change interleaving.
(*d*) Increase insulation thickness.
(*e*) Reduce insulation dielectric constant.

High capacitance is a common cause of poor performance and items (*b*) to (*e*) may often be changed to decrease the capacitance. It is sometimes possible to rearrange the circuit to better advantage and thereby make a deficient transformer acceptable. One illustration of this is the termination of a transmission line. Line termination resistance may be placed either on the primary or secondary side. If it is placed on the primary side there is usually a much improved front edge. Figure 231 does not show this improvement inasmuch as it was plotted for Fig. 229. For resistance on the primary side, the damping factor reduces to the single term

$$\alpha = \frac{R_1 R_2}{2(R_1 + R_2)L_s} \tag{140}$$

Improvement of the trailing-edge performance usually accompanies improvement of the front edge.

Core permeability is important because it requires fewer turns to obtain the necessary OCL with high-permeability core material. Permeability at the beginning of the trailing edge (point b', Fig. 236) is most important, for two reasons: the droop at this point depends on the OCL, so that for a given amount of droop the turns on the core are fixed; also, the normal permeability data apply to such points as b'. Flux density is chosen with two aims: it should be as high as possible for small size, but not so high as to result in excessive magnetizing current and backswing voltage.

(*D*) *Example.* Assume that the performance requirements are:

Pulse voltage ratio 2,000:10,000 volts.
Pulse duration 2 microseconds.
Pulse repetition rate 1,000 per second.
Impedance ratio 50:1,250 ohms (linear).
To rise to 90 per cent of final voltage in ¼ microsecond or less.
Droop not to exceed 10 per cent in 2 microseconds.
Backswing amplitude not to exceed 60 per cent of pulse voltage.
50-ohm source.

The final design has the following:

Primary turns = 20.
Secondary turns = 100.

Core: 2-mil silicon steel with 1-mil gap per leg.
Core area = 0.55 sq in.
Core length = 6.3 in. ($l_g/l_c = 0.0003$).
Core weight 0.75 lb, window $\frac{5}{8}$ in. $\times$ $1\frac{9}{16}$ in.
Primary leakage inductance = 2 microhenrys.
Effective primary capacitance = 1,800 $\mu\mu$f.
No-load loss equivalent to 400 ohms (referred to primary).

$$\text{Flux density} = \frac{10{,}000 \times 2 \times 10^2}{6.45 \times 100 \times 0.55} = 5{,}600 \text{ gauss.}$$

At 2 microseconds and $B = 5{,}600$ $\mu \approx 600$.

$$\text{Primary } OCL = \frac{3.2 \times 400 \times 0.55 \times 10^{-8}}{0.002 + (6.3/600)} = 550 \ \mu\text{h.}$$

Front-edge performance is figured as follows:

$$m = \frac{R_1}{2L_s} + \frac{1}{2R_2C_2} = \frac{50 \times 10^6}{4} + \frac{10^6}{0.1 \times 1.8} = 18 \times 10^6$$

$$T = 6.28 \times 10^{-6}\sqrt{2 \times 0.0018} = 0.375 \text{ microsecond}$$

$$k = 1.08$$

According to Fig. 231, this value of k gives 90 per cent of E_a in $0.35T$ or 0.131 microsecond.

The top is figured at

$$\frac{\tau R_1}{L_e} = \frac{2 \times 50 \times 10^{-6}}{550 \times 10^{-6}} = 0.18$$

and from the curve $R_1 = R_2$ in Fig. 234, the top droops 9 per cent.

The magnetizing current is

$(R_1 + R_2)/R_1 \times 9$ per cent or 18 per cent of the load current

For the backswing

$$m = \frac{10^6}{0.1 \times 1.8} = 5.5 \times 10^6$$

$$T = 6.28 \times 10^{-6}\sqrt{550 \times 0.0018} = 6 \text{ microseconds}$$

$$k = 5.2$$

From Fig. 235, the backswing is 20 per cent of E_a. If the load resistance is connected to the transformer when the pulse voltage is removed, the backswing superposed oscillation has the same k (1.08) as the front edge, that is, there is no oscillation and the total backswing voltage is 20 per cent of E_a.

Suppose the load were non-linear; the voltage would rise up to E within $\frac{1}{4}T$ or 0.094 microsecond. The front edge

$$m = \frac{50 \times 10^6}{4} + \frac{10^6}{0.8 \times 1.8} = 13.2 \times 10^6$$

and

$$k = 0.8$$

From Fig. 244,

$$\frac{T}{E}\frac{de}{dt} = 0.44$$

The secondary effective capacitance is 1,800/25 = 72 $\mu\mu$f and the initial load current is

$$C\frac{de}{dt} = \frac{72 \times 0.44 \times 10{,}000}{0.375 \times 10^6} = 0.84 \text{ amp}$$

Final load current is 10,000/1,250 = 8 amp, and current is non-uniform during the pulse. The backswing is calculated in Chapter 11.

Secondary current is 8 amp. The rms value of this current is, from Table I (p. 16),

$$I_{\text{rms}} = 8\sqrt{2 \times 10^{-6} \times 1{,}000} = 0.36 \text{ amp}$$

and the primary current is $5 \times 0.36 = 1.8$ amp. The wire insulation must withstand 10,000 ÷ 100 = 100 volts per turn, and with single-layer windings this normally requires at least 0.0014 in. of covering insulation. Heavy enamel wire, No. 28, has a margin of insulation over this value. This is further modified by the initial non-uniform voltage distribution as figured below. A sectional view of a two-coil design is shown in Fig. 245, with No. 28 heavy enamel wire

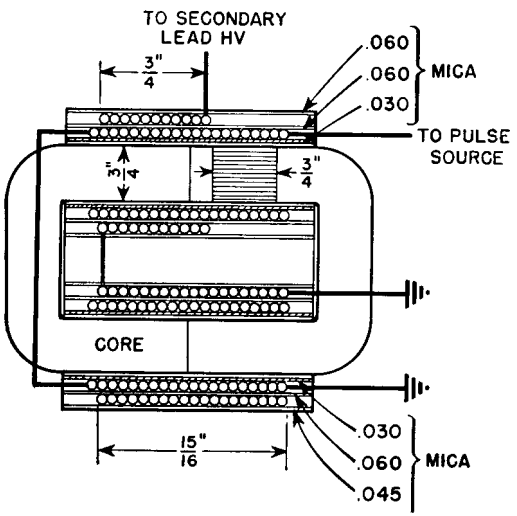

FIG. 245. Section of pulse transformer.

in the secondary and No. 22, wound two in parallel to occupy the form fully, in the primary. The core section is ¾ in. by ¾ in. The primary turn length is 3.75 in. and that of the secondary is 4.13 in. Primary and secondary d-c resistances are 0.05 and 2.3 ohms, and the respective copper losses are

$$\begin{aligned}(1.8)^2 \times 0.05 &= 0.162\\ (0.36)^2 \times 2.3 &= 0.3\\ \text{Total} \qquad &= 0.462\end{aligned}$$

The no-load loss is $[(2{,}000)^2/400] \times 1{,}000 \times 2 \times 10^{-6} = 20$ watts. Copper loss is therefore of little significance.

From the coil dimensions and insulation thicknesses we can figure the capacitances. The total winding traverse for both coils is 1.875 in. The primary-to-core capacitance is

$$\frac{0.225 \times 3.75 \times 1.875 \times 5}{0.030} = 264\ \mu\mu\text{f}$$

and the secondary-to-primary capacitance is

$$\frac{0.225 \times 4.13 \times 1.875 \times 5}{0.060} = 145\ \mu\mu\text{f}$$

so that these two capacitances in series are 94 $\mu\mu$f. Secondary turn-to-turn capacitance is, approximately,

$$\frac{0.225 \times 4.13 \times 0.0126 \times 3}{0.0019} = 18.4$$

or

$$C_w = 0.184$$

α is therefore $\sqrt{94/0.184} = 22.5$, and the wire enamel initially must withstand 2,250 volts per turn.

Figure 246 is a photograph of the transformer with Fosterite-treated coils.

135. Testing Technique. Tests for open circuits, short circuits, turns ratio, and d-c resistance are made on pulse transformers in the same manner as in other transformers. The instruments used must be suitable for the low values of inductance encountered, but otherwise no special precautions are necessary. Usually the d-c resistance is somewhat lower than the winding resistance during most of the pulse, but even the latter value is so low that it causes no significant part of the transformer loss. Losses are measured as described in Section 132.

Various methods have been used to check effective pulse *OCL*. These may involve substitution of known inductances, or current build-up, or decay, depending on the time constant of the transformer

inductance and an external known resistance. When such measurements are attempted under pulse conditions, there is usually a certain amount of error due to reflections, incidental capacitance, and the like. A method involving the measurement of pulse permeability and calculation by the OCL formula is given here.

If the air gap and pulse permeability are known, the OCL for a given core area and number of turns can be calculated. If the gap used is

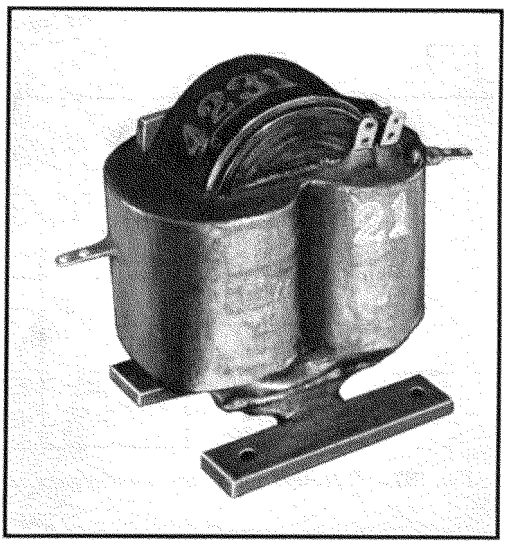

FIG. 246. Pulse transformer with coils of Fig. 245.

purposely made large to reduce saturation, proper allowance for it can be made in equation 38 (p. 97). If the gap is the minimum obtainable, it is necessarily included in the permeability measurement, but this is often done in taking pulse permeability data, as it was in the data of Fig. 241. With this definition of permeability equation 38 reduces to

$$OCL = (3.2\mu N^2 A \times 10^{-8})/l_c \qquad (141)$$

Equation 141 is valid only when $l_c/\mu \gg l_g$.

B-H data for a pulse transformer are taken by means of a circuit similar to that of Fig. 247. Primary current flowing through small resistor R_1 gives a horizontal deflection on the oscilloscope proportional to I and therefore H for a given core. R_1 should be low enough in ohmic value not to influence the magnetizing current wave form

appreciably. If the voltage drop across a high-resistance load R_2 (≈ 50 times normal pulse load) is almost the entire secondary voltage e_2, then voltage e_c applied to the vertical plates is the time integral of e_2 and is therefore proportional to flux density at any instant. (See equation 138.)

Short leads and the reduction of incidental capacitance are essential to obtain accurate measurements. Distributed capacitance of the winding, shown dotted, should be minimized, as it introduces extrane-

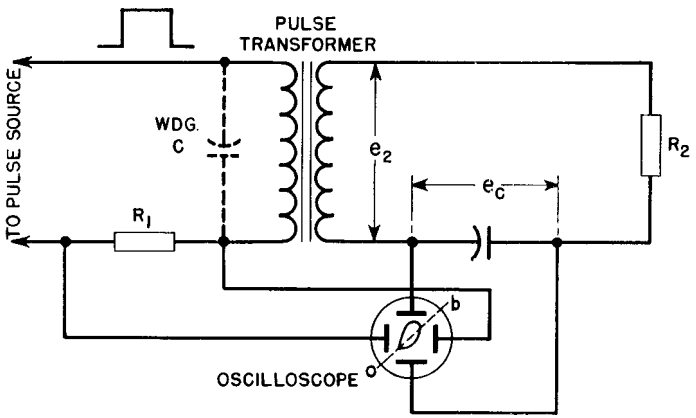

FIG. 247. *B-H* test for pulse transformers.

ous current into the measurement of H. One way to minimize this capacitance is to omit the high-voltage winding, and make all measurements from the low-voltage low-capacitance coil only.

The pulse source should be the kind for which the transformer is to be used. If it must be loaded to obtain proper pulse shape, a diode may be used to prevent backswing discharge through this load and therefore a reset core, unless reset core data are desired. Difficulty may be experienced in seeing the *B-H* loops of pulses having a low ratio of time on to time off because of the poor spot brilliance, unless an intensifier is used to brighten the trace.

With a calibrated oscilloscope it is possible to determine the slope of the dotted line *ob* in Fig. 247, drawn between the origin and the end of the pulse, and representing effective permeability μ at instant b, Fig. 226. This value of μ can be inserted in equation 141 to find OCL. Cores failing to meet the OCL should first be examined for air gap.

Effective values of leakage inductance and capacitance are difficult

to measure. The calculations of capacitance and leakage inductance are based on the assumption of "lumped" values, the validity of which can be checked by observing the oscillations in an unloaded transformer when pulse voltage is applied. The frequency and amplitude of these oscillations should agree with those calculated from the leakage inductance and effective capacitance. The pulse source should be

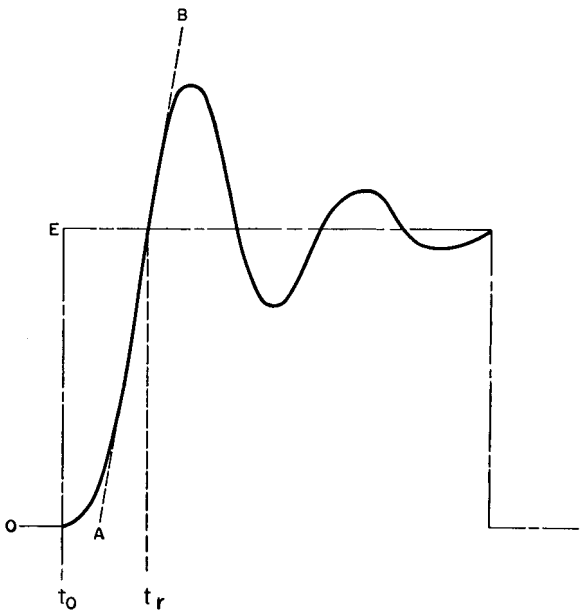

FIG. 248. Transformer constants may be found from pulse shape.

chosen for the squareness of its output pulse. Because of the light load, the transformer usually will be oscillatory, and produce a secondary pulse shape of the kind shown in Fig. 248. In this figure, the dot-dash line is that of the impressed pulse and the solid curve is the resulting transformer output voltage. This curve is observed by connecting the vertical plates of a synchroscope (oscilloscope with synchronized sweep) across the transformer output winding.

The first check of leakage L_s and C_2 is made by finding the time constant T from

$$T = 2\pi\sqrt{L_s C_2}$$

This time constant can be related to the time interval t_0–t_r in Fig.

248 by consulting Fig. 230. Formulas in this figure can be used for finding values of parameter k_1 using L_s, C_2, source resistance R_1 and load resistance R_2. This load resistance will be that corresponding to transformer losses only; hence R_2 R_1 for a pulse source with plenty of power, and

$$k_1 = \frac{\sqrt{L_s/C_2}}{2R_2}$$

With this value of k_1, the increase or overshoot of the first voltage oscillation over the flat top value E may be found from Fig. 230, and may be compared with that observed in the test. When the load is resistive, or when the voltage pulse is the criterion of pulse shape, these are the only checks that need to be made on leakage inductance and distributed capacitance.

When the load is a magnetron, triode, blocking oscillator, grid circuit, or other non-linear load, the shape of the current pulse is important. Ordinarily the current will not build up appreciably before time t_r in Fig. 248. The shape of this current pulse and sometimes the operation of the load are determined to a large extent by slope AB of the no-load voltage at time t_r. This time is the instant when the first oscillation crosses the horizontal line E in Fig. 248. As indicated in Fig. 244, there is a relationship between this slope and the parameter k_1. If the slope AB is confirmed, correct current pulse shape is also assured.

Insulation can be tested in one of two ways, depending on whether the insulation and margins are the same throughout the winding or whether the insulation is graded to suit the voltage. In the former case an equivalent 60-cycle peak voltage, applied from winding to ground at the regular 60-cycle insulation level, is sufficient. But, if the winding is graded, this cannot be done because the voltage must be applied across the winding and there is not sufficient OCL to support low-frequency induced voltage; hence a pulse voltage of greater than normal magnitude must be applied across the winding. Adequate margins support a voltage of the order of twice normal without insulation failure.

Such pulse testing also stresses the windings as in regular operation, including the non-uniform distribution of voltage gradient throughout the winding. The higher-voltage test ought to be done at a shorter pulse width so that saturation does not set in. In cases of saturation,

the voltage backswing is likely to exceed the pulse voltage of normal polarity and thus subject the insulation to an excessive test. This backswing may be purposely used to obtain higher voltage than the equipment can provide, but it must be carefully controlled. Corona tests are sometimes used in place of insulation tests, and this can be done, where the insulation is not graded, by using a 60-cycle voltage and a sensitive receiver to pick up the corona noise. With graded

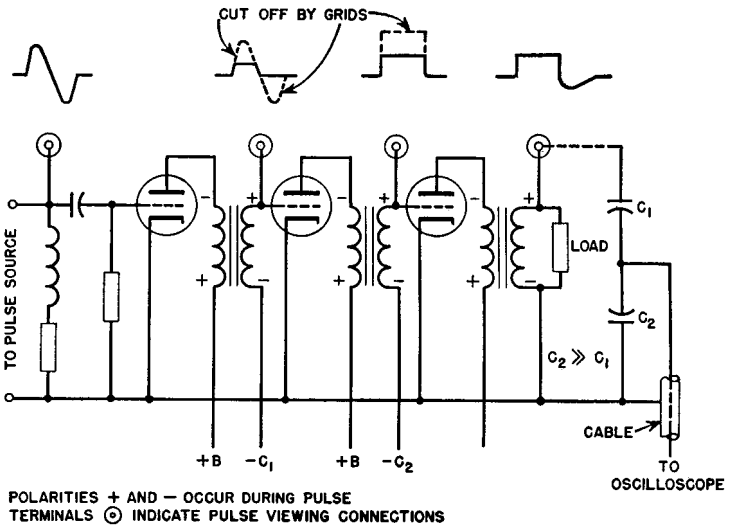

FIG. 249. Pulse amplifier with oscilloscope connections.

insulation a high frequency must be used. The method becomes too difficult to use because the receiver may pick up part of the high-frequency power emitted from the transmitter, or the transmitter parts may generate a certain amount of corona which is more troublesome than at 60 cycles.

In pulse amplifiers, the mode of operation of the tubes and circuit elements is important. A round irregular pulse may be changed by grid saturation, or by non-linear loading of some other sort, into a practically square wave pulse. It may take several stages of amplification to do this in certain instances, and a transformer may be used at each stage. Often the function of the transformer is to invert the pulse for each stage; that is, the transformer changes it from a negative pulse at the plate of one stage to a positive pulse on the grid of the next. Polarity is therefore important and should be checked dur-

ing the turns-ratio test. If the transformer fails to deliver the proper shape of pulse, it may be deficient in one of the properties for which tests are mentioned above. Figure 249 shows a pulse amplifier with normal pulse shapes for each stage. Checking each stage at the points indicated, without spoiling the pulse shape by the measuring apparatus, requires attention to circuit impedance, stray capacitance, cable termination, and lead length.

11. PULSE CIRCUITS

Pulse generation and utilization require the use of various non-sinusoidal devices. Formation of pulses from sine waves was mentioned briefly in Chapter 10. In the following sections, other methods of forming and using pulses are described.

136. Blocking Oscillators. Blocking oscillators are used to obtain pulses at certain repetition rates. The pulse may be used to drive a

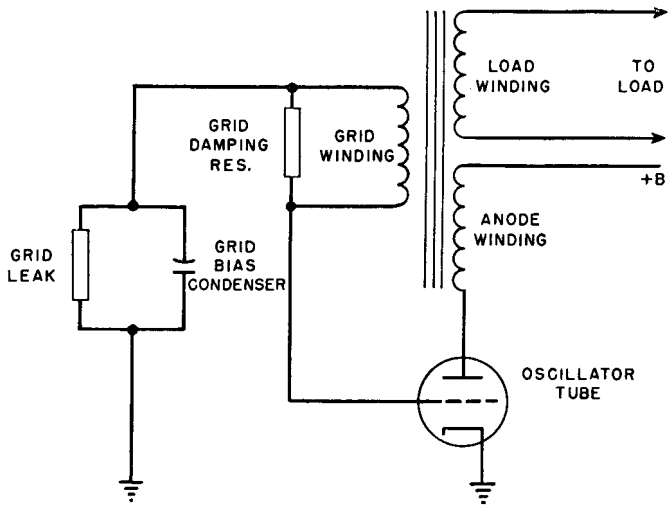

FIG. 250. Blocking oscillator.

pulse amplifier, or it may be used to modulate a *UHF* oscillator.

A typical blocking oscillator circuit is shown in Fig. 250. The grid is driven hard, and grid current usually is comparable in magnitude to anode current. Grid and anode winding turns are approximately equal. The oscillator operates as follows.

If the grid is only slightly negative, the tube draws plate current and because of the large number of grid turns the transformer drives the grid positive, increases the plate current, and starts a regenerative

action. During this period, the grid draws current, charging the bias capacitor to a voltage depending on the grid current flowing into the bias resistor-capacitor circuit. The negative plate voltage swing is determined by grid saturation, so that large positive swings of grid voltage result in virtually constant plate voltage. This continues for a length of time determined by the constants of the transformer, after which the regenerative action is reversed. Because of lowered plate voltage swing, the plate circuit can no longer drive the low impedance

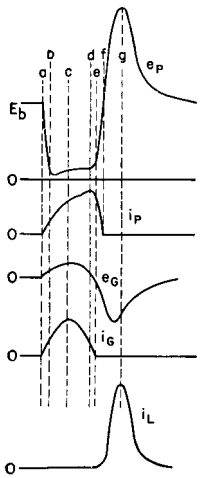

INSTANT a - PULSE STARTS. ANODE CURRENT RISES.

INSTANT b - SUDDEN RISE IN ANODE CURRENT INDUCES ANODE WINDING VOLTAGE PEAK, PROBABLY AT SATURATION VALUE.

INSTANT c - DUE TO COUPLING K < 1, GRID VOLTAGE PEAKS LATER. GRID CURRENT PEAKS SIMULTANEOUSLY.

INSTANT d - ANODE CURRENT MAXIMUM ANODE VOLTAGE STARTS TO FALL

INSTANT e - GRID VOLTAGE AND CURRENT ZERO

INSTANT f - ANODE VOLTAGE AND CURRENT ZERO.

INSTANT g - VOLTAGE BACKSWING REACHES PEAK. CAUSES PEAK LOAD CURRENT i_L.

FIG. 251. Blocking oscillator voltages and currents.

reflected from the grid, and the charge accumulated on the bias capacitor becomes great enough to decrease plate current rapidly in a degenerative action. Plate current soon cuts off, and then the plate voltage overshoots to a high positive value and the grid voltage to a high negative value. Grid voltage decays slowly because of the discharge of the bias capacitor into the grid leak. The next pulse occurs when the negative grid voltage decreases sufficiently so that regenerative action starts again. Hence the repetition rate depends on the grid bias R and C.

Either the negative or the positive pulse voltage may be utilized. Instantaneous voltages and currents are shown in Fig. 251 for a load which operates only on the positive pulse. The general shapes of these currents and voltages approximate those in a practical oscillator, except for superposed ripples and oscillations which often occur.

The negative pulse has a much squarer wave shape than the positive

pulse, and consequently it is used where good wave shape is required. No matter how hard the grid is driven, plate resistance cannot be lowered below a certain value; so a limit to the negative amplitude is formed. There is no such limit to the positive pulse, and this characteristic may be used for a voltage multiplier.

If the transformer has low OCL, the leakage inductance may be high enough to perform like an air-core transformer. That is, there are optimum values of coupling for maximum power transfer, grid drive, and negative pulse shape, but they are not critical. Comparison of peak voltages in Fig. 251 shows that the usual 180° phase relationship between grid and plate swings do not hold for such a blocking oscillator, if the term "phase" has any meaning in this case.

The front-edge slope of the negative pulse is determined by leakage inductance and capacitance as in Fig. 230, with two exceptions: the pulse is negative and the load is non-linear; hence there are no oscillations on the inverted top. The slope of this portion can be computed from Fig. 234, provided tube and load resistances are accurately known. The positive pulse can be found from Fig. 235 if these curves are inverted.

Pulse width, shape, and amplitude also are affected by the ratio of grid turns to plate turns in the transformer. Voltage rise is steeper as this ratio is greater, with the qualification that grid capacitance increases as the square of the grid turns; the ratio is seldom greater than unity. The exact ratio for close control depends on tube data which may not be available and must be determined experimentally. The situation parallels that of the class C low-Q oscillators mentioned in Chapter 6.

The circuit of Fig. 250 is called a free-running blocking oscillator. When it is desired to synchronize or otherwise control the pulse repetition rate, an external "trigger" pulse is applied to the blocking oscillator grid or cathode.

137. Line-Type Radar Pulsers. Figure 252 is the schematic diagram of a line-type pulser or modulator. This pulser is of the variety known as d-c resonant charging, with hold-off diode. The operation of the pulser is as follows:

During the charging period of each cycle, the diode permits direct current to flow through the charging reactor to the pulse-forming network and through the primary of the pulse transformer to ground. The rate of charging is governed largely by the inductance of the charging reactor and pulse-forming network capacitance. The inductances in the pulse-forming network and the leakage inductance

of the pulse transformer are so small as to be negligible during this period.

The pulse transformer load is the magnetron, which is operated with high negative potential on the cathode. A double winding is provided on the pulse transformer secondary to permit filament current to flow into the magnetron filament. The reactances of the pulse-forming network and the charging reactor at their resonant frequency are high compared to the circuit equivalent series resistance. Therefore, the pulse-forming network charges up to a voltage $2E$, where E

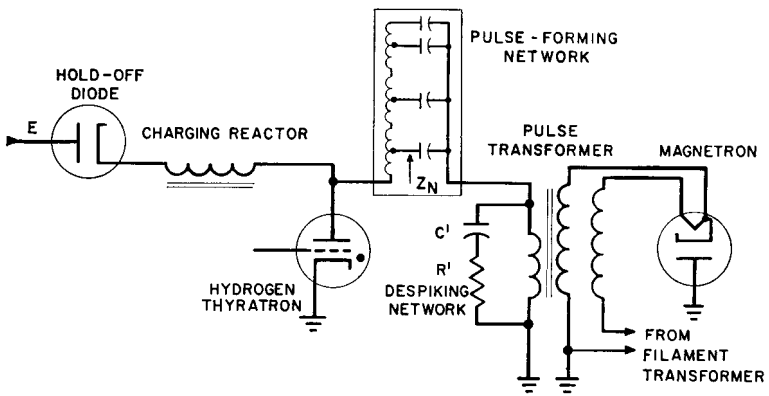

FIG. 252. Simplified schematic of modulator.

is the d-c supply voltage. Negligibly small voltage appears on the pulse transformer and magnetron during the charging interval.

After the pulse-forming network has charged up fully, it is prevented from discharging back through the d-c source by the hold-off diode. At some subsequent instant, a trigger voltage on the grid of the hydrogen thyratron causes the thyratron to conduct and permits the pulse-forming network to discharge through the very low internal resistance of the thyratron.

The sudden discharge of current through the thyratron causes a voltage wave to start down the pulse-forming network as in Fig. 253. This voltage is an inverted step function with a value $(2E - E) = E$. Initial voltage $2E$ on this network is divided equally between the network and the pulse transformer primary, and produces pulse voltage E, of duration τ. The pulse width τ is the length of time that the pulse takes to travel down the pulse-forming network (*PFN*) and back. After time t_1 the circuit is ready to charge slowly again through the charging reactor. Magnetron current and voltage rise at the

pulse leading edge in general accordance with the explanation of Section 133, but sometimes "despiking" network $R'C'$ is included to reduce current oscillations. In this pulser, the magnetron equivalent resistance R_M (referred to the pulse transformer primary) is equal to Z_N, the pulse-forming network impedance.

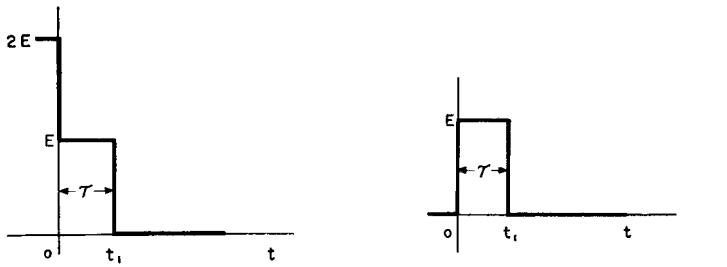

FIG. 253. Modulator voltages.

If the magnetron circuit opens during pulser operation, voltage applied to the pulse transformer primary is doubled. This may cause insulation failure if the open circuit continues. For this reason, spark gaps are often provided on pulse transformers in line-type pulsers.

138. False Echoes after Main Pulse. Trailing-edge oscillations are of two general types: (1) a long-term or low-frequency oscillation (see Fig. 254) dependent on capacitance C_D and pulse transformer open-circuit inductance L_e, and (2) a superposed high-frequency oscillation dependent on capacitance C_D and L'_N ($= PFN$ inductance L_N plus pulse transformer leakage inductance L_S). If these oscillations exceed zero in the positive or main pulse direction, false "echoes" of two kinds may occur: close echoes, adjacent to the main pulse, and distant echoes which appear later at a comparatively longer time interval. Either of these cause the magnetron to give a false indication. The distant echo corresponds to oscillation (1), and the close echo superposed on this long-term backswing to oscillation (2). These are represented in Fig. 254 as oscillations f_3 and f_2, respectively. With proper attention to the circuit constants, it is possible to eliminate both types of echoes.

The low-frequency backswing oscillation or axis is affected by C_N only while it is still in the circuit. When thyratron conduction ceases (soon after the trailing edge becomes negative) C_N is cut out of the circuit. Once this happens, the presence or absence of distant echoes is determined only by C_D in combination with L_e and R_e. More-

over, if $C_N \gg C_D$, close echoes are also determined by C_D and L'_N, regardless of whether or not the thyratron is conducting during the close-echo interval.

Both low- and high-frequency oscillation amplitudes depend on the amount of resistance in the circuit. At instant t_1 this resistance is R_M, the magnetron resistance E/i_2 (Fig. 243), in comparison with which the transformer core-loss equivalent resistance R_e is negligibly high. After the magnetron ceases conducting, only R_e remains. Dur-

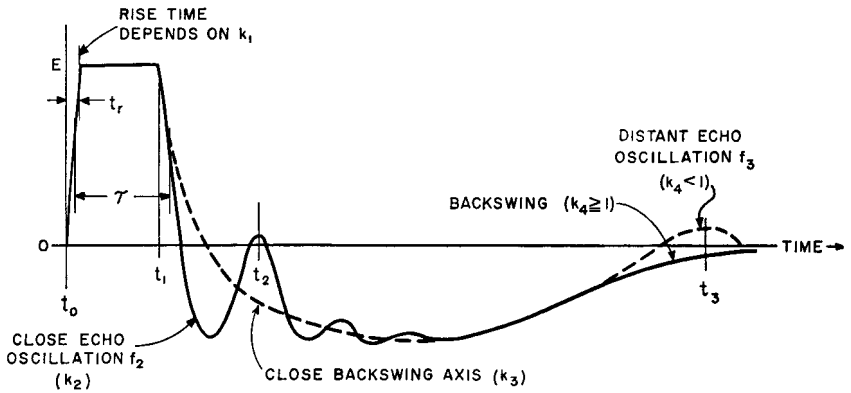

FIG. 254. Oscillations on pulse backswing.

ing the trailing-edge interval, circuit resistance varies from R_M to R_e. Resistances R_M and R_e may be replaced by their geometric mean R_I during the trailing-edge interval and the part of the backswing immediately following. This applies to both low- and high-frequency backswing oscillations during the interval t_2–t_1 (Fig. 254). The low-frequency or long-term axis of backswing may then be found from values of parameter k_3 determined by L_e, C_D, and R_I, as indicated in Fig. 235. If the oscillations are damped out, the impedance ratio still determines wave shape. This ratio is designated k_1, k_2, k_3, or k_4, depending on the portion of the pulse as indicated in Fig. 254.

If *PFN* produces an essentially square wave, front-edge wave shape at the magnetron is determined by impedance ratio

$$k_1 = \frac{R_M}{2\sqrt{L_s/C_D}}$$

It may be shown [1] that if $k_1 = 0.5$ the magnetron voltage and current

[1] See *Pulse Generators*, by Glasoe and Lebacqz, M.I.T. Radiation Laboratory Series, Vol. 5, McGraw-Hill Book Co., New York, 1948, p. 567.

rise without oscillations to final value at $t_r = 1.6\sqrt{L_s C_D}$. This k_1 has little influence on the trailing edge because L_s is usually small compared to L_e.

Oscillations occurring close to the trailing edge of the pulse are of frequency f_2 (determined by $L'_N C'_D$, where $C'_D = C_D C_N/(C_D + C_N)$, L'_N is the sum of the transformer leakage and *PFN* inductance), and of amplitude determined by

$$k_2 = \frac{1}{2R_I}\sqrt{\frac{L_N}{C'_D}}$$

This amplitude is superposed on the backswing as an axis, which, if oscillatory, has frequency f_3 determined by $L_e C'_D$. Since one purpose of good pulser design is the elimination of false echoes, the backswing axis considered here is always non-oscillatory. Assuming the thyratron is non-conducting for most of the backswing interval, the condition for non-oscillatory backswing is

$$\sqrt{\frac{L_e}{C'_D}} \geqq 2R_I \quad \text{for the close part of the backswing}$$

and

$$\sqrt{\frac{JL_e}{C_D}} \geqq 2R_e \quad \text{for the distant part}$$

where L_e is the *OCL* at time t_1 and J is the ratio of low-frequency core permeability to pulse permeability. If

$$k_3 = \frac{1}{2R_I}\sqrt{\frac{L_e}{C'_D}}$$

and

$$k_4 = \frac{1}{2R_e}\sqrt{\frac{JL_e}{C_D}}$$

then

$$k_3 > k_4$$

because generally

$$\frac{R_e}{R_I} > \sqrt{\frac{JC'_D}{C_D}}$$

So, if the pulser is designed to prevent distant echoes, $k_4 \geqq 1$ and k_3 is several times the value of k_4. Time intervals influenced by these

impedance ratios are illustrated in Fig. 254. In general, for a good pulse, the close part of the backswing axis follows a non-oscillatory pattern of relatively high-impedance ratio, such as those shown on Fig. 235 for $k_3 > 1$.

The general effect of pulse transformer magnetizing current is to depress the backswing axis. Magnetizing current does not affect the criterion for absence of false echoes $k_4 > 1$; hence a high ratio J is helpful in eliminating close echoes. The ratio Δ of magnetizing current to load current is much less for the close echo than for the distant echo because R_I is less than R_e. Close echo Δ is approximated by

$$\Delta = \frac{\tau R_I}{L_e} \tag{142}$$

To prevent close echo, the first positive peak of oscillation should be no greater than the negative backswing axis voltage at instant t_2. Backswing axis voltage may be equated to the amplitude of the first positive oscillation peak at time t_2 in Fig. 254. This equation leads to a transcendental relation between k_2, k_3, and Δ, which is plotted in

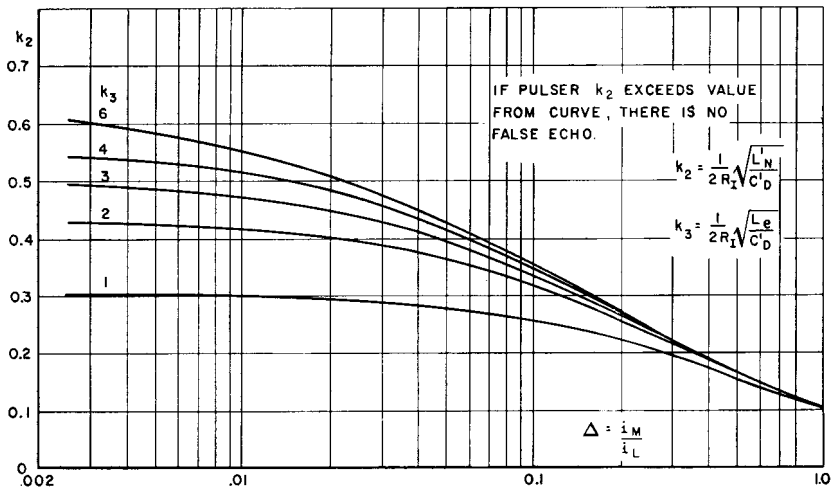

FIG. 255. Borderline of close false echoes.

Fig. 255.[1] It will be noted that all values of k_2 in Fig. 255 are less than unity. Hence, under the conditions here assumed, there is always

[1] This equation is developed in the author's "False Echoes in Line-Type Radar Pulsers," *Proc. I.R.E., 42,* 1288 (August, 1954).

a certain amount of high-frequency oscillation superposed on the backswing axis. But, if k_2 is greater than the value given by Fig. 255, there is no false close echo. Because of the approximation represented by equivalent resistance R_I, to prevent false echoes it is best if k_2 exceeds the curve value substantially. For convenience, the various impedance ratios are tabulated in Table XVII.

TABLE XVII. PULSER IMPEDANCE RATIOS

Part of Pulse Affected	Value of Load Resistance	Impedance Ratio Defined	Condition for Good Pulse Shape
Front edge	R_M	$k_1 = \dfrac{R_M}{2\sqrt{L_s/C_D}}$	$k_1 = 0.5$ for min. t_r with flat-top current pulse
Close echo	$R_I = \sqrt{R_M R_e}$	$k_2 = \dfrac{1}{2R_I}\sqrt{\dfrac{L'_N}{C'_D}}$	$k_2 \geqq$ value in Fig. 255 for no close echo
Backswing axis close to pulse	$R_I = \sqrt{R_M R_e}$	$k_3 = \dfrac{1}{2R_1}\sqrt{\dfrac{L_e}{C'_D}}$	$k_3 > k_4$ by definition
Distant echo	R_e	$k_4 = \dfrac{1}{2R_e}\sqrt{\dfrac{L_e J}{C_D}}$	$k_4 \geqq 1$ for no distant echo

Example. Suppose that the transformer of Section 134 were used in a line-type modulator with $L_N = 50\,\mu\text{h}$, $C_N = 0.02\,\mu\text{f}$, $R_I = \sqrt{50 \times 400} = 141$ ohms, $J = 2.0$. Using equation 142, for close echo,

$$\Delta = \frac{2 \times 141}{550} = 0.52$$

$$C'_D = \frac{0.02 \times 1{,}800 \times 10^{-18}}{(0.02 + 0.0018) \times 10^{-6}} = 1{,}650\ \mu\mu\text{f}$$

$$L'_N = 50 + 2 = 52\ \mu\text{h}$$

Impedance ratios:

$$k_2 = \frac{1}{2 \times 141}\sqrt{\frac{52 \times 10^{-6}}{1{,}650 \times 10^{-12}}} = 0.628$$

$$k_3 = \frac{1}{2 \times 141}\sqrt{\frac{550 \times 10^{-6}}{1{,}650 \times 10^{-12}}} = 2.04$$

$$k_4 = \frac{1}{2 \times 400}\sqrt{\frac{2 \times 550 \times 10^{-6}}{1{,}800 \times 10^{-12}}} = 0.98$$

From ratio k_4 we see that the long-term backswing is barely oscillatory. Hence some distant false echo is possible. In Fig. 255, minimum k_2 for close false echoes is 0.17. Since k_2 calculated above is 0.628, there are no close false echoes with this modulator. According to Fig. 235, the transformer has 56 per cent backswing. It can be improved by using 0.002 in. grain-oriented silicon steel having $\mu = 1{,}000$ at 5,600 gauss. L_e then becomes 1,000 μh, $\Delta = 0.283$, $k_3 = 2.75$, and $k_4 = 1.39$. Now there are no false echoes, distant or close, and the backswing is 30 per cent.

139. Charging Reactors. In the modulator of Fig. 252, a reactor is used to charge the pulse-forming network to nearly double d-c voltage E. The inductance of this reactor is not critical but should not be so great as to resonate with *PFN* at a frequency f_r less than half the pulse repetition frequency (*PRF*). That is, the voltage across *PFN* would not reach $2E$ if the resonant-charging frequency f_r were less than $PRF/2$, and the hold-off diode would be useless. It is the function of this diode to prevent discharge of *PFN* through the d-c source. This makes it possible to use reactors with normal manufacturing tolerances, or with variations in *PRF*, within the limit set by $f_r > PRF/2$.

When no hold-off diode is used, both reactor inductance and *PRF* must be held to close tolerances, to maintain high voltage across *PFN*, with resonant frequency f_r exactly equal to $PRF/2$. Linearity of inductance with change in direct current is also necessary for accurate control. Reactors designed by Fig. 71, p. 100, are usually linear enough for the purpose.

If $f_r < PRF/2$ the hydrogen thyratron fires before voltage across *PFN* reaches its peak, but after steady-state conditions obtain this voltage nearly equals $2E$. If f_r is low enough, the increase of voltage is approximately linear with time. This result is called linear charging. Reactor inductance is large in this case, and charging current flows continuously. Here also a range of *PRF*'s may be used, all greater than $2f_r$.

Reactor voltages and currents for the three methods of charging are illustrated by Fig. 256. In all cases, Q should be high (more than 10) for efficient pulser operation. Voltages in Fig. 256 are for infinite Q. Voltage is shown for the reactor terminal that connects to *PFN*. With a hold-off diode, this voltage appears on both terminals during the intervals when current is zero. Without the diode, or if diode and reactor in Fig. 252 are interchanged, the voltage at the left-hand terminal, Fig. 252, is E. Insulation may then be graded accordingly. In all cases, peak voltage across the reactor is E. A-c flux density may

be calculated as in a filter reactor, but the *effective* frequency is $2f_r$ because the flux excursion is in one direction only at frequency f_r.

In a-c resonant charging, reactor voltage would increase to QE, where E is the a-c input voltage, if charging continued for a sufficient number of cycles. If reactor $Q > 10$ and the thyratron is fired at the end of one full charging cycle, maximum PFN voltage is πE_{pk}, where E_{pk} is the peak value of applied a-c voltage. In a-c charging the sup-

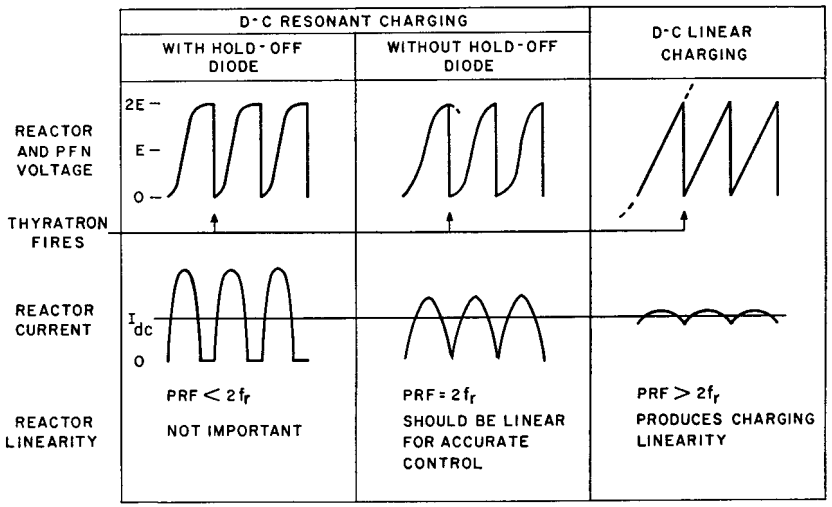

FIG. 256. Pulser charging reactor voltage and current.

ply transformer inductance may be used instead of a separate reactor and results in somewhat less total weight. A high reactance transformer is useful for this purpose, with shunts as in Section 104. If a hold-off diode is used with a-c charging, an ordinary plate transformer may be used and weight reduced still further.[1]

140. Sweep Generators. Successive pulses, which are separated in time and cause vertical deflection, can be displayed on an oscilloscope by a *horizontal sweep.* This is the term applied to deflecting means which move the oscilloscope beam horizontally from left to right, usually at a uniform time rate. If the sweep rate is non-uniform, picture distortion results. In *magnetic* deflection uniform sweep is produced by a sawtooth current which varies linearly with time during the sweep interval. A transformer for magnetic deflection is used in the

[1] For a detailed description of a-c charging, see Glasoe and Lebacqz, *op. cit.*, p. 380.

circuit of Fig. 257. Pulses of sweep duration τ_s applied to the grid of a beam tetrode cause plate current to increase throughout the pulse. If the transformer had no losses, a pulse of constant amplitude E_a

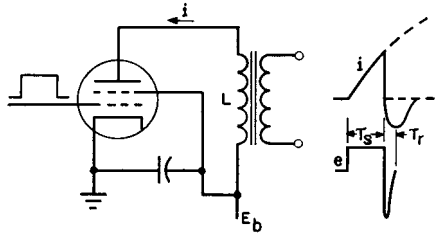

FIG. 257. Tetrode sweep generator.

would cause current to increase linearly with time until the pulse ended, in accordance with equation 40:

$$E_a = -L\frac{di}{dt} \tag{40a}$$

Losses in a practical transformer are equivalent to a resistance in series with L, and the rise in current is exponential. If the losses are small, current rise may be confined to the part of the exponential curve which is nearly linear, as indicated at the right in Fig. 257. The transformer load is usually the deflection coil of a picture tube. If this coil also has sufficiently low loss, the deflection coil current has the same wave form as the transformer primary, and a linear sweep results.

At the end of the pulse, current i does not stop flowing immediately, because of the transformer and deflection coil inductance. A large voltage backswing amplitude results, corresponding to large values of Δ in Fig. 235. Values of L, C, and R_e are such that the backswing is oscillatory with a period $2\tau_r$ which is small compared to sweep duration τ_s. During τ_r, the first or negative half of the backswing oscillation, the oscilloscope beam is usually "blanked" or cut off quickly, to allow the beam to retrace to the extreme left, ready for the next sweep period. For a bright picture, the retrace period τ_r should be short compared to τ_s, so that scanning occurs during a large percentage of the time. In television receivers, the sweep frequency is 15,750 cycles and the backswing frequency approximately 77,000 cycles. Thus the retrace time is about 10 per cent of the sweep period. Positive voltage backswing is used in starting the next sweep trace, as will be described later. Magnetic deflection sweep transformers are made

with low-loss cores. Manganese-zinc ferrites find wide use here. Design of sweep transformers is closely integrated with the sweep circuit, as will be shown in the next section.

Electrostatic deflection is accomplished by application of sawtooth voltages to the horizontal plates of an oscilloscope. Such a voltage is shown in Fig. 258. Sawtooth voltages may be formed in several ways

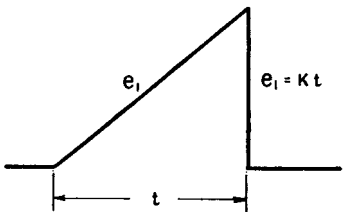

FIG. 258. Sawtooth wave.

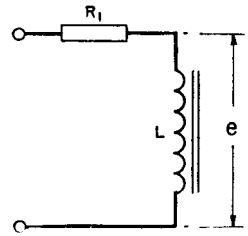

FIG. 259. Sawtooth transformer circuit.

from repetitive pulses.[1] If the pulse requires amplification before being applied to the tube plates, a sweep amplifier is necessary. Here again linearity is important. The spot is moved at a uniform rate across the screen and quickly returned to repeat the trace. In such a circuit, the load on the transformer can be regarded as negligible. Assume a linearly increasing voltage as shown in Fig. 258 to be applied to the equivalent circuit of Fig. 259.

$$e_1 = Kt$$

Then

$$Lpe_1 = LK$$

where $p = d(\ )/dt$, and the voltage across the transformer primary is

$$e = \frac{Lpe_1}{Lp + R_1}$$

$$= \frac{LK}{R_1}(1 - \epsilon^{-R_1 t/L}) \tag{143}$$

Slope of e is

$$de/dt = K\epsilon^{-R_1 t/L} \tag{144}$$

[1] See "Response of Circuits to Steady-State Pulses," by D. L. Waidelich, *Proc I.R.E., 37,* 1396 (December, 1949).

Thus voltage e has the same slope as the applied voltage times an exponential term which is determined by the resistance R_1 of the amplifier, the OCL of the transformer, and the time between the beginning and the end of the linear sweep. Under the conditions assumed, the value of the exponential for any interval of time can be taken from the curve marked $R_2 = \infty$ in Fig. 234. For example, suppose that the sweep lasts for 500 microseconds, that the sweep amplifier tube plate resistance is 800 ohms, and that the transformer inductance is 10 henrys. The abscissa of Fig. 234 is 0.04, and, since the slope of this exponential curve equals its ordinate, the slope of the voltage applied to the plates of the oscilloscope will be, at the end of the sawtooth interval, 96 per cent of the slope which it had at the beginning of the interval.

Assume that at the end of the time interval t (Fig. 258) the amplifier tube is cut off. Then the sweep circuit transformer reverts to that of Fig. 235, in which C_D has the same meaning as before but R_I includes only the losses of the transformer, which were neglected in the analysis for linearity of sweep. That is to say, the voltage does not immediately disappear but follows the curves of Fig. 235 very closely, as in magnetic deflection. Backswing voltage may be kept from affecting the screen by suitable spacing of the applied wave forms or biasing the cathode-ray tube grid.

Vertical sweep transformers are used in television receivers to displace the horizontal sweep lines at a 60-cycle rate, in order to produce a picture. The vertical displacement is fairly linear, retrace rapid, and sawtooth wave form is necessary here also. Because of the relatively slow vertical displacement, yoke inductance is negligible, so that vertical sweep amplifiers effectively operate into resistive loads during trace periods. The transformers present no particularly difficult problem beyond that of high OCL at low cost.

141. Magnetic Sweep Circuits. A simple television receiver sweep circuit is shown in Fig. 260. Pulse voltage applied to the tetrode grid appears across the transformer primary winding inverted. Current in the lower part of the transformer primary has the shape shown in Fig. 257. This is the current wave shape in the transformer secondary and deflection coil (termed the yoke). An autotransformer extension of the transformer primary winding is used to transform the pulse voltage backswing shown in Fig. 257 to a high value. This voltage is actually much larger than Fig. 257 indicates, and needs only 3:1 step-up to furnish 7 to 14 kv. It is then rectified and applied to the accelerating anode of the oscilloscope. In this way, a separate

high-voltage supply is avoided. A damper diode is used to convert the backswing current into useful current during the next sweep in-

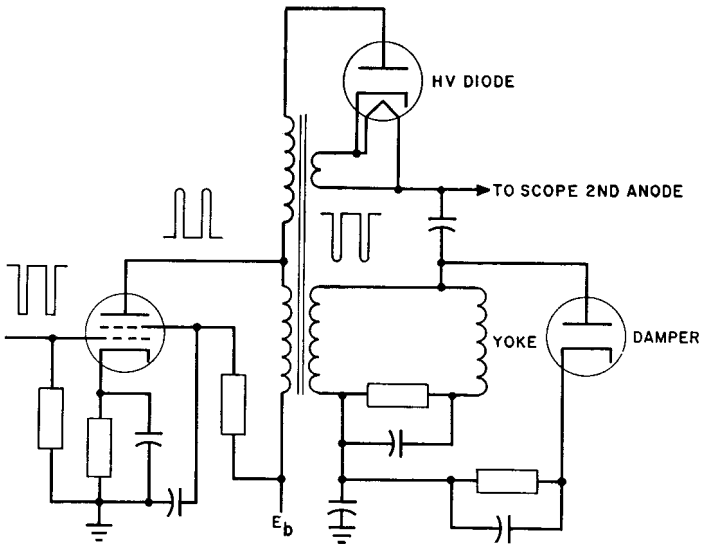

FIG. 260. Television sweep circuit.

terval. Backswing current reaches its negative peak at the end of retrace period τ_r. As indicated by the dotted oscillation at the left of Fig. 261, this current would continue to oscillate for some time if left undamped. With the damper diode circuit, this current never oscillates but instead charges the diode R-C network, which slowly discharges into the yoke. Before damper current reaches zero, the tetrode starts to conduct. Because of winding capacitance, the tetrode tube current is not initially linear. It is offset by exponential decay of damper tube current. Yoke current then proceeds in a linear manner, following the dotted line in the transition from damper to tetrode current, as in Fig. 261.

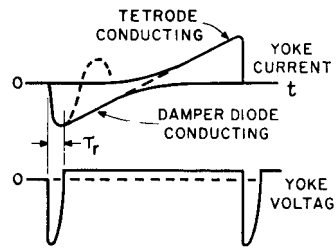

FIG. 261. Deflection yoke current and voltage.

With the large consumer demand for television receivers, there has been an incentive for improved efficiency of the basic sweep circuit. Partly this has been accomplished by ingenious schemes for improved

linearity with lower transformer Q, and partly by using the plate input resistance of the tetrode for the damper diode bias resistance. Thus otherwise wasted power is put to a useful purpose.[1]

142. Magnetic Pulse Generators. In Chapter 9 it was seen that thyratron operation can be approximated by self-saturating magnetic amplifiers. This fact points to a saturable reactor to replace the hydrogen thyratron in the pulser of Fig. 252. Several factors militate against the direct substitution of saturable reactors for thyratrons:

1. Departure of core material from sharp rectangularity interferes with steep pulse voltage rise.
2. Saturated value of inductance interferes with large current flow needed during pulse.
3. Reactors are a-c devices; hence a-c charging must be used. This limits the choice of *PRF*.

Despite these difficulties, saturable reactors have been used successfully in pulsers. Low power pulses may be formed by use of the circuit of Fig. 262. Reactor L_1 is linear and resonates with C_1 at the supply frequency. Resonance therefore tends to maintain current i sinusoidal in wave form. Current i is large enough to saturate reactor L_2, which has rectangular B-H loop core material. Twice each cycle current i passes through zero, and near these current zeros L_2 inductance becomes large. This large inductance forces most of current i instantaneously into C_2 and R_L, and builds up a comparatively large peak voltage across R_L. Such pulses are peaked in wave shape and alternate in polarity twice each cycle. Pulse durations of less than 0.1 microsecond have been obtained with this circuit. Owing to the large interval of time during which i is large, and not producing pulses, the power output is limited to small values.

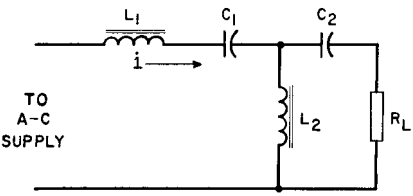

FIG. 262. Magnetic pulse generator.

In Fig. 262 the voltage across L_2 at a given line frequency f is nearly proportional to the saturation flux density B_s of the core for rectangular loop material. If the core area is A_c and turns N in L_2, then this voltage is, neglecting losses,

[1] See "Television Deflection Circuits," by A. W. Friend, *RCA Rev.*, March, 1947, p. 98; also "Magnetic Deflection Circuits for Cathode-Ray Tubes," by O. H. Schade, *RCA Rev.*, September, 1947, p. 506.

$$e_s \approx \frac{0.8 B_s f A_c N}{10^6 \theta_s} \tag{145}$$

where $\theta_s/2$ is the angle, starting from zero, at which saturation is reached, as in Fig. 193 (p. 247). If θ_s is very small, and $2\pi/\omega \gg R_L C_2 \gg \theta_s/\omega$, substantially all of e_s appears across R_L.

Higher power may be obtained from cascaded stages as in Fig. 263.

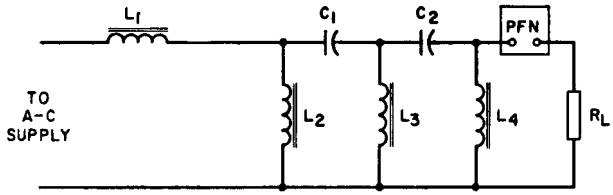

FIG. 263. Cascaded stages in magnetic pulse generator.

Reactor L_1 is linear and resonates with C_1 at the supply frequency. Reactors L_2, L_3, and L_4 are saturable; bias windings are used, but not shown. Suppose that L_2 and L_4 are initially unsaturated, and L_3 is saturated. C_1 charges in series with L_1 and L_3. As the voltage across L_2 reaches maximum, L_2 saturates and discharges C_1. Discharge current causes L_3 to become unsaturated and L_4 saturated; then C_2 charges until L_3 saturates again. As the wave proceeds towards R_L both charge and discharge times become successively shorter. Pulse duration in each stage is determined by the saturated value of inductance and associated C. In the last stage, the pulse is shaped by *PFN* to the desired duration and flatness at the top. As this sequence is repeated once each cycle, the line current is not sinusoidal, so a line capacitor is useful for supplying the current harmonics. One modification of this circuit is the use of saturating transformers instead of reactors in order to provide the stepped-up voltage necessary for magnetron operation. With a magnetron, R_L is replaced by a pulse transformer primary winding. In another modification saturable reactors are the series elements and capacitors the shunt.[1]

[1] See "The Use of Saturable Reactors as Discharge Devices for Pulse Generators," by W. S. Melville, *J.I.E.E.* (*London*), *98,* Part III, p. 185.

BIBLIOGRAPHY

TRANSFORMER THEORY

1. E. G. Reed, *Essentials of Transformer Practice,* McGraw-Hill Book Co., 2nd ed., New York, 1927.
2. L. F. Blume, Editor, *Transformer Engineering,* John Wiley & Sons, 2nd ed., New York, 1951.
3. M.I.T. Electrical Engineering Staff, *Magnetic Circuits and Transformers,* John Wiley & Sons, New York, 1943 (contains extensive bibliography).

CORE MATERIALS

4. *Magnetic Core Materials Practice,* Allegheny Steel Co., Brackenridge, Pa., 1937.
5. J. K. Hodnette and C. C. Horstman, "Hipersil, a New Magnetic Steel and Its Use in Transformers," *Westinghouse Engineer, 1,* 52 (August, 1941).
6. A. G. Ganz, "Applications of Thin Permalloy Tape in Wide-Band Telephone and Pulse Transformers," *Trans. AIEE,* April, 1946, p. 177.
7. ASTM Standards on Magnetic Materials A34-49 to A345-49 inclusive, American Society for Testing Materials, Philadelphia, Pa.
8. R. M. Bozorth, *Ferromagnetism,* D. Van Nostrand Co., New York, 1951.
9. C. C. Horstman, "Progress in Core Material for Small Transformers," *Westinghouse Engineer, 12,* 160 (September, 1952).
10. S. R. Hoh, "Evaluation of High Performance Magnetic Core Materials," *Tele-Tech, 12,* 86 (October, 1953).
11. James R. Wait, "Complex Magnetic Permeability of Spherical Particles," *Proc. I.R.E., 41,* 1664 (November, 1953).

RECTIFIERS

12. D. C. Prince and P. B. Vogdes, *Mercury Arc Rectifiers,* McGraw-Hill Book Co., New York, 1927.
13. A. J. Maslin, "Three-Phase Rectifier Circuits," *Electronics, 9,* 28 (December, 1936).
14. D. L. Waidelich and H. A. Taskin, "Analyses of Voltage-Tripling and -Quadrupling Circuits," *Proc. I.R.E., 33,* 449 (July, 1945).
15. R. S. Mautner and O. H. Schade, "Television High-Voltage R-F Supplies," *RCA Rev., 8,* 43 (March, 1947).
16. E. V. Blieux, "High-Voltage Rectifier Circuits," *General Electric Rev., 51,* 22 (February, 1948).

REACTORS

17. T. Spooner, "Effect of a Superposed Alternating Field on Apparent Magnetic Permeability and Hysteresis Loss," *Phys. Rev., 25* (2nd series), 527 (January–June, 1925).
18. L. B. Arguimbau, P. K. McElroy, and R. F. Field, *Iron-Cored Coils for Use at Audio Frequencies,* General Radio Co., Cambridge, Mass.
19. V. E. Legg, "Optimum Air Gap for Various Magnetic Materials in Cores of Coils Subject to Superposed Direct Current," *Trans. AIEE, 64,* 709 (1945).
20. George Katz, "Effect of Temperature on Iron Powder Cores," *Elec. Mfg., 53,* 135 (February, 1954).

AMPLIFIERS

21. H. S. Black, "Stabilized Feedback Amplifiers," *Bell System Tech. J., 13,* 1 (January, 1934).
22. R. Rüdenberg, "Electric Oscillations and Surges in Subdivided Windings," *J. Appl. Phys., 11,* 665 (October, 1940).
23. F. E. Terman, *Radio Engineers' Handbook,* McGraw-Hill Book Co., New York, 1943, Sections 2 and 3.
24. K. Schlesinger, "Cathode Follower Circuits," *Proc. I.R.E., 33,* 843 (December, 1945).
25. H. W. Bode, *Network Analysis and Feedback Amplifier Design,* D. Van Nostrand Co., New York, 1945, Chapters XVI to XIX.
26. D. T. N. Williamson, "Design for a High-Quality Amplifier," *Wireless World,* April, 1947, p. 118.
27. H. W. Lamson, "Advantages of Toroidal Transformers in Communication Engineering," *Tele-Tech, 9* (May, 1950).
28. T. Halabi, "Audio Transformer Design Charts," *Electronics,* October, 1953, p. 193.

NON-SINUSOIDAL WAVES

29. J. G. Brainerd, G. Koehler, H. J. Reich, and L. F. Woodruff, *Ultra-High Frequency Techniques,* D. Van Nostrand Co., New York, 1942, pp. 36–47.
30. H. E. Kallman, R. E. Spencer, and C. P. Singer, "Transient Response," *Proc. I.R.E., 33,* 169 (March, 1945).
31. C. E. Torsch, "A Universal-Application Cathode-Ray Sweep Transformer with Ceramic Iron Core," *Proc. Natl. Electronics Conf., 5,* 130 (1949).
32. L. W. Hussey, "Non-Linear Coil Generators of Short Pulses," *Proc. I.R.E., 38,* 40 (January, 1950).
33. H. W. Lord, "A Turns Index for Pulse Transformer Design," *Trans. AIEE, 71,* Part 1, pp. 165–168 (1952).
34. M. Chodorow, E. L. Ginzton, I. R. Nielsen, and S. Sonkin, "Design and Performance of a High-Power Pulsed Klystron," *Proc. I.R.E., 41,* 1595 (November, 1953).
35. M. B. Knight, "Practical Analysis of Vertical Deflection Circuits," *Tele-Tech, 12,* 62 (July, 1953).

MAGNETIC AMPLIFIERS

36. A. V. Lamm, "Some Fundamentals of a Theory of the Transductor or Magnetic Amplifier," *Trans. AIEE, 66,* 1078 (1947).

37. E. L. Harder and W. F. Horton, "Response Time of Magnetic Amplifiers," *Trans. AIEE, 69,* 1130 (1950).
38. A. I. Pressman and J. P. Blewett, "A 300 to 4000 Kilocycle Electrically Tuned Oscillator," *Proc. I.R.E., 39,* 74 (January, 1951).
39. James G. Miles, "Bibliography of Magnetic Devices and the Saturable Reactor Art," *Trans. AIEE, 70,* 2104 (1951) (containing a list of 901 references).
40. H. L. Durand, L. A. Finzi, and G. F. Pittman, Jr., "The Effective Ratio of Magnetic Amplifiers," *Trans. AIEE, 71,* 157 (April, 1952).
41. H. W. Lord, "Dynamic Hysteresis Loops of Several Core Materials Employed in Magnetic Amplifiers," *Trans. AIEE, 72,* 85 (1953).
42. S. B. Batdorf and W. N. Johnson, "An Instability of Self-Saturating Magnetic Amplifiers Using Rectangular Loop Core Materials," *Trans. AIEE, 72,* 223 (1953).
43. W. A. Geyger, *Magnetic Amplifier Circuits,* McGraw-Hill Book Co., New York, 1954.
44. R. W. Roberts, "Magnetic Characteristics Pertinent to the Operation of Cores in Self-Saturating Magnetic Amplifiers," *Trans. AIEE, 73,* 682 (1954).
45. H. F. Storm, *Magnetic Amplifiers,* John Wiley & Sons, New York, 1955 (contains extensive bibliography).

TRANSFORMER STANDARDS

46. ASA, American Standards for Transformers, Regulators, and Reactors C57.22-1948.
47. NEMA, Standards for Transformers, No. 48-132.
48. AIEE Standards: No. 1. General Principles Upon Which Temperature Limits Are Based. No. 551. Master Test Code for Temperature Measurement. "Progress Report of AIEE Magnetic Amplifier Subcommittee," *Trans. AIEE, 70,* 445 (1951).
49. RETMA Standards: Power Transformers for Radio Transmitters TR-102-B. Power Filter Reactors for Radio Transmitters TR-110-B. Audio Transformers for Radio Transmitters TR-121. Audio reactors TR-122. Iron-Core Charging Reactors TR-127. Pulse Transformers for Radar Equipment TR-129.

GENERAL

50. D. S. Stephens, "Lightweight Aircraft Transformers," *Trans. AIEE, 68,* 1073 (1949).
51. P. G. Sulzer, "Stable Electronic Voltage Regulator," *Electronics, 23,* 162 (December, 1950).
52. W. D. Cockrell, *Industrial Electronic Control,* McGraw-Hill Book Co., New York, 2nd ed., 1950.
53. R. E. Collin, "Theory and Design of Wide-Band Multisection Quarter-Wave Transformers," *Proc. I.R.E., 43,* 179 (February, 1955).

INDEX